Forschungszentrum Karlsruhe
Technik und Umwelt

Wissenschaftliche Berichte
FZKA 6324

Effects of Humic Substances on the Migration of Radionuclides: Complexation and Transport of Actinides

Second Technical Progress Report

G. Buckau (Editor)

Institut für Nukleare Entsorgungstechnik

Juni 1999

Forschungszentrum Karlsruhe
Technik und Umwelt

Wissenschaftliche Berichte
FZKA 6324

EFFECTS OF HUMIC SUBSTANCES ON THE MIGRATION OF RADIONUCLIDES: COMPLEXATION AND TRANSPORT OF ACTINIDES

SECOND TECHNICAL PROGRESS REPORT

EC Project No.: FI4W-CT96-0027

(Work Period 01.98 - 12.98)

G. BUCKAU (Editor)

Institut für Nukleare Entsorgungstechnik

Forschungszentrum Karlsruhe GmbH, Karlsruhe
1999

Als Manuskript gedruckt

Forschungszentrum Karlsruhe GmbH
Postfach 3640, 76021 Karlsruhe

Mitglied der Hermann von Helmholtz-Gemeinschaft
Deutscher Forschungszentren (HGF)

ISSN 0947-8620

Project Partners:

Partner No. 1 (Coordinator): FZK/INE, D
Partner No. 2: BGS, UK
Partner No. 3: CEA-SGC, F
Partner No. 4: FZR-IfR, D
Partner No. 5: KUL, B
Partner No. 6: LBORO, UK
Partner No. 7: CEA-LSLA, F (Associated to Partner No. 3)
Partner No. 8: GERMETRAD, F (Associated to Partner No. 3)
Partner No. 9: RMC-E, UK
Partner No. 10: NERI, Dk
Partner No. 11: GSF-IfH, D (Associated to Partner No. 1)
Temporary Contributor*: Uni-Mainz, D

Duration of the Project:

01.97-12.99

***: EC-TMR grant FI4W-CT97-5005**

Foreword

The present report describes progress within the second year of the EC-project "Effects of Humic Substances on the Migration of Radionuclides: Complexation and Transport of Actinides". The project is conducted within the EC-Cluster "Radionuclide Transport/ Retardation Processes". Without being a formal requirement of the Commission or co-funding bodies, this report documents results of the project in great technical detail and make the results available to a broad scientific community. Results of the first year of the project are published in an equivalent form in [1].

The report contains an executive summary written by the coordinator. More detailed results are given by individual contributions of the project partners in 17 annexes. Not all results are discussed or referred to in the executive summary report and thus readers with a deeper interest also need to consult the annexes.

The report reflects the successful integration of "cost shared research projects" and mobility research grants" by the European Commission. Annex 17 is from the temporary contributor University of Mainz (EC-TMR grant FI4W-CT97-5005). The annex reflects the objectives of the present project and is an important contribution to the understanding of possible artifacts leading to incorrect experimental results and associated misunderstandings concerning relevant actinide humate interaction processes.

[1] Buckau G. (editor) (1998) "Effects of Humic Substances on the Migration of Radionuclides: Complexation and Transport of Actinides, First Technical Progress Report", Report FZKA 6124, August 1998, Research Center Karlsruhe.

Content

*: Temporary contributor (EC-TMR grant FI4W-CT97-5005)

EXECUTIVE SUMMARY

EFFECTS OF HUMIC SUBSTANCES ON THE MIGRATION OF RADIONUCLIDES: COMPLEXATION AND TRANSPORT OF ACTINIDES

SECOND TECHNICAL PROGRESS REPORT

EC Project No.: FI4W-CT96-0027

(Work Period 01.98 - 12.98)

G. Buckau
(FZK/INE)

Content of Executive Summary

INTRODUCTION

The project started 01.97 and has a duration of three years. This report covers the second year, i.e. the period 01.98 - 12.98. Work has been conducted on all Tasks of the project. (Task 1 ("Sampling and Characterization"); Task 2 ("Complexation"); Task 3 ("Actinide Transport"), Task 4 ("Migration Model Development and Testing") and Task 5 ("Assessment of Impact on Long-Term Safety"). Definition of migration case studies for implementation of the present state-of-the-art is under preparation in a separate report.

The project encompasses development of the necessary input to judge upon the influence of humic substances on the long-term safety of radioactive waste disposal. The project focuses on long-lived radionuclides with high radiotoxicity, i.e. actinides and technetium, and their behavior in the far-field. To assess the impact of humic substances on the radionuclide migration in the far-field, relevant processes need to be introduced into models. These models rest on a step-wise approach where data of individual processes from relatively well defined systems are tested for their applicability on more complex laboratory systems on natural material (especially batch and column experiments under near-natural conditions). The processes described by models developed from laboratory experiments are limited by the size and time constraints of such studies. Furthermore, large-scale inhomogeneities and deviation from equilibrium in the real, more or less open, system cannot be easily developed through investigations on the laboratory scale. In order to achieve adequate confidence that relevant processes have been regarded in models developed, the real system is also investigated with respect to for example, chemical behavior of actinide analogue trace elements in natural humic colloids and the migration behavior of humic colloids present at a real site. A schematic description of the overall approach of the project is shown in Fig. 1.

Contrary to original intentions and for reasons beyond the reach of the project partners, an encompassed research site in France did not materialize and the Sellafield is not anymore a candidate site for disposal. Sellafield, however, is studied as a reference site for such geochemical conditions. Material relevant for the German "Königstein" and "Johanngeorgenstadt" uranium mining and milling sites is also used within the project. Some aspects are investigated on Boom Clay material. The German Gorleben site presently is questioned as a candidate site. For this site, however, a tremendous amount of data on geology, hydrology and geochemistry, are available. Furthermore, material for laboratory investigations still is available. For these reasons, site-specific work focuses on this site.

Main achievement of the project so far has been to demonstrate that the geochemical behavior of humic colloid bound actinide ions requires inclusion of kinetics, whereas approaches solely relying on an equilibrium approach fail to describe experimental findings. Furthermore, the chemical behavior of natural actinide homologues is different than actinides studied under laboratory conditions.

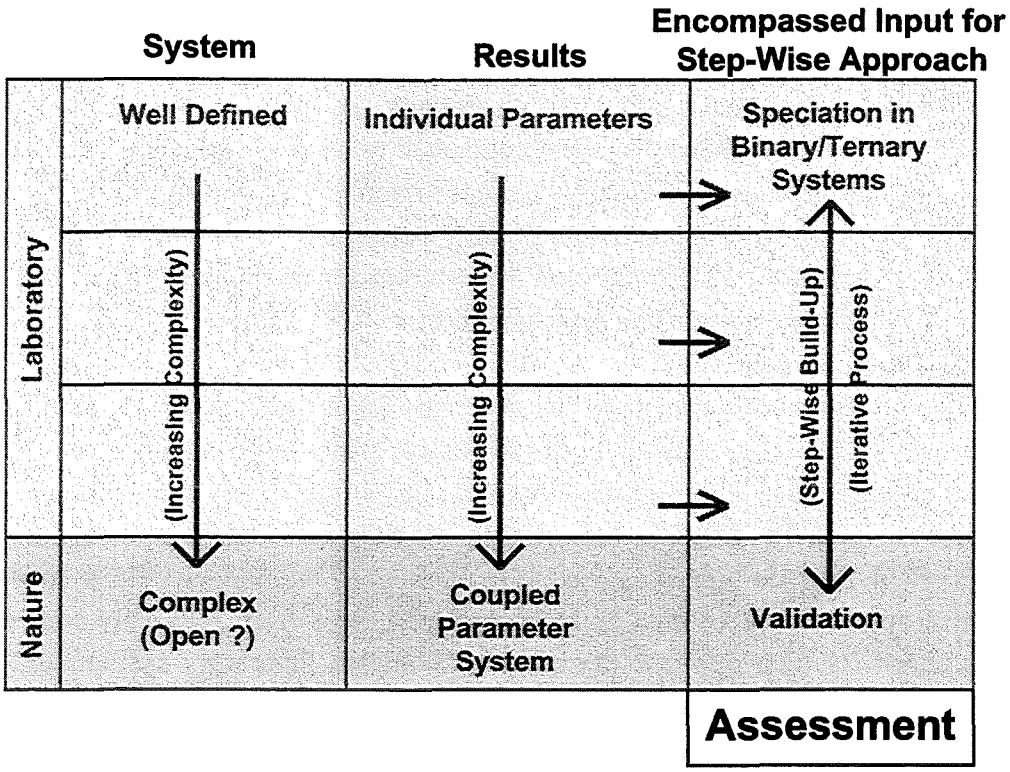

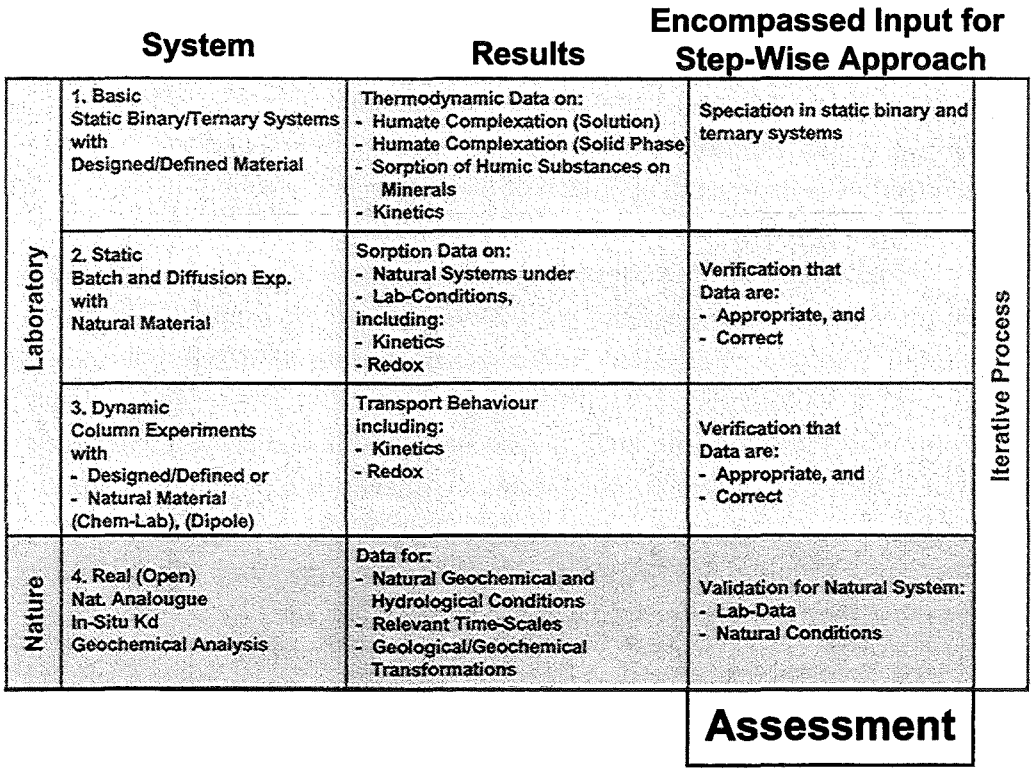

Fig. 1: Schematic description of the overall project approach

1. OBJECTIVES

The main objective of the project is to determine the influence of humic substances on the migration of radionuclides. For the long-term safety, long-lived highly radiotoxic nuclides are the most relevant. The project therefore focuses on actinide elements. In order to achieve the main objective a thorough understanding is needed for (i) the complexation of actinides with humic substances, (ii) the influence of humic substances on the sorption properties of sediments, and (iii) the mobility of actinide humic substance species in groundwater.

2. PARTNERS AND PROJECT STRUCTURE

The project has 11 partners and for the present period one additional temporary partner. Three partners are associated to other contractors. The partners and their partnership is as follows:

Partner No. 1 (Coordinator): FZK/INE, D
Partner No. 2: BGS, UK
Partner No. 3: CEA-SGC, F
Partner No. 4: FZR-IfR, D
Partner No. 5: KUL, B
Partner No. 6: LBORO, UK
Partner No. 7: CEA-LSLA, F, (Associated to Partner No. 3)
Partner No. 8: GERMETRAD, F, (Associated to Partner No. 3)
Partner No. 9: RMC-E, UK
Partner No. 10: NERI, Dk
Partner No. 11: GSF-IfH, D, (Associated to Partner No. 1)
Temporary Contributor: Uni-Mainz (EC-TMR grant FI4W-CT97-5005)

The project is divided into five tasks with a project structure as shown in Fig. 2.

3. SUMMARY OF RESULTS

The overall progress within individual tasks and contributions of individual partners is summarized below. Details can be found in the annexes.

Project Management Structure
(Overview)

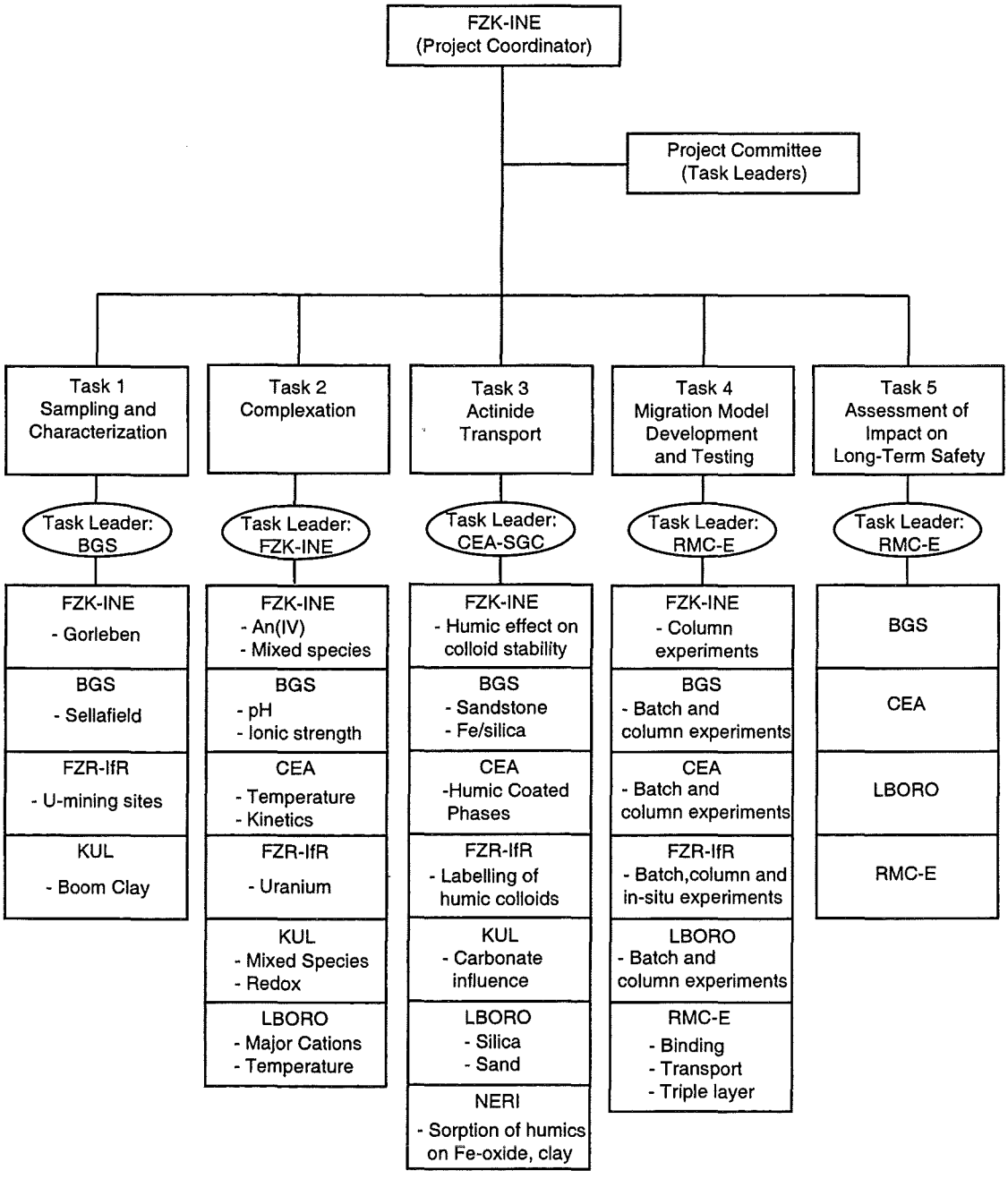

Fig. 2: Project structure

3.1 TASK 1 (Sampling and Characterization)

3.1.1 Objectives and General Achievements

The objectives of this task are to ensure appropriate sampling and characterization of relevant experimental material, ensure appropriate documentation of the sampling and characterization and thus provide the basis for trustworthy interpretation of results and intercomparison studies between different laboratories. Natural experimental material from Gorleben (D), Sellafield and Derwent Reservoir (UK), Johanngeorgenstadt (D), Königstein (D) and reference sites have been sampled and characterized. Man-made designed experimental material, such as humic acid coated silica beads and defined mineral phases have been prepared and characterized. Columns have been prepared with natural and designed material. Characterization results of appropriate detail for the material and experimental systems are given in the published "First Technical Progress Report" [1].

3.1.2 Characterization Results

Results of extensive characterization of Kranichsee humic and fulvic acids and Derwent fulvic acid have already been reported at earlier stages of the project. Because of its importance for the metal ion humate interaction, proton exchanging groups were characterized by pH titration at different ionic strength. Both fulvic acids were found to have proton exchange capacities of approximately 5 meq/g and Kranichsee humic acid approximately 4 meq/g. Excellent agreement is found between the present value from BGS and the previous direct pH titration value of 4.06±0.51 meq/g Kranichsee humic acid by FZR/IfR. In Figs. 3a and b, the titration curves of the both fulvic acids are shown. A striking difference is the strong ionic strength dependency of the Kranichsee fulvic acid compared to the Derwent fulvic acid. The Kranichsee humic acid also shows a strong ionic strength dependency (not shown). Such differences may be important for comparing the metal ion interaction properties (See also Annex 3).

A set of five columns have been prepared and conditioned under anoxic conditions (Ar + 1% CO_2) (Annex 16). Characterization was done of input material ranging from course irregular pebble to fine sand. The columns were conditioned for six weeks with synthetic humic-free "Gorleben Sweet Water" until hydraulic properties were acceptably stable. Thereafter, the columns were conditioned for 37 weeks with the Gorleben groundwater Gohy-2227. During conditioning with the groundwater, hydraulic properties of the columns and changes in chemical composition of the groundwater was monitored. The first fractions of Gohy-2227 groundwater showed a decrease in the DOC concentration of approximately 10 %. After approximately 12 weeks, DOC input and output concentrations showed no significant difference. During conditioning with the natural groundwater Gohy-2227, average values for

decrease in effective porosity was found to be 0.03 to 0.09 % per day and 0.04 to 0.32 % per day average increase in dispersivity. This shows that stable hydraulic properties of laboratory columns with natural material require approximately 10 months of conditioning. Furthermore, several months of conditioning with natural groundwater is required to achieve steady state conditions with respect to sorption of humic substances.

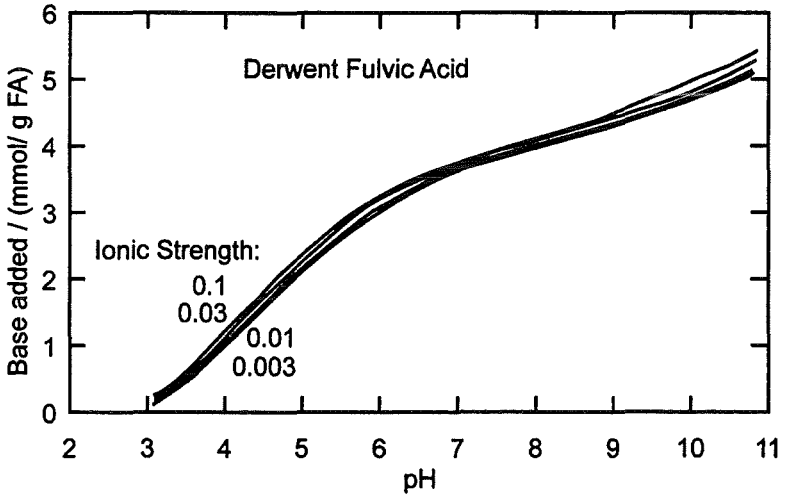

Fig. 3a: pH titration of Derwent fulvic acid at different ionic strength.

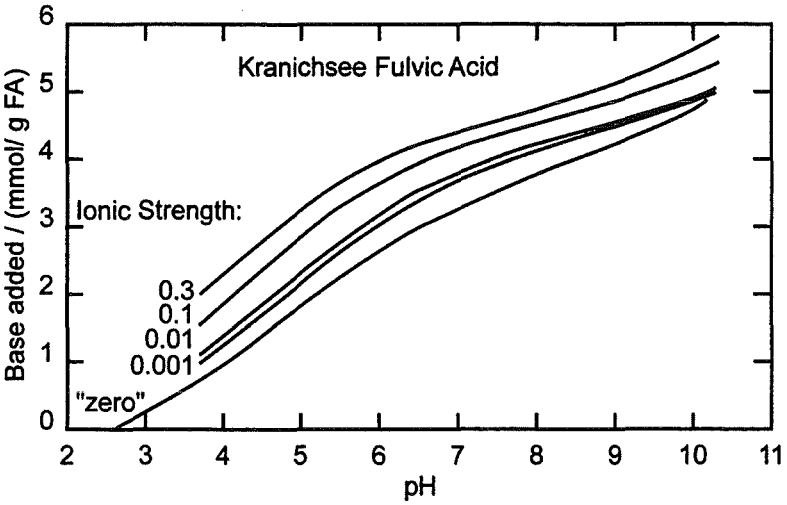

Fig. 3b: pH titration of Kranichsee fulvic acid at different ionic strength.

3.2 TASK 2 (Complexation)

3.2.1 Objectives and General Achievements

The objectives of this task are to provide relevant basic data on actinide/technetium humate complexation and the reduction of the redoxsensitive elements. Considerable progress has been achieved in a number of issues: (i) humate complexation of tri-, tetra- and hexavalent actinide ions by different methods, including mixed complexes in the pH neutral range; (ii) reduction of heptavalent technetium and pentavalent neptunium to their tetravalent states; (iii) humate interaction kinetics/reversibility of Eu(III), Th(IV) and U(VI), including influence of chemical conditions and temperature; (iv) kinetics/reversibility of natural humic colloid bound trace elements (geochemical actinide analogue elements). A first estimate of the humate interaction constant of tetravalent technetium has also been made. From these results, further data on the humate complexation has been added to the EC-Humics database. Work on fundamental approaches to the actinide-humate interaction processes has progressed well and this issue is considered basically finalized. A thorough investigation scrutinizing experimental methods has shown that experimental artifacts lead to the incorrect assumption of metal ion concentration dependent humate complexation constants.

3.2.2 Complexation Results

First results from a spectroscopic study on the humate complexation of the tetravalent neptunium ion in the non-hydrolyzing pH range have been achieved. This work is conducted in cooperation with SCK/CEN. The free ion and the humate complex are characterized by their absorption at 960 nm and 968 nm, respectively (Annex 1). The charge neutralization model proved to be successful in describing experimental data.

Work has continued on establishing a consistent set of actinide complexation constants for species distribution calculations (Annex 4). Speciation is done by time-resolved laser fluorescence spectroscopy, making use of excitation, emission and fluorescence life-time. For U(VI), the mixed $UO_2(OH)_3$-humate complex is found to be the dominant species under typical groundwater conditions. For Eu(III) evidence for mixed carbonate-humate complexes is found. The thorium humate complexation is studied by competition with silica colloids and humic acid coated silica beads between pH 2 and 9. First results show a very strong stabilization of thorium in solution. These results lead to the assumption that thorium in the pH neutral range generate humate complexes (and eventually hydroxo-humate complexes).

The influence of humic substances (from Boom clay and Gorleben) on the reduction of Tc(VII) to Tc(IV) was studied as a function of time in presence of synthetic systems of Fe(II) containing minerals (FeS and FeS2). Tc(VII) reduction was also studied in Boom Clay as a

natural reducing sediment. The enhanced solubility of Tc(IV) due to the presence of humic substances was interpreted as Tc(IV) - HS complexation. A first estimate of the Tc(IV) humate complexation constant has been made, resulting in $\log\beta = 21$. This value is deduced from speciation calculations with several Tc(IV) species, and thus is not very precise (Annex 11). Nevertheless, this value may be useful for comparison with forthcoming humate complexation constants of tetravalent actinide ions.

The uranium(VI) humate complexation has been studied at pH 4.0 and 5.0 and at an ionic strength of 0.004 and 0.1 M ($NaClO_4$). Two different experimental methods were critically examined. It was shown that the electrophoretic ion focusing leads to incorrect results due to experimental draw-backs. Anion-exchange chromatography was also investigated for its applicability. It was shown that the anion-exchanger also contains a small number of cation exchanging sites. The consequence is that if not corrected for, an increase in the stability constant is found with decreasing metal ion concentration. If this effect is corrected for, a single uranium(VI) humate metal ion concentration independent complexation constant is found ($\log\beta = 6.08 \pm 0.15$ (L/mol)) (Annex 17).

Investigations on the dissociation of the trivalent Eu ion by batch contact with the ion-exchanger Chelex 100 revealed differences between Eu added in the laboratory system and the natural Eu content of humic colloids. Eu was pre-equilibrated with Aldrich humic acid for contact times between 1 hour and 6 weeks prior to dissociation measurement by Chelex 100. The Eu dissociation was increasingly retarded with increasing pre-equilibration time (Annex 2). At about 1000 h dissociation time, however, only about 18 % of Eu remained on humic colloids for all four pre-equilibration times. More important, the natural Eu content of humic colloids show a very different dissociation kinetics. This dissociation of this Eu is much stronger retarded and after 1000 h still more than 40 % remains on the humic colloids. Rate constant for the Eu dissociation under different conditions indicate that the kinetic data from laboratory systems, including column experiments with radionuclides equilibrated with humic colloids in the laboratory, are not representative for the real system. Contrary to these laboratory investigations, much lower retardation of multivalent trace metal ions may be expected in the real system (Annex 2).

The dissociation of Th and U from fulvic acid has been investigated. For scavenging the dissociated actinide ions, the cation exchangers Cellphos and Hyphan were tested and used (no one exchanger was found to be ideal for both actinides tested under the range of experimental conditions). One example of results is shown as Figure 4. Limitations in sorption rates on the exchanger need to be taken into account for appropriate evaluation of dissociation rate constants from the fulvate complex. Furthermore, because of these limitations, actinide fulvate stability constants cannot be adequately evaluated through back-extrapolation of species distribution at the dissociation time-zero (Fig. 4). The thorium and uranyl fulvate dissociation rates were compared. Dissociation of U(VI) at pH 7 is rapid, with up to 70%

dissociation within the first hour, compared to less than 20% for Th(IV). Of the fraction remaining fulvic bound, long term dissociation kinetics depend on the preconditioning time between actinide and fulvic acid. For the U(VI) example and a preconditioning time of 1 day, about 65% of this fraction was dissociated within the following 20 hours. For a preconditioning time of 162 days, the corresponding number is approximately 35%.

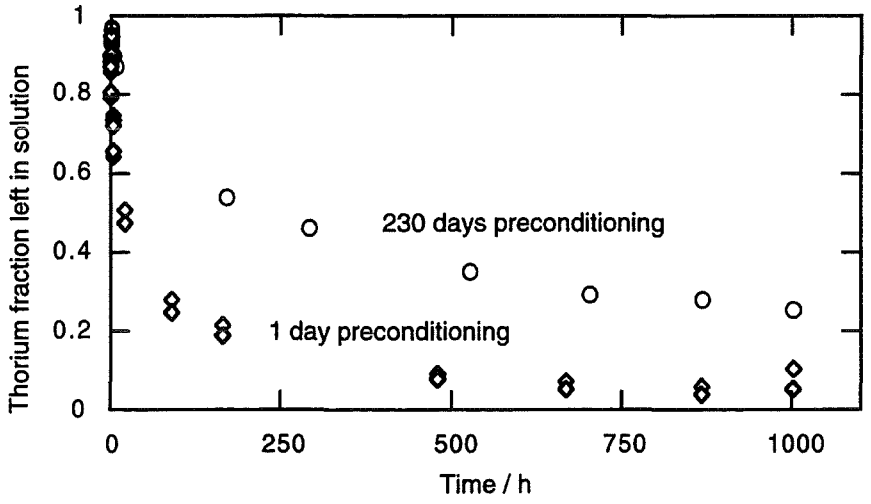

Fig. 4: Dissociation of Th from Derwent fulvic acid by exchange with Hyphan; 1 day preconditioning points are duplicates.

The association/dissociation of the europium ion (Annex 12) and the thorium ion with Derwent fulvic acid and Aldrich humic acid has been studied. Dissociation kinetics was studied by adding Dowex cation exchanger to scavenge dissociated ions. For Th, parameter variation was made on pH (4.5 and 6.5), temperature (up to 60 °C), humic substance and Th concentrations. In Fig 5, examples of the experimental observations are shown. No effect of temperature was observed. For a sufficient amount of Dowex cation exchanger it was shown that the results are not negatively influenced by saturation of the exchanger. Association is verified to be a very rapid process with 98 - 99 % of Th bound within 2 minutes. With increasing conditioning of the humate/fulvate complex, Th is transformed to kinetically hindered binding environments. This amount of less kinetically available Th humate/fulvate increased with pH, equilibration time, humic substance and Th concentrations.

Work on fundamental approaches to the actinide-humate interaction processes has progressed well. Based on experimental results on the temperature dependency, it is shown that dehydration of metal ions upon complexation and relaxation of the humate double layer upon progressive charge neutralization due to the metal ion complexation dominates over the

enthalpy contribution from local binding. Considerable improvement was achieved by introduction of an internal volume of humic acid instead of merely surface interaction. Work on this issue is considered basically finalized.

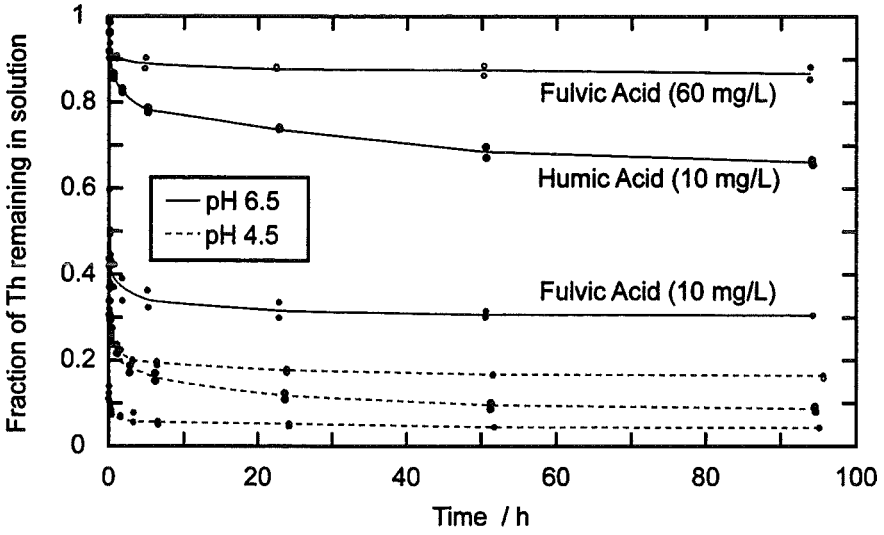

Fig. 5: Dissociation of Th from Aldrich humic acid Derwent FA by contact with Dowex cation exchanger. The relative sequence of the curves are the same at both pH values.

3.3 TASK 3 (Actinide Transport)

3.3.1 Objectives and General Achievements

The objectives of this task are to identify, describe and quantify relevant mechanisms influencing the actinide and technetium transport by batch and column experiments on both defined/designed and natural material. This includes not only sorption/migration of actinide elements and technetium on natural material and covalently humic acid coated silica beads, but also for example, the sorption of humic acid on mineral surfaces and the influence of humic acid on the reduction of redoxsensitive elements on various mineral surfaces.

The results show that batch and column experiments on natural material are not in equilibrium but a kinetic approach is required for a consistent description of the results. Furthermore, for redoxsensitive elements the migration behavior is mainly governed by the oxidation state. Uranium transport experiments on Gorleben column systems show that next to humic colloid bound uranium also ionic complexes are of importance. This is in agreement with speciation results (Annex 4). Investigations on the ternary system uranium, phyllite and humic acid show the importance of humic acid for sorption and stabilization of uranium in solution. The redox

state of Np and Tc will govern their geochemical behavior. Investigations show that the presence of active sediment surface sites accelerates the reduction to tetravalent Tc and Np. One of the key issues for humate mediated actinide transport is the humic acid interaction with mineral surfaces. Results show different behavior towards different minerals. It is also shown, that certain humic substance fractions are preferentially sorbed.

3.3.2 Actinide Transport Results

The transport behavior of neptunium is governed by the redox state. To allow interpretation of experimental results from column and batch experiments, the redox behavior of neptunium under relevant conditions has been investigated (Annex 1). The results on the reduction of Np(V) to Np(IV) can be summarized as (i) reduction rate and reduction capacity in groundwater is pH dependent; (ii) it is catalyzed by dissolved Fe(II) and Fe(III); (iii) there are possibly more than one reaction routes with different kinetics; and (iv) reduction is significantly accelerated in presence of sediment. Without contact with sediment approximately half of the Np(V) has been reduced after 25 days. In contact with sediment almost quantitative reduction is found after one day.

The transport behavior of uranium in the Gorleben groundwater Gohy-532 has been investigated (Annex 10). The results show that part of the uranium is transported with a velocity slightly higher than the groundwater matrix, i.e. the ideal tritium tracer. As also found for americium, the recovery depends on the pre-equilibration time between the radionuclide and groundwater humic colloids. Increasing the pre-equilibration time from 0.04 to 82 days, recovery increases from 0.4 to 7.8 %. Also in agreement with findings on the americium transport, the recovery decreases with the residence time in the column. Both these results verify the kinetic approach developed within this project.

Humic acid coated silica gel is investigated for application to humate complexation studies with easy and unambiguous separation between complex and non-complexed actinide ions. It is also investigated for application as model system for sediment sorbed humic acid. The sorption behavior of Eu(III) has been investigated at pH 5-8 in 50 mM $NaClO_4$. Within six hours more than 90 % of Eu(III) is sorbed (Annex 6).

Investigations on the sorption of humic acid on defined prepared minerals have continued. Two important questions are if there is specific sorption at defined sites with a maximum sorption capacity and if different fractions of humic acid are preferentially sorbed. It is shown that depending on the type of mineral either site specific binding with a limited loading and non-specific basically unlimited sorption occurs. Furthermore, selective fractions of humic acid show preferential sorption (Annex 15). The sorption of humic acid on goethite mineral and hematite colloids has been investigated (Annex 5). The humic acid sorption on goethite

strongly depends on pH, especially low sorption around pH = point of zero charge. The humic acid sorption was found to reach a saturation value (Fig. 6). Contrary to this, humic acid sorption on hematite was lower and no sorption saturation value was observed under the experimental conditions of the study.

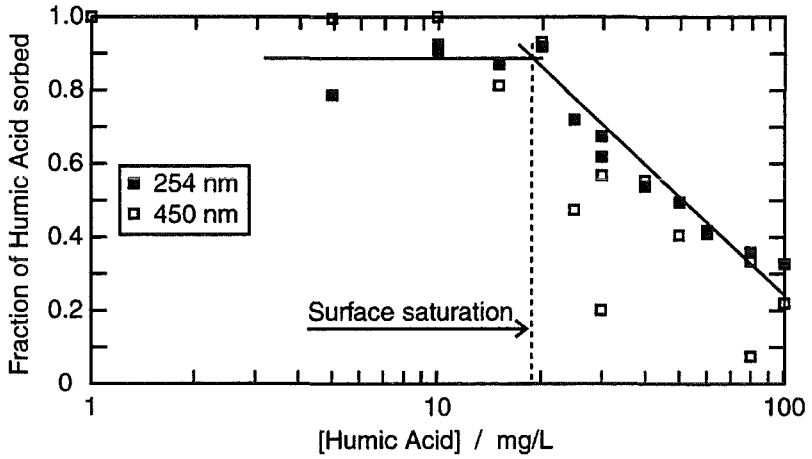

Fig. 6: Sorption of Aldrich humic acid on Goethite (500 mg/L) at pH 5 and I=0.1 M ($NaClO_4$). Humic acid is quantified by UV/Vis spectroscopy at 254 and 450 nm.

The influence of humic substance on the sorption of uranium(VI) on the natural mineral Phyllite has been investigated by batch experiments (Annex 9). The mineral was contacted with UO_2^{2+}, with and without Kranichsee humic acid. pH was varied between 3.5 and 9.5 at an ionic strength of 0.1 M ($NaClO_4$). In Fig. 7, an example is given for uranium(VI) and humic acid sorption at two different humic acid concentrations as a function of pH. At a low initial humic acid concentration (5 mg/L), both humic acid and the uranyl ion is mainly sorbed in the neutral pH region. At higher humic acid concentrations, a large fraction of humic acid remains in solution, stabilizing the uranyl ion.

Previously, batch experiments have been conducted to study the influence of geochemically relevant Fe(II)-containing minerals (FeS and FeS_2 (pyrite)) and the clay mineral illite on the chemical behavior of Tc, with and without humic acid. Reduction of Tc(VII) to Tc(IV) is of main importance. Furthermore, experiments were conducted with pyrite and 10^{-2} mol/L bicarbonate as well as with pyrite pretreated with dithionite-citrate solution in order to remove Fe(III)-oxides from the mineral surface. In the present period, the reduction of Tc(VII) has been studied in the natural system Gorleben groundwater/sand sediment (Annex 11). Experiments were conducted under inertgas atmosphere (N_2/H_2) (Eh $\approx$ -200 mV) with an

initial Tc concentration of 5 µmol/L at pH 7.9. Less than one third of technetium is found in solution after 24 hours. This is attributed to reduction from Tc(VII) to Tc(IV). It shows that in the real system Tc(VII) is expected to be readily reduced to Tc(IV).

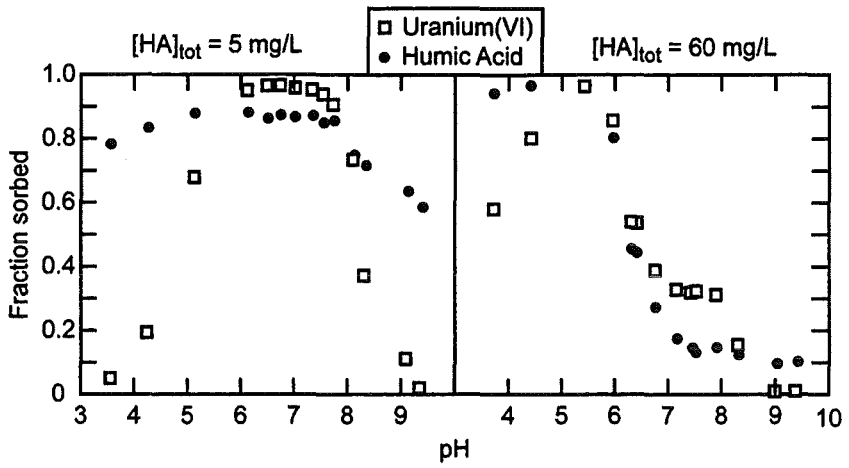

Fig. 7: Sorption of uranium(VI) and Kranichsee humic acid on Phyllite as a function of pH.

3.4 TASK 4 (Migration Model Development and Testing)

3.4.1 Objectives and General Achievements

The objectives of this task are to rationalize the state of understanding by establishing numerical models, test these models to ensure their applicability or identify processes still not adequately understood. Following conclusions already during the first project meeting, development of new models for transport modeling appears necessary. The major achievement has been to develop and test models taking the above mentioned non-equilibrium in batch and column experiments into account.

In the past, interpretation of actinide transport based on the thermodynamic equilibrium approach and filtering of humic colloids has been subject to major difficulties. These difficulties may be summarized as follows: (i) pulse injection column experiments show two different actinide fractions; one eluted slightly faster than ideal tracers and one which is not eluted within time-scales practicable for the lab experiments; (ii) batch experiments show time dependent distribution values; and (iii) combination of results from batch and column experiments on equivalent systems lead to inconsistencies. Furthermore, the fraction of the actinide ion recovered by elution with zero retention is found to vary with experimental conditions.

For these reasons, kinetic approaches have been developed. The open transport code K1D allows for incorporation of equilibrium and kinetics of different reactions, as appropriate. The code Column3 where equilibrium and kinetic parameters are fitted to experimental data has also been applied.

3.4.2 Modeling Results

The transport code K1D has been further developed to include mixed equilibrium/kinetically processes. Based on experiments, parameters have been carefully evaluated and the resulting code tested. The "Kinetically Controlled Availability Model" has been further developed and the charge neutralization model has been formulated for incorporation in modeling codes. These approaches are brought into the code for coupled equilibrium/ kinetics modeling of humate mediated actinide transport.

To model the real system, upscaling from laboratory findings is required with respect to time scale, spatial scale and variations in hydrological and geochemical conditions along a migration path. Upscaling of the time scale is a major problem because of differences in kinetics found in laboratory systems and the real system. Spatial upscaling is shown to be no problem for column experiments with column length varying between 0.5 and 10 m (Fig. 8). For comparable preconditioning prior to column injection, normalizing to the mobile fraction at the beginning of the column, the Eu-recovery is directly dependent of the residence time in the column but not of the column length.

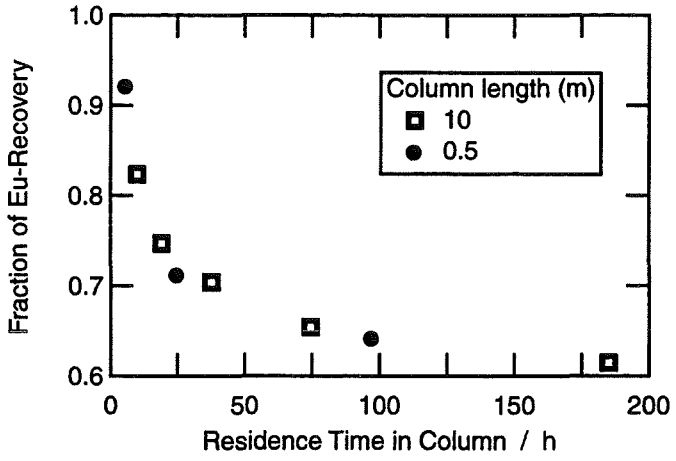

Fig. 8: Upscaling of humate mediated Eu transport in column experiments with 0.5 and 10 m column length.

The transport code Column3 has been applied to model the migration of Co and fulvic acid. Kinetic and equilibrium parameters are fitted from experiments and tested for different experimental conditions. In Fig. 9, the outcome is shown for modeling the transport of fulvic acid for 0.22 and 1.07 cm/min flow velocity. Experimental data and modeling results agree well for both the low and the high flow velocities verifying the applied kinetic approach for fulvic acid sediment surface interaction under these conditions. To which extent such exchange will occur in the real system is still not quite clear.

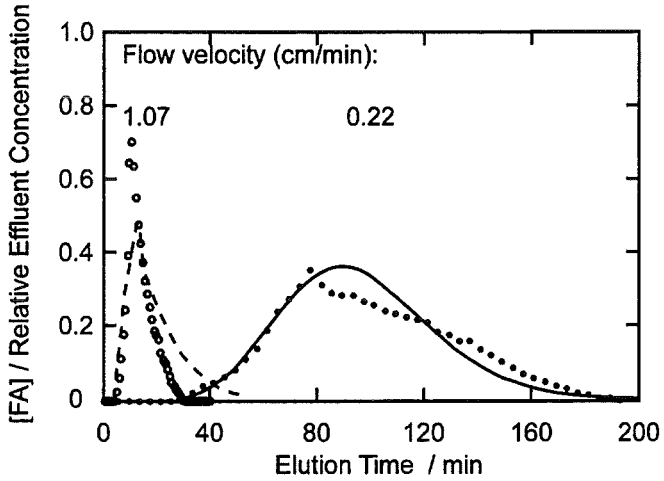

Fig. 9: Column transport of fulvic acid at 0.22 and 1.07 cm/min flow velocity. Experimental data and results from modeling by the code Column3.

3.4.3 Joint Database on Humate Complexation

A joint database of selected humate complexation data has been established. The data are restricted to results originating from the partners including their previous activities. The database contains direct speciation results and thus allows modeling by different approaches and model development. The database is available on the project homepage.

3.5 TASK 5 (Assessment of Impact on Long-Term Safety)

Commencement of activities on this task originally was not foreseen until the last year of the project. Nevertheless, considerable work has already been conducted. Experimental work and modeling has shown that several processes are best described by a kinetic approach. Depending on the conditions, however, the equilibrium approach may sometimes be used leading to considerable reduction in modeling efforts. Model calculations have been conducted to establish boundary conditions where either of these approaches is the most appropriate

(Annex 14). This will help in optimizing modeling efforts of the forthcoming migration case studies.

In order to apply the developed models on real systems, two migration case studies are under preparation. These are Gorleben and the Uranium Mining Rock Pile No. 250, Schlema/Alberoda, Saxony, Germany. These migration case studies will apply present knowledge on humate mediated actinide transport in real systems and also allow identification of weak points that require further studies. The migration case studies are included in a working document to be continuously developed throughout the last year of the project.

4. REFERENCES

[1] Buckau G. (editor) (1998) "Effects of Humic Substances on the Migration of Radionuclides: Complexation and Transport of Actinides, First Technical Progress Report", Report FZKA 6124, August 1998, Research Center Karlsruhe.

Annex 1

Redoxchemistry of Np in a Humic Rich Groundwater

(Marquardt et al., FZK/INE)

2st Technical Progress Report

EC Project:

"Effects of Humic Substances on the Migration of Radionuclides:
Complexation and Transport of Actinides"

FZK/INE Contribution to Task 2 (Complexation)

Redoxchemistry of Neptunium in a Humic Rich Groundwater

Reporting period 1998

C. Marquardt, R, Artinger, P. Zeh and J.I. Kim

Forschungszentrum Karlsruhe, Institut für Nukleare Entsorgungstechnik,
P.O. Box 3640, D-76021 Karlsruhe, Germany.

Redoxchemistry of Neptunium in a Humic Rich Groundwater

C.M. Marquardt, R. Artinger, P. Zeh, J.I. Kim

Abstract

The chemical behaviour of the redoxsensitive pentavalent neptunium was studied in a humic substances containing Gorleben groundwater Gohy 2227 mainly by absorption spectroscopy. Batch and column experiments showed a reduction of NpO_2^+ to Np^{4+}. Experiments at different pH values (4, 6-9) showed different reaction kinetics with assumed pseudo-first order rates in the orders of 10^{-4} h^{-1}. A detailed description of the rate is difficult due to the complexity of the groundwater and the humic acid itself. The rate of the reduction is accelerated by ferrous and ferric ions in solution. In a column experiment with a Gorleben sandy sediment NpO_2^+ is reduced to Np^{4+} very rapid within 15 hours, compare to the batch experiments without sediment contact. It is assumed that the Fe^{2+} on the sediment surface as well as in solution as humate complex expedites the NpO_2^+ reduction to Np^{4+}. The tetravalent neptunium is found as a humic colloid bound species in contrast to the pentavalent neptunium, which exists mainly in ionic forms as free NpO_2^+ and monocarbonato complexe $NpO_2CO_3^-$.

Introduction

Complexation and redox reactions of humic substances predominantly govern the chemical behaviour of actinide ions in natural aquatic systems. In many publications the complexation reactions of actinide ions with ligands occuring in natural waters like the humic and fulvic acids have been described. However, little information is available concerning their redox behaviour toward redoxsensitive metals in natural waters. Especially the redox effect of organic molecules like the ubiquitous humic substances and their reaction mechanism are hardly characterised, although a reductive effect is attributed to them [1, 2, 3, 4, 5, 6].

The lighter actinides can exist simultaneously in different oxidation states (III – VI), they are redoxsensitive. In aqueous solution each single oxidation state shows different chemical

interactions with inorganic and organic reaction partners. The actinide ions will change their oxidation state depending on the presence of different redox partners, and consequently, the chemical as well as the migration behaviour will change. Especially for the transition from pentavalent to tetravalent oxidation states the chemical properties, like tendency for hydrolysis, complexation and colloid formation, are altered drastically [7, 8], which result in entirely different migration behaviour. Therefore understanding the redox behaviour of actinides is essential for interpretations and modelling of migration studies.

The chemical behaviour of pentavalent neptunium is studied in a groundwater under reducing conditions (oxygen free argon atmosphere). A groundwater with high humic substances content from the Gorleben aquifer system (Lower Saxony, Germany) was used. This groundwater is selected because of the direct relevance to safety assessment of permanent disposal in the salt dome underlying the Gorleben aquifer system.

Experimental

For the experiments a stock solution of the neptunium isotop Np-237 was prepared in the pentavalent oxidation state (NpO_2^+) at a concentration of 0.05 M, ionic strength of 0.1 M $NaClO_4$ and pH 3. (for details see Ref [9]). Neptunium concentrations were measured by 1) alpha-liquid-scintillation counting with beta-discrimination of its daughter protactinium-233 and 2) NIR absorption spectroscopy of the Np(IV) and Np(V) absorption band at 960 nm and 980.4 nm with molare absorbance coefficients of 162 [10] and 395± 5 L $mol^{-1}cm^{-1}$ [9].

The humic containing groundwater Gohy 2227 was used and all its chemical and physical parameter are presented in detail in Artinger et al [11]. The pH value and the ionic strength of the water was pH 7.6 and 4.4 x 10^{-2} M, respectively. The DOC of the Gohy-2227 groundwater amounts 81.9 mgC L^{-1}. One part of the experiments were done in a CO_2-free system under 100% Argon atmosphere and the other part under 1% CO_2 /Argon atmosphere.

The CO_2-free system was used for basic studies of the redox reactions at higher pH values to avoid interference by carbonate complexation. The CO_2 was removed from the groundwater by bubbling it with Argon at pH 6. Investigations of the behaviour of Np(V) in the CO_2-free

system were carried out by batch experiments. NpO_2^+ was added to the groundwater yielding in neptunium concentrations of 0.5 to $1.5x10^{-4}$ mol/L. The experiments were done at pH values of 4, 6, 7, 8 and 9. To stabilise the pH values during the reduction 0.01 M buffer solutions of PES (pH 4), MES (pH 6), PIPES (pH 7) and TRIZMA (pH 8, 9) were used. Over a period of 82 days the absorption spectra of all solutions were taken in the wavelength range of 940 to 1040 nm at certain times to follow a change of the neptunium signal.

A dynamic experiment were carried with Np(V) in the Gohy 2227 groundwater and a column packed with a Gorleben near aquifer surface Pleistocene aeolian quartz sand. The set-up of the column experiments is explained in [11]. The columns are located in a glove box with inertgas atmosphere of 1 % CO_2 / 99% Argon, whereby the amount of oxygen is maintained below 10 ppm. This type of gas simulates mean anaerobic gorleben atmospheric conditions.
A pulse of 50 ml of sand-equilibrated Gohy 2227 groundwater with a neptunium concentration of 1 x 10^{-4} mol/L, pH-value of 7.6 and an initial ionic strength of 4.4 x 10^{-4} M passes through the column with a Darcy velocity of 3 x 10^{-4} cm/s. After the column the water was collected in different fractions and investigated by absorption spectroscopy.

The absorption spectra are recorded in 1cm quartz cuvettes by a Cary 5 spectrometer (VARIAN) via glass fibre optics.

Results and discussion

Redox behaviour at different pH-values

The reaction of neptunium in the Gohy 2227 groundwater were investigated spectroscopically at different pH values (4, 6, 7, 8 und 9) after certain time periods (few minutes to 83 days). For better evaluation and interpretation the experiments are performed under carbonate free atmosphere. Absorption spectra were taken in the wavelength range of 950 to 1020 nm. In Fig. 1, representative for each pH value, only the spectra at pH 8 are shown. The spectra are composed of one large absorption band for the NpO_2^+-ion at 980.4 nm and a weak absorption

band for the $NpO_2HA(I)$ at 989 nm, which can be recognized only as a shoulder. With increasing reaction time, the absorption of the NpO_2^+ as well as the $NpO_2HA(I)$ decreases. However, the shape of the spectra does not change and new absorption bands are not created. The decrease in the absorption of the neptunium species was observed for all investigated pH values.

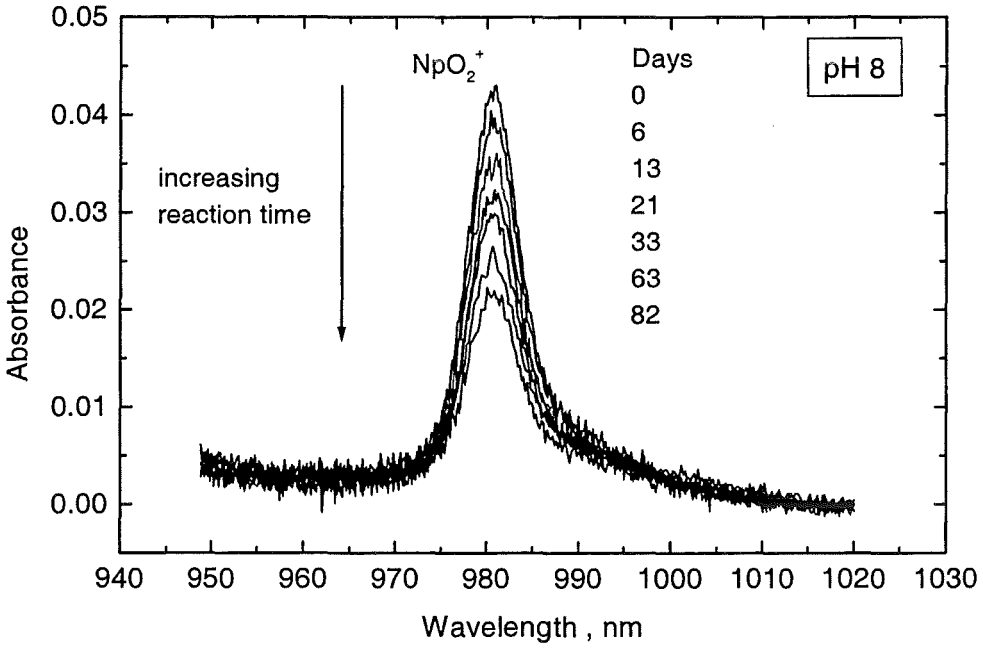

Fig. 1: Change of the absorption spectra of $NpO2^+$ with reaction time in the carbonate-free Gohy-2227-groundwater at pH 8.

From the significant diminution of the NpO_2^+ absorption it is assumed that neptunyl ions react with components of the Gohy water resulting in species which show no or only very small absorption. An adsorption of the neptunium on the surface of the vessels can be excluded, because the total amount of neptunium keeps constant in solution within the error margins of a liquid-liquid scintillation counting.

As mentioned before humic substances show reductive properties and are able to reduce metal ions. By comparison of the normal redox potential of the reduction of Np(V) to Np(IV) (E_0 = -0.79 V) and oxidation of HA_{red} to HA_{ox} (E_0 = 0.5-0.7 V [12,13]), where the latter are

synonyms for reduced and oxidized form of the humic substances, a reduction reaction is conceivable. From these facts it is assumed that a diminution of the absorbance of NpO_2^+ is correlated to the reduction of it. If tetravalent neptunium is produced, it reacts stronger then the pentavalent neptunyl cation with humic substances, even after acidifying the solution [14].

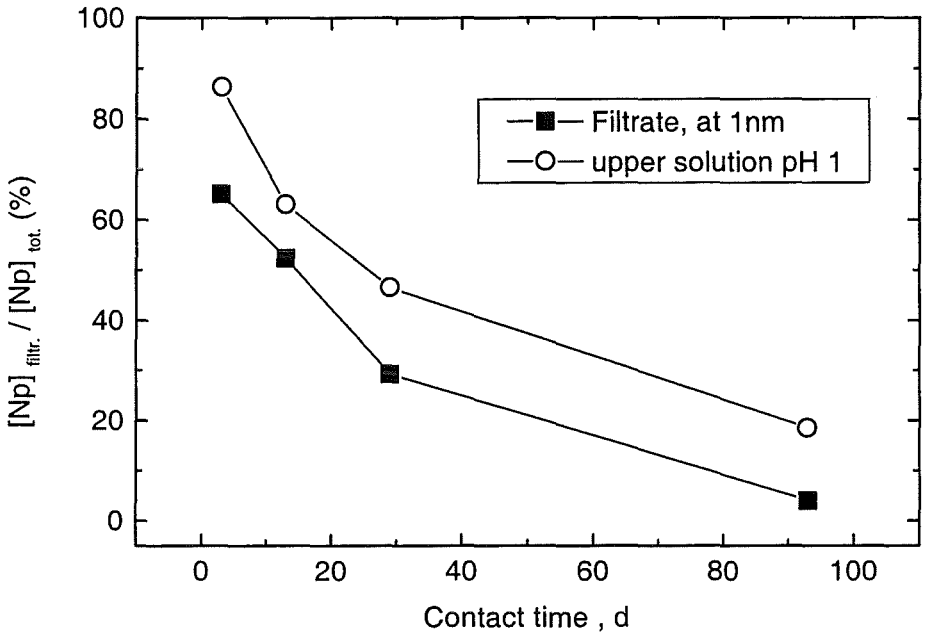

Fig. 2: Temporal alteration of neptunium concentration in Gohy 2227 groundwater in the filtrate of 1 nm pore size ultrafiltration and in solution after precipitation of the humic acid at pH 1.

With ultrafiltration experiments it can be shown, how much of the neptunium is bound to the humic substances. Almost all humic substances can be removed from the Gohy-2227 water by means of ultrafiltration with a membran of 1000 Dalton cut-off (Pallfiltron). As a consequence the neptunium bound to the humic will follow the humic fraction and can also be separated. In such an ultrafiltration experiment a increase of neptunium removeable at 1 nm and hence a decrease of neptunium in filtrat is observed with a simultaneously decrease of the spectroscopic absorption of NpO_2^+. This is illustrated in Fig.2. If such a solution is acidified to pH 1, the humic acid precipitates and settled down together with humic acid-bound neptunium. The amount of non bound neptunium in ionic form is found in the solution above the precipitate. The concentration of free neptunium in solution decreases parallel to that in

the filtrat of the previous ultrafiltration experiment. The difference between both is attributed to the fulvic acid bound neptunium which remains soluble at pH 1. The neptunium precipitated at pH 1 increases from 14% to 81% and the 1 nm filterable neptunium from 31% to 96%.

As tetravalent cations absorb very strong on humic substances and desorb weakly at low pH values in contrast to pentavalent oxy-cations, the ultrafiltration results point out, that NpO_2^+ is reduced to Np^{4+} in the used humic containing groundwater. This reduction of NpO_2^+ was confirmed by separation of tetravalent Np by means of liquid-liquid extraction with TTA for Gohy 2227 and by absorption spectroscopy, where the concentration of protons were extremely raised by means of gaseous HCl. At these conditions a Np(IV) humate complex should not be stable and neptunium exist as a Np^{4+} cation. The spectrum without HCl exhibits only the basic spectrum of the humic substances without significant characteristics. After saturation with gaseous HCl two absorption bands of Np^{4+} emerge, at 723 nm and 960 nm and the absorption of the humic substances disappears due to the precipitation of them [15]. Although it is known that NpO_2^+ disproportionates at low pH to Np^{4+} and NpO_2^{2+}, the disproportionation can be neclected, because the reaction kinetic is slow compare to the time which is need for the experiment.

From the absorption spectra recorded at pH 4 to 9 the concentration of free NpO_2^+ and $NpO_2HA(I)$ were calculated according to the method described in our previous publication [9]. The results are illustrated in Fig. 3 and the corresponding values of certain species concentrations are listed in table 1. The neptunyl concentrations ($[NpO_2^+]$) are normalized to the free neptunyl concentration at the beginning of the reaction ($[NpO_2^+]_{t=0}$) and the ratio log $[NpO_2^+]/[NpO_2^+]_{t=0}$ is plotted against the time. In this picture the slowest reaction takes place at pH 7 and by going to higher (pH 9) and lower (pH 4) values the reaction rates increase, whereas the reduction is faster at pH 9 than at pH 4.

The humic substances belong to a class of molecules which are in general inadequatly characterised with respect to their structure and functional groups. This include the mechanisms of redox processes and the question which groups in the molecules are involved

in the reduction process. If we visualize how many functional groups of the humic substances enables any reduction processes [1], one can suppose that the observed kinetic is the sum of many different kinetics. Therefore, the observed reaction represents more an empirical than a mechanistic reaction rate. Only if any reducing group dominates over all others, we have a chance to describe the rate with simple mathematics like the humate complexation of actinides. Such groups might be the quinones/hydroquinones. Studies of the reducing properties of natural quinones show, that they have a redox potential between 0.3 and –0.4 V in the pH range 0 to 12 and are capable as reducing agents [16]. The reducing mechanism depends in a very complicated way on the pH value. With the pH the quinones forms different protonated and deprotonated species which are involved in the reaction process and as a result the number of involved electrons vary between 2 and 4 [16]. Besides the quinoidic groups other groups can also act as reducing species. Additionally, the Gorleben groundwater is a complex mixture of different components of organic and inorganic components, where the Fe(II) ion must be mentioned.

However, a first attempt was made to plot the data as a reaction of first order with respect to neptunium ($\log([NpO_2^+]/[NpO_2^+]_{t=0})$ against the reaction time (Fig. 3). In the beginning the curves for each pH value are not linear and obey not a first order kinetic, but after 20 days it seems that the curves change to a linear relationship. A first approximation can be made to calculate rate constants in this range resulting in the following experimental first-order rate constants K_{obs}:

pH value	rate constant K_{obs} : x $10^{-4}(h^{-1})$
4	1.4 ± 0.14
6	1.9 ± 0.23
7	1.62 ± 0.086
8	3.23 ± 0.069
9	6.3 ± 0.28

It is obvious that the rate constants increase from pH 7 to 9, whereas at pH values lower than 7 similar values are obtained. Due to the complexity of the Gorleben water and the humic substances, the reaction rate can not be elucidate in detail from this experiment. But

nevertheless, the rate of the reduction reaction is very small and is in the magnitude of order found for the reduction rate of Np(V) to Np(IV) in presence of citric acid [17]

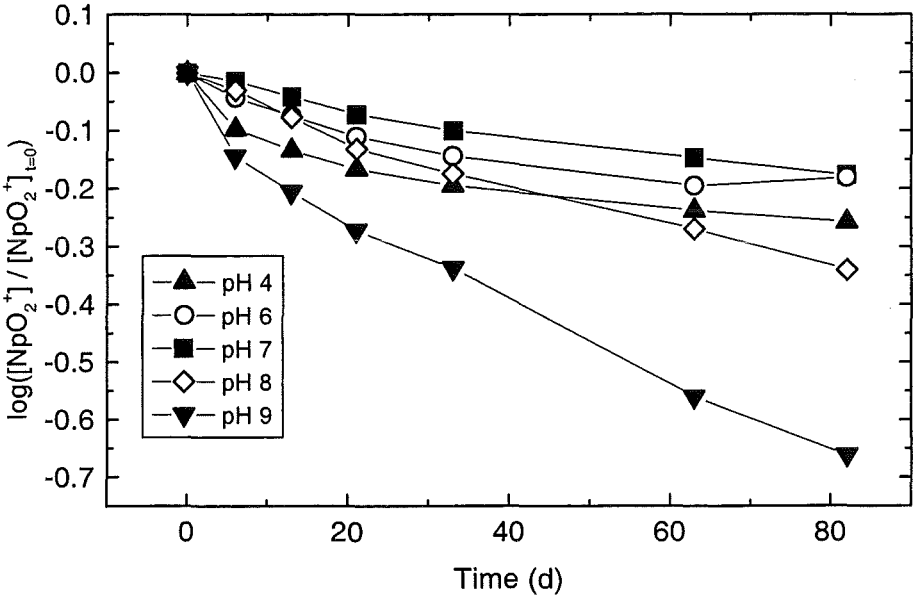

Fig. 3: Normalized free Np(V) concentration log $[NpO_2^+]/[NpO_2^+]_{t=0}$ as a function of time in carbonate-free Gohy 2227 groundwater sample at different pH

Influence of the reduction reaction on the Np(V) humate complexation

Parts of the neptunium(V) in the groundwater is complexed by humic substances. Now the question arises if the reduction process of Np(V) has an influence of the NpO_2^+ humate complexation reaction. It`s conceivable that the partly oxidized humic molecules have other complexing properties than the original HA. On the other side, the newly formed Np(IV) might block binding sites of the HA molecule, because it interacts much stronger with humics than NpO_2^+. From the spectra the amount of NpO_2^+ and $NpO_2HA(I)$ can be calculated by a peak deconvolution according to the method described in our previous papers [9,18]. The

concentrations of all species are summarized in table 1. The complexation constant β is calculated by

$$\beta = \frac{[NpO_2HA(I)]}{[NpO_2^+]([HA(I)]_t \cdot LC - [NpO_2HA(I)])} \qquad (2)$$

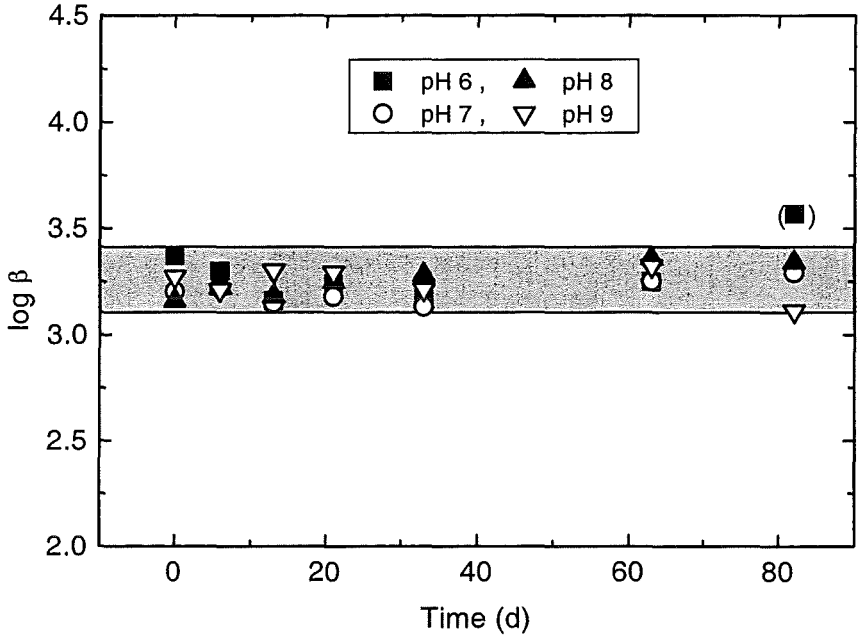

Fig. 4: Calculated complexing constants log β of the Np(V) humate complexation in Gohy 2227 groundwater at different pH values as a function of contact time.

with loading capacities LC picked up from [9,18]. In Fig. 4 and Table 1 the calculated log β values are shown. However, the log β values remain constant within the error margins for every pH value and over the examined time period of 83 days and a grand average value of 3.23 ± 0.03 is obtained. It is supposed that the complexation of NpO_2^+ by the humic acid is not considerably influenced by the reduction process, although the humic acid is partly oxidized and the concentration of the complexing groups of the humic acid might be diminished by complexation of tetravalent Np(IV). The contribution of Np(IV) humate in this

experiment is smaller than the actual free humic acid concentration, which is available for the Np(V) complexation process.

By comparing the values of log β with values obtained with extracted Gorleben humic and fulvic acid Gohy 573 (log β(HA) = 3.58, log β(FA) = 3.53), these values are 0.2-0.3 units higher than the values determined in this work. The reason might be higher metal loading (calcium, iron) of the humics remaining in the groundwater resulting in a lower loading capacity compare to isolated and purified humic substances. But the differences are not dramatic compare with the heterogeneity of the humic substances.

Influence of divalent and trivalent iron cations on the Np(V) reduction

Iron is an ubiquitous component of significant concentrations in natural waters. In the following experiments the influence of Fe^{3+} ions on the Np(V) reduction in Gohy 2227 groundwater is shown. To a solution of carbonate-free groundwater 1 x 10^{-5} and 5 x 10^{-6} M Fe^{3+} and subsequently NpO_2^+ were added. To avoid hydrolysis of the Fe^{3+} the pH was adjusted to 6. At certain times the absorption spectra were taken in the wavelength range 950-1020 nm and from the absorbance the concentration of NpO_2^+ was calculated. In Fig. 5 the ratio log $[NpO_2^+]/[NpO_2^+]_{t=0}$ is plotted in dependence on time for the experiment with and without adding Fe^{3+}. In presence of the Fe^{3+} ions, the concentration of NpO_2^+ decreases with time, but compare to the experiment without adding iron, the kinetic is faster.

No distinction is observed for the two different ferric concentrations, ergo the reaction is independent of the Fe^{3+} concentration in this concentration range. 7.9 and 7.6 x 10^{-5} mol/L Np(V) were reduced in presence of ferric ions in this experiment, whereas without adding Fe^{3+} only 3.8 x 10^{-5} mol/L was changed. It is assumed from this observation, that the ferric ions interfere the reduction reaction. From literature [12,19] it is known, that ferric ions are reduced to ferrous ions by humic substances, which can reduce NpO_2^+ in a subsequent reaction. If we suppose that all of the added ferric ions (1 x 10^{-5} und 5 x 10^{-6} M) are reduced to Fe^{2+}, only equivalent concentrations of Np(V) can be reduced for a one electron reduction mechanism [20]. In the present experiment more than the seven-fold amount of reduced Np(V) was yielded. Only when the ferric ions act as catalysts in a cyclic reaction mechanism,

as proposed in Fig. 6, a higher turnover can be expected. In details the reduction consist first of the reduction of Fe^{3+} to Fe^{2+} by humic acid and second the subsequent reduction of NpO_2^+ to Np^{4+} by Fe^{2+}.

In order to prove the reduction of Np(V) in presences of ferrous ions, a second experiment was performed. Therefore Fe^{2+} and Np(V) were added to a Gohy 2227 groundwater resulting in concentrations of 1 x 10^{-4} mol/L and 2 x 10^{-4} mol/L, respectively. The absorption spectra of the solution were taken at certain times in the wavelength range 940 to 1020 nm in order to determine the NpO_2^+ concentration.

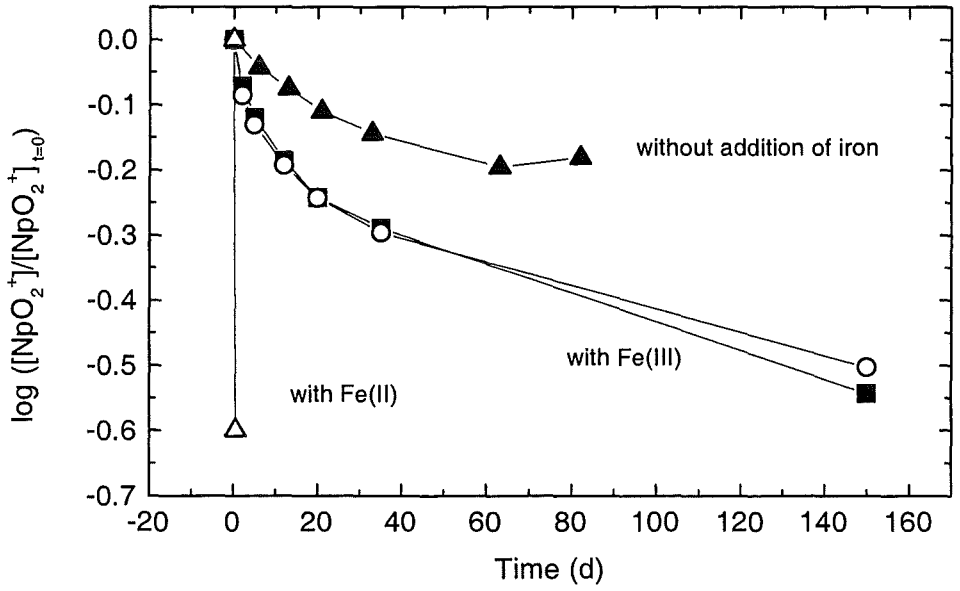

Fig. 5: Normalized free NpO_2^+ concentration against the contact time of Np(V) in Gohy 2227 ground water without addition of iron, in presence of ferric (1 x 10^{-5} und 5 x 10^{-6} M) at pH 6 and ferrous iron (1 x 10^{-4} M) at pH 7.6.

In Fig. 5 the result of the experiment is shown in dependence upon the time. The reaction kinetic is very fast and already after minutes the reduction is observed and after one day no pentavalent neptunium is detectable by absorption spectroscopy. The kinetic is much faster than for reactions in absence of Fe^{2+} ions. From this experiment, the assumption, that the

reduction of Np(V) can be achieved and accelerated by Fe^{2+} is confirmed. Additionally, it shows that the reduction of NpO_2^+ by humic acid only is much slower.

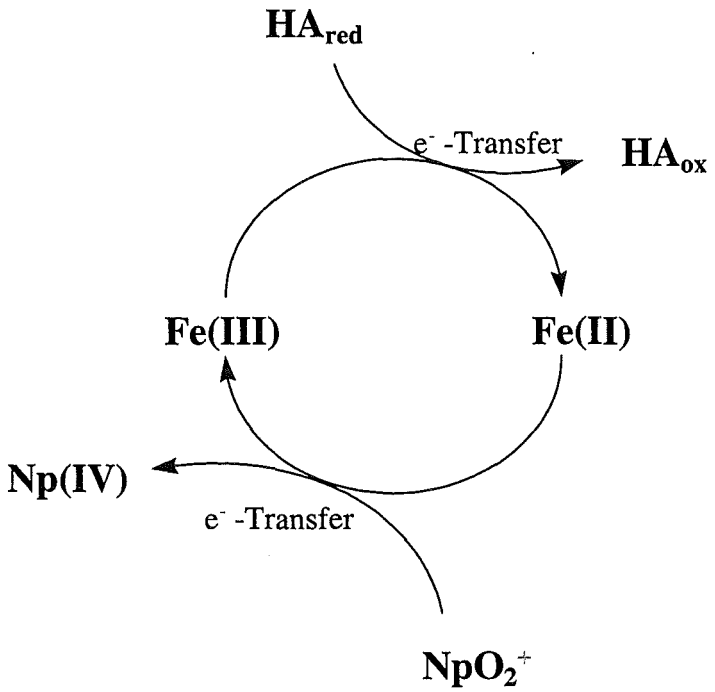

Fig. 6: Possible reaction cyclus of the indirect reduction of Np(V) by humic acid in presence of Fe(III).

Redox behaviour in a migration experiment

In order to assess the migration behaviour of Np(V) a column experiment was performed under repository relevant and natural-like conditions. For that a solution of 9.2×10^{-5} mol/L Np(V) in a Gorleben sand equilibrated Gohy 2227 groundwater was prepared under 1% CO_2 / 99% Argon atmosphere. The spectroscopic characterisation of this solution results in three species, the free NpO_2^+ ion, the neptunium(V)monocarbonato complex ($NpO_2(CO_3)^-$) and Np(V)-humate. 50 ml of this neptunium(V) spiked groundwater passed a column which was thightly packed with a Gorleben sand. The other part of the solution was stored in a vessel without contact to the sediment and investigated by absorption spectroscopy at certain times (up to 25 days).

After passing the column the solution was collected in several fractions. The residence time of the solution in the column was about 15 h. The fraction with the highest neptunium concentration was characterized spectroscopically and compared with the results obtained for the solution, which had no contact to the sediment. Beside the spectra taken at 940 – 1020 nm to identify the absorption bands for NpO_2^+ (980.4 nm) and Np^{4+} (960 nm), the wavelength range 650 – 780 nm was investigated. In this range another absorption band of the free Np^{4+} is usually found at 723 nm. The spectra are shown in Fig. 7. After flowing through the column the absorption spectra of the solution has changed dramatically in the range of 940 to 1030 nm. The strong absorption bands at 980 and 992 nm disappear and a weak absorption band is recognized with a maximum at 986 nm and a width which is larger than of the original absorption bands of the 3 species (Fig. 7). The original species of pentavalent neptunium are no more detectable, although the total concentration of neptunium in solutions was 2.85×10^{-5} mol/L . In contrast to this, the solution which was not in contact with the sediment shows no significant change after the first 4 days. Only after 25 days the absorption bands of the pentavalent neptunium species are diminished considerably, but they are still observable.

The kinetic of the neptunium(V) reduction is accelerated in presence of the sediment. In the wavelength range 650 - 780 nm a new absorption band is formed after the reaction, which is illustrated in Fig. 7. The shape of these absorption curve suppose the superposition of several indiviual absorption bands. The characteristics of these absorption curve is a absorption maximum at 742 nm with a shoulder at 723 nm. One can suppose that the absorption is caused by Np(IV) species, like hydrolysis products, mixed humate complexes as well as carbonate complexes and colloids. These species couldn´t been related to individual characterisitic of the spectrum up to now. If we compare qualitatively the absorption spectra of both solutions in this range (with and without sediment contact) after different reaction times of one day in the column and 3 weeks in solution only, one cannot see any significant distinction in the shape of the curves. For better comparison the absorbances of both spectra are adjusted and a quantitative assertion is not possible. Despite different reaction kinetics and mechanisms the spectra are similary and it is supposed, that it is obtained the same species distribution of the tetravalent neptunium.

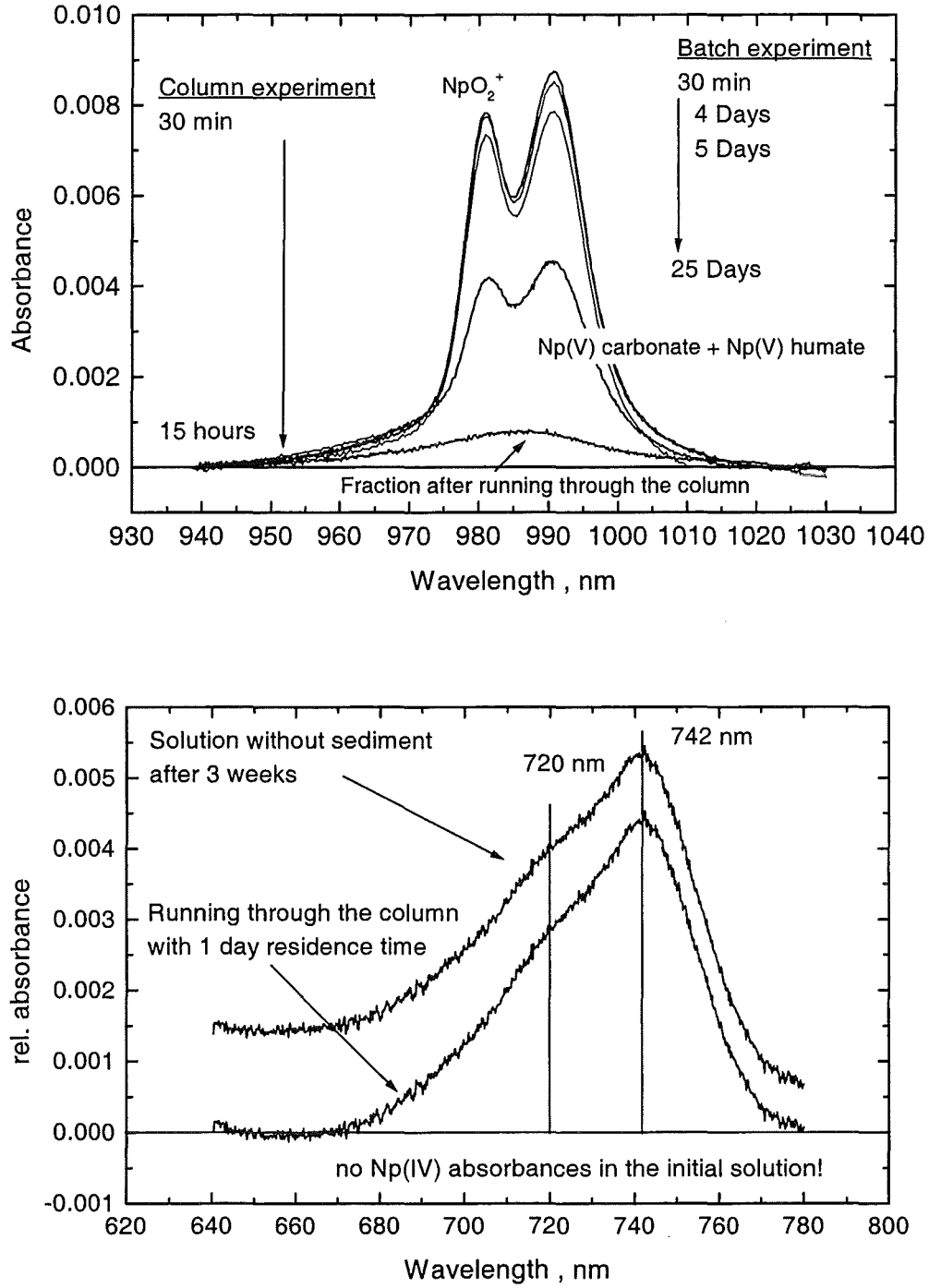

Fig. 7: Temporal alteration of Np(V) spectra in sediment equilibrated Gohy 2227 ground water in two wavelength ranges. For explanation, see text.

It remains to be explained, why Np(V) is reduced faster in the column as in solution only. The batch experiments already exhibits, that the reduction rate is enhanced by the presence of Fe^{2+}. It´s obvious to hold the iron on the sediment surface responsible for the acceleration. The

mean iron content of the total sand was determined to 0.1 atom-% by x-ray fluorescence analysis. More important than the total content of the sand is the element composition on the surface of the sand, where the reaction takes place. This surface consist of 2.6 atom-% Fe, which is a factor 20 more than referring to the total composition. The sand equilibrated groundwater has got a remarkable ferrous content of 41 x 10^{-6} mol/L. During the contact of the water with the sediment iron will always be leached, which is under anaerobic conditions stable as Fe^{2+} and can act as reducing agent for Np(V). Usually Fe(II) complexes are stronger reducing agents than free Fe^{2+}. If ferrous ions are complexed by humic acid, it can be assumed that the reduction potential is enhanced, which is known from the literature for citric acid, EDTA and other oxygen donor complexing molecules [21]. Additionally, the iron on the surface itself of ferrous oxides is a stronger reducing component. From these facts all feasibilities are given from the chemistry of iron and humic substances in natural groundwater systems to reduce the pentavalent neptunium into the tetravalent state.

From the fractions collected after passing the column 95 % of the total neptunium concentration is separated by ultrafiltration with 1 nm pore size filters and only 5 % is found in the filtrate. Because almost all of the humic acids are filtered at 1 nm filter pore size, we conclude that the neptunium is bound to the humic acid fraction. To confirm this assumption tetravalent neptunium (Np^{4+}, 3.9 x 10^{-5} or 1.3 x 10^{-4} mol/L) was added to an acidified carbonate-free Gohy 2227 groundwater. The solution was subsequently neutralized by adding carbonate-free NaOH and filtered through membranes with 1nm and 400 nm pore sizes. It is observed a remarkable separation of the neptunium with increasing pH at pore size of 1 nm (Fig. 8), which corresponds to a sorption of neptunium to humic colloids. In difference to pentavalent neptunium, which interacts only weak with humic colloids, tetravalent neptunium is bound to 84 % to the colloid at pH 2.4. Below pH <4 the humic acids remains insoluble and are settled down on the bottom of the vessels. These large particles can also be removed by filtration with 400 nm pore size membranes. After the dissolution of the humic acid at pH values >4, no neptunium is filtered with 400 nm but is still removed with 1 nm almost quantitatively. This drastic change in the behaviour corresponds to a decrease in the particle size of the humic colloid due to the dissolution and the neptunium remains to be bound on the colloid.

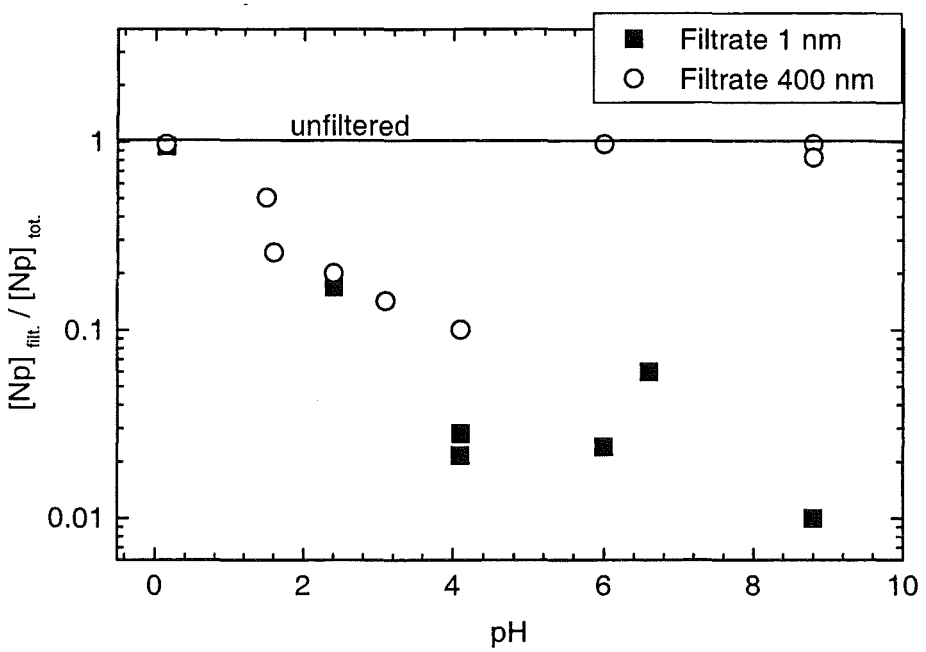

Fig. 8: Relative Np concentration in filtrates (at 1nm and 400 nm pore sizes) of Np(IV) (3.9×10^{-5} or 1.3×10^{-4} mol/L) in Groundwater Gohy 2227 as a function of pH.

Summary and Conclusions

The experiments have clearly illustrated that pentavalent neptunium is reduced to tetravalent neptunium in Gorleben groundwater Gohy 2227. Due to the reduction, the speciation of the neptunium changes from predominant ionic form (NpO_2^+, $NpO_2CO_3^-$) to totally humic colloid bound form. The kinetic of the reduction reaction is pH dependent and the description of it is not solved. The difficulties arise from the fact that on the one hand probably different groups of the humic substances could reduce the neptunium and on the other hand other components of the groundwater might reduce the neptunium. This results in superposed kinetics, which change with time depending on the individual concentration of the each component. For the neptunium(V) reduction the description may be possible by means of multicomponent models, how one can find in the literature for first approaches [22], but which must be developed further for the Gohy-2227 and neptunium. Hereto, more experiments are necessary.

Finally, it must be mentioned, that a solution containing 160 mg L^{-1} (= 80 mg DOC L^{-1}) of a isolated and purified Gohy 2227 humic acid [15] showed no reduction of Np(V) to Np(IV).

The separation and purification of humic acid may destroy the reducing groups, because the method is usually performed in alkaline solutions under air atmosphere and reductive hydroquinone and aldehyde groups lose their cabability to reduce metals.

Table 1: Concentrations of Np(V) and Np(V) humate (NpHA) determined spectroscopically with the corresponding stability constants log β as a function of time. (All concentrations in mol/L). At pH 4 neptunium humate is not detectable.

	pH 4	**pH 6**			**pH 7**			**pH 8**			**pH 9**		
Time (d)	$[Np(V)_{free}]$	$[Np(V)_{free}]$	[NpHA]	log β	$[Np(V)_{free}]$	[NpHA]	log β	[Np(V)-frei]	[NpHA]	log β	[Np(V)-frei]	[NpHA]	log β
0	1.10E-04	1.10E-04	1.21E-05	3.37	1.08E-04	1.50E-05	3.20	9.80E-05	2.33E-05	3.16	4.84E-05	2.80E-05	3.24
6	8.78E-05	9.92E-05	9.83E-06	3.30	1.05E-04	1.52E-05	3.22	9.14E-05	2.44E-05	3.22	3.47E-05	1.80E-05	3.18
13	8.08E-05	9.24E-05	6.96E-06	3.16	9.85E-05	1.24E-05	3.15	8.20E-05	2.07E-05	3.18	3.01E-05	1.93E-05	3.27
21	7.49E-05	8.51E-05	7.74E-06	3.24	9.19E-05	1.24E-05	3.18	7.24E-05	2.13E-05	3.25	2.58E-05	1.64E-05	3.26
33	7.01E-05	7.87E-05	6.22E-06	3.17	8.61E-05	1.05E-05	3.13	6.56E-05	2.07E-05	3.28	2.22E-05	1.19E-05	3.18
63	6.35E-05	6.99E-05	6.57E-06	3.25	7.72E-05	1.22E-05	3.25	5.27E-05	2.00E-05	3.36	1.33E-05	9.22E-06	3.29
82	6.08E-05	7.22E-05	1.26E-05	3.57	7.22E-05	1.26E-05	3.29	4.48E-05	1.68E-05	3.34	1.05E-05	4.52E-06	3.08
$\log \beta_{mean}$	-	3.25 ± 0.08			3.20 ± 0.06			3.25 ± 0.08			3.21 ± 0.08		

References

[1] Stone, A.T., Godtfredsen, K.L., Baolin Deng, in G. Bidoglio and W. Stumm (eds.), *Chemistry of Aquatic Systems: Local and Global Perspectives,* p. 337 (1994)

[2] Nash, K., Fried, S., Friedman, A.M., Sullivan, J.C., Redox Behavier, Complexing, And Adsorption Of Hexavalent Actinides By Humic Acid And Selected ClaysEnviron; Sci. Techn., **15**, 834 (1981).

[3] Choppin, G.R., Humics and Radionuclide migration, Radiochim. Acta, **44/45**, 23 (1988).

[4] Yaozhong, C., Bingmei, T., Zhangji, L., A kinetic study of the reduction of Np(VI) with humic acid, Radiochim. Acta **62**, 199 (1993)

[5] Jianxin J., Yoazhong C., Zhangji L., A kinetic study of the reduction of plutonium with humic acid, Radiochim. Acta **61**, 73 (1993).

[6] Marquardt, C., Herrmann, G., Trautmann, N.: Complexation of Neptunium(V) with Humic Acids at Very Low Metal Concentrations, Radiochim. Acta, **73**, 119-125 (1996).

[7] Kim, J.I.: Chemical behaviour of the transuranic elements in natural aquatic systems, in A.J. Freeman, C. Keller(Eds.): *Handbook on the Physics and Chemistry of the actinides*, Elsevier 1986, Band 5, p. 413

[8] Choppin, G.R., Allard, B.: Complexes of actinides with naturally occuring organic compounds, A.J. Freeman, C. Keller (Eds.*): Handbook on the Physics and Chemistry of the actinides*, Elsevier 1986, Band 3, p. 407

[9] Marquardt, C., Kim, J.I.: Complexation of Np(V) with Humic Acid: Intercomparison of Results from Different Laboratories, Radiochim. Acta **80**, 129 (1998).

[10] Hagan, P.G., Cleveland, J.M., The Absorption Spectra of Neptunium Ions in Perchloric Acid Solution, J. inorg. nucl. Chem. **28**, 2905 (1966)

[11] Artinger, R., Kienzler, B., Schüßler, W., Kim, J.I.: Effects of humic substances on the ^{241}Am migration in a sandy aquifer: column experiments with Gorleben groundwater/sediment systems, accepted for publication in J. Contam. Hydrol. 1998

[12] Skogerboe, R.K., Wilson, S.A.: Reduction of Ionic Species by Fulvic Acid, Anal. Chem. **53**, 228 (1981).

[13] Matthiessen, A.: Evaluating the redox capacity and redox potential of humic acids by redox titrations; in Senesi, N. and Miano, T.M., Eds.*: Humic Substances in the Global Environment and implications on Human Health*, S.187, Elsevier Science B.V. 1994.

[14] Kim, J.I., Zeh, P., Delakowitz, B.,: Chemical Interaction of Actinide Ions with Groundwater Colloids in Gorleben Aquifer Systems, Radiochim. Acta **57/58**, 147 (1992).

[15] Zeh, P., Kim, J.I.: Chemische Reaktionen von Aktiniden mit Grundwasser-Kolloiden, Report RCM 00994, TU München 1994

[16] Petrova, S.A., Kolodyazhny, M.V., Ksenzhek, O.S.: Electrochemical properties of some naturally occuring quinones; J. Electroanal. Chem. **277**, 189-196 (1990).

[17] Reed, D.T., Wygmans, D.G.., Aase, S.B., Banaszak, J.E., Radiochim. Acta **82**, 109 (1998)

[18] Marquardt, C., Kim, J.I., Complexation of Np(V) with Fulvic Acid, Radiochim. Acta **81**, 143 (1998)

[19] Deiana, S., Gessa, C., Manunza, B., Rausa, R., Solinas, V.: Iron(III) reduction by natural humic acids: a potentiometric and spectroscopic study, European J. Soil Science, **46**, 103 (1995).

[20] Cohen, D., Fried, S., Inorg. Nucl. Chem. Lett., **5**, 653 (1969)

[21] Stumm, W., *Chemistry of the Solid-Water* Interface, John Wiley and Sons, New York (1992), p. 312.

[22] Wittbrodt, P.R., Palmer C.D.: Reduction of Cr(VI) in the Presence of Excess Soil Fulvic Acid, Environ. Sci. Technol. **29**, 255 (1995)

Annex 2

Kinetic Aspects of Metal Ion Binding to Humic Substances

(Geckeis et al., FZK/INE)

2nd Technical Progress Report

EC Project:

"Effects of Humic Substances on the Migration of Radionuclides: Complexation and Transport of Actinides"

Project No.: FI4W-CT96-0027

FZK/INE Contribution to Task 3 (Actinide Transport)

Kinetic Aspects of the Metal Ion Binding to Humic Substances

H. Geckeis, Th. Rabung, J.I. Kim

Forschungszentrum Karlsruhe GmbH, Institut für Nukleare Entsorgungstechnik, P.O.Box 3640, D-76021 Karlsruhe, Germany

1. Introduction

The relevance of humic colloid mediated transport of radionuclides from a nuclear repository to the biosphere strongly depends on the kinetic properties of the nuclide binding to colloidal species. Recent investigations have shown that the migration behaviour of actinides in column experiments can not be described by a thermodynamic equilibrium approach but kinetically governed processes need to be regarded [1]. Earlier investigations on the dissociation kinetics of actinide humate complexes have been published by Cacheris and Choppin [2]. They determined dissociation rates for thorium humate by using a competing ligand as a function of pH (pH<6) and temperature. Slowest rates were found to lie in the range of 10^{-3} min^{-1}. The authors interpret their experimental results by postulation of different thorium species bound either in the interior of a coiled humic colloid structure or bound to peripheral binding sites showing slow and fast dissociation kinetics, respectively. It was also shown that with increasing equilibration time, thorium becomes less available. This is interpreted as migration of the metal ion into the interior of the humic macromolecule. Similar experimental observations have been made during the investigation of the influence of humic acid on the sorption reaction of Eu(III) [3, 4].

For the purpose of application of above discussed findings from laboratory investigations to the real system, however, there are several uncertainties:

- Experimental results obtained with purified humic acid under laboratory conditions might not be valid for natural conditions.
- Concentrations of metal ions studied may not be relevant for the real system.
- Predictions on the basis of short term laboratory experiments might not be relevant for long term migration processes in a natural aquifer system.

2. Objectives

The aim of the present work is to investigate the dissociation kinetics of actinide ions and their chemical homologues by the Chelex batch technique [5, 6, 7]. A chelating cation exchanger is used to scavenge dissociated ions of (1) Eu(III) complexed with purified humic acid as a function of the equilibration time; and (2) actinides and actinide homologues which are constituents of natural non-purified humic colloids in groundwater. The groundwater samples originate from the Gorleben aquifer system. Dissociation rates are measured and used to compare the dissociation behaviour of "laboratory" and "real" systems.

3. Experimental

"Laboratory" system

A solution (pH=8.0, buffered with 1 mmol/L Tris, ionic strength: 0.1 mol/L $NaClO_4$) with purified Aldrich humic acid (30 mg/L) and Eu(III) ($1 \cdot 10^{-6}$ mol/L) was prepared under aerobic conditions. After different equilibration periods (1 h; 1 d; 1 w; 6 w) the purified chelating cation exchanger (Chelex 100) was added (5.5 g /L). The functional groups of the resin are imino diacetic acid bound to a polystyrene back-bone and the exchange capacity amounts to 2.0 meq/g dry weight. After different time periods, the resin is sedimented by centrifugation and the supernatant solution is analysed by ICP-mass spectrometry (Perkin-Elmer; Elan 6000).

"Natural" system

Two natural groundwaters from the Gorleben aquifer system (Gohy-532 and -2227) are studied. For the purpose of this investigation, the most important difference between these groundwaters are their concentrations of dissolved organic carbon (DOC), namely 29.9 and 81.9 mgC/L, for Gohy-532 and -2227, respectively (Shimadzu; TOC 5000). More detailed information on chemical and physico-chemical properties of these groundwaters can be found in ref. [8]. Throughout the experiments, the groundwater samples were handled under inert gas atmosphere (Ar + 1% CO_2). pH values were 8.9 and 7.7, for Gohy-532 and -2227, respectively. Sampling of supernatant solution (cf. above) was conducted after contact time between 1 and 105 days.

4. Results and discussion

In principle the following reactions, their kinetics and the final equilibrium need to be regarded for application of the chelex method:

$$M^{x+} + Chelex \longleftrightarrow M - Chelex + xNa^{+} \qquad \text{Eq. (1)}$$

and

$$MHA_i \longleftrightarrow M^{x+} + HA_i \qquad \text{Eq. (2)}$$

where MHA_i represent kinetically different metal humate species.

It was shown that humic acid does not sorb significantly to the resin during the experimental period and that no degradadion of the resin occured. The Chelex resin is well separated from the solution by centrifugation and moreover the complexation constants of a variety of metal ions lie in the same order of magnitude as found for the humic acid. Therefore, the Chelex exchange method is not hampered by such experimental artifacts and thus is appropriate for the present investigations.

Measurement of the sorption kinetics of Eu(III) from an aqueous solution without humic acid (Fig. 1) shows a comparatively fast reaction with the Chelex resin (Eq.1). For evaluation of the results, therefore, the assocation kinetics of eq. (1) can be neglected. Compared to the metal ion concentration ($< 1 \cdot 10^{-6}$ mol/L), a large excess of Chelex exchanger is used (11 meq/L). Therefore, the backward reaction of Eq. 1 can be neglected and thus the Eu concentration in solution can be considered governed by the humic colloid bound fraction. Consequently, the decrease of Eu (or other metal ions) in solution can be used directly to evaluate the dissociation kinetics from humic colloids.

With respect to eq. (2), the overall dissociation kinetics is measured. Individual kinetic components could be interpreted as chemically different humic acid ligands. As has already been mentioned above, however, reorientation of the humic acid macromolecule or diffusion

of the metal ion into the interior of the humic colloid appears to be the more likely reason for different kinetic components.

"Laboratory " system

Results of the desorption experiments obtained for the Aldrich HA/Eu(III) system at pH=8.0 are shown in Fig. 1. The dissociation kinetics depends on both the contact time with the Chelex exchanger and the equilibration time of the Eu(III) with the humic acid prior to measurement of the dissociation [2]. In all experiments a similar Eu(III) concentration is reached after ca. 1000 h. In the absence of HA the Eu(III) concentration declines rapidly to below 5 % of the original concentration.

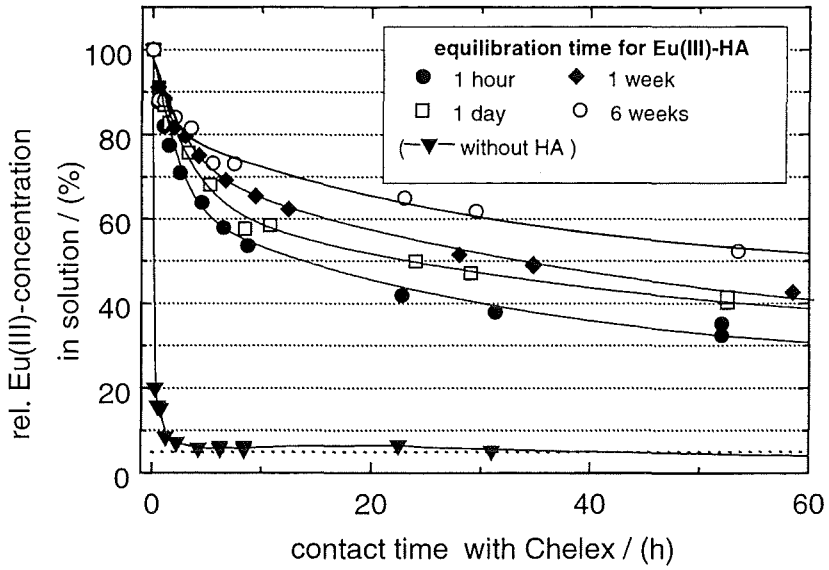

Fig. 1: Eu(III)-concentration in solution as a function of the contact time with Chelex exchanger and the equilibration period of the Eu(III)-humate complex ([HA] = 30 mg/L; [Eu(III)] = $1 \cdot 10^{-6}$ mol/L; pH=8.0; I=0.1 M $NaClO_4$). For comparison, the Eu(III) sorption kinetics on Chelex in the absence of HA is also shown.

The removal rate of Eu(III) from solution can be described by a pseudo-first-order kinetics (Eq.3), which has been also reported by different authors to be appropriate for other metal humate complexes [4, 5, 6, 7]. The postulation of at least two kinetically different Eu(III)-humate components is necessary to describe the experimental results:

$$Eu_{diss}(t)\,[\%] = Eu_{eq}\,[\%] + A_1 \exp(-t/\tau_1) + A_2 \exp(-t/\tau_2) \qquad \text{Eq. (3)}$$

$Eu_{diss}(t)$: dissolved Eu(III)-fraction as a function of time t [h]
Eu_{eq}: equilibrium concentration of Eu(III) in solution
A_1: fraction of Eu(III)-humate dissociating with a time constant τ_1 [%]
A_2: fraction of Eu(III)-humate dissociating with a time constant τ_2 [%]
τ_1, τ_2: time constants [h]

The results obtained by fitting the experimental data to the kinetic model (Eq.3) are listed in Tab. 1. The data suggest that (1) an equilibrium state for the Eu(III) in solution is attained at about 14 % of the originally present Eu(III) and (2) the time constants for the "fast" and the "slow" component remain the same for all equilibration times but that the fractions of Eu(III) in the respective kinetic modes change (Fig.2). With increasing equilibration time the Eu(III) moves from the "fast" to the "slowly" dissociating fraction.

Tab. 1 Fit parameters obtained by fitting experimental data to the kinetic equation Eq. (3). (Calculations were made using the Fit Routine of ORIGIN Vers. 4.1; errors correspond to the uncertinty of the fit calculation)

System	τ_1 [h]	A_1	τ_2 [h]	A_2	Eu eq [%]
Eu(III) –Aldrich Humic acid; Eq. Time = 1 h	4.6±0.5	49±2	139±19	32.6±2	12.8±1
Eu(III) –Aldrich Humic acid; Eq. Time = 24 h	4.6±0.4	41.7±2	141±10	42±1	13.1±0.8
Eu(III) –Aldrich Humic acid; Eq. Time = 168 h	4.7±0.6	33±2	115±9	50.7±2	12.5±0.8
Eu(III) –Aldrich Humic acid; Eq. Time = 1008 h	3.6±1	25±3	150±25	52.4	19±2

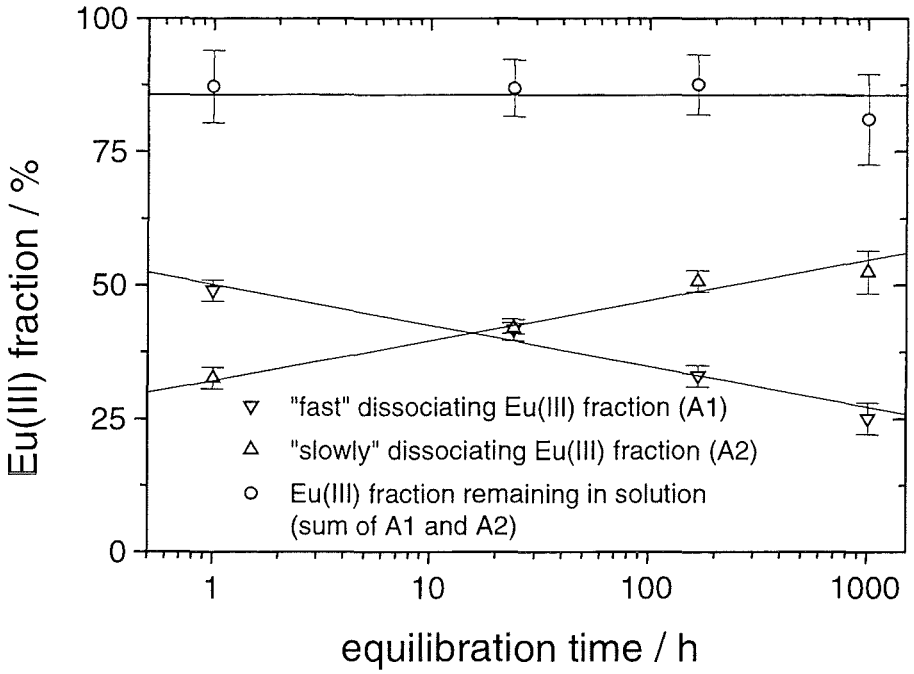

Fig. 2 Fractions of "fast" (A1) and "slowly" (A2) dissociating Eu(III) as a function of equilibration or ageing time of Eu(III)-humate

Findings from kinetic investigations by other authors are consistent with those from the present study. For the description of the Am(III) migration behaviour in the Gorleben groundwaters Gohy-532 and -2227 in column experiments with a sandy sediment, dissociation time constants in the same order of magnitude (τ_1=3 h, τ_2=250 h) are required for the parameterization of the kinetic model applied [1]. The ageing effect of Am(III)-humate and Eu(III)-humate on the dissociation behaviour is also found to be qualitatively the same. The slight differences might result from different properties of the non-alterated groundwater humic acid and the purified Aldrich humic acid. Both experiments – column experiments with natural groundwater and natural sand as well as batch experiments in a model system – show consistent kinetic effects as previously reported by Cacheris and Choppin [2] and Rao et al. [4]. Similar time constants have been also determined by Bryan et al. (separate contribution in the report).

The two kinetic components presumably reflect that after complexation of metal ions to the external humic acid functional groups, the availability for exchange will diminish with

increasing equilibration time due to (1) rearrangement of the metal-humate complex, (2) diffusion of the metal ion into the interior of the humic acid macrostructure and/or (3) formation of mixed organic/inorganic colloid species.

Due to restrictions in the experimental precision, it still remains unclear to which extent part of metal ions are bound in a fashion that they can be considered "irreversibly" bound to the humic colloids. Furthermore, for practical reasons the equilibration time and geochemical conditions prior to measurement of the dissociation kinetics in these laboratory experiments cannot reflect the natural situation. Therefore, direct investigations on natural humic colloids and their constituents are necessary.

"Natural" System

The experiments described above suggest an increase of the kinetic stabilization with increasing equilibration/ageing time of the Eu(III) humate over the entire experimental time span (upto 1000 h). In order to reflect the equilibration time span and chemical conditions in the real system, the desorption of the naturally occuring trace elements in Gorleben groundwater colloids are investigated by the Chelex method under near natural conditions. Chemical and physico-chemical parameters of the groundwaters can be found in [8].

The dissociation of the Th, Eu, U, Pb and Sr from the Gorleben-2227 humic colloids is shown in Fig. 3. The desorption kinetics of the individual elements reflect the element specific kinetic properties. The dissociation rates qualitatively follow the sequence Th < Eu < U < Pb < Sr and thus qualitatively follow their affinity to the humic acid. Quantitative statements, however, require knowledge of the equilibrium concentration for the individual metal species which presently are not known.

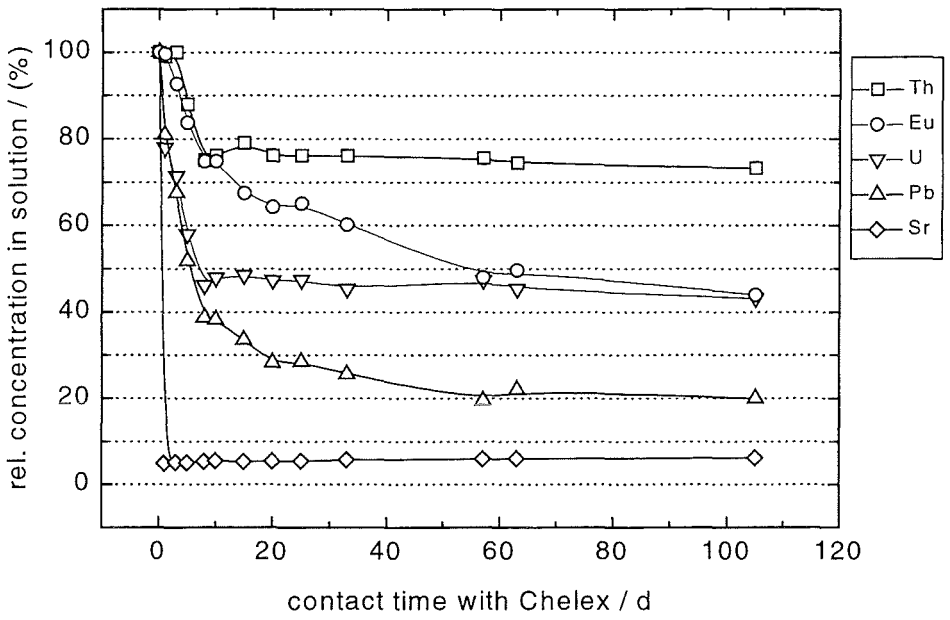

Fig. 3 Th-, Eu-, U-, Pb- and Sr-concentration dependency with time in groundwater Gohy-2227 after contact with Chelex (pH=8.1; Ar/1% CO_2 atmosphere).

A direct comparison of the dissociation rates of Eu(III) in the "laboratory" system with that in the "natural" system is shown in Fig. 4. Fitting of the experimental data to the kinetic equation Eq(3) result in time constants for the natural groundwaters which are higher by approximately one order of magnitude than observed for the Eu(III)-humate experiments using purified Aldrich HA (Gohy-2227: τ_1 = 140 h; τ_2=1200 h; Gohy-532: τ_1=70 h; τ_2=1200 h). In Fig. 4, these differences between the laboratory and real systems are visualized.

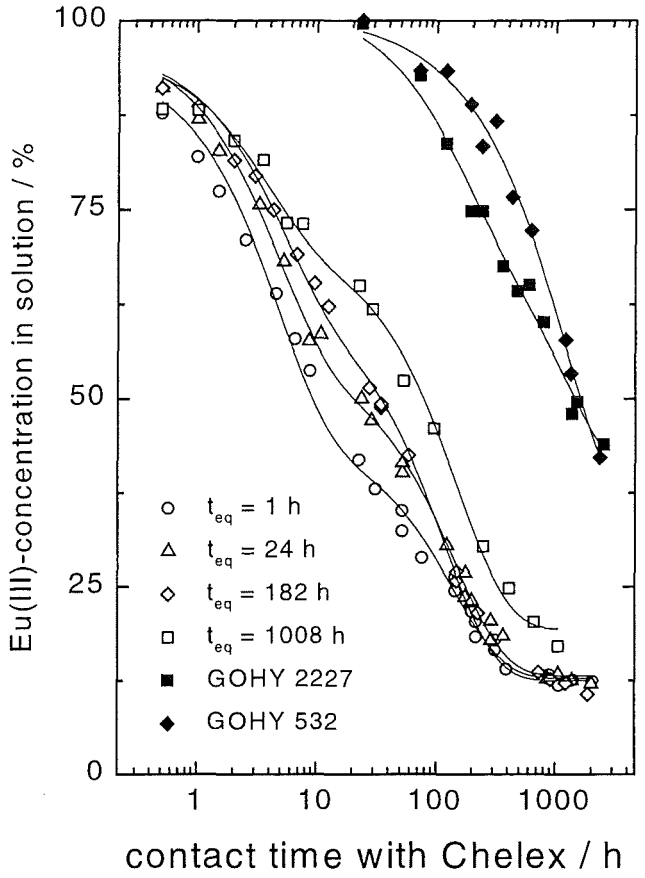

Fig. 4 Eu(III)-concentration in humic acid containing solutions as a function of the contact time with Chelex. Open symbols correspond to experiments with Aldrich HA and filled symbols to similar experiments with natural Gorleben groundwaters Gohy-532 and -2227.

5. Conclusions and Outlook

The dissociation of humic colloid bound metal ions is considerably kinetically hindered. Desorption rates of humic colloid bound actinides and homologues decrease with increasing equilibration time and the kinetic behaviour of naturally bound homologues is different from that of actinides freshly spiked to humic acid solution. Therefore, it can not be excluded that the kinetic behaviour of the actinides released from a repository might be very different from that observed in relatively short laboratory experiments.

In case of very slow dissociation kinetics related to the time scales required for the migration from the tentative repository to the biosphere, a part of the actinides might be transported unretarded through the geosphere. The presence of such an "irreversibly" bound fraction of actinides or homologues can only be estimated if the equilibrium concentration of the individual metal ion species in the experiments described above is known. Further investigations will concentrate on the determination of equilibrium concentrations by using isotopic exchange techniques. Furthermore, investigations on the exchange rates by isotope exchange under quasi-stationary conditions (constant metal ion loading) could be beneficial.

6. References

[1] W. Schüßler, R. Artinger, B. Kienzler, J.I. Kim in G. Buckau (edr.), Effects of Humic Substances on the Migration of Radionuclides: Complexation and Transport of Actinides; First Technical Progress Report, August 1998, Forschungszentrum Karlsruhe, FZKA 6124, p.91-103

[2] W.P.Cacheris, G.Choppin, Radiochim.Acta.42 (1987), 185-190

[3] Th. Rabung, Einfluß von Huminstoffen auf die Europium(III)-Sorption an Hämatit, Thesis, Universität Saarbrücken (1998)

[4] L.Rao, G.R.Choppin, S.B.Clark, Radiochim. Acta 66/67 (1994), 141-147

[5] Yanjia Lu, C.L. Chakrabarti, M. H. Back, D. C. Grégoire, W.H. Schroeder, Intern. J. Environ. Anal.Chem., 60 (1995), 313-337

[6] C.H.Langford, D.W.Gutzman, Analyt.Chim.Acta 256 (1992), 183-201

[7] W.Rate, R.G.McLaren, R.S.Swift, Environ.Sci.technol. 26 (1992), 2477-2483

[8] B. Artinger, B. Kienzler, W. Schüßler, J.I.Kim, Sampling and Characterization of Gorleben Groundwater/Sediment Systems for Actinide Experiments, in G. Buckau (edr.), Effects of Humic Substances on the Migration of Radionuclides: Complexation and Transport of Actinides; First Technical Progress Report, August 1998, Forschungszentrum Karlsruhe, FZKA 6124, p.23-43

Annex 3

The Characterization of a Fulvic Acid and its Interaction with Uranium and Thorium

(Davies et al., BGS)

2nd Technical Progress Report

EC Project:

"Effects of Humic Substances on the Migration of Radionuclides:
Complexation and Transport of Actinides"

BGS Contribution to Task 1 (Characterisation) and Task 2 (Complexation)

The Characterisation of a Fulvic Acid and its Interactions with Uranium and Thorium

Reporting Period 1998

J. Davis, J.Higgo, Y. Moore and C. Milne

British Geological Survey
Nottingham
NG12 5GG
United Kingdom

ABSTRACT

The transport of actinides via colloids is very important to the production of a performance assessment for a nuclear waste repository e.g. Kersting et al. (1999). Organic colloids in the form of humic substances (HS) could constitute a major pathway for the migration of actinides away from the repository to the biosphere. The greater the stability of the actinide-HS complex the longer the potential migration pathway.

BGS has continued with the laboratory experiments studying the interactions between U and Th and the Derwent Water-derived DE72 fulvic acid.

DE72 FA has now been fully characterised, with data supplied for proton and copper binding titrations. Two different experimental methods have been developed to study complexation properties of actinides with DE72 FA.

Conditional stability constants have been derived for thorium binding to DE72 fulvic acid and these are comparable to literature data.

Dissociation constants for thorium (IV) and the uranyl ion from DE72 FA have been obtained. After initial rapid dissociation the dissociation rates decrease to around 10^{-5} min^{-1}, for both uranium and thorium at pH between 6.5 –7.4. The most important controlling parameter appears to be length of preconditioning time, or 'ageing' of solutions.

1. INTRODUCTION

This section of the project aims to investigate the role which humic substances may play in the migration of radionuclides, by focussing on a fuller characterisation of DE72 Derwent fulvic acid and on the dissociation of complexed UO_2^{2+} and Th^{4+} from this fulvic acid. For Task 1 proton and copper titrations have been completed and for Task 2, two methods have been developed;

- a batch solvent extraction method similar to that of Nash and Choppin (1979) to determine stability constants;
- a batch method, using chelating resins, to generate data on the kinetics of dissociation of fulvic acid and the actinides at room temperature.

To investigate the dissociation kinetics of these complexes a resin method was used. The resin (R) selectively collects trace metals within a salt solution. The dissociation of Fa-A(ctinide) releases free A ions, the vast majority of the free ions will then bind to the resin as:

$$Fa - A + R \leftrightarrow Fa + A + R \leftrightarrow Fa + A - R$$

If the rate limiting step is the dissociation of the Fa-A complex and the free A ions are instantly sorbed to the chelating resin, then the proportion of A sorbed to the resin is directly proportional to the rate of the dissociation of the complex.

2. CHARACTERISATION (Task 1)

The following completes the characterisation of DE72 Derwent fulvic acid first outlined by Higgo et al. (1998) and shows comparative proton and copper binding titrations.

2.1. Proton Binding

Data are supplied, as a comparison, for proton binding by Derwent FA (DFA) and the well characterised Kranichsee Fulvic acid (KSFA) and humic acid (KSHA)

Experimental procedures for proton binding of KSFA/KSHA are essentially the same as described for DFA Higgo et al. (1998) but the range of data has been altered slightly in two of the controlling parameters to try to improve the method:

- The ionic strength range was increased from 0.001 – 0.3M (compared to a previous range of 0.003 – 0.1M) in order to improve the definition of the salt effect.
- The pH range was contracted slightly, to approximately 3.7 – 10.3 c.f 3.3 – 10.7, in order to minimise errors associated with the correction for titration of the background electrolyte (the size of the correction increases logarithmically at pH 'outside' about 3.5 and 10.5).

During experiments on the Derwent Fulvic Acid data points were recorded at approximately 0.1 pH intervals, the titrator adjusting the size of acid or base doses in order to maintain constant pH increments. Electrode drift was monitored following each addition, for a minimum of 2 minutes and until the pH drift was less than 0.001 pH/min (at regions of low buffer capacity, monitoring was up to 20 minutes). Separate pH and reference half cells were used, with a saturated calomel reference fitted with a continuously refreshed double-junction electrolyte bridge (0.1 M KNO3). The reaction vessel was thermostatted at 25° ± 0.1°C and was continuously purged with a trickle flow of O2- and CO2-free N2. The complete four-cycle titration took 72 hours.

2.1.1. Results and discussion

It should be noted that a degree of caution is needed when interpreting proton charging curves, thus:

- The Y axis scale is not always the same in each case;
- The dQ axis is change in charge, not necessarily absolute total charge;
- The initial pH of the solutions, (which these curves are all referenced to) can also be used, so if the purification is perfect the translation from dQ to Q might be exact, but these limitations should be noted;
- The spread of ionic strength dependency between the curves is slightly misleading because the same I values were not used for DFA as for KS. DFA curves should be bunched more tightly because the spread of I is less. Nevertheless the apparent I dependency of KSHA and KSFA is interesting, and work is on-going to see if this effect is real.

A plot of the comparison between the three humic substances is shown below.

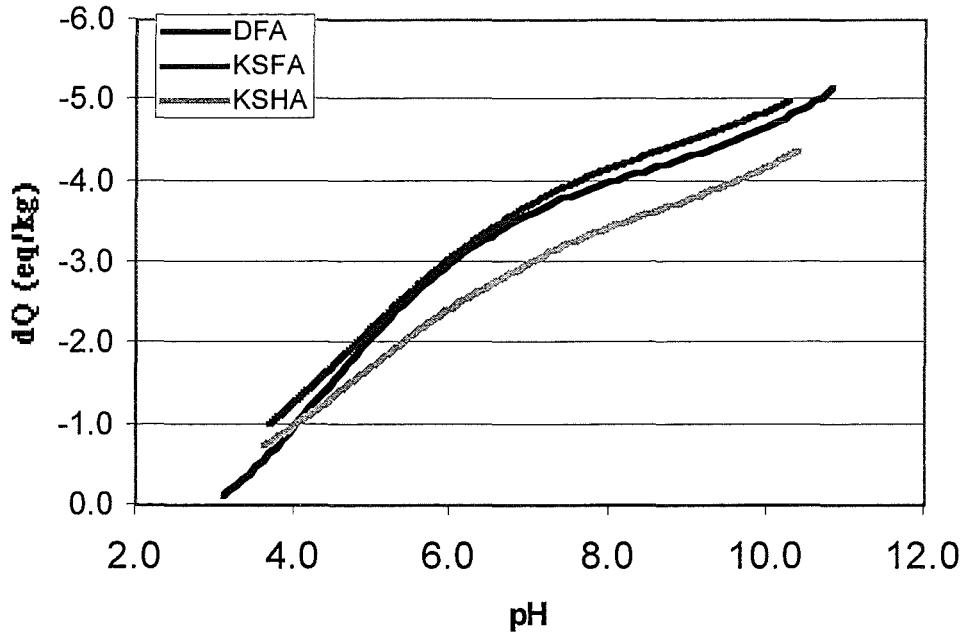

Figure 1. Comparative plot of proton charging (using lowest I for each)

The I value is slightly nominal because I changes with titration. At high I the effect is negligible e.g. 0.3 to 0.31 or so. At low I it can be significant with 0.001 altering to 0.004 or 0.006 during the course of the titration. The I value quoted (on all the plots) is generally the target value at the beginning of the titration leg. The three curves on the comparison plot (Figure 1) are all nominally between 0.001 and 0.003. To be rigorous, when modelling with Model VI or NICA etc. the I value can be taken specifically for each data point, thereby correctly allowing for the variation over the experiment.

Proton binding capacity from pH 3 – 10.5

DFA, KSFA 5 eq/kg

KSHA nearer 4 eq/kg

DFA and KSFA seem to have similar binding capacities. Fulvics have been reported up to about 8 eq/kg and in fact the NICA-Donnan fit quoted in Higgo et al. (1998) predicted for DFA a total charge of 8 eq, by extrapolating the curves beyond the experimental window. Humics are always less than fulvics, sometimes by a factor of 2 but as the KSHA is not markedly less than KSFA it suggests a low molecular weight humic. An examination of the shape of the curves shows DFA has a sharper 'hip' in the middle. This is quite common with fulvics, but humics seem to be much straighter (behaving almost like an ideal buffer). The typically steeper charging at low pH of the fulvics reflects the generally higher proportion of carboxylic type groups occurring in fulvics than in humic acids. The KSHA and KSFA curves have quite a similar shape, but a different total capacity from each other. There is little literature data of such direct comparisons where it has been possible to titrate the fulvic and the humic fractions from the same source.

A collation of proton data from various sources and authors is on-going.

2.2. Copper Binding

Copper binding by DFA compared with a fulvic acid (PUFA) from Switzerland has also been performed using a similar method and is illustrated in Figure 2.

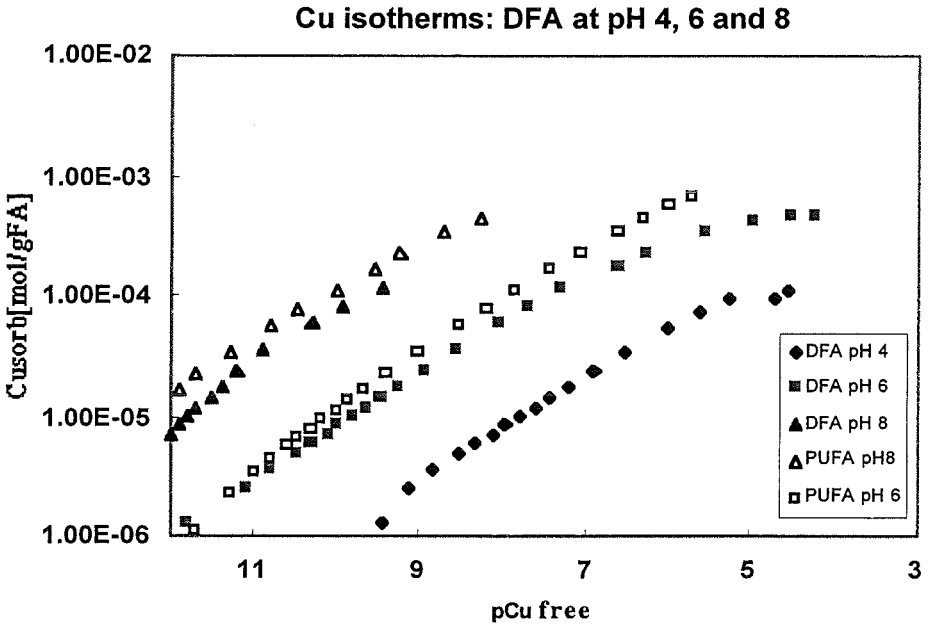

Figure 2. Copper isotherms for DE72 fulvic acid at pH 4,6 and 8.

Interpretation of this work is still on-going at BGS. Provisionally, however, DFA and PUFA gave similar results, and a quick comparison with other humics gave a similar figure. When the proton constants are available and the I dependency is confirmed, NICA-Donnan copper parameters can be derived from this data set.

3. COMPLEXATION (Task 2)

Two batch methods were used to study the complexation behaviour of fulvic acid with uranium and thorium over the pH range 4 to 8. The speciation of uranium, as the uranyl ion, and thorium within these ranges is well documented. As the pH increases the uranyl ion increasingly speciates

with carbonates but over the series of experiments these did not appear to interfere significantly with fulvate-metal binding.

3.1. Competitive Solvent Extraction Method

This work began during the first year of the project. Results for the uranyl ion (but at only one pH and ionic strength) were outlined in Higgo et al. (1998). Thorium data are provided here.

In a generalised reaction between metal ion (M) and organic ligand (L):

$mM + nL = MmLn$ where m and n = moles of M and L respectively

The overall stability constant is derived from :

$$\beta_{mn} = \frac{\{MmLn\}}{\{M\}^m\{L\}^n}$$

where { } represent thermodynamic activity. Each species that can be formed by M and L has a unique βmn which is a true thermodynamic constant at a given temperature (and is independent of solution composition). However, experiments tend to yield concentrations rather than activities, so instead the "concentration quotient" is determined:

$\beta mn,c = \frac{[MmLn]}{[M]^m[L]^n}$ is determined where :

$$\beta mn = \frac{\delta MmLn}{(\delta M)^m(\delta L)^n}\ \beta mn,c$$

where δ = activity coefficients.

Often the term "conditional stability constant" is used. This refers to the calculation of β in terms of:

Mf (total metal not bound to the ligand)

Lf (total ligand not bound to the metal).

$$\beta^* mn,c = \frac{[M_mL_n]}{[M_f]^m[M_L]}$$

where: β^*mn,c = conditional stability constant.

Humic substances are large complex organic molecules which limits the description of complexation reactions. Due to the polyelectrolytic nature of humics it is not possible to report stoichiometries on a mole : mole basis. Instead a site binding approach is often employed. The complexes are assumed to have a 1:1 stoichiometry in terms of binding sites per mole of ligand. Various authors have accounted for non-integral relationships. Nash and Choppin (1979) assumed there was more than one type of binding site on the humic molecule forming 1:1 or 1:2 complexes with the metal ion. Smith et al. (1986) explained the non-integral relationships with a single binding site on the humic molecule capable of forming 1:1 and 1:2 complexes with the metal ion.

3.1.1. Experimental

The method was altered slightly from that outlined in Higgo et al. (1998);

- Higher concentrations of the solvent phase, HDEHP in toluene, were needed to attain workable distribution coefficients (in the absence of fulvic acid) with increasing pH, and for comparable experiments using thorium ;
- Silanised vessels were used to minimise the sorption of uranium to vessels at high pH.

Aqueous solutions containing fulvic acid and actinide where equilibrated for 24 hours at varying ionic strengths and pH. These were shaken with an equal volume of HDEHP in toluene for 24 hours and the two phases separated by centrifugation. The two phases were counted by liquid scintillation. Sorption to the walls was very much less than that reported in Higgo et al. (1998) and recoveries were greater than 95%.

3.1.2. Results and discussion

The uranium experiments were carried out with $1x10^{-5}$ M HDEHP in toluene at pH 4 to 6, and with $2x10^{-4}$ M HDEHP in toluene at pH values above this range. The thorium experiments were carried out with 0.01 M HDEHP. Throughout uranium and thorium concentrations were $2x10^{-7}$ M.

Actinide	pH	Ionic Strength M/l NaCl	Log beta l/g
uranium	3.9	0.1	2.9
uranium	4.1	0.03	2.7
uranium	5.9	0.1	3.2
uranium	7.2	0.1	3.9
thorium	5.3	0.01	2.0
thorium	5.5	0.01	1.5
thorium	6.5	0.1	2.6

Table 1 Log beta values derived from uranium and thorium solvent extraction experiments.

Stability constants are calculated in terms of total unbound metal in solution (Moles/l) while the humic concentration is in g/l. The uranium values agree well with those reported previously Higgo et al. (1992).

The solvent extraction method worked well for thorium at low pH values but at higher values a third layer appeared and more thorium appeared to be extracted by the solvent in the presence of humic than in the absence of humic. It is difficult to compare our thorium values with those in the literature without the aid of a model because of the differences in experimental techniques and reporting methods. Tipping (1993) used the humic ion binding model to analyse the two small thorium-humic binding datasets available Nash and Choppin (1979) and Ibarra et al. (1981). The two datasets are for similar (low) pH values but widely different metal concentrations. In analysing the data of Nash and Choppin (1979) correction had to be made for the high degree for complexation of Th by acetate, acetate complexes being calculated to account for 99.6% of the solution Th not bound by humic acid. This meant that there was uncertainty about the concentrations of Th^{4+} and its hydrolysis products.

In order to display these data graphically Tipping (1993) plotted graphs of $p[Th^{4+}]$ against $p\nu$ for these two data sets (ν = mole thorium metal bound per gram humic matter). It is clear from these graphs that the two data sets are very different. Thus Nash and Choppin's values for log beta = $p[Th^{4+}] - p\nu$ are around 7.5 at pH 3.9 whereas Ibarra obtained values around 3.5. These data are

based on the concentration of Th^{4+}. Lower values would have been obtained if the concentration of total unbound thorium (including hydrolysis products) had been used in the calculation.

Log beta values given in Table 1 have been calculated in terms of total unbound thorium in solution and appear low compared with Nash and Choppin's values. However, if we base our calculations on the concentration of Th^{4+} then our values (log beta =9.8 at pH 6.5 and 6.0 at mean pH of 5.4) are comparable with those of Nash and Choppin - after correction for acetate complexation. Of course this approach requires accurate thermodynamic data for the modelling of thorium speciation. There is still some uncertainty in these data, and for this reason we do not add buffers to control the pH and we prefer to calculate values in terms of total (measurable) thorium in solution.

3.2. Batch Kinetic experiments

Batch kinetic experiments were used to measure the rate of dissociation of actinides from an actinide-fulvic complex. All the experiments followed the same basic protocol as follows.

The test solution was made by adding the relevant actinide to an aqueous solution of either NaCl or $NaClO_4$ at the required pH and ionic strength. Fulvic concentration varied from 0 to 50 mg/l. Either ^{233}U or ^{230}Th was used as a purchased carrier free source or ^{234}Th was 'milked' from ^{238}uranyl nitrate, using a method from Toribara and Koval (1967).

The solutions were 'aged' from 1 day to 262 days, simulating a range of contact times approximating to real field conditions. A measured amount of purified resin was added to the test solution and mixed vigorously. At intervals the test vial was centrifuged, to separate fulvic-bound and resin-bound metal. A sub-sample was taken from the aqueous, fulvic-bound, fraction. This sub-sampling was repeated over long time periods of up to 42 days. The method assumes that upon dissociation from the fulvic complex, the metal is immediately and irreversibly bound to the resin. The applicability of each tested resin to the varying experimental conditions is outlined later.

The sub-samples were counted on an LKB Wallac 1219 Rack-Beta liquid scintillation counter. Where ^{234}Th was used, counting can only proceed after 60 hours when the two immediate short-lived proctactinium daughters (which have not bound to the resin) have decayed. Any activity left in the vial is then only due to ^{234}Th and the Pa daughters that have grown into equilibrium after this time period.

Relative kinetics were calculated using the following procedure. The kinetic dissociation data are parameterised using a function which is a sum of decaying exponentials,

$$f(t) = \sum_{i=1}^{n} a_i e^{-k_i t}$$

with n=3 in most cases. The fitting process is carried out in two stages. An initial estimate is made for the parameter pairs (a_i, k_i) using an iterative graphical approach. These parameters are then optimised using a non-linear least squares routine. The two stage approach is required because the optimisation step is not robust and requires a good initial estimate to ensure convergence. Even with this two step procedure, "outliers" can cause convergence failures in the optimisation routines and it has been necessary on occasion to omit certain data points from the fitting process.

The graphical procedure involves plotting the data as log(count rate) vs. time and making a straight line fit to the late time data points. The intercept and slope of this line provide estimates of a_n and k_n respectively. This exponential term is then subtracted from the data, the residuals are replotted, and the process repeated to obtain a_{n-1} and k_{n-1}, etc.

3.2.1. Results and discussion

The effect of pH, ionic strength, and preconditioning time have been investigated on the kinetics of dissociation of thorium and uranium from Derwent fulvic acid. No one resin was found to be ideally suited over the full range of experimental parameters. Cellulose Phosphate used by Padilha (1997) was selected for uranium experiments at pH of around 4, and Cellulose Hyphan used by Burba (1993) for uranium and thorium experiments around pH 7.

3.2.1.1. Effect of Preconditioning time

This was varied between 1 day and 262 days for thorium. The kinetics of dissociation are shown in Table 2.

Pre-conditioning time, days	Total contact time, days	k3, Min^{-1}	k3 extent, percent	k1, Min^{-1}	k2, Min^{-1}
1	41.8	-3.14E-05	18.2	5.03E-03	2.36E-04
1	41.8	-2.31E-05	17.1	5.76E-03	1.96E-04
262	41.8	-1.20E-05	54.6	7.22E-04	3.73E-04
244	41.8	-1.33E-05	52.6	8.88E-03	3.93E-04
242	41.8	-1.37E-05	57.9	3.17E-02	3.51E-04

Table 2 Effect of pre-conditioning time on kinetic rates for thorium-fulvic dissociation.

All experiments at unbuffered pH of between 6.5 and 7.0 and ionic strength 0.1M

An example of this dissociation is illustrated in Figure 3.

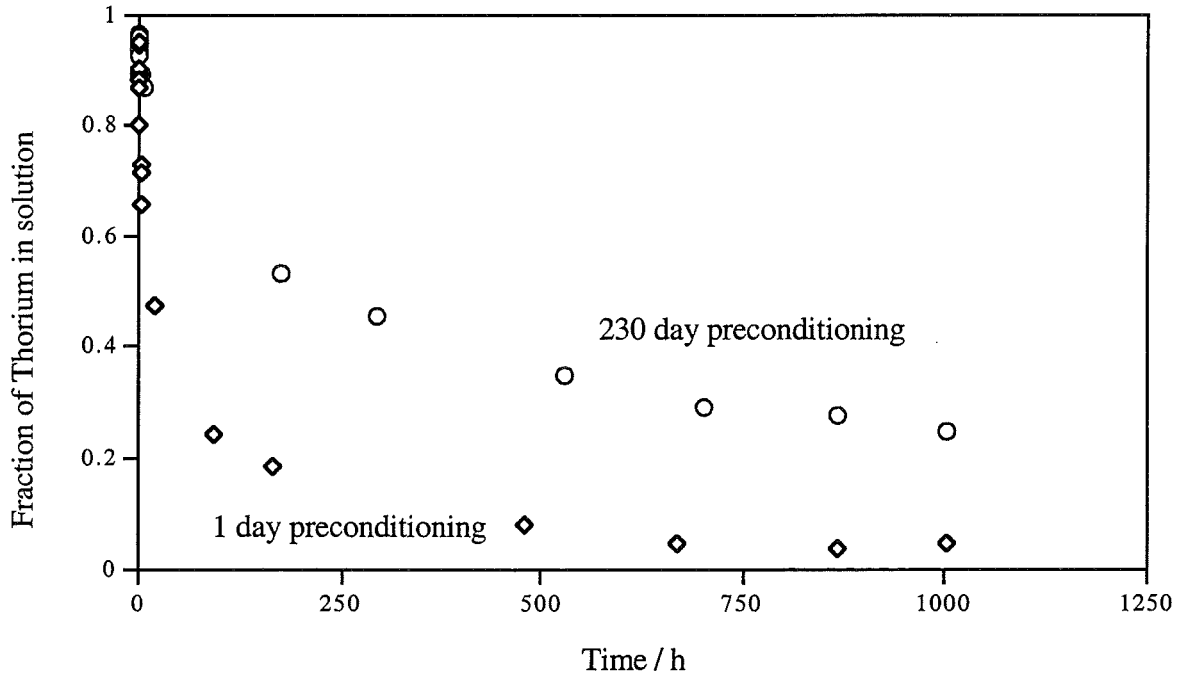

Figure 3. Dissociation of Thorium from DE72 fulvic acid

Using this method the dissociation rate is artificially divided into three stages. The first and fastest has a dissociation rate k1, the intermediate has a dissociation rate k2 and the final slow stage has a dissociation rate k3. Because k3 is calculated first it is the most accurate. It is also the most important because it is this stable complex that is likely to be mobile in the field. By the time k1 is calculated (after two subtractions) the error might be quite high. Table 2 lists k1, k2 and k3 and also shows the percentage that decays with a rate of k3 min^{-1}. Thus with incubation time of 262 days 54.6% of the Th-complex decays slowly whereas after one day pre-conditioning only 18% decayed slowly. The other 78% dissociated rapidly and would not be mobile in a field situation. The effect of pre-conditioning time seems to be most significant during the first few days. Proviosonal data, to be verified and published in future reports seems to indicate there is a larger increase in the percentage of slowly-dissociating complex between one to four days than between four and 240 days.

Table 3 shows similar work done with uranium, again at an unbuffered pH between 7.0-7.4. The ionic strength of the 1 day preconditioned samples was 0.1M and that of the longer term conditioned is 0.01M. Competition effects would produce relatively faster dissociation in a higher ionic strength solution (but see 3.2.1.3)

Pre-conditioning time, days	Total contact time, days	k3, Min^{-1}	k3 extent, percent	k1, Min^{-1}	k2, Min^{-1}
1	41.8	-7.49E-04	3.0	6.39E-02	1.17E-02
1	41.8	-7.73E-04	5.2	6.40E-02	1.07E-02
162	37	-1.59E-05	8.0	9.27E-03	2.43E-04
162	37	-1.76E-05	6.5	7.92E-03	1.79E-04

Table 3 Effect of pre-conditioning time on kinetic rates for uranium-fulvic dissociation.

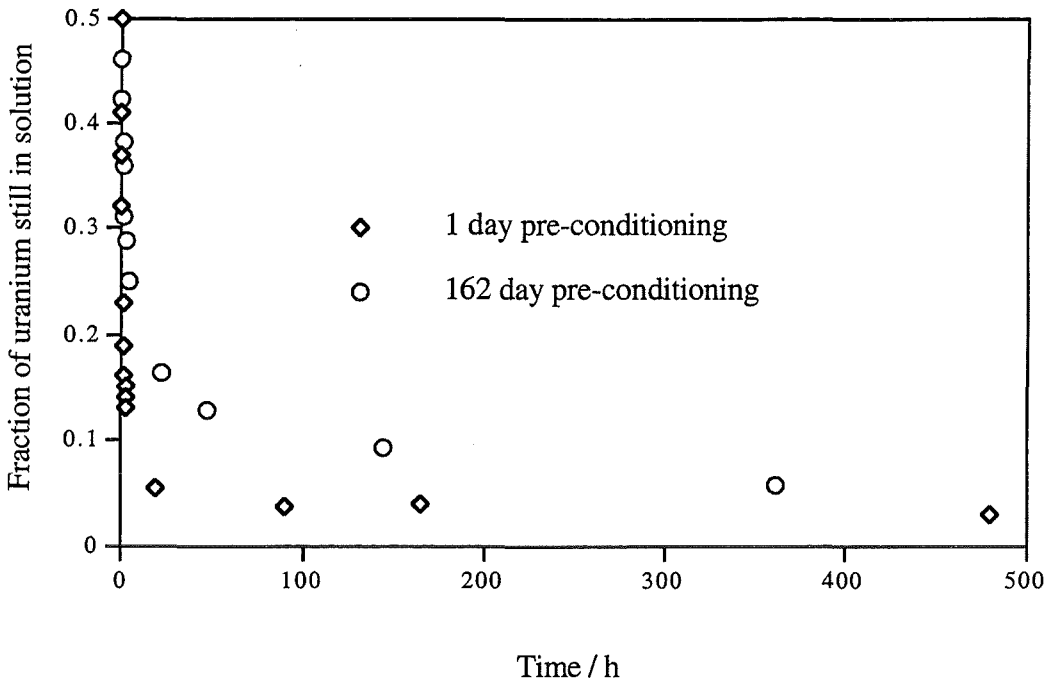

Figure 4. Dissociation of Uranium from DE72 fulvic acid

Figure 4 shows the effect of contact time with the resin on the amount of uranium still in aqueous phase i.e. complexed with the fulvic.

The proportion of U-FA complex that dissociated slowly was far smaller than in the case of thorium. Thus, only ≈4 % and ≈7% dissociated slowly for pre-conditioning times of 1 and 162 days respectively. Nevertheless, the actual values for k3 were similar and it is possible that this residual complex ($K3 < 10^{-5}$) could travel some distance through the far field.

It is unfortunate that the technique does not allow sampling *ad infinitum*, but it is constrained by problems of the short-half of the radio-isotope and the fact that sub-samples are non-replaceable after liquid scintillation counting.

3.2.1.2. Effect of pH

The bulk of the experiments carried out with Hyphan were at pH more akin to the field, in the range 6.5-7.5. A number of experiments were carried out using Cellphos at a lower pH with uranium (see Table 4).

Precondition time days	pH	Ionic Strength, Na+, M	k3 extent, percent	k1, Min-^{1}	k2, Min-^{1}	k3, Min-^{1}
1	3.4	0.01	3.0	-7.20E-02	-9.79E-03	-1.15E-04
13	3.2	0.01	3.6	-6.80E-02	-1.01E-02	-2.55E-04
20	3.4	0.01	N/A	-7.25E-02	-2.17E-03	N/A
1	3.3	0.1	3.6	-2.31E-01	-5.09E-02	-2.56E-03
20	3.2	0.1	4.9	-2.77E-01	-4.98E-02	-1.21E-03

Table 4 Summary of uranium dissociation from DE72 fulvic acid at low pH.

As expected dissociation at this lower pH is much more rapid and the amount of uranium still in solution, as bound fulvate, after only 24 hours is negligible. Preconditioning again has little effect on the slow dissociation rate (k3) but despite the percentage being so low, seems to have an effect on the ratio of rapidly- (k1 + k2) to slowly- (k3) dissociating complexes.

3.2.1.3. Effect of Ionic Strength

Table 4 also includes data on the ionic strength of the background electrolyte. In general fulvic-metal binding decreases with increasing ionic strength as the thickness of the double layer decreases. It appears from our results that dissociation rates also increase as the ionic strength increases. This may be because other free aqueous ions such as Na+ are able to bind to sites within the fulvic molecule occupying sites that at lower ionic strengths would delay the emergence of actinide ions from the molecule.

The range of dissociation rates from fast (k1) to slow (k3) probably reflects

- the different binding strengths of the sites within the molecule and;
- the rate at which actinide ions are released from deep within the fulvic molecule.

During migration to the edge of the molecule there is a high probability that they will bind to other unoccupied sites, thus, being delayed further. At high ionic strengths many of these sites my be occupied by cations such as Na+ and dissociation will be more rapid.

4. CONCLUSIONS

- Characterisation of the DE72 fulvic acid is now complete. Both proton-binding and copper-binding titrations have shown that this fulvic acid is similar in terms of pH dependency to other fulvic acids studied. This is important because it means that results using this material can be extrapolated to other environments.

- A solvent extraction method has been developed to obtain conditional stability constants for uranium and thorium complexation to DE72 fulvic acid. Values obtained for uranium are similar to those derived in previous research. The thorium values appear to be low in comparison to others in the literature but a re-examination of the published data removes this apparent discrepancy.

- A resin method was used to generate kinetic data to describe the dissociation of uranium and thorium from DE72 fulvic acid. After initial rapid dissociation the dissociation rates decrease to around 10^{-5} min^{-1}, for both uranium and thorium at pH between 6.5 –7.4. The proportion of slowly dissociating complex depends on the preconditioning time as well as pH and ionic strength.

- Throughout thorium has slower dissociation kinetics than uranium.

- No single resin was found ideal at all experimental parameters and the dataset still has some gaps.

In the next phase of the work a number of experiments will be conducted to attempt to fill in some gaps in the current dataset for thorium kinetics with emphasis on a range of pre-conditioning times and to quantify the relationship between pre-conditioning time and k3 extent.

5. ACKNOWLEDGEMENTS

This work was funded by the European Commission and the UK Environment Agency. The results will be used in the formulation of Government policy but do not necessarily represent that

policy. This paper is published by the permission of the Director of the British Geological Survey (NERC).

6. REFERENCES

Burba, P. (1993). Labile / inert metal species in aquatic humic substances: an ion-exchange study. Fresenius Journal of Analytical Chemistry **348**, 301-311

Higgo, J.J.W., Davis, J., Smith, B., Din, S., Crawford, M.B., Tipping, E., Falck, W.E., Wilkinson, A.E., Jones, M.N. and Kinniburgh, D. (1992). Comparative study of humic and fulvic substances in groundwaters: 3. Metal complexation with humic substances. British Geological Survey Technical Report no. WE/92/12.

Higgo, J.J.W., Davis, J., Smith, B. and Milne C. (1998). Extraction, purification and characterisation of fulvic acid British Geological Survey Technical Report no. WE/98/22.

Higgo, J. J. W., D. Kinniburgh, Smith, B. and Tipping, E. (1993). Complexation of Co^{2+}, Ni^{2+}, UO_2^{2+} and Ca^{2+} by humic substances in groundwaters. Radiochimica Acta **61**: 91-103.

Ibarra, J. V., Oscar, J. and Gavilan, J.(1981). Acidos humicos de lignitos: II. Complejos con los iones estroncio, plomo, uranilo y torio. Medida de sus constantes de estabilidad. Anal. Quim **77**.

Kersting, A.B., Efurd, D.W., Finnegan, D.L., Rokop, D.J., Smith, D.K. and Thompson, J.L. (1999). Migration of plutonium in groundwater at the Nevada test site. Nature, **397**, 56-59.

Nash, K.L. and Choppin, G.R. (1979). Interaction of humic and fulvic acids with Th(IV). Journal of Organic Nuclear Chemistry, **42**, 1045-1050.

Padilha, P.M., Rocha,J.C., Moreira, J.C., Sousa Campos, J.T., Carmo Federici, C. (1997) Preconcentration of heavy metal ions from aqueous solutions by means of cellulose phosphate: an application in water analysis. Talanta., **45**, 317-323.

Smith, G.C., Rees, T.F., McCarthy, P., Daniel, S. (1986). On the interpretation of Schubert plots for metal-humate systems. Soil Science, **141**, 7-9.

Tipping, E. (1993). Modelling the binding of europium and the actinides by humic substances. Radiochimica Acta **62**: 141-152.

Toribara, T.Y. and Koval, L. (1967). Isolation of thorium in biological samples. Radiochimica Acta , **14**, 403 – 407.

Zuyi, T. and Huanxin, G. (1993). Use of the ion exchange method for determination of stability constants of thorium with humic and fulvic acids. Radiochimica Acta , **65**, 121-123.

Annex 4

Complexation of Eu(III), Th(IV), and U(VI) by Humic Substances

(Moulin et al., CEA)

2nd Technical Report
EC Project

"EFFECTS OF HUMIC SUBSTANCES ON THE MIGRATION OF RADIONUCLIDES: COMPLEXATION AND TRANSPORT OF ACTINIDES"

CEA Contribution to Task 2

COMPLEXATION OF Eu(III), Th(IV) and U(VI) BY HUMIC SUBSTANCES

Reporting period 1998

Valérie MOULIN, Pascal REILLER, Christian DAUTEL
Gabriel PLANCQUE, Ivan LASZAK, Christophe MOULIN*,

CEA, CE-Saclay, Fuel Cycle Division, DESD/SESD/LMGS
91191 Gif-sur-Yvette, FRANCE
**CEA, CE-Saclay, Fuel Cycle Division, DPE/SPCP/LASO*
91191 Gif-sur-Yvette, FRANCE

ABSTRACT

Complexation of actinides by humic substances has been studied by different techniques depending on the actinide and its oxidation state. For trivalent actinide (using a rare earth element, Eu as an analogue of trivalent actinide), Time-Resolved Laser-Induced Fluorescence (TRLIF) has been retained as a method for direct speciation at low level. By varying pH and physicochemical conditions (absence of carbonate ions) and at fixed ionic strength, it is possible together to identify spectrally and temporally, all the hydroxo and carbonato complexes. This approach has also been retained for U(VI) as a model of hexavalent actinide, for which hydroxo complexes have been characterized by TRLIF (the simple carbonato complexes are not fluorescent). In the case of U(VI), titrations by humic acids of U(VI) solutions at various pH have allowed to characterize organic complexes formed with U(VI): single complexes (UO_2HA) and mixed complexes ($UO_2(OH)_3HA$). The impact on U(VI) speciation has then been identified. In the case of Th(IV) as a model of tetravalent actinides, a competitive method has been used to obtain data on the Th-HA system by studying the ternary system silica colloid/HA/Th at constant pH (Schubert method). Apparent interaction constants have been calculated depending on Th hydrolysis constants used. A study of the system Th/HA/silica has a function of pH and for different HA concentrations has shown the strong complexing character of humic acids towards Th in the pH range 4-9.

Content

1. GENERAL INTRODUCTION

The understanding of radioelement behaviour in natural systems in relation with nuclear waste disposals in geological formations necessitates the knowledge of their speciation in these systems including their distribution between the solution and the mineral phases. In particular, this implies to determine the influence of *humic substances* (humic and fulvic acids, HA/FA) as natural organic substances present at different concentrations in groundwaters on the migration of radionuclides, particularly actinide elements. This induces to study

- the complexation of actinides with humic substances as complexing agents,
- their influence on actinide sorption properties towards mineral surfaces and
- the mobility of actinide-humic substances complexes in groundwaters.

In this framework , our objectives are the following:

- to obtain data (interaction constants, complexing capacities) on the interactions between humic/fulvic acids and actinides under relevant geochemical conditions (pH, ionic strength, presence of competing cations);
- to study the effect of humic substances on actinide migration by batch experiments.

For the part relative to the **complexation** of actinides with humic substances (HA/FA), the aim is to obtain the actinide speciation under relevant geochemical conditions (pH, ionic strength, presence of competing cations), and for the following elements:

- Eu(III) chosen as a chemical analogue of trivalent actinides such as Am, Cm, Pu,
- Th(IV) chosen also as a chemical analogue of tetravalent actinides such as U, Np, and Pu;
- U(VI) as a model of hexavalent actinides (U, Pu).

For this purpose, it is also important to focus on the possible existence of *mixed complexes*, namely M-OH/CO_3-HA/FA, which will then completely modify the actinide speciation compared to the absence of such complexes, in particular in the case of Eu(III) and U(VI). The technique retained to study such complexes is *Time-Resolved Laser-Induced Fluorescence*, which has been used, up to now, by both CEA laboratories for the study of trivalent actinides and lanthanides for pH<7.

For Th(IV), as the data on such oxidation state are scarce in the literature, the objective is to obtain informations on the interactions between Th(IV) and humic substances under conditions relevant to natural systems. As thorium is a non fluorescent element, the technique retained is based on the Schubert method using a mineral phase as an extracting phase. The system under study is *silica colloids/humic acids/Th* as a

function of pH, ionic strength and humic acids concentration.

2. CASE OF URANIUM : URANIUM ORGANIC SPECIATION DETERMINED BY TIME-RESOLVED LASER-INDUCED FLUORESCENCE

Ivan Laszak, Valérie Moulin, Christophe Moulin, Gabriel Plancque

2.1. INORGANIC SPECIATION : SUMMARY OF RESULTS

The different hydrolysed species of U(VI) have been characterized from a spectroscopic point of view [temporally (lifetime) and spectrally (fluorescence spectrum)]. Six main hydroxo complexes have been perfectly identified (Laszak et *al.*, 1998a, 1998b ; Moulin et *al.*, 1995, Moulin et *al* ., 1997; Moulin et *al.*, 1998). Figure 1 represents the spectra of the uranyl ion UO_2^{2+} and the main hydroxide complexes: the first hydroxo - complex UO_2OH^+, the third $UO_2(OH)_3^-$ and the polynuclear species $(UO_2)_3(OH)_5^+$ together with fluorescence lifetime. The simple carbonato complexes of U(VI) are not fluorescent.

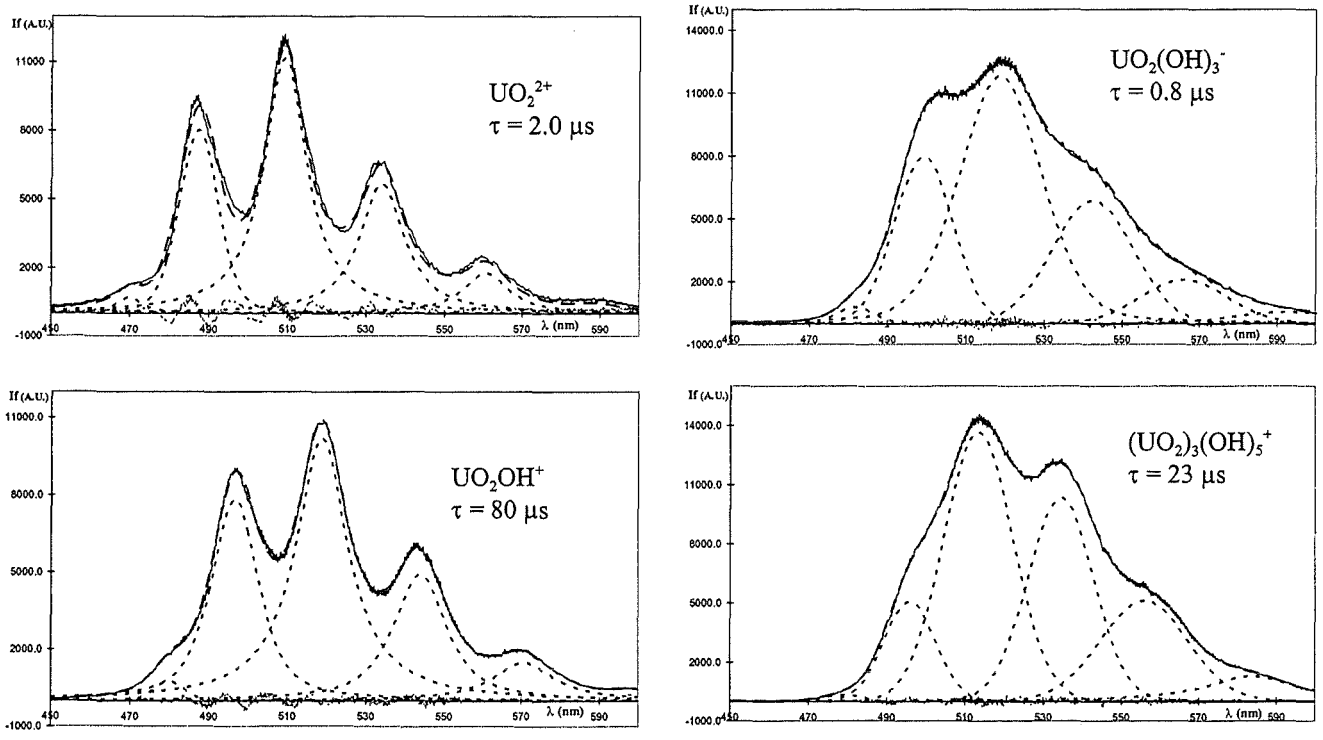

Figure 1 : Fluorescence spectra of U(VI) hydroxo complexes : UO_2^{2+}, $UO_2(OH)^+$, $UO_2(OH)_3^-$ and $(UO_2)_3(OH)_5^+$

2.2. COMPLEXATION OF U(VI) WITH HUMIC SUBSTANCES STUDIED BY TRLIF

2.2.1. EXPERIMENTAL

Apparatus

Time-resolved laser-induced fluorescence : A Nd-YAG laser (Model minilite, Continuum) operating at 266 nm (quadrupled) or 355 nm (tripled) and delivering about 5 mJ of energy in a 4 ns pulse with a repetition rate of 20 Hz is used as the excitation source. The laser output energy is monitored by a laser power meter (Scientech). The laser beam is directed into the cell of the spectrofluorometer "FLUO 2001" (Dilor, France) by a quartz lens. The radiation coming from the cell is focused on the entrance slit of the polychromator. Taking into account dispersion of the holographic grating used in the polychromator, measurement range extends to approximately 200 nm into the visible spectrum with a resolution of 1 nm. The detection is performed by an intensified photodiodes (1024) array cooled by Peltier effect (-20°C) and positioned at the polychromator exit. Recording of spectra is performed by integration of the pulsed light signal given by the intensifier. The integration time adjustable from 1 to 99 s allows for variation in detection sensitivity. Logic circuits, synchronised with the laser shot, allow the intensifier to be active with determined time delay (from 0.1 to 999 μs) and during a determined aperture time (from 0.5 to 999 μs). The whole system is controlled by a microcomputer.

Fluorescence measurement procedure

All fluorescence measurements are performed at 20°C. The pH of the solution in the cell is measured with a conventional pH meter (Model LPH 430T, Tacussel) equipped with a subminiature combined electrode (Model PHC 3359-9).

Titrations of U solution (at 0.1 or 1 mg/l) by humic acids have been performed either under atmospheric pressure for pH 4, 5.5 and 6.4 or in an inert glove-box avoiding the presence of CO_2 for pH 10.5. Lifetimes (τ) are measured at the beginning and at the end of the titrations; fluorescence spectra are also recorded.

Fluorescence spectra were analysed using the deconvolution software GRAMS 386®. All peaks were described using mixed Gaussien-Lorentzian profile (the apparatus function was previously recorded using a mercury lamp). Fluorescence lifetime measurements were made by varying the temporal delay with fixed gatewidth. Fluorescence intensities are corrected of dilution effect during the titration, of prefilter effects (if there exist) and normalised at the same incident laser energy (2.5 mJ).

Materials

Standard solutions of uranium (VI) in sodium perchlorate ($NaClO_4$ 0.1 M) are obtained from suitable dilution of a solution prepared by dissolution of high purity uranium with concentrated perchloric acid (Merck). Due to the hazardous properties of perchloric acid, this reaction is performed in a hood with absolutely no grease on vessels. Uranium concentration of the initial standard solution is measured by mass spectrometry.

Purified Aldrich humic acids (HA) are used in a protonated form. Their main characteristics are detailed in Kim et *al.* (1991), as part of an EC Mirage project (Kim, 1990). Their proton capacities are 5.4 meq/g for HA-Aldrich (determined by potentiometric titrations). Their apparent acidity constants (determined as the pH at mid-equivalence) are: $pK_a^{HA} = 4.3$. Stock solutions of 125 mg/l for Aldrich HA in 0.1 M $NaClO_4$ have been prepared after dissolution in NaOH medium (pH~10; ratio 1/10) in the case of HA.

Perchloric acid and sodium hydroxide (Merck) are used for pH adjustment. The ionic strength is fixed by the sodium perchlorate concentration at 0.1 M for most of the experiments excepted those realised in potassium carbonate (K_2CO_3 0.1 M or 1 M). All chemicals used are reagent grade and Millipore water is used throughout the procedure

2.2.2. RESULTS

The interaction of humic acids with U(VI) has been studied at different pH according to the predominant inorganic species (Laszak, 1997, Laszak et *al.*, 1999) *i.e.* :

- at pH 4 with UO_2^{2+}
- at pH 5 with $UO_2(OH)^+$
- at pH 6.4 with $(UO_2)_3(OH)_5^+$
- at pH 10.5 with $UO_2(OH)_3^-$

by using **TRLIF** as technique of investigation of organic complexes as performed in other studies (Moulin et *al.*, 1992, 1996). Titration experiments have been performed in order to obtain characteristic data, namely the complexing capacities (W) and interaction constants (β): a solution of the inorganic species is titrated by the humic ligand until saturation is reached at constant pH and for a fixed ionic strength.

For each titration curve and each system, initial and final spectra are recorded as well as the lifetimes. These measurements are essential since,

- if the initial and final lifetimes τ are identical, static quenching occur which permits to conclude on complexation between both species (U species and HA) ; on contrary, a variation of τ implies a dynamic quenching.

- if the initial and final spectra are the same, there are two possibilities : either there is formation of a non fluorescent complex or there is formation of a mixed complex.

Moreover, during titrations performed at the excitation wavelength of 355 nm, the variation of fluorescence intensity (ΔF) has been calculated between the end and the beginning of the titration. From titration curves, the fraction of free U at each point (x) is also calculated as well as the Δx as the variation of x between the beginning and the end of the titration. From the Δx and ΔF values, it is considered that if both values are different with $\Delta x > \Delta F$, then a mixed complex is formed.

Each previously identified inorganic U species has been titrated by humic acids. The main results are the following:

The titration of $\mathbf{UO_2^{2+}}$ at pH 4 by humic acids leads to a the fluorescence decrease with no lifetime variation (τ_i = 1.5 µs and τ_f = 1.3 µs). This is due to a static inhibition initiated by the formation of a complex between UO_2^{2+} and humic acids. The exploitation of the titration curve leads to a β value of $10^{5.4\pm0.5}$ and a complexing capacity of 1.3 meq/g.

Figure 2 presents a titration curve of $\mathbf{UO_2(OH)^+}$ at pH 5 by humic acids which shows a fluorescence decrease with no lifetime variation (τ_i = 82 µs and τ_f = 84 µs). This is again due to a static inhibition initiated by the formation of a complex between both species under study, the nature of which is probably not a mixed complex. (analysis of the Δx and ΔF values).

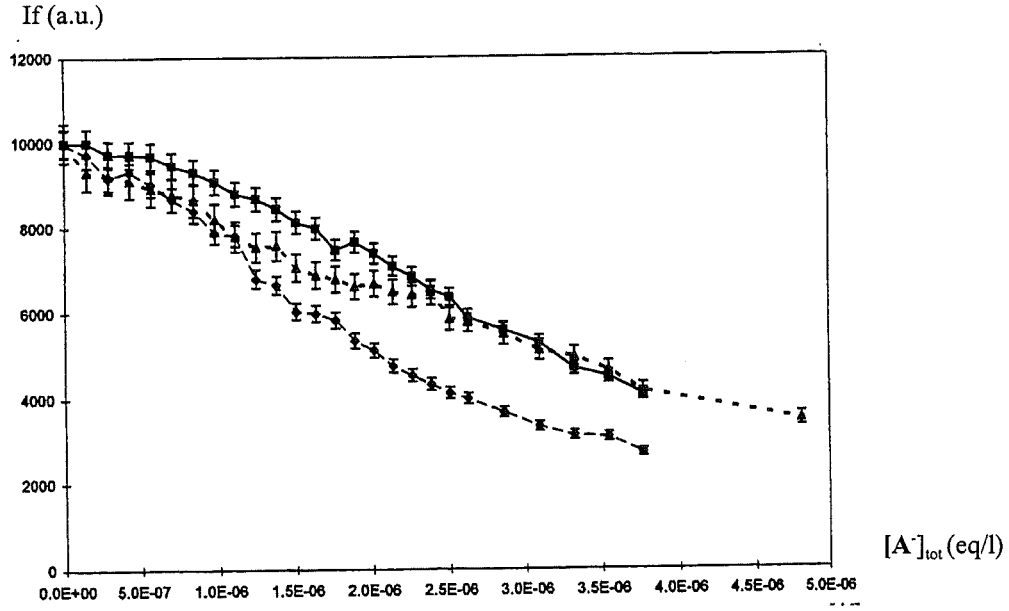

Figure 2 : Titration curve of the first uranium hydroxo complex by HA at pH 5, I=0.1 M

By the same token, titration of $\mathbf{(UO_2)_3(OH)_5^+}$ at pH 6.4 by humic acids leads to a fluorescence decrease with constant lifetime (τ_i = 27 µs and τ_f = 25 µs). This is due to a static inhibition initiated by the formation of a complex between both species under study, the nature of which is probably not a mixed

complex (analysis of the Δx and ΔF values).

Figure 3 presents a titration curve of $UO_2(OH)_3^-$ at pH 10.4 by humic acids which presents a drastic fluorescence decrease with no lifetime variation (τ_i = 1.5 µs and τ_f = 1.3 µs). The exploitation of the titration curve leads to a β value of $10^{6.8\pm0.5}$ and a complexing capacity of 0.5 meq/g. Through the analysis of the Δx and ΔF values, the complex formed is a mixed complex.

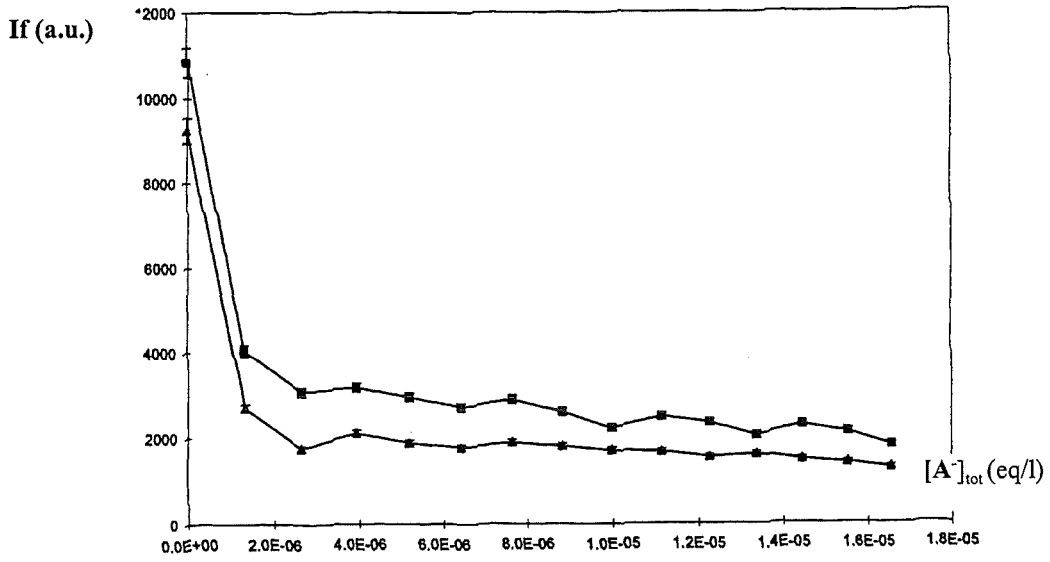

Figure 3 : Titration curve of the three hydroxo uranium complex by HA at pH 10.4, I=0.1 M

All the results are summarised in table 1. Through this study, two complexes have been identified: the fluorescent complex UO_2AH and the mixed complex with $UO_2(OH)_3^-$.

Species	Conclusion
UO_2^{2+}	presence of a fluorescent complex UO_2A with log β = 5.4
UO_2OH^+	absence of a mixed complex
$UO_2(OH)_3^-$	presence of mixed complex $UO_2(OH)_3A$ with log β = 6.8
$(UO_2)_3(OH)_5^+$	absence of a mixed complex

Table 1 : Organic complexes of uranium identified by TRLIF

2.2.3. *CONSEQUENCES ON U SPECIATION*

From this study, the impact of humic substances on the speciation diagram of uranium is clearly seen on figure 4: the uranium speciation under atmospheric conditions even in the presence of 1 mg/l of humic acids is governed by organic complexes in the neutral pH range (6.5-8).

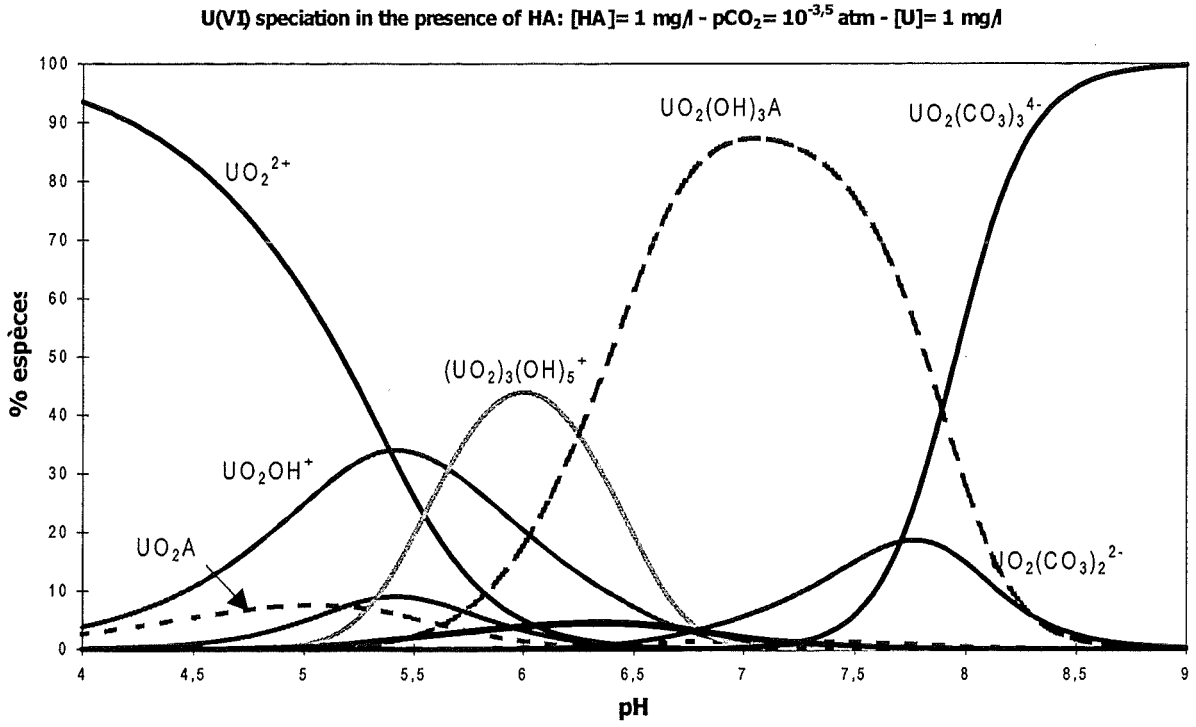

Figure 4: U speciation taking into account mixed complexes identified by TRLIF

2.3. REFERENCES

Kim, J.I., Buckau, G., Klenze R., Rhee D.S., Wimmer H. (1991) Characterisation and complexation of humic acids. CEC Report EUR 13181.

Kim, J.I. (1990) Geochemistry of actinides and fission products in natural aquifer systems. In " *CEC Project Mirage-Second Phase on Migration of Radionuclides in the Geosphere* " (B. Côme, Ed.), EUR Report 12858.

Laszak I. (1997) Etude des interactions entre substances humiques et Uranium(VI) par Spectrofluorimetrie Laser à résolution temporelle. Etude chimique et spectroscopique, Thèse de l'Université PARIS VI, November.

Laszak I., Moulin V., Moulin C. and Mauchien P. (1998a) Uranium inorganic speciation determined by time-resolved laser-induced fluorescence. In " *Effects of humic substances on the migration of radionuclides : complexation and transport of actinides*. First Technical Progress Report (Ed. G. Buckau). Rapport FZKA 6124, pp. 129-146.

Laszak I. , Moulin V. and Moulin C. (1998b) Spéciation inorganique de l'uranium déterminée par spectrofluorimétrie laser à résolution temporelle. Technical Report CEA/DESD 98-188.

Laszak I., Moulin V., Moulin C. and Tondre C. (1999) Uranium speciation in the presence of humic substances studied by time-resolved laser-induced fluorescence. *Talanta*, to be published.

Moulin C., Decambox P., Moulin V and. Decaillon J.G (1995) Uranium speciation in solution by Time-Resolved Laser-Induced Fluorescence. *Analytical Chemistry* **34**, 348.

Moulin C., Decambox P and Mauchien P (1997) State of the art in time-resolved laser-induced fluorescence : applications and trends. *Journal of Radioanalytical and Nuclear Chemistry* **226**, 135.

Moulin C., Laszak I. , Moulin V. and Tondre C. (1998) Time-resolved laser-induced fluorescence as a unique tool for uranium speciation at low level. *Applied Spectroscopy* **52**, 528.

Moulin V., Tits J., Moulin C., Decambox P., Mauchien P. and De Ruty O. (1992) Complexation behaviour of humic substances towards actinides and lanthanides studied by Time-Resolved Laser-Induced Fluorescence. *Radiochimica Acta* **58/59**, 121.

Moulin V., Moulin C and Dran J.C. (1996) Role of humic substances and colloids on the behaviour of radiotoxic elements in relation with nuclear waste disposals: confinement or enhancement of migration? In ACS Volume on *"Humic and Fulvic Acids and organic colloidal materials in the environment"*, pp 259-272.

3. CASE OF EUROPIUM : Eu INORGANIC SPECIATION DETERMINED BY TIME-RESOLVED LASER INDUCED FLUORESCENCE

Gabriel Plancque, Christophe Moulin, Valérie Moulin

3.1. INORGANIC SPECIATION

The approach developed on uranium (see previous paragraph) has been also applied in the case of europium, namely the acquisition of a spectrum data base of Eu complexes (hydroxo and carbonato complexes) before looking at the interaction with humic substances. Hence, europium as a chemical analogue of trivalent actinides can be analyzed at low level by TRLIF (Badort et *al.*, 1989; Decambox et *al.*, 1989) and its hypersensitive transition is a very good indicator of the complexation phenomena (Horrocks et *al.*, 1979; Dobbs et *al.*, 1989; Moulin et *al.*, 1999).

3.1.1. EXPERIMENTAL

Apparatus

Time-resolved laser-induced fluorescence: The same system than the one described for U(VI) (§ 2.2) has been used.

Fluorescence measurement procedure

All fluorescence measurements are performed at 20°C. The pH of the solution in the cell is measured with a conventional pH meter (Model LPH 430T, Tacussel) equipped with a subminiature combined electrode (Model PHC 3359-9).

For each identification, europium concentration, pH, ionic strength were perfectly fixed and controlled. From a spectroscopic point of view, various gate delay and duration were used to certify the presence of only one complex by the measurement of a single fluorescence lifetime and spectrum.

Fluorescence spectra were analysed using the deconvolution software GRAMS 386®. All peaks were described using mixed Gaussien-Lorentzian profile (the apparatus function was previously recorded using a mercury lamp). Fluorescence lifetime measurements were made by varying the temporal delay with fixed gatewidth.

Materials

Standard solutions of europium (III) in sodium perchlorate ($NaClO_4$ 0.1 M) or in potassium carbonate (K_2CO_3 0.1 M or 1 M) are obtained from suitable dilution of a solution prepared by dissolution of high purity europium oxide powder (Alfa) with concentrated perchloric acid (Merck).

Perchloric acid and sodium hydroxide (Merck) are used for pH adjustment. The ionic strength is fixed by the sodium perchlorate concentration at 0.1 M for most of the experiments excepted those realised in potassium carbonate (K_2CO_3 0.1 M or 1 M). All chemicals used are reagent grade and Millipore water is used throughout the procedure

3.1.2. RESULTS

The characterisation of the inorganic complexes (with hydroxides and carbonates ligands) of europium implies to identify them temporally, *i.e.* by the determination of the lifetime and spectrally *i.e.* by the determination of the fluorescence spectrum. These different species under study are the hydroxide and carbonate complexes, in addition to free europium.

With the interaction constants (log β) listed in the literature (Dierckx et *al.*, 1994, Wolery et *al.*, 1992) (table 2), the Eu speciation diagram at atmospheric pressure in which the hydroxide and carbonate complexes are only taken into account, can be built (figure 5). No mixed Eu complexes (Eu-OH-HCO_3/CO_3) are considered.

Species	$EuOH^{2+}$	$Eu(OH)_2^+$	$Eu(OH)_3$(aq.)	$Eu(OH)_4^-$	$Eu(CO_3)^+$	$Eu(CO_3)_2^-$	$Eu(CO_3)_3^{3-}$
log β	5.55	10.72	15.71	17.71	6.96	12.45	14.1

Table 2 : Interaction constants of inorganic complexes of europium at I=0.1 M

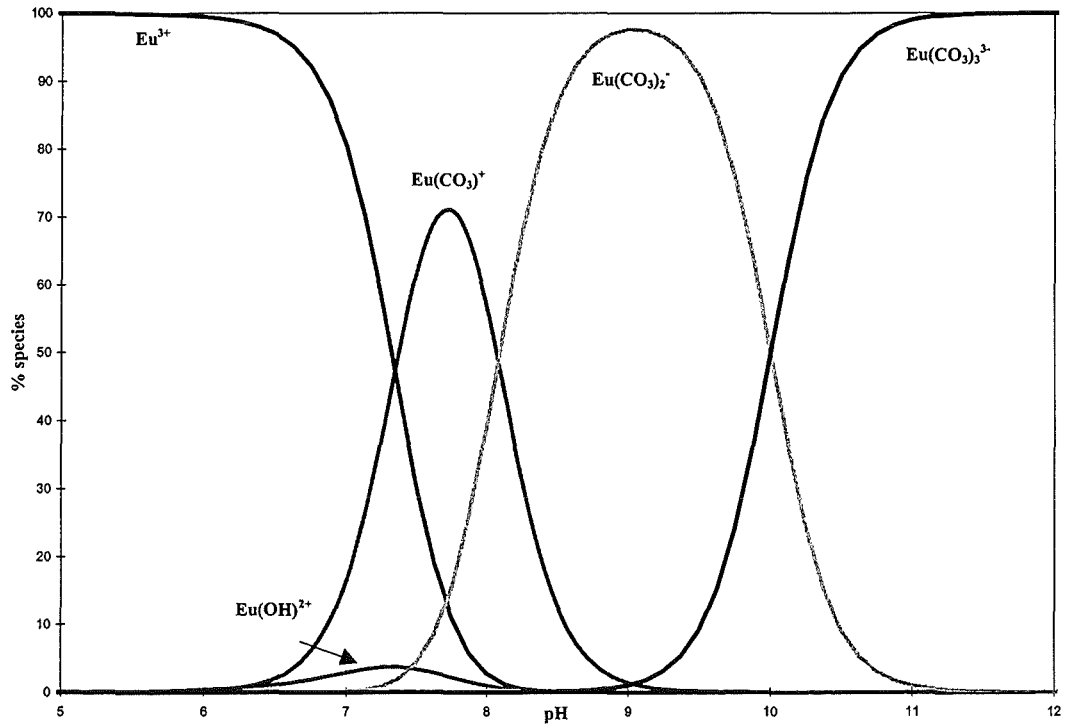

Figure 5 : Speciation diagram of europium at atmospheric pressure

It is also possible to work under a controlled atmosphere (without air) and then to consider the hydroxide complexes as seen on figure 6.

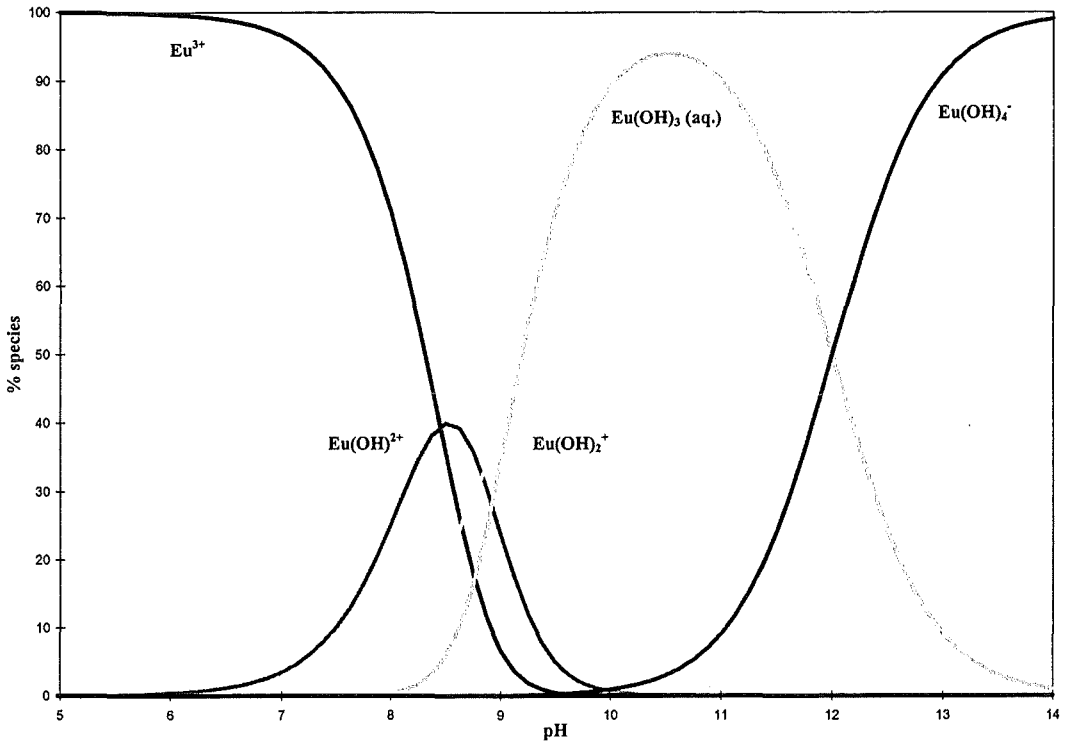

Figure 6 : Speciation diagram of europium at $pCO_2 = 0$

These diagrams allow us to determine the best chemical conditions to identify one particular species. In our case, the following conditions were chosen:

- atmospheric pressure and acidic pH to see free europium Eu^{3+}, namely pH 2 and [Eu]= 5.10^{-7} M
- controlled atmosphere ($pCO_2 = 0$) and alkaline pH to see the trihydroxi-complex $Eu(OH)_3$ (aq.), namely pH 10 and [Eu]= 5.10^{-7} M
- carbonate medium and alkaline pH to see the tricarbonate-complex $Eu(CO_3)_3^{3-}$, namely pH 10 and [Eu]= 5.10^{-7} M.

The identification of the first and second hydroxo complexes will be difficult as seen on Figure 10.

The following figures present fluorescence spectra obtained under these conditions:

➢ The spectrum of **free europium** (figure 7) presents two peaks : 593 nm with a full width at mid height (FWMH) equals to 6.5 nm and 618 nm with a FWMH equals to 9.5 nm. The peak ratio 593 / 618 is equal to 4 to 1. This is characteristic of europium which presents a fluorescence spectrum in the red with strongest lines around 580, 593, 618, 650 and 700 nm ($^5D_0 \rightarrow {}^7F_J$, J = 0-4)), the transition at 618 nm ($^5D_0 \rightarrow {}^7F_2$) being hypersensitive. This feature is very important in complexation studies since its

intensity is enhanced in the case of complexation with a ligand, relative to its intensity in aqueous medium (no complexation).

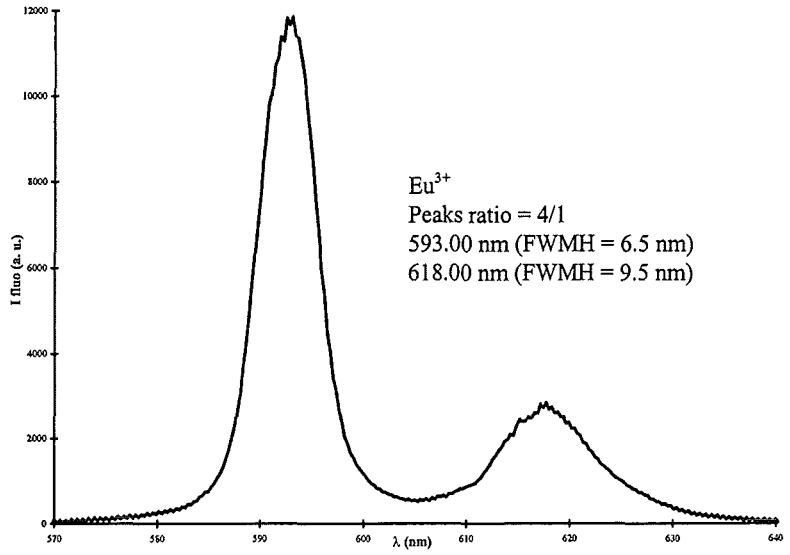

Figure 7: Spectrum of free europium Eu^{3+}.

- For the tri carbonate complex $\mathbf{Eu(CO_3)_3^{3-}}$ (figure 8), two peaks are present : 594 nm with a FWMH equals to 8.0 nm, and 618 nm with a FWMH equals to 9.5 nm. A little shoulder is observed on the 618 nm peak. Under these conditions, due to complexation with carbonate ions, the peak ratio 594 / 618 is equal to 1 to 6.

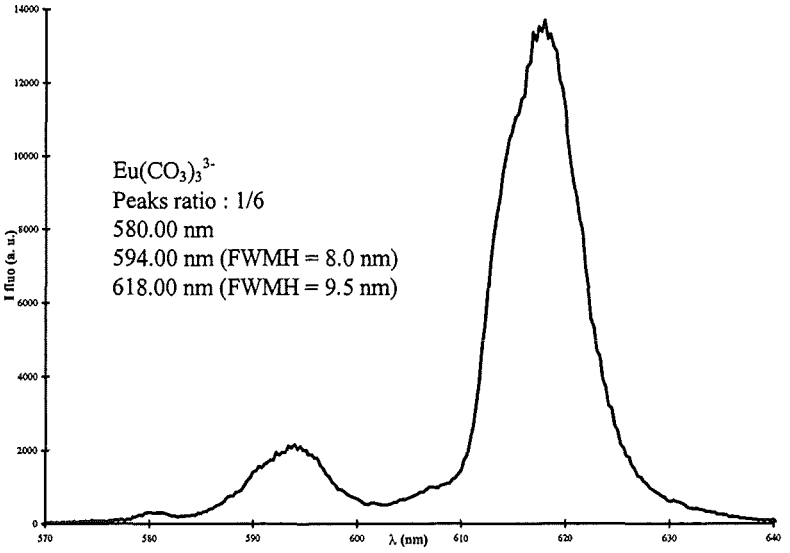

Figure 8 : Spectrum of the tri carbonate complex $Eu(CO_3)_3^{3-}$

- For the tri- hydroxo complex **$Eu(OH)_3$** (figure 9): at 593 nm, two peaks can be observed with a total FWMH equals to 12.5 nm and one at 615 nm with a shoulder at 623 nm. The peak ratio is equal to 2 to 3.

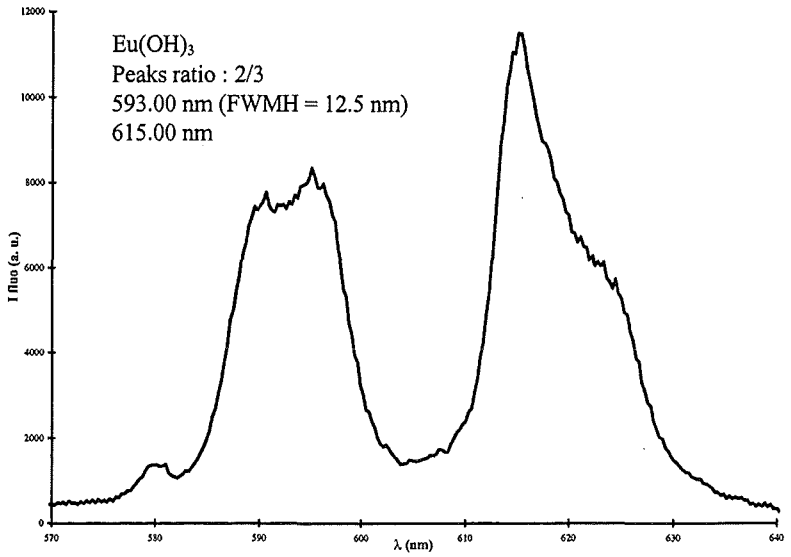

Figure 9 : Spectrum of the tri- hydroxo complex $Eu(OH)_3$.

In order to illustrate the complexity of the spectral identifications of Eu species, an example of the spectrum obtained at pCO2 = 0 and at pH = 7.5 (where free europium Eu^{3+} and the first hydroxo complex are the main species) is presented figure 10.

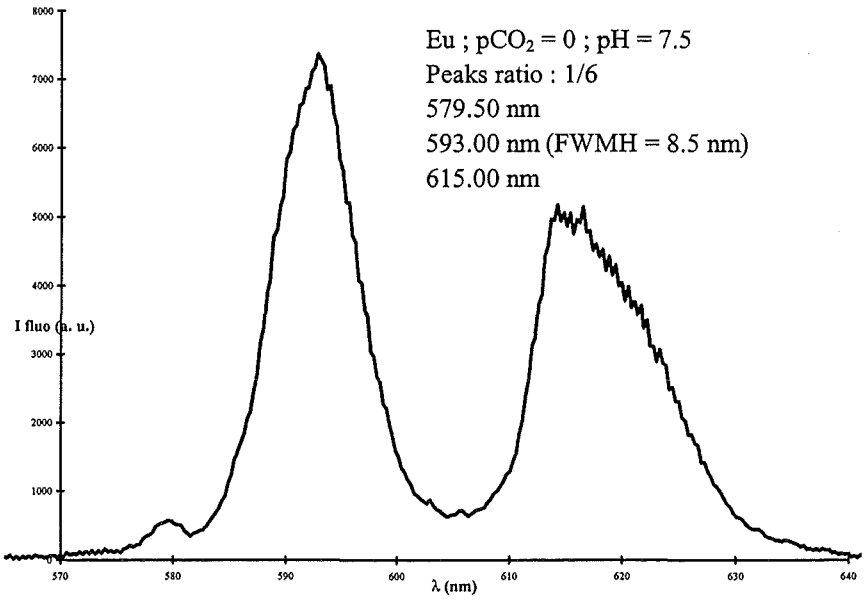

Figure 10 : spectrum at $pCO_2 = 0$ and pH = 7.5.

All the results are summarised in the table 3: for each species, the spectral data (main fluorescence wavelengths and full width at mid height) and the lifetimes are presented. The identification of the other hydroxide complexes is in progress (Plancque et *al.*, 1999). Results obtained for the tricarbonate are in good agreement with literature data (Kim et *al.*, 1994).

Species	Fluorescence wavelength (nm) and peak ratio [ ]	FWMH (nm)	Lifetime (μs)
Eu^{3+}	593 / 618 [4/1]	6.5 / 9.5	110 ± 10
$EuOH^{2+}$	identification under progress	-	-
$Eu(OH)_2^+$	identification under progress	-	-
$Eu(OH)_3(aq.)$	593 / 615 [2/3]	12.5 / -	-
$Eu(OH)_4^-$	identification under progress	-	-
$Eu(CO_3)^+$	to perform	-	170 ± 10
$Eu(CO_3)_2^-$	to perform	-	230 ± 15
$Eu(CO_3)_3^{3-}$	594 / 618 [1/6]	8.0 / 9.5	400 ± 30

Table 3 : Spectral data and lifetimes for inorganic complexes of europium.

3.2. PERSPECTIVES

The next step will be to study the interactions between the trivalent Eu and humic acids by time-resolved laser-induced fluorescence in order to determine if there is formation of mixed complex. Then, their interaction constants and the impact on the speciation diagram will be performed.

3.3. REFERENCES

Bador R., Morin M., Dechaud H. (1989) Detection of Eu and Sm by chelation and laser excited time-resolved fluorimetry. *Analytica Chimica Acta* **219**, 66

Decambox P., Berthoud T., Kirsch B., Mauchien P. and Moulin C. (1989) Direct determination of traces of lanthanide ions in aqueous solutions by laser-induced time-resolved spectrofluorimetry. *Analytica Chimica Acta* **220**, 235.

Dierckx, A. Maes A. and Vancluysen J. (1994) Mixed complex formation of europium with humic acid and competing ligand. *Radiochimica Acta* **66/67**, 149.

Dobbs J.C., Susetyo W., Knight F.E., Castles M.A., Carreira L.A., Azaraga L.V. (1989) Characterization of metal binding sites in fulvic acids by lanthanide ion probe spectroscopy. *Analytical Chemistry* **61**, 483.

Horrocks W.deW., Sudnick D.R. (1979) Lanthanide ion probes of structure in biology. Laser induced luminescence decay constant provide a direct measure of the number of metal coordinated water molecules. *Journal of the American Chemical Society* **101**, 334.

Kim J.I., Klenze R., Wimmer H., Runde W. and Hauser W. (1994) A study of the carbonate complexation of Cm and Eu by Time-Resolved Laser-Induced Fluorescence. *Journal of Alloys and Compounds* **213/214**, 333.

Moulin C., Larpent C., Gazeau D. (1999) Interaction studies between europium and a surfactant cage TAC8 by Time-Resolved Laser-Induced Fluorescence. *Analytica Chimica Acta* **378**, 47.

Plancque G., Moulin V., Toulhoat P. and Moulin C. (1999) Inorganic speciation of europium by Time-Resolved Laser-Induced Fluorescence. *Analytica Chimica Acta*. To be published.

Wolery T., Daveler S.A. (1992) EQ6, a computer program for reaction path modeling of aqueous geochemical systems. UCRL-MA-110662, LLNL.

4. CASE OF THORIUM : EFFECTS OF THE PRESENCE OF HUMIC SUBSTANCES UPON THE SORPTION OF Th ONTO SILICA COLLOIDS

Pascal Reiller, Valérie Moulin, Christian Dautel

Thorium is usually regarded as an analogue for the other tetravalent actinides. The available data about the complexation of Th(IV) with humic substances have been obtained by Nash and Choppin (1980) revised by Choppin and Allard (1985). Unfortunately, these data have been obtained in a pH range which is irrelevant of natural media ($3.5 \leq pH \leq 5$), and have to be taken with care when used in the conditions of natural waters. Nevertheless, on the basis of those data, a sensitivity study recently led by Reiller and Moulin (1998), showed that the humic acids (HA) complexes of Th(IV) can be the major species in clayey waters up to pH 7. Otherwise, Negrel and Toulhoat (1995) noted that in deep granitic waters, thorium is associated with particulate matter.

Hence, there lies a need for the determination of complexation constants for the system Th(IV)-HA, in order to ascertain the speciation of this element in the pH range relevant of natural media. In this study, an indirect method has been used to reach the complexation constants related to the system Th-HA, using the competition between humic complexation and the sorption onto silica colloids. These reactions will actually be competitive reactions in natural waters. Silica colloids have been chosen because of their weak interaction with humic acids (Labonne-Wall (1997)). Recently, the influence of humic and fulvic acids on the americium(III) and uranium(VI) sorption onto silica has been quantified by Labonne-Wall *et al.* (1997). The authors have clearly demonstrated, especially in the case of silica-Am-humic acid system, that the complexation of organic matter implies the decrease of the sorption onto the mineral surface. Hence, an enhancement of the mobility of Am(III) can be postulated in this peculiar system.

In the case of Th(IV), Cromières *et al.* (1998) quantified the interaction with hematite – α-Fe_2O_3 – colloids using non electrostatic and diffuse double layer surface complexation models, and the hydrolysis constants recommended by Bäes and Mesmer (1976). The Kurbatov approach (non electrostatic approach), for I = 0.1 M, allow the description of Th retention onto hematite colloids by considering equilibria involving different hydroxo surface complexes, $\equiv FeOH\text{–}Th^{4+}$, $\equiv FeOTh(OH)_2^+$, $\equiv FeOTh(OH)_3$ and $\equiv FeOTh(OH)_4^-$.

Östhols (1995) and Östhols *et al.* (1997) studied the adsorption of thorium onto amorphous pyrogenic silica colloids ($d \approx 30$ nm, 0.44 meq/g at 0.1 M), considering the following equilibrium at I = 0.1 M, using the surface complexation theory:

$$2 \equiv SiOH + Th^{4+} \leftrightarrows (\equiv SiO)_2Th^{2+} + 2\,H^+ \qquad \log K = -1.98 \pm 0.48 \qquad (1),$$

but the authors have only investigated a narrow range of pH irrelevant of natural waters, and rather high Th/SiO_2 ratios – $2 \leq pH \leq 4$; $8.35\ 10^{-8}$ to $9.9\ 10^{-6}$ mol Th /g SiO_2 –.

The objectives of this work are to study the influence of humic acids upon the sorption of a tetravalent actinide upon silica, one of the major component of the colloidal matter contained in natural waters (Degueldre (1994)), and to deduce from this study interaction constants relative to the system Th-HA. In a first part, the thorium-silica system is characterised using the Kurbatov approach of a surface complexation model. In a second part, the behaviour of thorium in a ternary system composed of Th(IV), silica and humic acids is investigated.

4.1. EXPERIMENTAL

Materials

The sol-gel silica used was obtained from AEA Harwell in the form. The size distribution is monomodal centred on a diameter of 98 nm. The specific surface is calculated to be 50 $m^2.g^{-1}$. The proton exchange capacity is 0.3 $meq.g^{-1}$.

Purified Aldrich humic acids (HA) are used in a protonated form. Their main characteristics are detailed in Kim et *al.* (1991), as part of an EC Mirage project (Kim, 1990). Their proton capacities are 5.4 meq/g for HA-Aldrich (determined by potentiometric titrations). Their apparent acidity constants (determined as the pH at mid-equivalence) are: $pK_a^{HA} = 4.3$.

The initial solution of thorium – ^{228}Th in 2 N HNO_3 – was obtained from Amersham. This solution was diluted in order to obtain a 1.09 10^{-9} M stock solution in 0.9 M $NaClO_4$ and HNO_3 0.2 M. All other chemicals were reagent grade, and Millipore water was used.

The sorption experiments were conducted in batch procedure at room temperature in polycarbonate vials sealed with screwcaps. The concentration of the silica suspension was fixed at 50 $mg.L^{-1}$, *i.e.* 1.5 10^{-2} $meq.L^{-1}$, by diluting the stock solution in the background electrolyte, and aliquots of humic acid was added and the pH was adjusted at the desired value with a TACUSSEL pHmetre (PHM 220 MeterLab) equipped with a combined TACUSSEL electrode (Radiometer type XC 161). The ionic strength were kept constant – I = 0.1 M – through all of the experiments. The obtained suspension was shaked for 24 hours to allow equilibration of the adsorbent. The radionuclide was added to obtain a final concentration of 1.15 10^{-12} M, corresponding to a ratio of 2.29×10^{-11} mol/g or 1.31×10^{7} eq of sites/mol; the pH was adjusted again. The solution was shaked again for 24 hours, and 2 mL of the suspension was sampled for thorium activity measurement (A_1), in order to get rid from Th(IV) adsorption upon the vial walls as described by Cromières (1996) and Cromières *et al.* (1998). The colloids are separated from the liquid phase by ultracentrifugation (90 min, 40 000 rpm), the pH of the supernatant is measured and another aliquot of 2 mL is sampled from the supernatant for thorium activity measurement (A_2).

The activities of ^{228}Th are measured by liquid scintillation counting. The previous samples are added to 4 mL of liquid scintillator. The activity measurements are performed after one month in order to attain the

secular equilibrium of ^{228}Th with its daughters. No quenching effects due to either silica or humic acids affects the counting. The initial thorium activity (A_o) was determined by direct addition into the liquid scintillator.

Sorption percentage is calculated form the activities of the suspension (A_1) and of the supernatant (A_2) according to the following equation:

$$P\,(\%) = \frac{A_1 - A_2}{A_1} \times 100$$

The distribution coefficient, K_d, is given by:

$$K_d\,(mL.g^{-1}) = \frac{[Th]_{sorbed}}{[Th]_{solution}} = \frac{P \times 10^6}{[SiO_2](mg.L^{-1})\,(100 - P)}$$

4.2. RESULTS AND DISCUSSIONS

4.2.1. SORPTION OF THORIUM ONTO SILICA WITHOUT HUMIC ACIDS.

The results for the thorium sorption onto silica without HA obtained for 4 independent experiments are shown on figure 11. It can be seen that the Th sorption onto silica surface increase with the pH increase. As a comparison, results obtained by Östhols (1995) are also reported on figure 11.

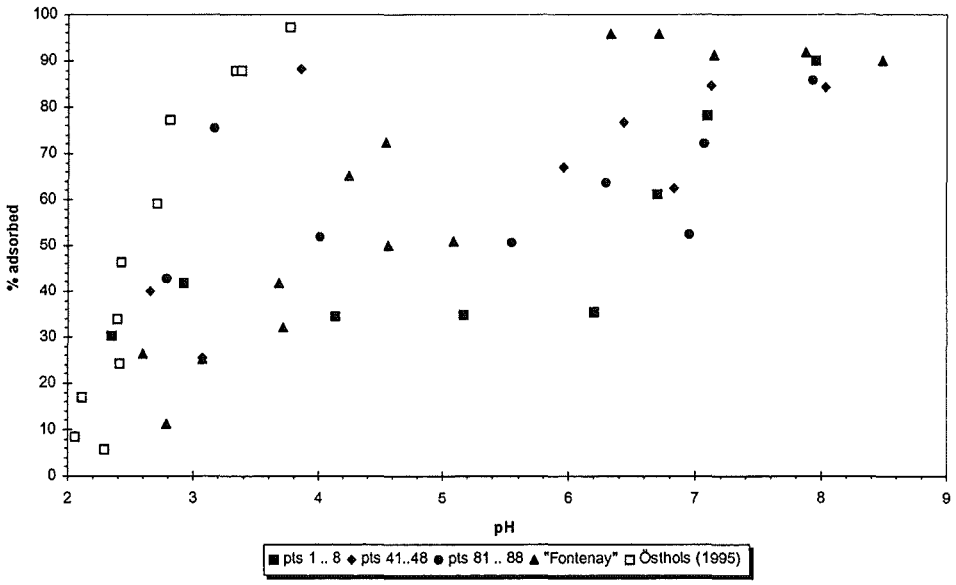

Figure 11 : Different sorption experiments of Th onto silica as a function of pH. [Th] = 1.15 10^{-12} M, [SiO_2] = 50 mg.L^{-1}, I = 0.1 M ($NaClO_4$)

If a trend can be inferred, the dispersion of our primary data set is clearly too high to be totally satisfactory. Furthermore, only few points from our data are in agreement with the ones obtained by Östhols (1995). This fact is to be related with the long time observed difficulty to conduce adsorption works on this element (Rydberg and Rydberg (1952), and Cromières (1996) for our experimental conditions). One has to take into account the differences between:

- specific surface of the colloids: 50 $m^2.g^{-1}$ in our case and 163 $m^2.g^{-1}$ for Östhols (1995);
- the synthesis method: sol-gel in our case and pyrogenic for Östhols (1995).

Nevertheless for pH range above 5.5, the results are in fair agreement with those obtained by Cromières *et al.* (1998).

Interpretation of results: proposition of sorption mechanisms

Regarding to the low Th concentration, and the isolation of the system from atmospheric CO_2, only the monomers induced by the hydrolysis are taken into account. There is a discrepancy in the various published data on Th(IV) hydrolysis. The most accepted values are those determined by Bäes and Mesmer (1976) and confirmed by Grenthe and Lagerman (1991). Recently, Fuger (1993) proposed corrected values of these reactions referring to I.A.E.A. works (Fuger *et al.* (1992)). The cumulative constants of thorium(IV), corrected for 0.1 M ionic strength, are reported in table 4 – $\varepsilon_{Th(IV)}$ were taken as equal to $\varepsilon_{U(IV)}$ in Grenthe *et al.* (1992) –.

Table 4 : Hydrolysis cumulative constants of Th^{4+}, corrected for 0.1 M ionic strength using SIT method (Grenthe *et al.* (1992)) except for Ryan and Rai (1987).

Equilibrium	$\log \beta_i^*$ Fuger (1993) $I = 0.1$ M	$\log \beta_i^*$ Bäes and Mesmer (1976) I = 0.1 M
$Th^{4+} + H_2O \rightleftarrows Th(OH)^{3+} + H^+$	– 4.14	–3.86
$Th^{4+} + 2\ H_2O \rightleftarrows Th(OH)_2^{2+} + 2\ H^+$	– 8.07	–8.01
$Th^{4+} + 3\ H_2O \rightleftarrows Th(OH)_3^{+} + 3\ H^+$	-	–12.99
$Th^{4+} + 4\ H_2O \rightleftarrows Th(OH)_4 + 4\ H^+$	≤ – 19.7 Ryan and Rai (1987) I = 0.1 M	–17.16
$Th^{4+} + 5\ H_2O \rightleftarrows Th(OH)_5^{-} + 5\ H^+$	≤ – 33.1 Ryan and Rai (1987) I = 0.1 M	

The protonation of the surface sites of silica, referring to Labonne (1993) can be represented using

the following equilibria and the related constants at the considered ionic strength:

$$\equiv SiOH_2^+ \leftrightarrows \equiv SiOH + H^+ \qquad Ka_1 = \frac{[\equiv SiOH]\,[H^+]}{[\equiv SiOH_2^+]} = 10^{-2.99} \tag{2}$$

$$\equiv SiOH \leftrightarrows \equiv SiO^- + H^+ \qquad Ka_2 = \frac{[\equiv SiO^-]\,[H^+]}{[\equiv SiOH]} = 10^{-6.54} \tag{3}$$

The point of zero charge is thus equal to 1.77, close to a pH value of 2 (Brady, 1992).

Referring to the surface complexation approach (Stumm & Morgan (1996)), the sorption of thorium, referring to Th^{4+}, upon the surface of silica colloids is described by:

$$\equiv SiOH + Th^{4+} + n\,H_2O \leftrightarrows \equiv SiOTh(OH)_n^{(3-n)+} + n\,H^+$$

with the apparent stability constant K_n:

$$K_n = \frac{[\equiv SiOTh(OH)_n^{(3-n)+}]\,[H^+]^n}{[\equiv SiOH]\,[Th^{4+}]} \tag{4}$$

including the electrostatic term.

The Kurbatov equation is then written as:

$$\log\left(\frac{K_d\,\alpha_{SiOH}\,\alpha_{Th^{4+}}}{C_e}\right) = n \times pH + \log K_n \tag{5}$$

where C_e is the proton exchange capacity (here 0.3 meq.g^{-1}), and α_{SiOH} and $\alpha_{Th^{4+}}$ are defined as follows:

$$\alpha_{SiOH} = 1 + Ka_1\,[H^+] + \frac{Ka_2}{[H^+]} = 1 + 10^{-2.99-pH} + 10^{-6.54+pH} \approx 1 + 10^{-6.54+pH}$$

$$\alpha_{Th^{4+}} = 1 + \sum_n \frac{\beta_i}{[H^+]^n}$$

and K_d as expressed previously.

The plot of the Kurbatov term as a function of pH gives a straight line with a slope n and an y intercept log K_n.

Figure 12 shows the plots of the Kurbatov term *vs.* pH compared with the speciation of Th according to both sets of hydrolysis constants (Bäes and Mesmer (1976) and Fuger (1993)). Three different regions can be distinguished:

- $2 \leq pH \leq 4$;
- $4 \leq pH \leq 5.5$;
- $5.4 \leq pH \leq 8.5$.

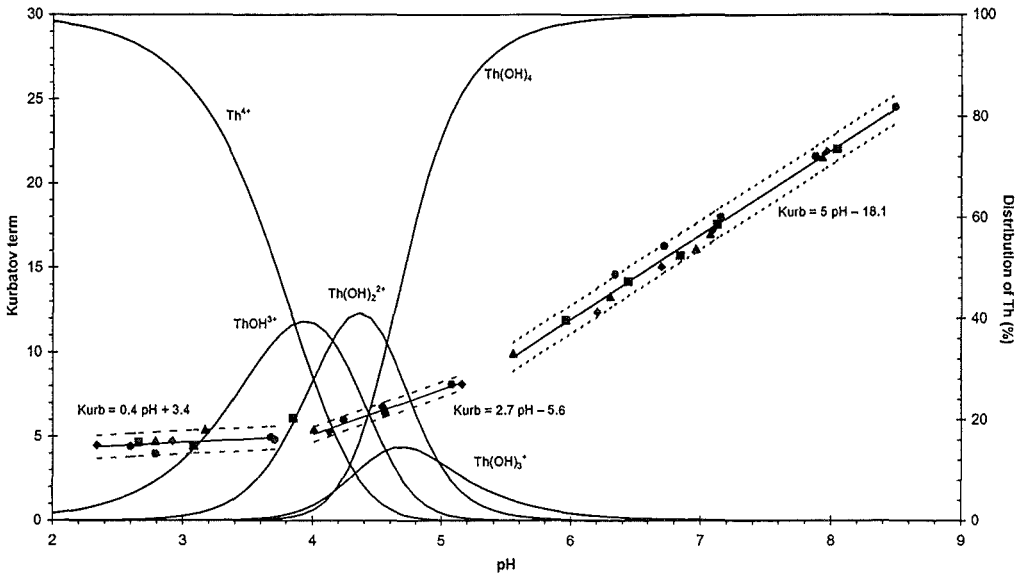

a.

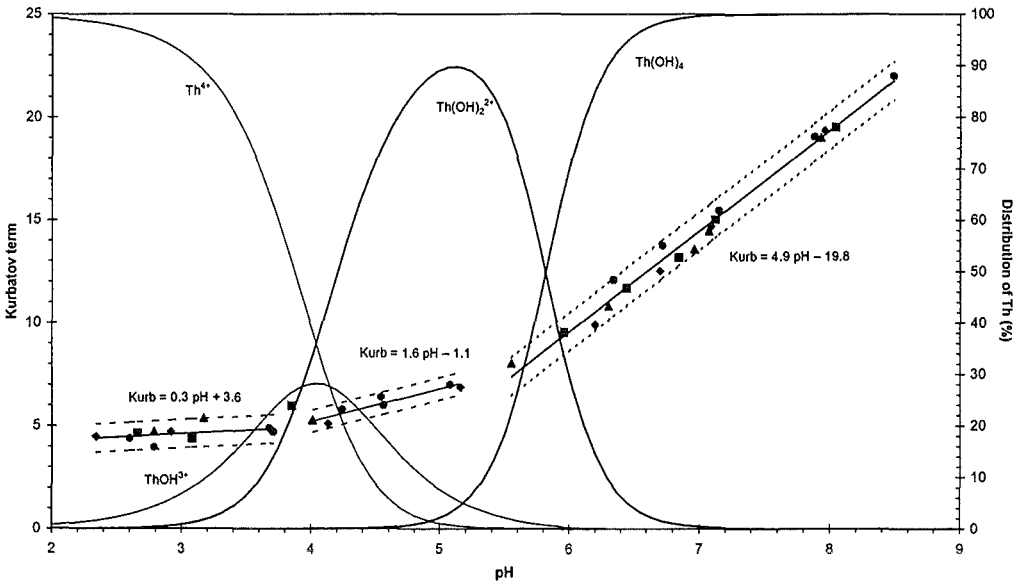

b.

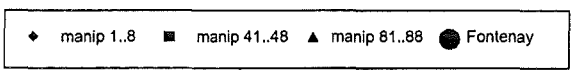

Figure 12 : Comparison of the Kurbatov plots for thorium adsorption on silica colloids, and the speciation of thorium; a. Bäes and Mesmer (1976) constants ; b. Fuger (1993) constants.

In the first region, $2 \leq pH \leq 4$, the slope obtained from the linear regression shows a combination between adsorbed species. We can propose the resulting combination of the following mechanisms:

$$\equiv SiOH + Th^{4+} \leftrightarrows \equiv SiOHTh^{4+}$$

$$\equiv SiOH + Th^{4+} \leftrightarrows \equiv SiOTh^{3+} + H^{+}$$

as it has been proposed by Cromières *et al.* (1998) for the sorption of thorium upon hematite.

In the second region, $4 \leq pH \leq 5.5$, the estimation of the slope is slightly different according to both assumptions due to the differences between the values of the hydrolysis constants:

- n = 1.6 in the case of Fuger (1993);
- n = 2.7 for the constant of Bäes and Mesmer (1976).

These values can be represented by the mean behaviour in solution of the mono, di and tri hydroxo-complexes of Th(IV) as all these species are present in this pH range – see speciation diagrams –. Thus it seems difficult to assign a weight for each complex.

In the third region, $5.4 \leq pH \leq 8.5$, the Kurbatov expressions give the following slopes:

- Kurb = (5 ± 0.3) pH – (18.1 ± 1.9), in the case of Bäes and Mesmer (1976) data;
- Kurb = (4.9 ± 0.3) pH – (19.8 ± 2.1), in the case of Fuger (1993) data.

The values of the slopes of both expressions – n = 5 – refer to the same sorbed species, whose formation is described by the equilibrium:

$$\equiv SiOH + Th^{4+} + 4\ H_2O \leftrightarrows \equiv SiOTh(OH)_4^{-} + 5H^{+}$$

This is inferred by the fact that $Th(OH)_4$ is the dominant species above pH 5.5.

The apparent stability constants are thus given by the intercepts as:

- $\log K_{S5} = -18.1 \pm 1.9$ for the Bäes and Mesmer (1976) constants;
- $\log K_{S5} = -19.8 \pm 2.1$, for the Fuger (1993) constants.

Considering 95 % confidence (2σ).

Although these values has to be taken with care, regarding to the dispersion of the data, it is interesting to compare these results with those obtained by Cromières *et al.* (1998) for the same species, with the same sorption model and the Bäes and Mesmer (1976) constants $\log K_{S5} = -18.5$ for the hematite/Th(IV) system at the same ionic strength (0.1 M).

A further assignment of the contribution of the different complexes, especially in the more acidic region, to these global results could not be ascertained. The next step of this study will be the establishment of a procedure that permits us to obtain less dispersed data in the acidic region.

4.2.2. *THORIUM SORPTION IN THE PRESENCE OF HUMIC ACIDS.*

i) sorption at constant pH

The objective of this experiment is to study the complexing behaviour of HA towards Th(IV) using silica colloids as a competing agent. Figure 13 presents the results of the sorption experiments conducted in the presence of humic acids at a constants pH, *i.e.* pH = 6.3. The concentration range covered in the experiment represents the widest range at which humic acids can be encountered in the natural media.

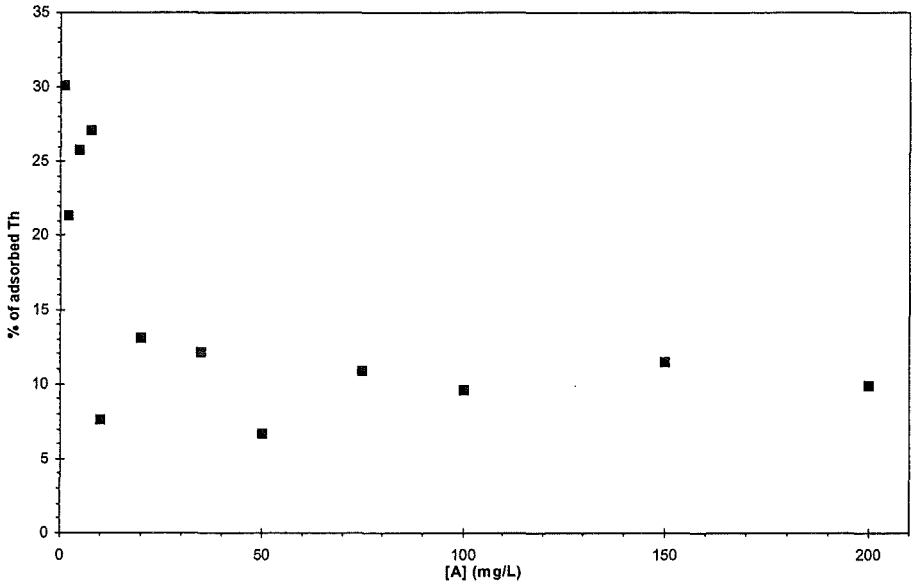

Figure 13 : Sorption of Th(IV) onto silica in the presence of Aldrich humic acid pH = 6.29 ± 0.08, [Th] = 1.15 10^{-12} M, [SiO_2] = 50 mg.L^{-1}, 1 ≤ [AH] (ppm) ≤ 200, I = 0.1 M ($NaClO_4$) .

The competitive reaction systems are easily studied using the Schubert's methods (Schubert (1948), Schubert and Richter (1948)). The following expression is used to analyse the obtained data from which the interaction constant β of the Th(IV)-HA system can be determined.

$$\log B = \log\left(\frac{K_d^o}{K_d} - 1\right) = n \log [A] + \log \beta_{obs} \qquad (6)$$

where K_d and K_d^o are the distribution coefficients defined above corresponding to the system with HA

and without HA respectively, n is the number of ligand reacting per metal, [A] is the concentration of humic acid, and log β_{obs} is the observed interaction constant of the Th-HA system. In our pH conditions, all carboxylic sites are ionised. Hence the humic acid concentration [A] is equal to the total HA concentration.

Taking into account the speciation of thorium in the experimental conditions, the conditional stability constant becomes:

$$\log \beta_{obs} = \log \frac{\beta}{\alpha(Th^{4+})} \Rightarrow \log \beta = \log \beta_{obs} + \log \alpha(Th^{4+}) \quad (7)$$

with β the apparent interaction constant referring to the equilibrium :

$$Th + A \leftrightarrows ThA$$

The variation of log B *vs.* log [A] shown on figure 14 is rather satisfactorily and is represented by the following linear relation:

$$\log B = (0.32 \pm 0.05) \log [A] + (0.81 \pm 0.07) \; ; \; r^2 = 0.818 \quad (8)$$

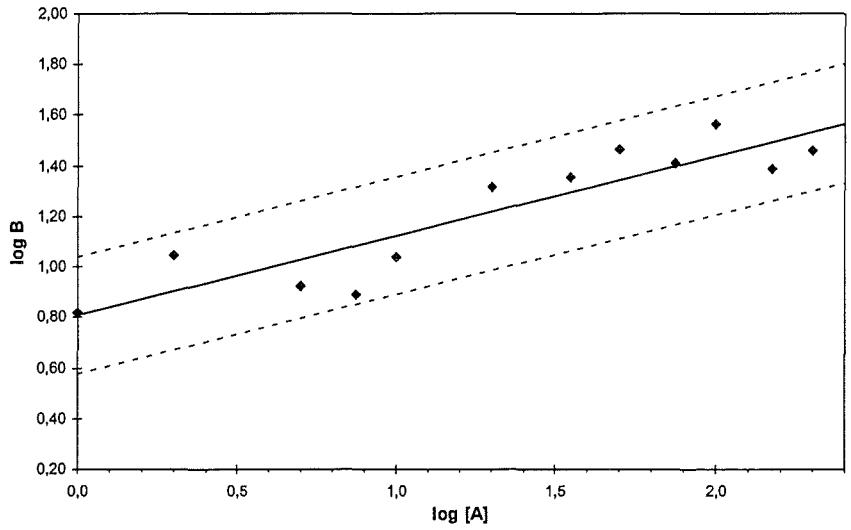

Figure 14: Determination of the parameters of thorium-AH-silica system using the Schubert method, pH = 6.3, *I* = 0.1 M.

As in the precedent case, the value of log $\alpha(Th^{4+})$ is directly dependant upon the values of the thermodynamic constants used to evaluate the speciation of thorium in the considered solution. The different values obtained using both hypothesis, for the pH value considered, *i.e.* pH = 6.29 ± 0.08, are reported in table 5, were log $\beta_{corrected}$ refers to the log β value corrected for proton capacity

Table 5 : Values of log $\alpha(Th^{4+})$ and log β for both hypothesis considered.

Ref.	log $\alpha(Th^{4+})$	log β	log $\beta_{corrected}$
Fuger (1993)	5.5 ± 0,3	6.3 ± 0.3	8.6 ± 0.6
Bäes and Mesmer (1976)	8.0 ± 0.3	8.8 ± 0.3	11.1 ± 0.7

The value of the slope of expression (8) is not equal to unity. As noted by Dierckx (1995), this implies the existence of a more complicated stoichiometry than the one stated: i) a mixed hydroxo-humic-Th(IV) complex can be adsorbed at the silica interface as in the case of other actinides (Dierckx *et al.*, 1994; Labonne-Wall *et al.*, 1997; Laszak, 1997; Marquardt and Kim, 1998), which has not been taken into account in our description; ii) the possible formation of mixed complexes in solution $Th(OH)_nHA$.

It is also important to notice that the adsorption reactions between thorium and all types of surface, including polyethylene, has always hindered the thorough study of the chemistry of this element at trace level. As noted by Östhols (1995), referring to Rydberg and Rydberg (1952), "it is probably difficult to find any vessel material that would allow studies at neutral and alkaline pH values". It is clear from the obtained results that the competitive sorption reactions took place between several systems including vessel walls, silica and humic acids. Different hypothesis can be proposed:

- as stated above, the physico-chemical properties of the silica solution are not nominal in term of dimension due to aggregation;
- the solubility of silica has not been taken into account;
- a mixed complex could be formed in solution;
- the complicated system induced by the collateral adsorption reactions between all the surfaces and thorium could lead to an apparent straight line, the slope of which may not be significant of the reaction postuled, including the adsorption of the thorium-HA complex at the surface of silica.

ii) sorption vs. pH

The variation of Th(IV) sorption onto silica in the presence of humic acids at different concentrations, has been measured *vs.* pH (I = 0.1 M, $[SiO_2]$ = 50 $mg.L^{-1}$). The experimental conditions were the same as for the previous experiments, and the results are presented on figure 15.

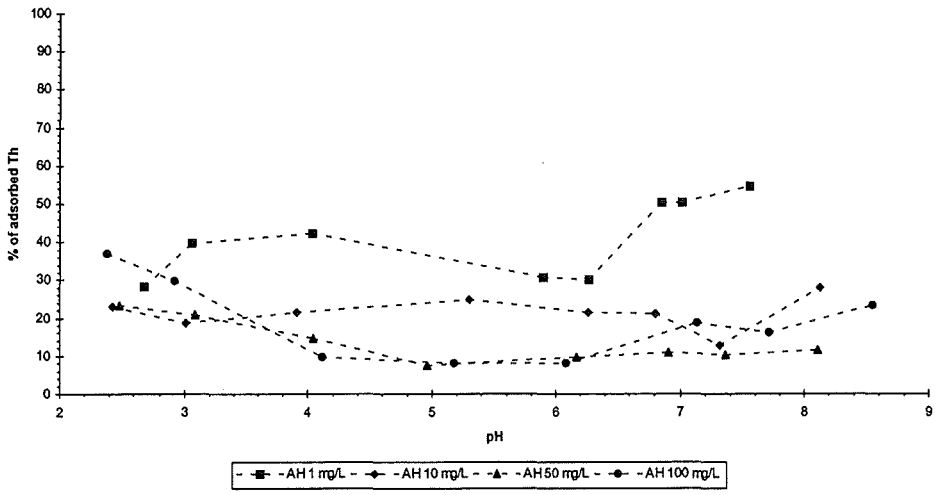

Figure 15: Sorption of thorium onto silica in the presence of humic acid *vs.* pH; [Th] = 1.15 10^{-12} M, [SiO_2] = 50 mg.L^{-1}, I = 0.1 M.

It is clearly seen on this figure that the presence of HA in solution strongly decreases Th sorption onto silica and even at 1 mg.L^{-1} of HA, demonstrating the strong complexing behaviour of HA toward Th(IV). The trend of releasing Th bound to HA in solution is clearly demonstrated and the quantification of the system is under progress.

The results obtained at pH relevant to natural waters ($6 \leq pH \leq 9$) in the presence of HA clearly put out in evidence the influence of humic acids upon the adsorption properties of thorium onto silica colloids. As it was previously demonstrated by Labonne-Wall *et al.* (1997), in the case of trivalent Am^{3+} and hexavalent uranium (UO_2^{2+}), humic acids present in natural solution are also able to desorb tetravalent actinides. The subsequent mobilisation of those elements bonded to humic substances, and the influence upon their migration behaviour has to be taken into account. The quantification of these phenomena is of a great importance in order to build an exhaustive data base about those peculiar reactions. These results also shed a light on the need of reliable thermodynamical data upon hydrolysis and carbonatation of thorium(IV).

4.3. PERSPECTIVES

Further works are under progress in order to have a better understanding of the Th-HA-Silica system. Firstly a new stock solution of silica will be used to carry out the same experiments in order to reduce the data dispersion; secondly, if the new silica solution exhibit the same behaviour, the whole system should be characterised as for retention mechanisms. The silica-thorium system will also be characterised using the more complex diffuse double layer surface complexation model. The ternary system will also be interpreted according to both surface complexation model (Kurbatov and diffuse double layer) in order to determine interaction constants for HA-Th(IV) system.

4.4. REFERENCES

Bäes and Mesmer (1976), The hydrolysis of cations, Wiley-Interscience Publications, New York.

Brady P.V. (1992), Silica surface chemistry at elevated temperatures, *Geochim. Cosmochim. Acta*, **56**, 2941-2946.

Capdevila H. and Riglet-Martial C. (1997), Données thermodynamiques sur l'oxydoréduction et la complexation des actinides en milieu hydroxocarbonate, *CEA Technical Note*, NT SESD N° 97.08.

Choppin G.R. and Allard B. (1985), Complexes of actinides with naturally occurring organic compounds, *in* "Handbook on the Physics and Chemistry of the Actinides" Chap. 11, Ed. Freeman A.J. and Keller C., Elsevier Sci. Pub.

Cromières L. (1996), Sorption d'éléments lourds (I(VI), Np(V), Th(IV), Am(III), Co(II), Cs(I), I(-I)) sur des colloïdes d'hématite. Proposition de mécanismes réactionnels, Thèse de doctorat de l'université PARIS XI ORSAY, N° 4601, 13 décembre 1996.

Cromières L., Moulin V., Fourest B., Guillaumont R. and Giffaut E. (1998), Sorption of thorium onto hematite colloids, *Radiochim. acta*, **82**, 249-256.

Degueldre C. (1994), Colloid properties in groundwaters from crystalline formations, NAGRA Report NTB 92-05.

Dierckx A., Maes A. and VanCluysen J. (1994), Mixed complex formation of Eu^{3+} with humic acid and a competing ligand, *Radiochim. Acta*, **66/67**, 149-156.

Dierckx A. (1995) Complexation of europium with humic acid : influence of cations and competing ligands. Katholieke Universiteit Leuwen. PhD thesis.

Fuger J., Khodakovski I., Sergeyeva E.I., Medvedev V.A. and Navratil J.D. (1992), The chemical thermodynamics of actinides elements and coumpounds. Part 12 : the actinides inorganic complexes, AIEA, Wien.

Fuger J. (1993), Problems in the thermodynamics of the actinides in relation with the back-end of the nuclear fuel cycle, *J. Nucl. Mat.*, **201**, 3-14.

Grenthe I. and Lagerman B. (1991), Studies on metal carbonate equilibria. 23. Complex formation in the Th(IV)-H_2O-CO_2(g) system, *Acta Chem. Scand.*, **45**, 231-238.

Grenthe I., Fuger L., Konings R.G.M., Lemire R.J., Muller A.B., Nguyen-Trung C. and Wanner H. (1992), Chemical thermodynamics of uranium, NEA-OCDE Wanner and Forest Eds. Amsterdam.

Kim, J.I., Buckau, G., Klenze R., Rhee D.S., Wimmer H. (1991) Characterisation and complexation of humic acids. CEC Report EUR 13181.

Kim, J.I. (1990) Geochemistry of actinides and fission products in natural aquifer systems. In " *CEC Project Mirage-Second Phase on Migration of Radionuclides in the Geosphere* " (B. Côme, Ed.), EUR Report 12858.

Labonne N. (1993), Rôle des matières organiques dans les phénomènes de rétention des actinides sur la silice, Thèse de doctorat de l'université PARIS XI ORSAY, N° 2911, 10 novembre 1993.

Laszak I. (1997), Etude des interactions entre substances humiques et Uranium(VI) par Spectrofluorimetrei Laser à résolution temporelle. Etude chimique et spectroscopique, Thèse de l'université PARIS VI, 18 novembre 1997.

Labonne-Wall N., Moulin V. and Villarem J.P. (1997), Retention properties of humic substances onto amorphous silica: consequences for the sorption of cations, *Radiochim. acta*, **79**, 37-49.

Marquardt C. and Kim J.I. (1998), Complexation of Np(V) with humic acid: Intercomparison of results from different laboratories, *Radiochim. acta*, **80**, 129-137.

Nash K.L. and Choppin G.R. (1980), Interaction of humic and fulvic acids with Th(IV), *J. Inorg. Nucl. Chem.*, **42**, 1045-1050.

Negrel G. and Toulhoat P. (1995), Chimie des eaux profondes en milieu granitique, *CEA Technical Report*, RT DESD N° 95.122.

Östhols E. (1995), Thorium sorption on amorphous silica, *Geochim. Cosmochim. acta*, **59**, 1249-1249.

Östhols E., Manceau A., Farges F. and Charlet L. (1997), Adsorption of thorium on amorphous silica, *J. Colloid Interface Sci.*, **194**, 10-21.

Reiller P. and Moulin V., Incidences des matières organiques naturelles sur la spéciation des radionucléides : calculs de sensibilité, *CEA Technical Report*, RT DESD 98.177.

Rydberg J. and Rydberg B. (1952), Adsorption on glass and polythene from solutions of thorium complexes in tracer concentrations, *Sv. Kem. Tidskr.*, **64**, 200-211.

Schubert J. (1948), *J. Phys. Coll. Chem.*, **52**, 340.

Schubert J. and Richter J.W. (1948) *J. Phys. Coll. Chem.*, **52**, 350.

Stumm W. and Morgan J.J. (1996), *in* "Aquatic Chemistry, chemical equilibria and rates in natural waters, Third Edition", Wiley Interscience, Chap. 9, p. 516.

Annex 5

Sorption Behavior of Humic Substances towards Iron Oxides

(Reiller et al., CEA)

2nd Technical Report
EC Project

"EFFECTS OF HUMIC SUBSTANCES ON THE MIGRATION OF RADIONUCLIDES: COMPLEXATION AND TRANSPORT OF ACTINIDES"

CEA Contribution to Task 3

SORPTION BEHAVIOUR OF HUMIC SUBSTANCES TOWARDS IRON OXIDES

Reporting period 1998

Pascal REILLER, Valérie MOULIN, Florence CASANOVA
CEA, CE-Saclay, Fuel Cycle Division, DESD/SESD/LMGS
91191 Gif-sur-Yvette, FRANCE

ABSTRACT

The sorption behavior of humic substances (HS) towards iron oxides has been studied as a function of various physico-chemical parameters, such as pH, ionic strength, nature and concentration of humic substances. The selected iron oxide is goethite as a reference mineral studied in the HUMICS project. The results show a strong influence of the different parameters under study : the HS sorption decreases when pH increases, decreases with ionic strength and is higher for humic acids compared to fulvic acids. The surface complexation approach has been applied to describe the retention of humic substances onto the goethite surface. The Kurbatov model (without electrostatic term) successfully describes the HS sorption onto goethite.

Content

1. GENERAL INTRODUCTION

The understanding of radioelement behaviour in natural systems in relation with nuclear waste disposals in geological formations necessitates the knowledge of their speciation in these systems including their distribution between the solution and the mineral phases. In particular, this implies to determine the influence of *humic substances* (humic and fulvic acids, HA/FA) as natural organic substances present in more or less concentrations in groundwaters on the migration of radionuclides, particularly actinide elements. This induces to study

- the complexation of actinides with humic substances as complexing agents,
- their influence on actinide sorption properties towards mineral surfaces and

the mobility of actinide-humic substances complexes in groundwaters.

In this framework, are objectives are the following:

- to obtain data (interaction constants, complexing capacities) on the interactions between humic/fulvic acids and actinides under relevant geochemical conditions (pH, ionic strength, presence of competing cations);
- to study the effect of humic substances on actinide migration by batch experiments.

For the part relative to the **migration** of actinides with humic substances (HA/FA), the aim is to determine for which conditions humic substances modify the migration, and in particular the **retention** of actinides onto mineral surfaces and under relevant geochemical conditions (pH, ionic strength, presence of competing cations). For this purpose, the behaviour of humic substances towards mineral phases is important to know, and particularly the formation of an organic film. The focus has been put on the systems constituted by iron oxides, and in particular goethite, and humic substances. Iron oxides are widely encountered in natural environments and present strong scavenging properties towards actinides. The effect of humic/fulvic acids on actinide sorption onto such substrate is then important to determine. The objective of the present work is to study the retention of humic and fulvic acids onto goethite (Carlsen et *al.*, 1999) as a function of physico-chemical parameters (pH, ionic strength, humic/fulvic concentration) and to propose retention mechanisms through the surface complexation approach.

2. SORPTION OF HUMIC SUBSTANCES ONTO GOETHITE

2.1. *EXPERIMENTAL*

Materials

Goethite

Goethite has been prepared according to the method of Atkinson *et al.* (1967) by NERI (Carlsen et *al.*, 1999). No further determination of surface properties were performed.

Humic substances

Purified Aldrich humic acids (HA) and fulvic acids (FA) from Fanay-Augères (granitic site) were used in a protonated form. Their main characteristics are detailed in Dellis and Moulin (1989), and Moulin *et al.* (1991) for Fanay-Augères FA and in Kim *et al.* (1991) for Aldrich HA, as part of an EC Mirage project (Kim, 1990). Their proton capacities are respectively 5.4 meq/g and 5.7 meq/g for HA-Aldrich and Fanay-Augères FA (determined by potentiometric titrations). Their apparent acidity constants (determined as the pH at mid-equivalence) are: $pK_a^{HA} = 4.3$ and $pK_a^{FA} = 3.9$. Stock solutions of Aldrich HA and Fanay-Augères FA in 0.1 M $NaClO_4$ were prepared (after dissolution in NaOH medium (pH~10; ratio 1/10) in the case of HA). All other chemicals were reagent grade, and Millipore water was used.

Procedure

The sorption experiments were conducted in batch procedure at room temperature in polycarbonate vials sealed with screwcaps. The concentration of the goethite suspension was fixed at 500 $mg.L^{-1}$, by diluting the stock solution in the background electrolyte: the pH was adjusted at the desired value with a ORION 520 A pH-metre equipped with a Radiometer XC 161 combined electrode (modified $NaClO_4$ 0.1 M, NaCl 10^{-2} M), at the desired ionic strength. The obtained suspension was shacked for 24 hours to allow equilibration of the adsorbent, and aliquots of humic acid was added: pH was checked. The solution was shacked again for 72 hours. The colloids are separated from the liquid phase by ultracentrifugation (60 min, 40 000 rpm), and the HS concentration is measured spectrophotometrically at 254 nm (Shimadzu UV-2100).

The distribution coefficient of HS, K_d, is given by:

$$K_d\ (mL.g^{-1}) = \frac{[HA]_{sorbed}}{[HA]_{solution}} = \frac{P \times 10^6}{[\alpha\text{-FeOOH}](mg.L^{-1})\ (100 - P)}$$

where P is the fixed percentage of HS onto goethite.

2.2. *RESULTS*

2.2.1. SORPTION OF HUMIC ACIDS ONTO GOETHITE AT CONSTANT PH

Figure 1a shows the sorption isotherm of HA onto goethite at pH = 5 at 0.1 and 0.001M ionic strength. Figure 1b allows an evaluation of the complexing capacity of goethite towards humic acids, and it will be calculated precisely further when the specific surface of the goethite sample will be determined.

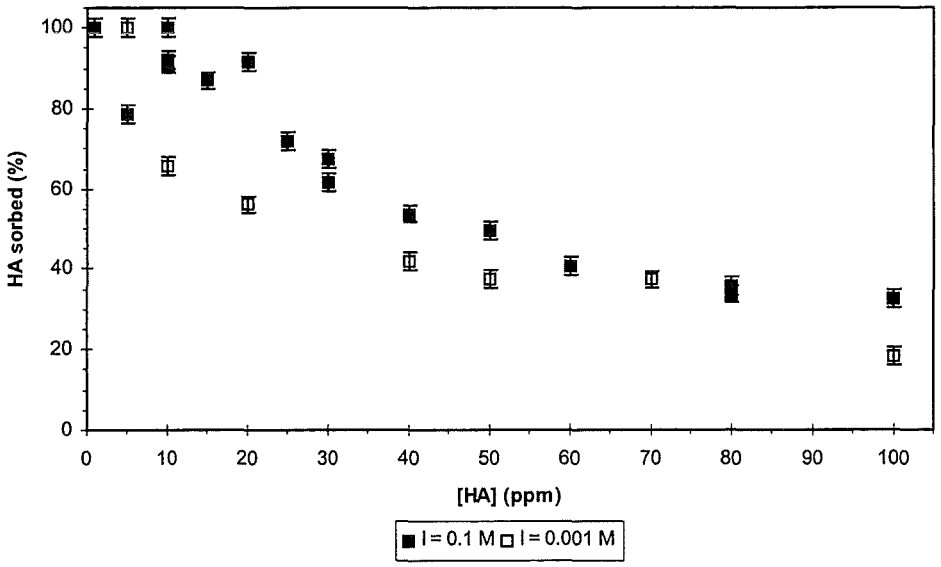

a.

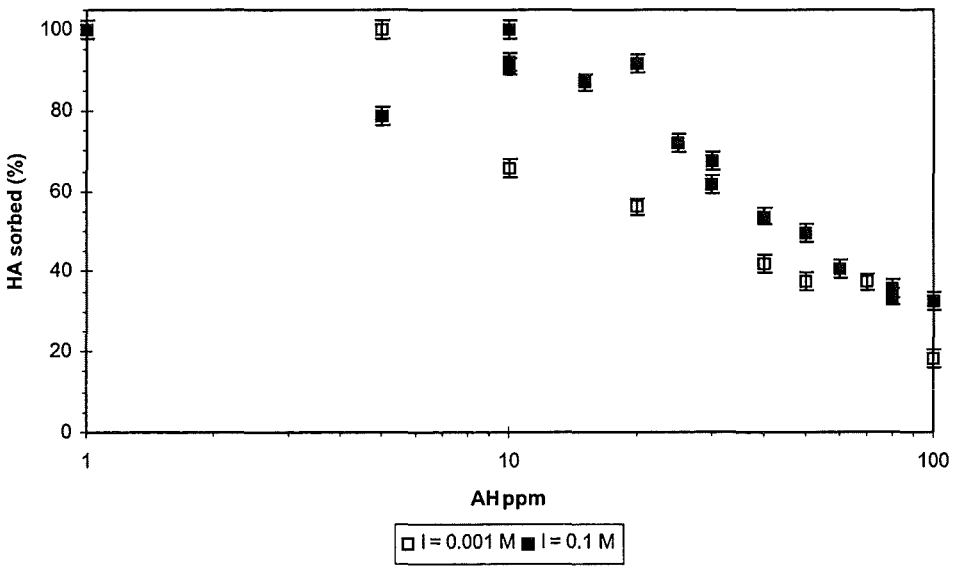

b.

Figure 1 : Sorption isotherm of Aldrich humic acid onto goethite at pH = 5 for two ionic strengths ;[α-FeOOH] = 500 mg/L

2.2.2. EFFECT OF PH ONTO THE SORPTION OF HUMIC ACIDS (HA)

The variation of retention of HA onto goethite *vs.* pH at 0.1 M ionic strength is shown on figure 2. As observed generally for iron oxides, the sorption of humic acids onto goethite decreases when pH increases. The sorption is favoured in the acidic-neutral pH range where the goethite surface is positively charged (PZC = 7.5), whereas humic acids are negatively charged in this pH range.

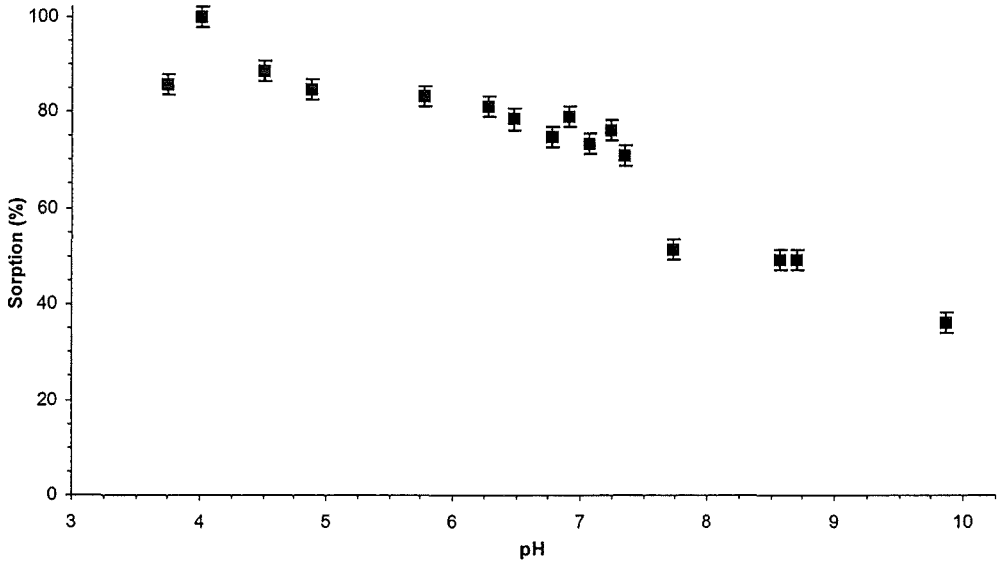

Figure 2 : Sorption of Aldrich humic acid onto goethite *vs.* pH; [α-FeOOH] : 500 mg.L^{-1}, [AH] = 10 ppm.

2.2.3. EFFECT OF THE NATURE OF HUMIC SUBSTANCES

The differences observed between both types of HS used are shown on figure 3, which shows that the retention of humic acids onto goethite is larger than that of fulvic acids. As already observed by Gu et *al.* (1995), in the case of hematite (α-Fe_2O_3), this difference may be due to the preferred sorption of larger hydrophobic molecules (HA) than smaller hydrophilic ones (FA) onto this mineral.

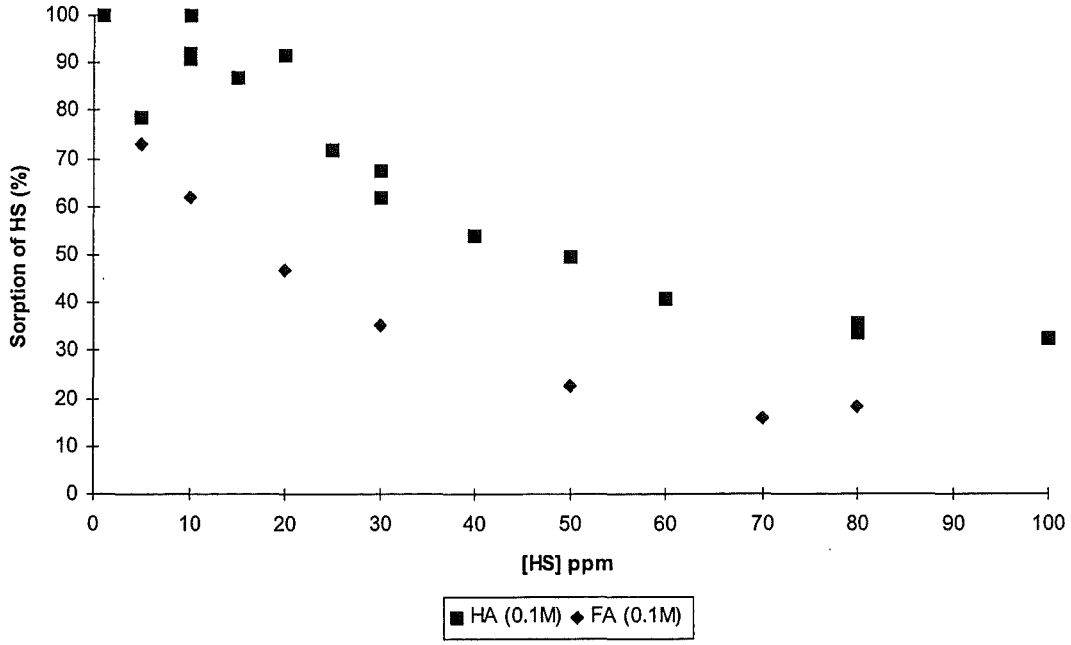

Figure 3 : Sorption of Humic Substances onto goethite; [α-FeOOH] = 500 mg/L, I = 0.1 M.

2.2.4. EFFECT OF IONIC STRENGTH

The influence of the ionic strength upon the sorption of HA and FA is shown on figure 4a in the case of the variation of pH, and figure 4b for the sorption isotherm at 10 ppm of HS. In both cases, the retention of humic substances onto goethite decreases with ionic strength. The effect is more pronounced in the case of humic acids. This is probably in relation with the fact that when decreasing ionic strength, the conformation of humic/fulvic molecules goes from a folded structure to an opened and unfolded structure (Buffle, 1988). Then at high ionic strength the molecules are smaller than at low ionic strength, which explains the higher sorption capacity at higher ionic strength.

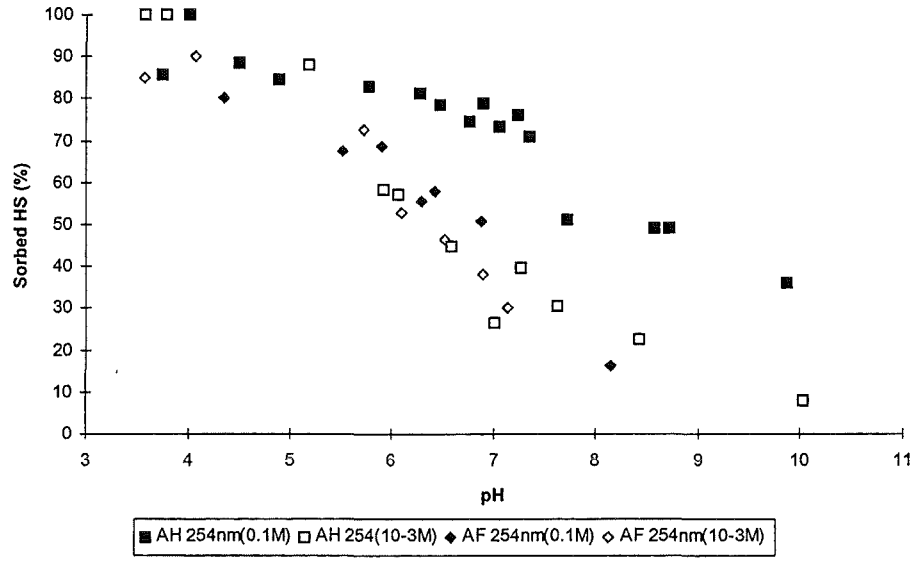

a.

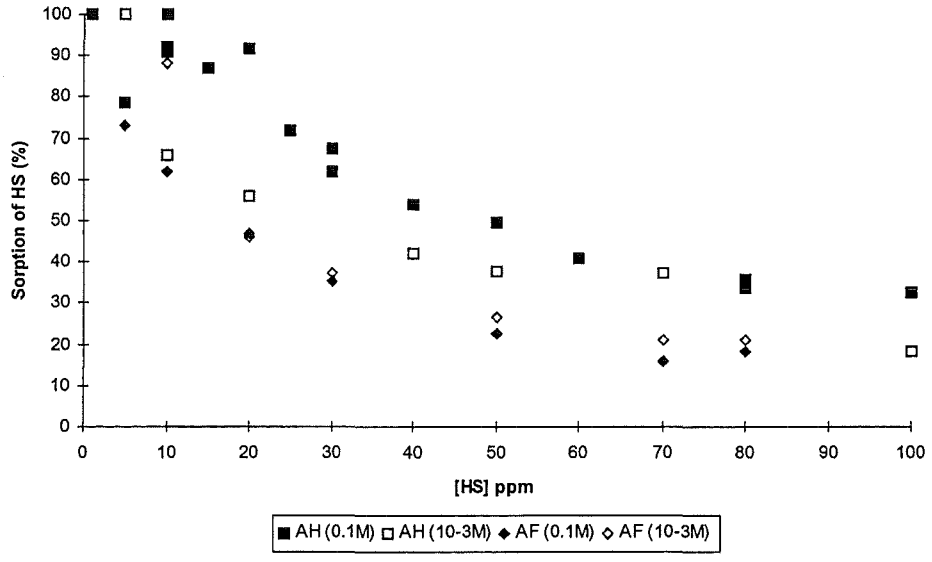

b.

Figure 4 : Sorption of Humic Substances onto goethite at different ionic strengths [α-FeOOH] = 500 mg/L; a. effect of pH, [HS] = 10 ppm; b. effect of HS concentration, pH = 5

2.3. INTERPRETATION OF DATA : PROPOSAL OF RETENTION MECHANISMS

There is a large discrepancy in between the values of PZC and of the acidity constants of the surface site of goethite that can be found in the literature: from PZC = 7.4 (Tipping and Cooke (1982), to PZC > 9 (Zeltner and Anderson (1988), Lumsdon and Evans (1994)). This can be assigned to the different degree of carbonatation as noted by Evans *et al.*(1979), Zeltner and Anderson(1988), or Lumsdon and Evans (1994).

As noted by Lumsdon and Evans (1994), the quantification of carbonatation of gœthite, and its direct influence upon the surface site, cannot be made straightforwardly. Hence, in the following, the surface sites will be noted ≡SOH and not ≡FeOH in order to take this phenomenon into account.

Referring to the surface complexation approach (Stumm and Morgan (1996)), the sorption of HA, upon the surface of goethite can be described by:

$$\equiv SOH_n^{(n-1)+} + AH \leftrightarrows \equiv SOAH + n\,H^+$$

with n = {0, 1}.

The apparent stability constant K_n^{AH} can be written:

$$K_n^{AH} = \frac{[\equiv SiOAH]\,[H^+]^n}{[\equiv SiOH_n^{(n-1)+}]\,[AH]}$$

including the electrostatic term into the constant.

The Kurbatov equation is then written as:

$$\log\left(\frac{K_d\,\alpha_{\equiv SOH}\,\alpha_{HA}}{C_e}\right) = pH + \log K$$

where α_{HA} is the ionisation factor for humic acid:

$$\alpha_{HA} = 1 + \frac{K_a}{[H^+]}$$

The protonation of the surface sites of goethite can be represented using the following equilibria and the related constants:

$$\equiv SOH + H^+ \leftrightarrows \equiv SOH_2^+ \qquad K_1^{int}$$

$$\equiv SOH \leftrightarrows \equiv SO^- + H^+ \qquad K_2^{int}$$

The ionisation factor can be written regarding to the different types of surface sites. For the positive sites ($\equiv SOH_2^+$), it can be written

$$\alpha(\equiv SOH_2^+) = 1 + \frac{1}{K_1\,[H^+]} + \frac{K_2}{K_1\,[H^+]^2} = 1 + 10^{(pK_1 + pH)} + 10^{(pK_1 - pK_2 + 2\,pH)};$$

and for the neutral sites (≡SOH)

$$\alpha(\equiv SOH) = 1 + K_1\,[H^+] + \frac{K_2}{[H^+]} = 1 + 10^{-(pK_1 + pH)} + 10^{-(pK_2 - pH)}$$

As noted in the section Materials, the goethite used has been synthesised according to the method of Atkinson *et al.* (1967), and the PZC is estimated to be 7.5 by Carlsen *et al.* (1999) according to Schwarzenbach *et al.* (1993).

In a first approach and in reference to the synthesis method, the acidity constants used were taken from Davis *et al.* (1978), $pK_1 = 4.2$ and $pK_2 = -10.8$ (PZC = 7.5), which corresponds to a carbonated goethite. The correction of ionic strength was made using the Davies equation. The total exchange capacity C_e was taken from Sigg and Stumm (1980), *i.e.* 0.2 meq.g^{-1}.

The plot of the Kurbatov term as a function of pH gives a straight line with a slope indicating the number of exchanged H^+, and an y intercept giving log K.

Figure 5 shows the plot of the Kurbatov terms for the different types of surface sites. The obtained straight lines are satisfactorily described by the following equations (± 3 σ):

$$Kurb(\equiv SOH_2^+) = (1{,}68 \pm 0{,}09)\ pH - (1{,}74 \pm 0{,}65)$$

$$Kurb(\equiv SOH) = (0{,}68 \pm 0{,}09)\ pH + (2{,}46 \pm 0{,}65)$$

These both equations lead to the proposition of the following equilibria:

$$\equiv SOH_2^+ + AH \leftrightarrows SOAH + 2\,H^+ \qquad \log K_2^{AH} = -1.74 \pm 0.65$$

or

$$\equiv SOH + AH \leftrightarrows SOAH + H^+ \qquad \log K_1^{AH} = 2.46 \pm 0.65$$

which are strictly equivalent because $\Delta \log K^{AH} = 4.2 \approx pK_1 = 4.17$ in our conditions.

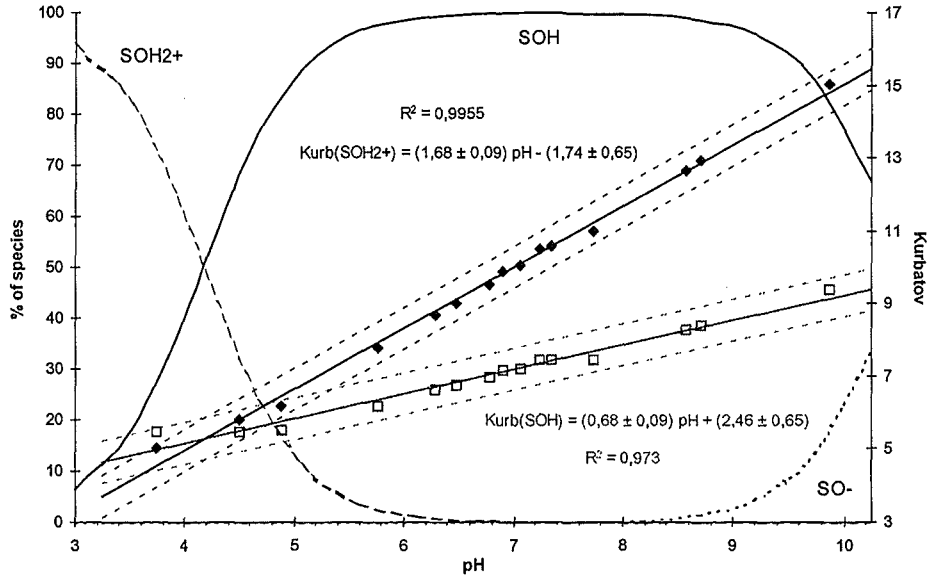

Figure 5 : Comparison of the Kurbatov plots for HA sorption onto goethite, and the repartition of the surface site.

3. PERSPECTIVES

The obtained interaction constants are deeply dependant of the stated surface properties of the goethite sample, *i.e.* acidity constants and total exchange capacity. Hence, further works are under progress to obtain the needed parameters. Afterwards, the application of the diffuse double layer model would be applied to represent the speciation of the surface site of goethite under the experimental conditions.

After having characterised the binary systems constituted by HA,FA/goethite, the impact of such organic molecules on a radionuclide sorption will be investigated. The case of Th(IV) (or Am(III)) will be studied.

4. REFERENCES

Atkinson R.J., Posner A.M. and Quirk J.P. (1967) Adsorption of potential-determining ions at the ferric oxide-aqueous electrolyte interface, *J. Phys. Chem.*, **71**, 550-558.

Buffle J. (1988), Complexation reaction in aquatic system. An analytical approach, Ellis-Horwood, Chichester.

Carlsen L., Lassen P. and Volfing M.B. (1999) Sorption of humic acids to kaolinite and goethite. Contribution to the technical report 1998 for the HUMICS project.

Davis J.A., James R.O. and Leckie J.O. (1978) Surface ionization and complexation at the oxide/water interface I. Computation of electrical double layer properties in simple electrolytes, *J. Colloid Interface Sci.*, **63**, 480-499.

Dellis T. and Moulin, V. (1989) Isolation and characterisation of natural colloids, particularly humic substances, present in a groundwater. In: *Proceedings of the 6th International Symposium on Water-Rock Interaction/Malvern* (E. Miles, Ed.), Balkema, Rotterdam, pp 197-201.

Evans T.D., Leal J.R. and Arnold P.W. (1979), The interfacial electrochemistry of goethite (α-FeOOH) especially the effects of CO_2 contamination, *J. Electroanal. Chem.*, **105**, 161-167.

Gu B., Schmitt J., Chem Z., Liang L. and McCarthy J.F. (1995), Adsorption and desorption of different organic matter fraction on iron oxide, *Geochim. Cosmochim. Acta*, **59**, 219-229.

Kim, J.I. (1990) Geochemistry of actinides and fission products in natural aquifer systems. In: *CEC Project Mirage-Second Phase on Migration of Radionuclides in the Geosphere* (B. Côme, Ed.), EUR Report 12858.

Kim, J.I., Buckau, G., Klenze R., Rhee D.S. and Wimmer H. (1991) Characterisation and complexation of humic acids. CEC Report EUR 13181.

Lumsdon D.A. and Evans L.J. (1994) Surface complexation model parameters for goethite (α-FeOOH), *J. Colloid Interface Sci.*, **164**, 119-125.

Moulin V., Billon, A., Theyssier, M. and Dellis T. (1991) Study of the interactions between organic matter and transuranic elements. CEC Report EUR 13651 (1991).

Schwarzenbach, R.P., Gschwend, P.M. and Imboden, D.M. (1993), in "Environmental Organic Chemistry", Wiley, New York, Table 11.5.

Sigg L. and Stumm W. (1980), The interaction of anions and weak acids with the hydrous goethite (α-FeOOH) surface, *Colloids and Surf.*, **2**, 101-117.

Tipping E. and Cooke D. (1982), The effect of adsorbed humic substances on the surface charge of goethite (α-FeOOH) in freshwaters, *Geochim. Cosmochim. Acta*, **46**, 75-80.

Wang, L., Chin, Y.-P., Traina, S. J. (1997), Adsorption of (poly)maleic acid and an aquatic fulvic acid by goethite, *Geochim. Cosmochim. Acta*, **61**, 5313-5324.

Zeltner W.A. and Anderson M.A. (1988), Surface charge development at the goethite/aqueous solution interface: effects of CO_2 adsorption, *Langmuir*, **4**, 469-474.

Annex 6

Influence of Organic Coating and calcium Ions on the Sorption of Europium on a Silica Gel

(Fleury et al., GERMETRAD)

Second technical report

EC Project

"Effect of humic substances on the migration of radionuclides : complexation and transport of actinides"

GERMETRAD – Contribution to Task 3

Influence of the organic coating and calcium ions on the sorption of europium on a silica gel

Reporting period 1998

C. FLEURY, C. BARBOT, J. PIERI, J.P. DURAND, F. GOUDARD

GERMETRAD
2, rue de la Houssinière BP 92208 F-44322 NANTES Cédex 3

ABSTRACT

Humic substances, ubiquitous polyelectrolyte and polydisperse macromolecules, have a great affinity towards heavy metals and radionuclides. It is important to understand the role of these substances in the migration of contaminants that could be accidentaly released from radioactive waste repositories. The migration of these radionuclides is also governed by different influent parameters like pH, flow rate, ionic strength and presence of competing cations.

Lab experiments have been undertaken, they allowed us to confirm that the behaviour and dispersion of europium (used as analog of actinides) depends on the presence of humic acids. If the latter are bound to mineral surfaces, they immobilize the radionuclides. On the other hand, if they are in a suspended form, they are able to decrease the influence of some parameters (pH, flow rate or ionic strength) and to stabilize europium onto the mineral surfaces.
The presence of calcium cations tends to increase the migration of Eu at lower flow rates and at most alcaline pH.

INTRODUCTION

The storage of radioactive waste is a topical subject. Concerning the actinides, the security of the site must be ensured for thousand years. In the case of an accidental release of radionuclides in the environment, the natural phenomena implicated in their dispersion have to be known.

Humic substances (HS), polyelectrolyte and polydisperse macromolecules, are ubiquitous in natural waters. It is well known that HS have a great affinity for metallic cations and particularly for the actinides. Numerous studies have already been achieved concerning uranium, neptunium or americium (Moulin and Ouzounian, 1992; Moulin and Moulin, 1995; Moulin et al., 1996).
Humic substances are mainly composed of humic acid HA (soluble at alcaline pH but insoluble at acid pH) and fulvic acid FA (soluble at all pHs). For this study, only HA have been used. Their molecular weight is often high and Mc Carthy et al. (1993) have isolated quite all the HS of a natural water sample with 1 nm to 5 nm filters corresponding to MW of 3,000 to 100,000 daltons. The elementary composition of HA shows a great amount of carbon and oxygen (50-60 % C, 30-35 % O and 4-6 % H, Stevenson, 1982). The main functional groups are carboxyls

(34-50 %), carbonyls (15-30 %), phenols (7-14 %) and alcohols OH (1-8 %) (Stevenson, 1982).

These functional groups give HA a large "cationic exchange capacity": CEC. Kim et al. (1990) determined a 5.43 meq/g CEC for the commercial humic acids from Aldrich, these HA are often considered as a reference.

We decided to study the role of humic acids in the behaviour of a lanthanide: europium. This research has been facilitated by the creation of a new material at the laboratory: a silica gel has been coated with HA which have been chemically immobilised. The advantage of this "humic acid gel" is its capability to keep HA in the solid phase. The study of the influence of humic acids in static systems "batch" or in dynamic systems "column" is then facilitated.

Parameters such as pH and incubation time (in static systems) and pH, ionic strength, flow rate, presence of calcium cations and organic coating (in dynamic systems) may thus be studied.

EXPERIMENTAL PROCEDURE

The aim of this study is to show the influence of humic acid and calcium on the sorption of europium on a silica gel. Two experimental protocoles have been performed:

- Static system (batch) to study the sorption kinetics of Eu on the "humic acid gel" and to calculate the distribution coefficient Kd of Eu between HA-gel and sodium perchlorate;
- Dynamic system (affinity chromatography column) to study the influence of some parameters (pH, ionic strength, flow rate and presence of calcium) on the migration of europium.

Material

The stationnary phase for the affinity chromatography is a silica gel C5OO which features are summarised below:

- specific surface area: 320 m^2/g;
- BET pore volume: 1.75 mL/g;

- SiO_2: 99.5 % mini.

This gel has been coated with humic acids (Aldrich). An epoxy cycle has been used to bind the silanol groups of the gel to the phenolic groups of HA. The binding of HA to silica has been schematised:

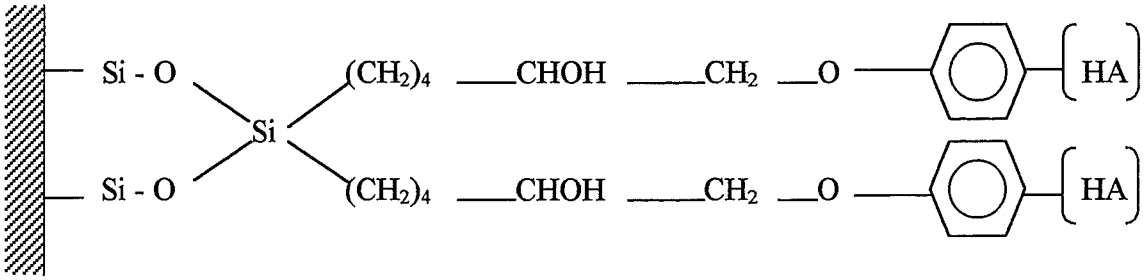

The features of this HA-gel are:
- a dark brown colour
- 18 mg HA per g of silica gel
- CEC = 2.54 10^{-2} meq/g HA-gel for a gel with only 2.3 mg HA / g silica gel (Czerwinsky et al.).

The humic acid gel has been used for the chromatographic experiments and for the batch experiments because it is easily centrifuged (10,000 rpm). Another advantage of this gel is that the carboxylic groups of the HA are available for the binding of cations because only the phenolic groups of the HA have been used to bind to the silica gel.

Europium (^{152}Eu) was chosen for its similarities with americium (that will be the dominant actinide in the radioactive waste for the next centuries). The gamma emission at 340 keV is detected with a gamma counting Packard Cobra II. A 10^{-8} M concentration is used in all experiments.

Sodium perchlorate has been used as liquid phase. The ionic strength was 5 10^{-2} or 5 10^{-3} M. For the experiments concerning the influence of calcium, the humic acid gel was preliminary equilibrated with $CaCl_2$ 10^{-2} M + $NaClO_4$ 2 10^{-2} M (I = 5 10^{-2} M).

The glass column used for the chromatographic experiments have a 1.1 cm diameter and are 12 cm long. The stationnary phase is only 2 cm heigh (0.7 g silica or HA-gel).

Procedure

Batch experiments allow us to determine the sorption kinetic of europium onto the HA-gel as a function of pH and presence of calcium cations. 4 mg HA-gel were incubated in $NaClO_4$ 5 10^{-2} M with europium; the concentration of HA was then 72 µg/mL suspension. Five incubation times were chosen: 10, 30, 60, 120 and 360 minutes. At the end of the experiment, an aliquot fraction (100 µL) of the suspension was taken and counted for radioactivity. The sample was then centrifuged (10,000 rpm during 2 minutes) and an aliquot fraction of the supernatant was taken and counted. In the first fraction, Eu under free form and bound to the HA was present whereas in the second fraction only free europium was detected. The percentage of Eu bound to the gel was then calculated and presented as a function of pH and incubation time. With this method, europium bound to the walls of the tubes was not taken into account.

Concerning the column experiments, the solid matrix was equilibrated overnight with sodium perchlorate at the desired ionic strength and pH. The europium sample was prepared by diluting concentrated Eu in $NaClO_4$ and adjusting the pH with NaOH or HCl (Vt = 200 µL). The sample was then injected in the column and eluted with $NaClO_4$. 1 mL fractions were collected and counted (Eu not bound to the gel). The solid phase was then taken and counted too (Eu bound to the gel). The percentage of radionuclide bound to the matrix was plotted as a function of pH, ionic strength, flow rate, presence of calcium or organic coating was calculated.

RESULTS

Batch

The results of the sorption kinetic of Eu onto HA-gel as a function of pH are presented (Figure 1). This kinetic is very fast: the maximum of retention of Eu is attained within the first hour (pH 5 to pH 7). At pH 8 the sorption seems to be slower but the same percentage is reached after 6 hours incubation.

The speciation diagram of europium has been drawn (Figure 2) to try to explain the results obtained with batch and column experiments. The dominant forms are Eu^{3+}, $Eu(OH)^{2+}$, $Eu(CO_3)^{+}$ and $Eu(CO_3)_2^{2-}$ depending on the pH and on the total inorganic carbon (TIC).

Distribution coefficients Kd have been calculated with the results obtained in batch experiments after 6 hours incubation (Figure 3). The affinity of europium towards HA-gel can be visualized. The log Kd have been calculated as the amount of europium bound per mg HA (and not HA-gel). The values are comprised between 5 and 6.

Column

Sorption of europium onto the humic acid gel has been studied with column experiments. Figure 4 presents the percentage of Eu bound to the gel as a function of pH, ionic strength and flow rate. The sorption of europium is always between 80 and 100 %. The influence of the different parameters is always moderate.

Influence of the humic coating on the retention of europium onto the silica gel has been investigated (Figure 5). Reference experiments have been realized with silica gel without organic coating. The sorption of Eu onto this matrix has been studied as a function of pH and flow rate in $NaClO_4$ 5 10^{-2} M. The influence of flow rate on the retention of Eu onto silica gel is more important than in the case of HA-gel. The percentage of sorption of the radionuclide is weaker in the absence of organic coating. pH seems to have a limited impact on the retention of Eu.

The influence of competing cations on the sorption of Eu onto the HA-gel seems to be interesting to study. Column experiments in presence of calcium have been performed. In this case, the HA-gel was preliminary equilibrated with $CaCl_2$ 10^{-2} M and $NaClO_4$ 2 10^{-2} M (I = 5 10^{-2} M). The results are presented Figure 6 with the reference values of retention of Eu onto HA-gel without calcium ions. Ca^{2+} seems to be more influent at alkaline pH. At pH 5 the sorption of Eu is the same with and without calcium whatever the flow rate.

DISCUSSION

It is now well known that humic acids have a great affinity for actinides and their homologues the lanthanides. Batch experiments (Figure1) allowed us to confirm the strong affinity and the rapidity of the binding between europium and humic acids. Clark and Choppin (1996) have

already remarqued this rapidity and they estimated that europium could sorb to HA (and to synthetic polyelectrolytes) within the first minute and then 90 % of Eu is bound to HA in 24 hours. The kinetics that we obtained also show that the maximum of sorption of Eu was attained after only 10 minutes of incubation (pH 5 to pH 7).
At pH 8, the sorption kinetic seems to be slower. However, the amount of available sites on the HA increases with pH principally because of the deprotonation of carboxyl groups. Kim et al. (1989) found a cationic exchange capacity CEC equal to 81.5 % at pH 6 for Aldrich humic acids ($NaClO_4$ 0.1M), this CEC increases with pH.

To understand the behaviour of europium we have to consider the speciation forms of the radionuclide as a function of pH and total inorganic carbon (Figure 2). The amount of Eu^{3+} decreases from 100 % at pH 5 to 0 % at pH 8. The hydrolysed and carbonated species appear from pH 6; $Eu(CO_3)^+$ is the dominant species at pH 8. The steric hindrance of these species may explain the relative slowness of the sorption at alkaline pH.

The affinity of europium towards humic acids is however always important: this is confirmed by the high values of Kd obtained in these experimental conditions (Figure 3). The Kd values are comprised between 10^5 and 10^6 for pH 5 to pH 8. The same experiments realized with the silica gel gave us values between 10^2 and 10^4. Ephraim et al. (1994) calculated Kd around 10^2 and $10^{3.5}$ for Eu and a humic acid coated silica (at pH values between 3 and 10). Our experimental Kd show that the presence of organic coating on a mineral matrix increases the affinity of the support towards radionuclides and then increases the impact of humic acids (in natural media) on the migration of these radionuclides.

Column experiments allow us to investigate the influence of flow rate that is another important factor. The influence of this parameter and also those of pH and ionic strength is shown on Figure 4. The strong affinity of Eu and HA that we already observed in batch experiments is confirmed with the high percentage of sorption of the radionuclide onto the HA-gel (80-100 %) whatever the pH, ionic strength and flow rate. Maes et al.(1991) remarked that this high affinity does not depend on the origine of the humic acids.

Column experiments have been investigated to study the influence of humic acid coating on the sorption of Eu onto the silica gel. The results have been grouped together in the Figure 5. The amount of radionuclide sorbed to the gel is once again relatively high (72 to 96 %) probably because the silica gel has a great specific surface area and a large amount of binding sites. We observed however that the influence of pH and flow rate is more pronounced than in the previous experiments with HA-gel.

These column experiments have been initially done at high and low ionic strength (5 10^{-2} and 5 10^{-3} M respectively). Unfortunately, the results obtained at the lower ionic strength were too dispersed to be used. This problem did not occur with the humic acid gel: HA seem to stabilize the binding of Eu. Their affinity for the radionuclide is greater than that of the silica gel; thus, they decrease the influence of the different parameters.

The results obtained with column experiments confirm those obtained in batch: europium binds to HA more quickly and in a stronger way than onto silica.

In natural waters, many competing cations are present; they can disturb the equilibrium existing between heavy metal ions and humic substances. We decided to study the influence of calcium on the sorption of europium onto the HA-gel. Column experiments have been performed and the results are presented in Figure 6. The sorption results obtained without calcium (figure 3, [NaClO4]=5 10^{-2} M) are considered as a reference.

In the presence of calcium, the influence of pH and flow rate is greater; calcium cations seem to disturb the sorption of europium on the HA binding sites. At pH 5, no difference is observed between the systems (with or without calcium). As the pH increases, sorption of Eu decreases and this decrease is deeper at the lower flow rate.
Higgo et al. (1993) have shown that the sorption of Ca^{2+} on fulvic acids increases with the pH. This phenomenon could explain the greater competition between Ca^{2+} and Eu for the binding sites that results in a decreasing retention of Eu onto HA. Some authors demonstrated however that Ca^{2+} don't displace Al^{3+} from HA binding sites (Tipping et al., 1988) and that humic acid preferentially bind uranium than Ca^{2+} when they can choose (Nefedov et al., 1998).
The chromatographic systems used in our experiments were preliminary equilibrated with $CaCl_2$. The calcium cations probably bind to the HA and then modify their conformation because they neutralize the negative charges. The HA molecules consequently retract and then the amount of available sites decreases.
At the lower flow rate (5 mL/h), the sorption of europium is weaker than at the higher flow rate (19 mL/h) when Ca^{2+} are present. We can do the hypothesis that europium binds to "weak sites" in a non specific way (at 19 mL/h), as suggested Rao et al. (1994). These sites could be available at the HA surface even if their conformation has been modified by calcium cations. On the other hand, at the lower flow rate, "strong" bindings occur between europium and HA sites located in the molecules. It could be supposed that these strong sites are less available in the presence of calcium and then the sorption of europium is weaker. Thus, at pH 8 (5 mL/h) the sorption of Eu on HA is three times smaller when calcium is added to the medium.

Calcium seems to have non negligeable impact on the migration of europium when the systems has been preliminary equilibrated with $CaCl_2$.

CONCLUSIONS

The security of the radioactive waste repositories is a topical problem and many laboratories are working to elucidate the natural processes involved in the dispersion of radionuclides if an accidental release occurs.

Humic substances, ubiquitous in natural waters, are known to have a great affinity towards actinides. These high molecular weight macromolecules have been intensively studied but many features are still uncertain.

Static and dynamic experiments have demonstrated that the binding between europium and humic acid is a very quick reaction and that the different parameters that we studied did not influence the high retention rate of Eu in a great extend (variations in pH, ionic strength or flow rate). However, the presence of the organic coating increases the stability of the binding with a decrease of the influence of the different parameters. Thus, we observed that the sorption of europium onto the silica gel was important but the influence of flow rate is visible.

Competing cations play a role in the sorption of Eu onto HA-gel. We remarked that calcium decreases the sorption of Eu on HA particularly when the pH increases and the flow rate decreases.

We can conclude that mineral surfaces like silica bind Eu but the retention depends on the natural parameters: flow rate and ionic strength. If these surfaces are coated with humic acids, the influence of these parameters is decreased. However, calcium ions seem to compete with europium for the HA binding sites in some specific conditions of pH and flow rate (high pH and low flow rate).

REFERENCES

CLARK S.B. and CHOPPIN G.R. (1996). A comparison of the dissociation kinetics of rare earth element complexes with synthetic polyelectrolytes and humic acid. . *ACS Symp. Series (Humic and Fulvic acids)*; 651, 207-219.

CZERWINSKI K.R., BUCKAU G., KIM J.I., MILCENT M.C., FLEURY C. and PIERI J. (1998). Quantifying the sorption of europium to humic acid coated material : understanding the role of humic acid. Submitted to Radiochimica Acta.

EPHRAIM J.H., SZABO G., and BULMAN R.A. (1994). Potentiometric titrations of chemically immobilsed humic acid and salicylic acid and their uptake of Eu(III) as a function of pH and ionic strength. *Environment International*, 20(1), 121-125.

HIGGO J.J.W., KINNIBURGH D., SMITH B. and TIPPING E. (1993). Complexation of Co^{2+}, Ni^{2+}, UO_2^{2+} and Ca^{2+} by humic substances in groundwaters. *Radiochimica Acta*, 61, 91-103.

KIM J.I. and BUCKAU G. (1991). Characterization of reference and site specific humic acid. *Rapport Européen EUR 13181 EN*, 1-59.

KIM J.I., BUCKAU G., BRYANT E. and KLENZE R. (1989). Complexation of americium (III) with humic acid. *Radiochimica Acta*, 48, 135-143.

McCARTHY J.F., WILLIAMS T.M., LIANG L., JARDINE P.M., JOLLEY L.W., TAYLOR D.L., PALUMBO A.V. and COOPER L.W. (1993). Mobility of natural organic matter in a sandy aquifer. *Envir. Sci. Technol.*, 27, 667-676.

MAES A., DE BRABANDERE J. and CREMERS A. (1991). Complexation of Eu^{3+} and Am^{3+} with humic substances. *Radiochimica Acta*, 52/53, 41-47.

MOULIN V., CASANOVA F., LABONNE N., VILAREM J.P., DRAN J.C., DELLA MEA G. and RIGATO V. (1996). Sorption mechanisms : formation of pseudocolloids, interaction of colloids and pseudocolloids with mineral surfaces. *Rapport européen* EUR 16880 EN, 115-152.

MOULIN V. and MOULIN C. (1995). Fate of actinides in the presence of humic substances under conditions relevant to nuclear waste disposal. *Applied geochemistry*, 10, 573-580.

MOULIN V. and OUZOUNIAN G. (1992). Role of colloids and humic substances in the transport of radioelemnts through the geosphere. *Applied geochemistry*, 1, 179-186.

NEFEDOV V.I., TETERIN Y.A., LEBEDEV A.M., TETERIN A.Y., DEMENTJEV A.P., BUBNER M., REICH T., POMPE S., HEISE K.H., and NITSCHE H. (1998). Electron spectroscopy for chemical analysis investigation of the interaction of uranyl and calcium ions with humic acids. *Inorganica Chimica Acta*, 273, 234-237.

RAO L., CHOPPIN G.R. and CLARK S.B.(1994). A study of metal-humate interactions using cation exchange. *Radiochimica Acta*, 66/67, 141-147.

STEVENSON F.E. (1982). Humus chemistry. Wiley Interscience New York, 443pp.

TIPPING E., BACKES C.A. and HURLEY M.A. (1988). The complexation of protons, aluminum and calcium by aquatic humic substances : a model incorporating binding-site heterogeneity and macroionic effects. *Wat. Res.*, 22 (5), 597-611.

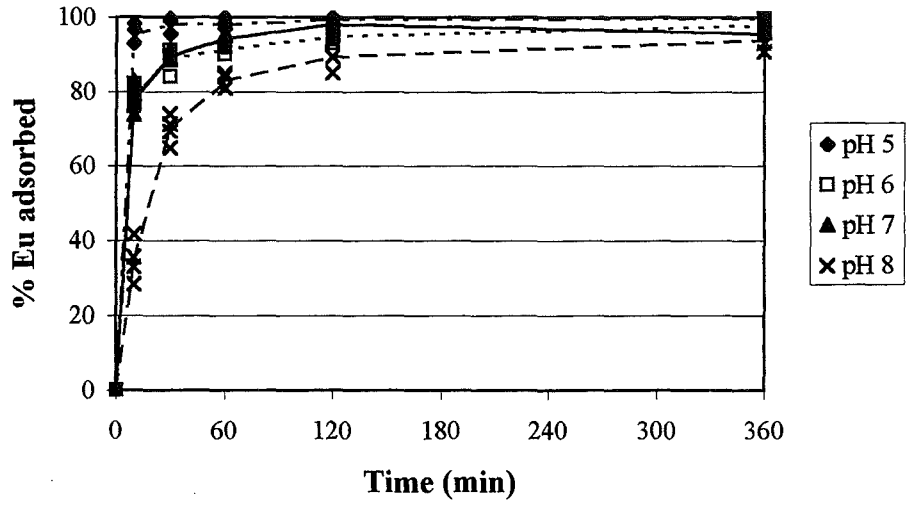

FIGURE 1: Sorption kinetic of europium onto "humic acid gel". Batch experiment. $[NaClO_4] = 5\ 10^{-2}$ M, $[Eu] = 10^{-8}$ M, 4 mg humic acid gel /mL (=72 µg HA/ mL).

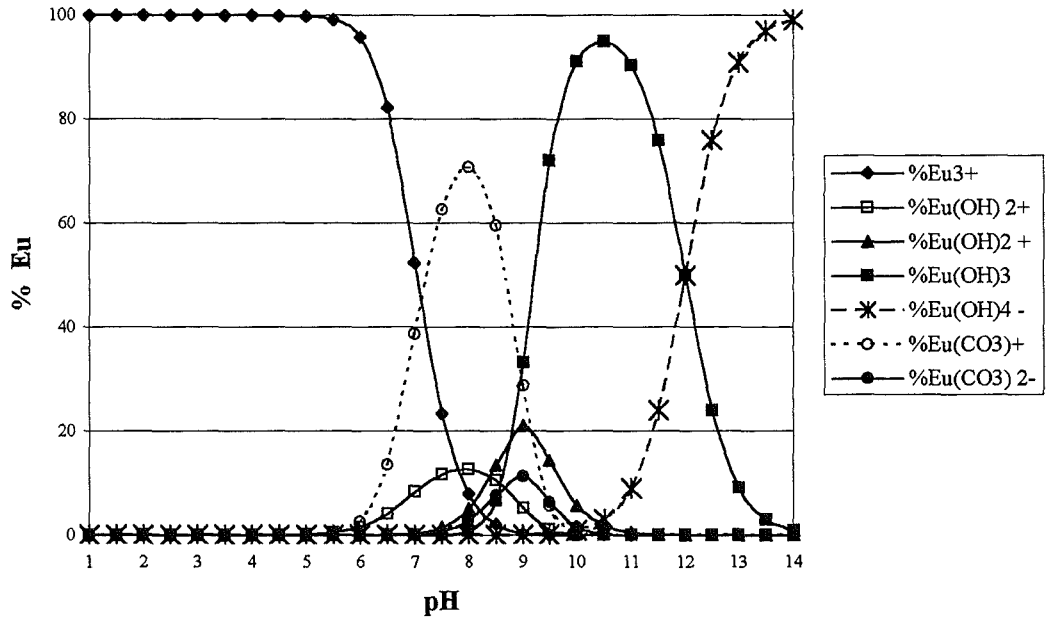

FIGURE 2: Speciation diagram of Eu (I = 0 M). $[Eu] = 10^{-8}$ M. $[TIC] = 10^{-5}$ M.

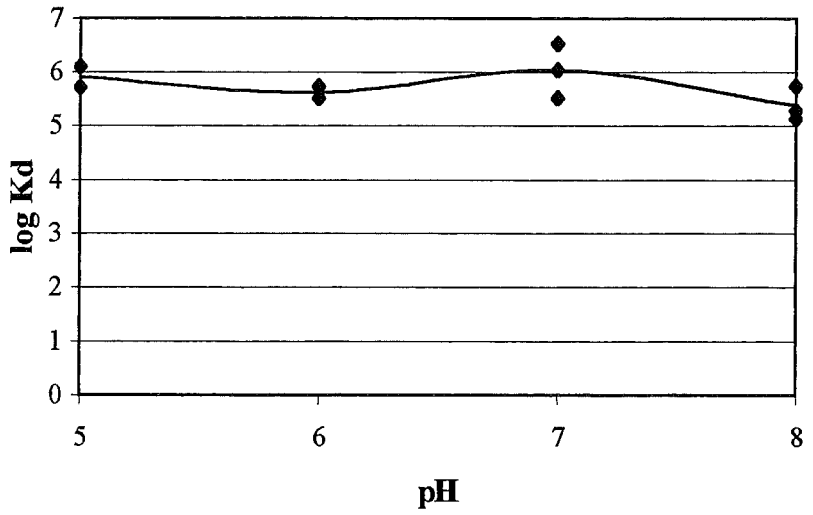

FIGURE 3: Distribution coefficient of Eu between "humic acid gel" and $NaClO_4$ 5 10^{-2} M. [Eu] = 10^{-8} M. Equilibration: 6 hours.

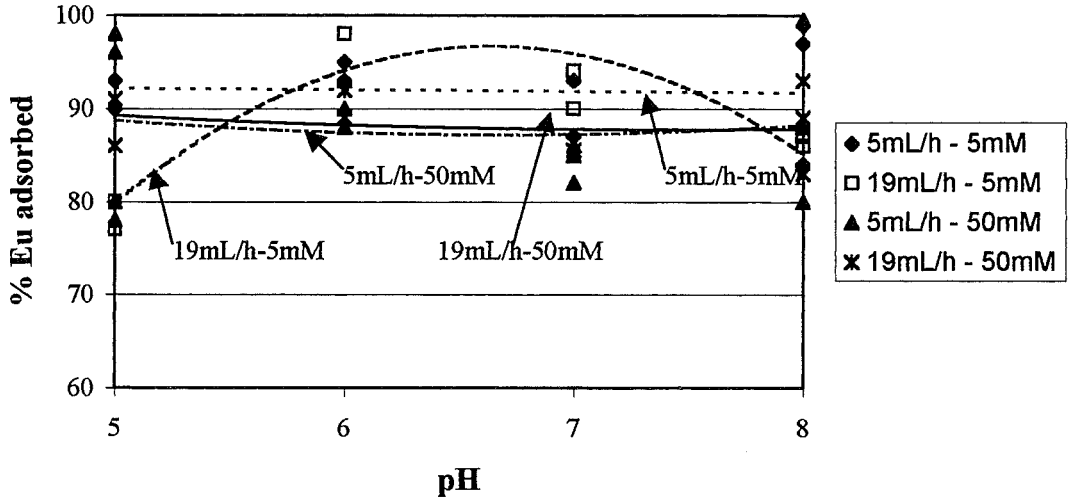

FIGURE 4: Sorption of Eu onto "humic acid gel" as a function of pH, ionic strength and flow rate. Eluent = $NaClO_4$.

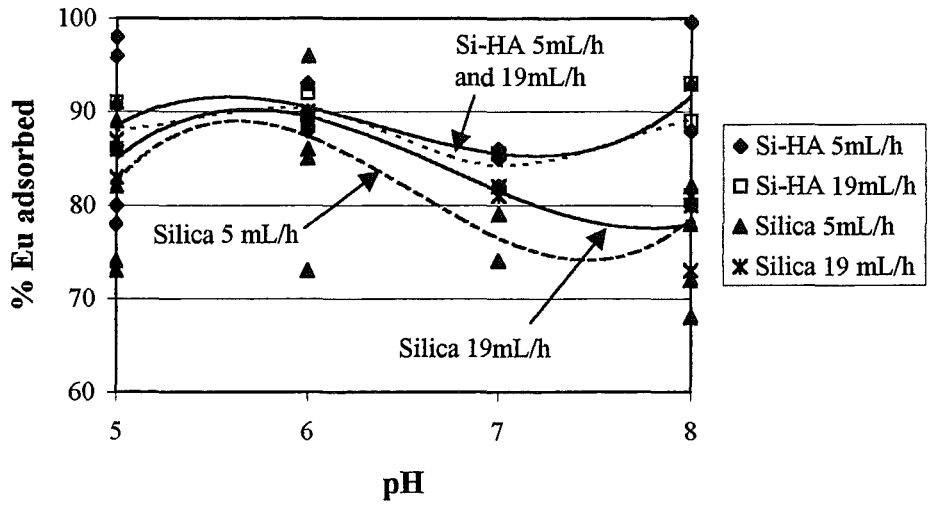

FIGURE 5: Comparison of the sorption of Eu onto "humic acid gel" and onto silica gel as a function of pH and flow rate in $NaClO_4$ 5 10^{-2} M. [Eu] = 10^{-8} M.

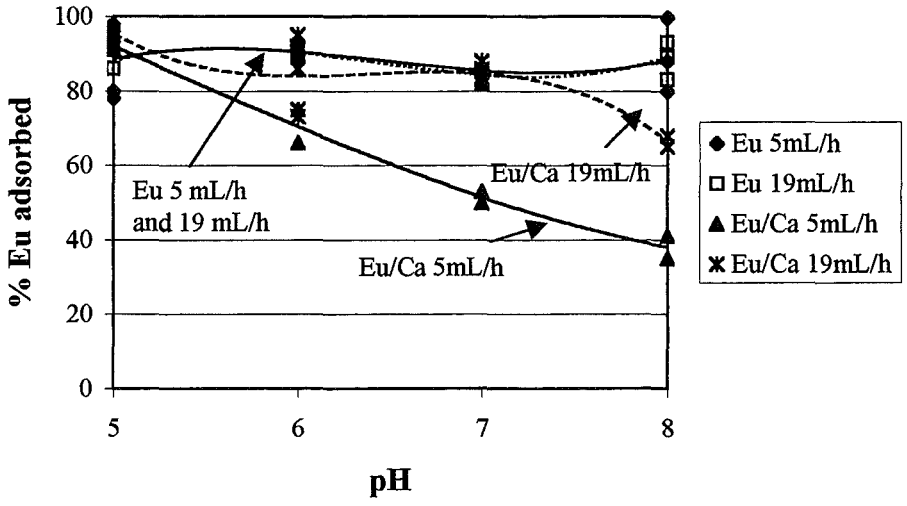

FIGURE 6: Influence of calcium on the sorption of europium onto "humic acid gel". [Eu] = 10^{-8} M. [$CaCl_2$] = 10^{-2} M. I = 5 10^{-2} M.

Annex 7

The Colloidal State of Humic Acid

(Zänker et al., FZR/IfR)

2nd Technical Progress Report

EC Project

"Effects of Humic Substances on the Migration of Radionuclides: Complexation and Transport of Actinides"

Project No.: FI4W-CT96-0027

FZR/IFR Contribution to Task 1 (Sampling and Characterization)

The Colloidal States of Humic Acid

Reporting Period 1998

H. Zänker, M. Mertig*, M. Böttger, G. Hüttig

Forschungszentrum Rossendorf e.V., Institute of Radiochemistry
P. O. Box 510119, D-01314 Dresden, Germany

* Technische Universität Dresden, Institute of Material Science
D-01062 Dresden, Germany

Abstract. Natural peat humic acid was studied by photon correlation spectroscopy in aqueous solution and scanning force microscopy after deposition (spin-coating) on a mica substrate. Two of the various particle types found on the mica surface are representative of the aqueous solution (and not only of the deposition process on the mica). One of these representative particle types is the humic acid macromolecule itself. Its conformation on the mica shows pronounced reactions to alterations of the pH value of the spin-coated solution indicating the validity of the random coil model of charged flexible polyelectrolyte molecules for humic acid. The second particle type representative of both the mica surface and the solution are small chunks of the lower submicron size range (70 to 160 nm). They are relatively inert and do not react to changes of the solution conditions. The micelle hypothesis is not supported is by our experiment.

1. Introduction

Whereas the metal complexation chemistry of humic acid or the chemistry of the reactions between humic acids and organic contaminants have relatively often been studied, the colloid chemistry of humic acid solutions (see also Jones and Bryan, 1998) has less frequently been viewed. Nevertheless, the transport behavior of humic acid or metal humate complexes in natural waters is significantly influenced by the colloid chemistry of the humics. Colloid particle size and thus agglomeration behavior, for instance, are decisive for the absence or presence of migration-enhancing size exclusion effects in rock fissures. In this chapter investigations into the colloid-chemical properties of humic acid are reported. Commercial Aldrich humic acid, a typical peat humic acid, served as the object of study. The experiments were primarily based on photon correlation spectroscopy (PCS) and scanning force microscopy (SFM). The results are a contribution to relatively fundamental humic acid research (see also Zänker et al., 1999).

Irrespective of what is assumed about the existence of agglomerates in humic solutions, the individual *humic acid molecules* alone belong to the size range of colloid particles. The molecular weight of humic acid is so far not very well understood, although it has been investigated for many years by different methods such as vapor pressure osmometry (Aiken and Gillam, 1989), size exclusion chromatography (Aster et al., 1996; Beckett et al., 1989; De Nobili et al., 1989; Wagoner et al., 1997, ultrafiltration (Aster et al., 1996; Buffle et al.,1982; Burba et al., 1995; Gaffney et al., 1996; Kliduff and Weber, 1992), ultracentrifugation (Jones et al., 1995; Reid et al., 1990), field-flow fractionation (Beckett et al., 1987; Beckett et al., 1989; Klein and Nießner, 1997; Schimpf and Petteys, 1997; Schimpf and Wahlund, 1997), and static light scattering (Reid et al., 1991; Underdown and Langford, 1981; Underdown et al., 1985; Varadachari et al., 1985; Wagoner et al 1997; Wershaw, 1989). Reported values of the molecular weight of single humic acid molecules vary from about 500 to several 100 000 Dalton, depending not only on the origin of the humic acid but also on the method of investigation. This discrepancy can be attributed to the nature of humic acid as was for instance

demonstrated by Burba et al. (1995). Performing a sequential five-stage tangential flow ultrafiltration with molecular weight cut-off membranes of 1 kD, 5 kD, 10 kD, 50 kD, and 100 kD, they found that the content of humic acid in the respective five filtration fractions depends dramatically on parameters such as the ionic strength, the humic acid concentration, and the pH value of the solution. This behavior can be best explained by the random coil model of organic macromolecules if the existence of charge carriers in the organic structures is considered (see, e.g., Swift, 1989). At high pH values, for instance, it is assumed that the functional groups are deprotonated. The molecule will expand because negative charges repel one another. At low pH values protons occupy the negative charge carriers. Then the molecules tend to contract. A similar influence is caused by increasing ionic strength. Because electrolyte ions shield negative charge carriers of organic molecules, the molecules will shrink with increasing ionic strength of the solution. Thus, the molecular weight of humic acid determined by ultrafiltration may depend on the ambient conditions and is an 'apparent molecular weight', characterizing the particular conformation of the molecule, rather than a real molecular weight (apart from the problem that significant systematic errors arise from the fact that ultrafilters are calibrated with substances quite different from humic acids). Similar conclusions on the reliability of molecular weight data of humic acid have been drawn from other methods of molecular weight determination such as size exclusion chromatography (Murphy et al., 1994).

Increasing humic acid concentration, protonation of the molecule or shielding of negative charge carriers from each other due to increasing ionic strength will not only change intra-molecular forces but may result in a reduction of the inter-molecular repulsive forces as well. Attractive forces (Van-der-Waals forces, hydrogen bonding) will then increase the tendency to form *molecule agglomerates.* However, the formation of humic acid molecule agglomerates is very complex and has scarcely been investigated so far. Thus, the nature of the agglomerates observed by the various methods is not well understood. A number of investigators hypothesized that these agglomerates are micelles or 'micelle-like' structures (Caceci and Billon, 1990; Engebretson et al., 1996; Skytte Jensen et al., 1996). This point of view, however, has recently been questioned in a study by Guetzloff and Rice (1996) who discovered by surface tension measurements that humic acid indeed forms micelles, but only at concentrations larger than 5 g/L which is far above both the concentrations considered in the former experiments and the concentrations that are of environmental relevance. One method occasionally used to study the size of humic acid agglomerates is PCS. Caceci and Billon (1990) measured the particle size distributions of several soil, surface water and groundwater humic acids employing PCS. They detected a small but significant concentration of relatively large scatterers in all investigated humic acid solutions. The size of these scatterers (50 nm to 200 nm) is far above the size of humic acid molecules which is expected to be between 1 nm and 10 nm. Therefore, Caceci and Billon classified these large scatterers as molecule agglomerates. They could confirm their existence by removing the small fraction of large light scatterers with a 15 nm Nuclepore filter. Also Reid et al. (1991) found particles of 448 nm and 81 nm in solutions of a peat humic acid and a water humic acid, respectively. Particles of tens to hundreds of nanometers were also detected in humic acid solutions by

Pinheiro et al. (1996) and by Ren et al. (1996). Objects of sizes between 2 nm and 3000 nm were reported by Muller (1996) who investigated humic acid extracted from water of an estuary. Results quite similar to those of the PCS studies were obtained from small angle neutron scattering experiments (Österberg and Mortensen, 1992; Österberg and Mortensen 1994; Österberg et al.,1994; Österberg et al., 1995) and small angle X-ray scattering experiments (Wershaw, 1989; Wershaw and Pickney, 1973). According to these investigations, too, humic acid solutions tend to contain particles of tens to hundreds of nanometers in size. Kim et al. (1990) could also identify a small fraction (< 5 %) of large particles of ≥ 100 000 Dalton in Aldrich humic acid and Gorleben humic acid by gel permeation chromatography. To provide a direct measure of the agglomerates, SFM investigations on air-dried humic acid and fulvic acid were accomplished by Österberg et al. (1995) and by Namjesnik-Dejanovic and Maurice (1997), respectively. In both experiments, the samples were prepared by drying a drop of solution on graphite or mica, respectively. Namjesnik-Dejanovic and Maurice (1997) found that under such conditions both structure and conformation of fulvic acid particles depend on the sample preparation. More recently, SFM in air was carried out on humic acid and other natural macromolecular organic substances by Santschi et al. (1998) and by Buffle et al. (1998).

2. Experimental

Aldrich humic acid (Aldrich Chemical Co., Steinheim, Germany), a natural humic acid obtained from peat (Aldrich Chemical Co., pers. comm. 1995), was purified according to the triplicate dissolution-precipitation procedure described by Kim and Buckau (1988). It was studied in aqueous solution by photon correlation spectroscopy (cf. Ford, 1985; Schmitz, 1990) and scanning force microscopy (cf. Magonov et al.,1997; Schmitz, 1997) after deposition (spin-coating, cf. Mertig, 1997) on freshly cleaved mica. The concentration of the humic acid was varied between 20 and 1000 ppm and the pH value between 2.7 and 11.3.

We used a BI-90 photon correlation spectroscope with a BI-9000 AT high-performance digital correlator (Brookhaven Instruments Corp., Holtsville, U.S.A.) which works at a fixed angle of 90°. An argon ion laser operated at a wavelength of 514.5 nm and in most cases at a laser power of 200 mW (LEXEL Laser, Inc., Fremont, U.S.A.) served as the light source. Rectangular SUPRASIL cuvettes (Hellma GmbH, Müllheim, Germany) that emit very little scattered light were used. The temperature of the solution was 25 °C, and the duration of the measurements was set at 300 s in most cases. For deriving the particle size distribution from the autocorrelation functions, we used the Cumulant Analysis (Koppel, 1972), the non-negatively constrained least squares (NNLS) deconvolution (Grabowski and Morrison, 1983), and the CONTIN deconvolution (Provencher, 1982). For a comparison of common deconvolution methods for PCS autocorrelation functions cf. Schurtenberger and Newman (1993) or Stock and Ray (1985).

Freshly cleaved mica sheets with a lateral size of 1 cm x 1 cm were used as the substrate for the SFM experiments on the humic acid solutions. Humic acid solution films with an initial thickness of about 2 µm were prepared by spin-coating at room temperature. For this procedure, a 30 µL drop of humic acid solution was placed onto the substrate. The drop was allowed to stand for 1 min before the spinning of the substrate was started at 5000 rpm for 60 s. At ambient conditions (25 % relative humidity), the spin-coated films dried within about 5 seconds providing a homogenous deposition of the organic material onto the substrate (cf. Mertig et al., 1997). The dry humic acid films were examined within one hour after preparation by SFM using a commercial multimode microscope NanoScope IIIa with phase extender (Digital Instruments, Santa Barbara, U.S.A.) operated in tapping mode at about 300 kHz under ambient conditions. Tapping mode is particularly advantageous on soft surfaces since there are nearly no lateral forces involved. Scanning with a scan rate of about 1 Hz (lines/s) was performed with silicon tip cantilevers (NanoProbe^{TM}, 125 mm) with typical tip radii $\leq$ 5 nm (cf. Mertig et al., 1997). For the humic acid imaging, a tapping amplitude of about 40 nm was chosen.

3. Results and Discussion

PCS indicated the presence of particles of about 130 nm in diameter (Fig. 1 shows a NNLS deconvolution of the autocorrelation function). This was independent of the pH and the humic acid concentration.

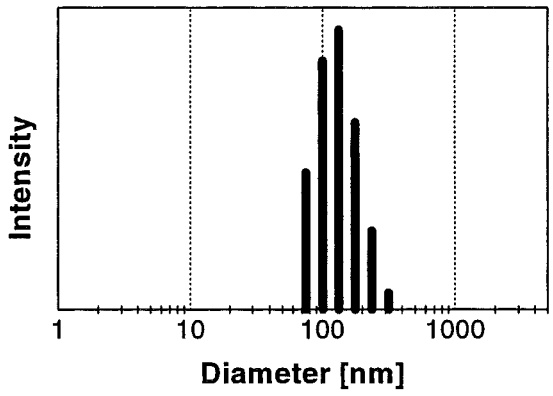

Fig. 1: Typical PCS particle size distribution of a humic acid solution. Prefiltration through a 1000 nm Nuclepore filter. Concentration 200 ppm; pH 6.2. Particles were found in the size range from 50 to 300 nm with the light intensity weighted peak being at 130 nm. Similar particle size distributions were obtained for the other pH values and humic acid concentrations studied.

Four particle classes were found on the mica substrate by SFM:

Class (1) Relatively large 'submicron chunks' of several hundreds of nm in diameter and up to 50 nm in height (the equivalent spherical diameter lies between 70 and 160 nm),

Class (2) 'Elongated agglomerates' of several hundred nm in length and only few nm in height (the equivalent spherical diameter is 30 to 40 nm),

Class (3) 'Disk-like agglomerates' of about 50 nm in diameter and only few nm in height (equivalent spherical diameter 10 to 25 nm),

Class (4) 'Subunits' of only few nm in diameter and height (the equivalent spherical diameter is 1.5 to 8 nm).

The first three particle classes can be discerned in the SFM micrograph in Fig. 2. Classes (2) and (3) can better be seen in Figures 3 and 4 which are SFM scans of higher magnification. Figures 3 and 4 also reveal that the particles of Classes (2) and (3) consist of a substructure: 'subunits' of a diameter of 12 to 14 nm are discernible (Class 4).

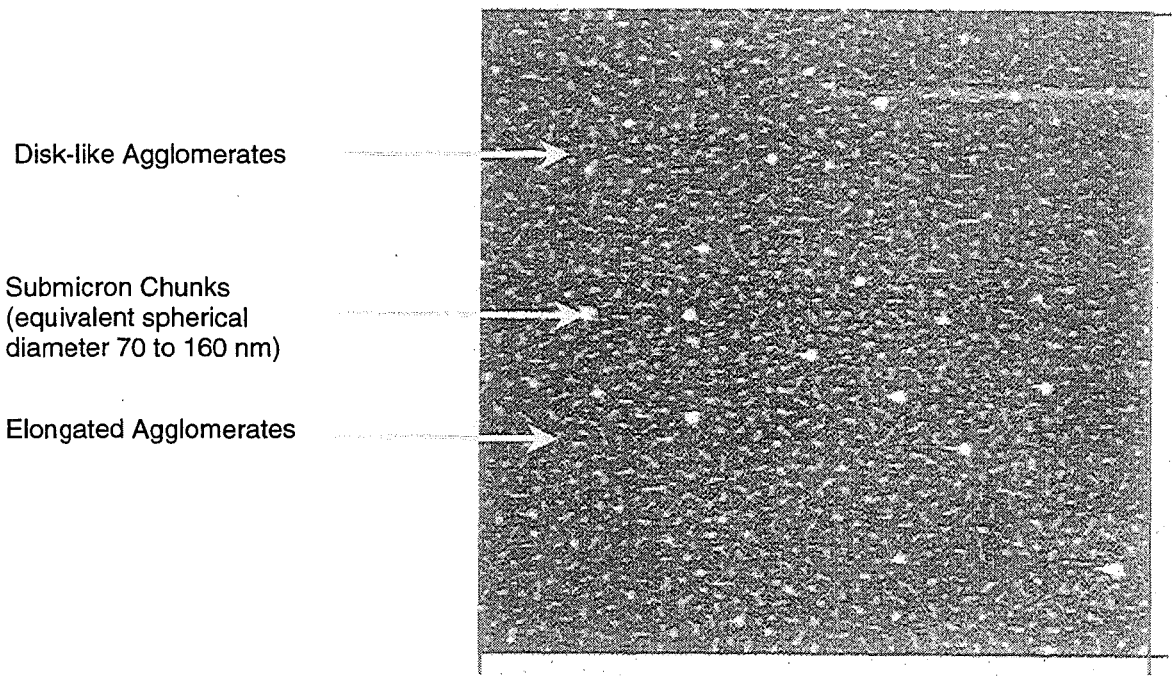

Fig. 2: SFM image of humic acid deposited on mica by means of spin-coating. Prefiltration through a 1000 nm Nuclepore filter. Concentration 200 ppm; 10 µm x 10 µm scan; pH 11.3; 'Submicron chunks', 'elongated agglomerates' and 'disk-like agglomerates' can be discerned.

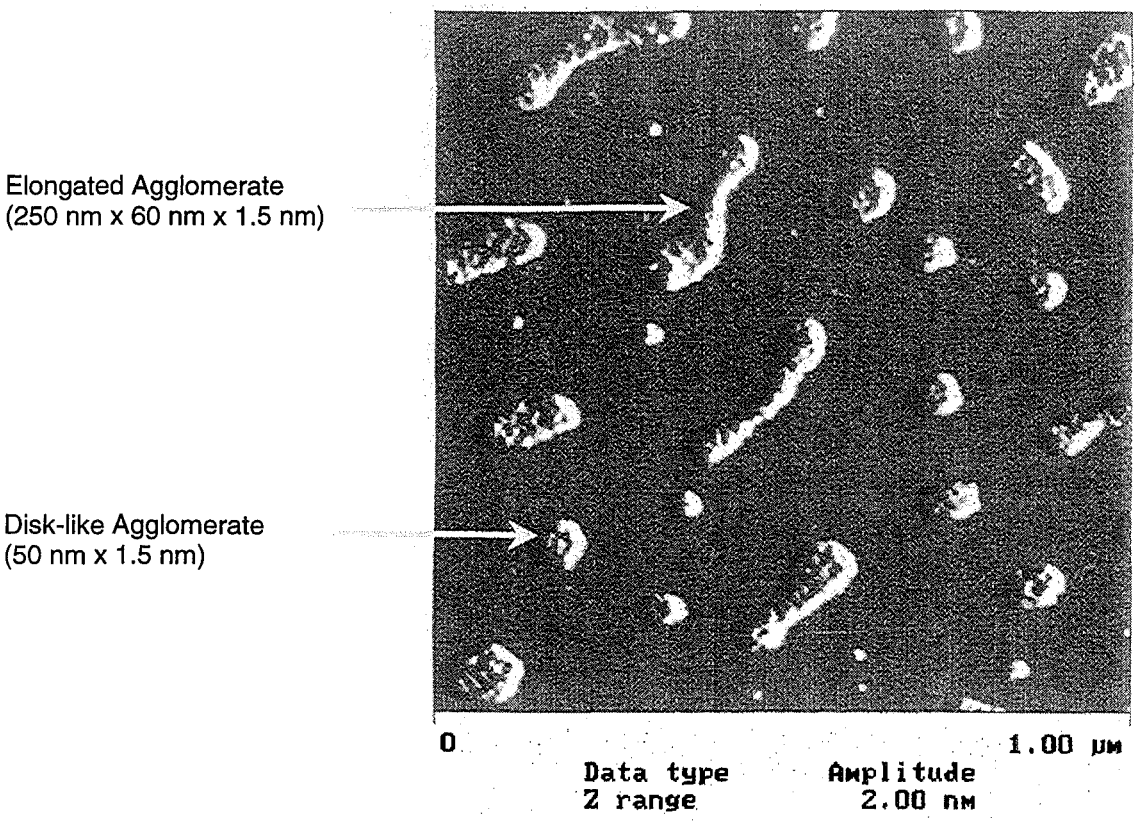

Fig. 3: SFM image of humic acid deposited on mica by means of spin-coating. Prefiltration through a 1000 nm Nuclepore filter. Concentration 200 ppm; 1 µm x 1 µm scan; pH 11.3; 'Elongated agglomerates' and 'disk-like agglomerates' with a characteristic substructure are visible. Height of the deposits: 1.5 to 2 nm. Periodicity of the substructure: 12 to 14 nm.

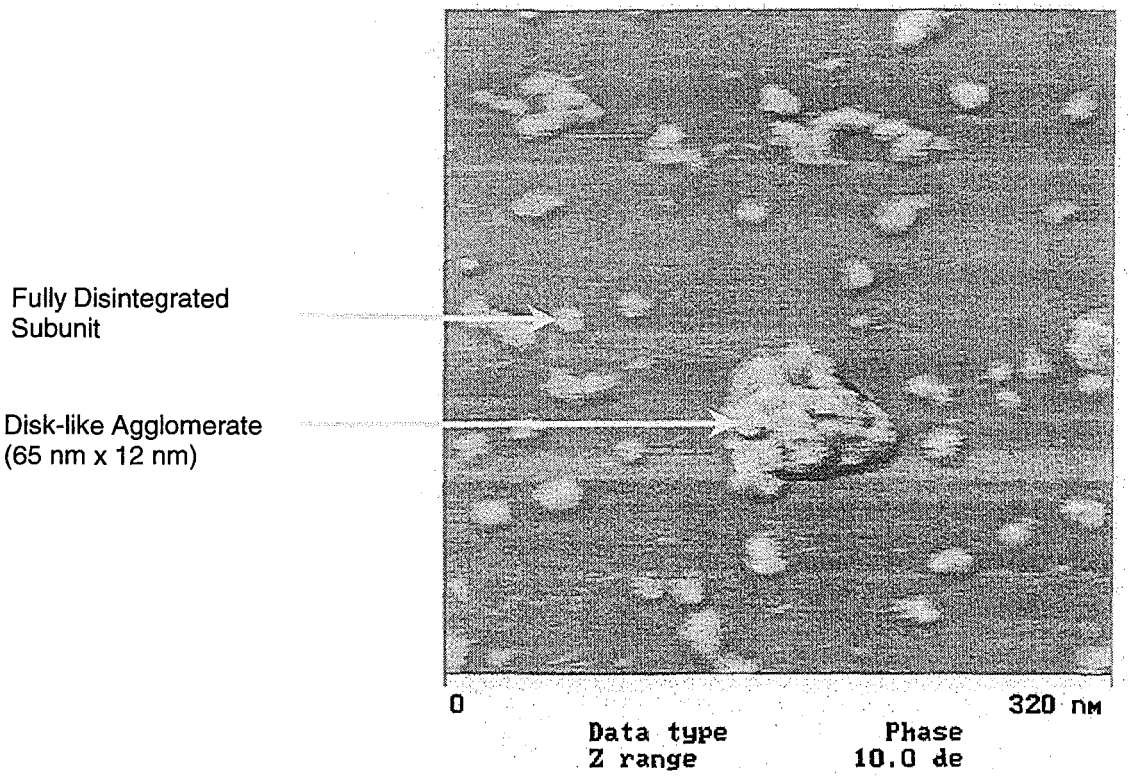

Fig. 4: SFM image of humic acid deposited on mica by means of spin-coating. Prefiltration with 1000 nm Nuclepore filter. Concentration 200 ppm; 320 nm x 320 nm scan; pH 4.2; Individual 'subunits' and a larger agglomerate with a characteristic substructure are visible. Height of the fully disintegrated 'subunits': 3.5 nm. Height of the agglomerate in the center: 12 nm ('subunits' are obviously laying on top of each other in this type of 'disk-like agglomerates' which was only found at low pH values). Periodicity of the substructure: about 12 nm.

Dilution experiments (Fig. 5) further specified the nature of the fourth particle class. Fully disintegrated 'subunits' are found at a humic acid concentration of 20 ppm, *i.e.*, the 'subunits' forming the objects in Figures 3 and 4 and the fine spots in Fig. 5 (c) are identical.

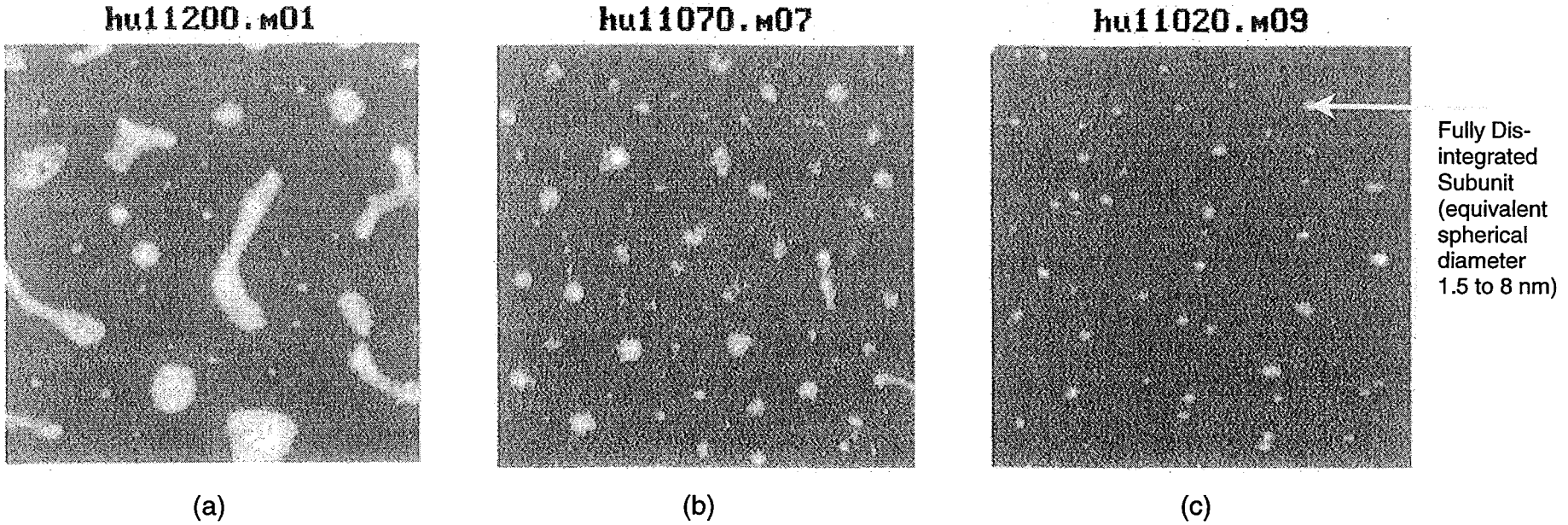

Fig. 5: Comparison of SFM images of humic acid at three humic acid concentrations. 1 µm x 1 µm scans. pH 11.3; Concentrations (a) 200 ppm, (b) 70 ppm, (c) 20 ppm. Dilution of the solution results in the appearance of fully disintegrated 'subunits' on the mica surface.

The aim of our light scattering experiments was to elucidate which of the objects found on the mica are representative of states in solution and which are only formed on the substrate during the spin-coating process. Particle Class 1 can be classified relatively easy as to exist also in aqueous solution. These particles show physico-chemical properties different from those of the other particle classes: they are chemically inert, *i. e.*, they do not change when humic acid concentration or solution pH are changed. The remaining particle classes show a much lower height on the mica surface than do the Class 1 particles. Furthermore, the Class 2 and 3 particles consist of Class 4 particles (subunits). If the concentration of the humic acid solution is low enough, the subunits appear in their fully disintegrated state (Fig. 5). From their spherical equivalent diameter we classify the subunits as the humic acid molecules. The still open question is if the Class 2 and Class 3 agglomerates exist in solution or if the original humic acid solution consists of the individual molecules. PCS on the unfiltered solutions or the 1000 nm filtrates gives particle sizes of 50 to 300 nm, *i. e.*, PCS finds exclusively the submicron chunks (Fig. 1). This is because the smaller particles are optically masked by the chunks although these chunks provide only < 5 mass % of the humic material. The idea was to investigate the humic acid solution after removing the disturbing submicron chunks. Fig. 6a shows an example of the autocorrelation functions obtained on a 1000 nm filtrate whose deconvolution yields the 50 nm to 300 nm particles. The shape of the autocorrelation function changes completely after the filtration through the 50 nm filter (Fig. 6b). Note that the scattered light intensity of the 50 nm filtrate is about 50 times that of the pure solvent, *i.e.*, the Milli-Q water. This autocorrelation function shows that no correlation can be found in the light scattering fluctuations of the 50 nm filtrate, not even after the shortest delay times (first delay time used in this experiment: 5 μs). The explanation for this lack of autocorrelation is that the light fluctuations are caused by very small, fast-moving particles, *i.e.*, a particle size of significantly less than 10 nm is indicated. The proper function of our PCS device in the particle size range of interest here was verified by measurements on 3 particle standards of known particle size: 28 nm polystyrene particles, 12 nm silica particles, and toluene, a Rayleigh scatterer of relatively high scattered light intensity consisting of particles (molecules) of less than 1 nm in diameter. This is shown in Figs. 6c through 6e.

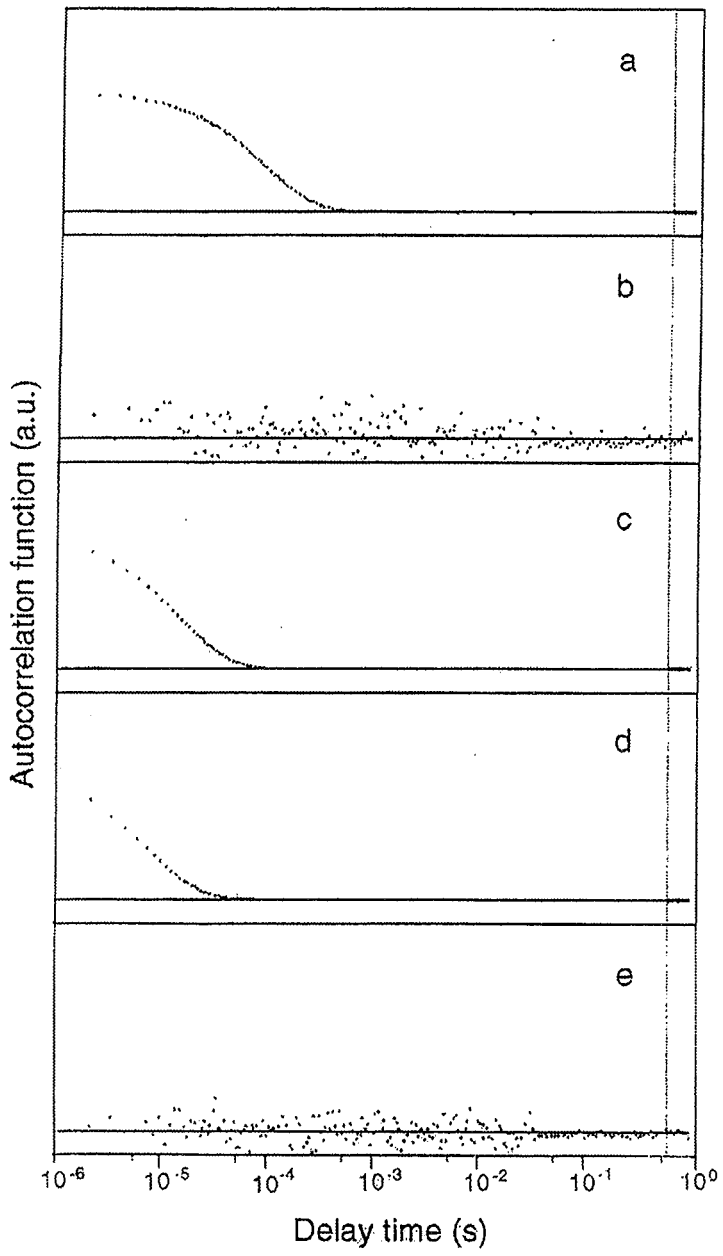

Fig. 6: Autocorrelation functions. (a) 1000 nm filtrate of humic acid. (b) 50 nm filtrate of humic acid. (c) 28 nm polystyrene latex particles. (d) 12 nm silica particles. (e) Toluene.

It follows that the elongated and the disk-like particles (Classes 2 and 3) do probably not exist in solution. The equivalent spherical diameter of these particles would be high enough to make them already detectable by PCS. The Class 2 and 3 particles result from agglomeration processes during the deposition on the mica surface. Thus, the particles representative of the aqueous solution are the chemically inert submicron chunks and the humic acid molecules. As mentioned above, several authors hypothesized that micelles are formed in humic acid solutions. Our experiment does not

support the micelle hypothesis (for humic acid concentrations ≤ 500 ppm). Micelles react very sensitively to changes in the solution conditions such as dilution or alteration of pH. The 'inertness' of the 'large scatterers' (submicron chunks) found by our experiment is in accordance with the results of other investigators who unsuccessfully tried to disintegrate such particles by the addition of surfactants such as Triton X-100 (Caceci and Billon, 1990; Reid et al. 1991). According to Kim et al. (1990), these small humic acid fractions of high molecular weight also show IR and ^{1}H-NMR spectra that differ considerably from those of the main fractions of the humic acid.

A very important property of the humic acid molecules (particles of Class 4) was observed by SFM. Table 1 gives the heights of the 'subunits' on the mica surface as determined by SFM as a function of the pH of the spin-coated solution. From the flatness of these units (heights of ≤ 2 nm in alkaline solution) we conclude that the humic acid structures possess a high flexibility (deformability).

Tab.1: Height of the 'subunits' in dependence on the pH; error of SFM height measurement: < 5 %

pH Value	Height of the 'Subunits' (nm)
4.2	3.5
6.2	2.5
11.3	1.5 to 2

It is , however, striking that this flexibility decreases if the pH value is lowered. In the more acidic region the 'subunits' are significantly higher than in the alkaline region. This 'response' of the SFM images to the pH value provides direct experimental evidence that the random coil hypothesis of polyelectrolyte molecules is correct for humic acid. In alkaline and neutral solutions the humic acid molecules are obviously 'expanded' (deprotonated form), whereas they are 'contracted' in the more acidic pH region (protonated form). Thus, their inner stiffness increases if the pH is lowered making them lay higher on the mica surface. Fig. 7 demonstrates schematically the response of molecule conformation to pH variations.

Conformation of Spin-Coated Humic Acid on Mica

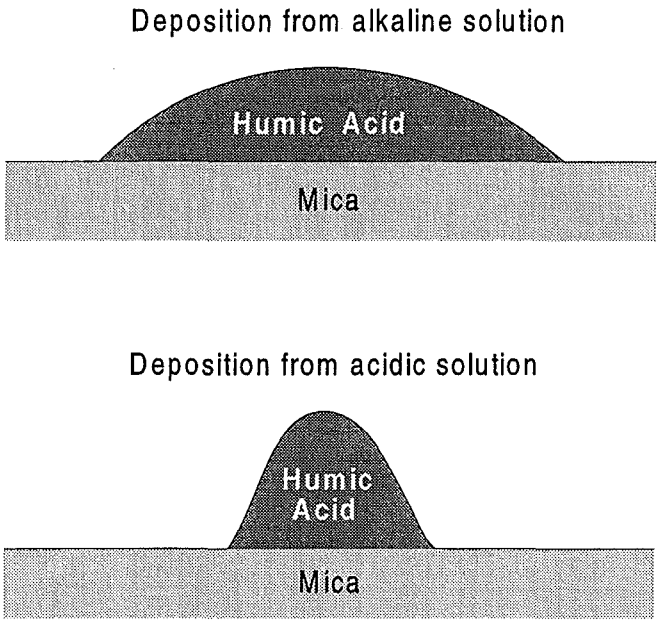

Fig. 7: Diagrammatic representation of the conformation of spin-coated humic acid on mica. Note that height measurement by SFM is much more reliable than the measurement of lateral dimensions.

Not much is known about the strikingly inert 'submicron chunks' yet. They seem to be an inherent constituent of the investigated peat humic acid that can not even be removed by the relatively thorough purification according to the method by Kim and Buckau (1998). The chunks might consist of insoluble humin (or even of inorganic matter, *i.e.*, silica-rich or iron-rich material). Investigations into the chemical nature of these submicron chunks are underway.

4. Conclusions

We used a novel approach to study the particle size distribution of natural peat humic acid by simultaneously investigating the system with both photon correlation spectroscopy in aqueous solution and scanning force microscopy after spin-coating onto mica. Two different particle configurations were observed with corresponding states in solution and on the substrate: 'submicron chunks' and individual humic acid molecules. Both particle classes have distinct sizes and properties. The submicron chunks

have equivalent spherical diameters between 70 nm and 160 nm. They behave inert when the ambient conditions are changed. Although their mass fraction is only < 5 percent, they scatter the majority of the light, thus masking smaller particles. Therefore, photon correlation spectroscopy exclusively detects submicron chunks, falsely indicating a unimodal particle diameter distribution in the solution. The submicron chunks can be removed from solution by filtration through a 50 nm pore size filter. Subsequent photon correlation spectroscopy investigations indicate the presence of particles with diameters significantly below 10 nm in solution. The maximum equivalent spherical diameter of the humic acid molecules resulting from scanning force microscopy data is found as 8 nm. Thus, the results of PCS and SFM for both the submicron chunks and the individual humic acid molecules are in agreement with each other. The micelle hypothesis is not supported by our experiment. The height of the deposited molecules varies between 1.5 nm and 3.5 nm, depending on the solution's pH value. This particle height alteration with changing pH is in accordance with the random coil model for organic polyelectrolyte molecules and probes indirectly the mechanical flexibility (deformability) of the molecules as a function of their protonation degree. Not much is known about the chemical nature of the strikingly inert submicron chunks yet.

5. References

Aiken, G.R and Gillam, A.H. (1989) Determination of Molecular Weights of Humic Substances by Colligative Property Measurements. In *Humic Substances II. In Search of Structure* (ed. Hayes, M. H. B. et al.) p. 515-544. John Wiley & Sons.

Aster, B., Burba, P., and Broekaert, J. C. (1996) Analytical fractionation of aquatic substances and their metal species by means of multistage ultrafiltration. *Fresenius J. Anal. Chem.* **354**, 722-728.

Beckett, R., Zhang, J., Giddings, J.C. (1987) Determination of Molecular Weight Distributions of Fulvic and Humic Acids Using Flow Field-Flow Fractionation. *Environ. Sci. Technol.* **21**, 289-295.

Beckett, R., Bigelow, J.C., Zhang, J., and Giddings, J. C. (1989) Analysis of Humic Substances Using Flow Field-Fractionation. In *Influence of Aquatic Humic Substances on Fate and Treatment of Pollutants* (ed. P. Mac Carthy and I. H. Suffet), ACS Advances in Chemistry Series 219, Chapter 5, ACS, Washington DC.

Buffle, J., Deladoey, P., Zumstein, J., and Haerdi, W. (1982) Analysis and characterization of natural organic matters in freshwaters. *Schweiz. Z. Hydrol.* **44/2**, 325-362.

Buffle, J., Wilkinson, K. J., Stoll, S., Filella, M., and Zhang, J. (1998) A Generalized Description of Aquatic Colloidal Interactions: The Three-colloidal Component Approach. *Environ. Sci. Technol.* **32**, 2887-2899.

Burba, P., Shkinev, V. Spivakov, and B. Ya (1995) On-line fractionation and characterization of aquatic humic substances by means of sequential-stage ultrafiltration. *Fresenius J. Anal. Chem.* **351**, 74-82.

Caceci, M.S. and Billon, A. (1990) Evidence for large organic scatters (50-200 nm) in humic acid samples. *Org. Geochem.* **15**, 335-350.

Engebretson, R. R., Amos, T., and Von Wandruszka, R. (1996) Quantitative Approach to Humic Acid Associations. *Environ Sci. Technol.* **30**, 990-997.

Ford, N.C. Jr. (1985) Light Scattering Apparatus. In *Dynamic Light Scattering* (ed. Pecora, R.), pp. 7-58. Plenum Press.

Gaffney, J. S., Marley, N. A., and Orlandini, K. A. (1996) The Use of Hollow-Fiber Ultrafilters for the Isolation of Natural Humic and Fulvic Acids. In: *Humic and Fulvic Acids. Isolation, Structure, and Environmental Role.* ACS Symp. Series 651. Symp. at the 210th National Meeting of the Amer. Chem. Soc., Chicago, Aug. 20-24, 1995 (ed. J. S. Gaffney et al.), pp. 26-40.

Grabowski, E. E. and Morrison, I. D. (1983) Particle Size Distribution from Analysis of Quasi-Elastic Light-Scattering Data. In *Measurement of Suspended Particles by Quasi-Elastic Light Scattering* (ed. Dahneke, B.E.), Wiley-Interscience.

Guetzloff, T. F. and Rice, J. A. (1996) Micellar Nature of Humic Colloids. In: *Humic and Fulvic Acids. Isolation, Structure, and Environmental Role.* ACS Symp. Series 651. Symp. at the 210th National Meeting of the Amer. Chem. Soc., Chicago, Aug. 20-24, 1995 (ed. J. S. Gaffney et al.), pp. 18-25.

Jones, M. N. and Bryan, N. D. (1998) Colloidal properties of humic substances. *Advances in Colloid and Interface Science* **78**, 1-48.

Jones, M. N., Birkett, J. W., Wilkinson, A. E., Hesketh, N., Livens, F. R., Bryan, N. D., Lead, J. R., Hamilton-Taylor, J., and Tipping, E. (1995) Experimental determination of partial specific volumes of humic substances in aqueous solution. *Anal. Chim. Acta* **314**, 149-159.

Kim, J. I. and Buckau, G. (1988) Preparation of References of Humic Acids. *Report RCM* 0288. Technische Universität München, Institut für Radiochemie.

Klein, T. and Nießner, R. (1998) Characterization of Heavy Metal Containing Seepage Water Colloids by Flow FFF, Ultrafiltration, ELISA and AAS. *Microchim. Acta* **129**, 47-55.

Stock, R. S. and Ray, W. H. (1985) Interpretation of Photon Correlation Spectroscopy Data: A Comparison of Analysis Methods. *J. Polym. Sci.: Polym. Phys.* Ed. **23**, 1393-1447.

Swift, R. S. (1989) Molecular Weight, Size, Shape, and Charge Characteristics of Humic Substances: Some Basic Considerations. In *Humic Substances II. In Search of Structure* (ed. Hayes, M. H. B. et al.) p. 449-465. John Wiley & Sons.

Underdown, A. W. and Langford, C. H. (1981) Light Scattering of a Polydisperse Fulvic Acid. *Anal. Chem.* **53**, 2139-2140.

Underdown, A. W., Langford, C. H., and Gamble, D. S. (1985) Light Scattering Studies of the Relationship Between Cation Binding and Aggregation of a Fulvic Acid. *Environ. Sci. Technol.* **19**, 132-136.

Varadachari, C., Nayak, D. C., Barman, A. K., and Gosh, K. (1985) Light Scattering Studies on Soil Humic Substances. *J. Indian Soc. Soil Sci.* **33**, 11-14.

Wagoner, D. B., Christman, R. F., Cauchon, G., and Paulson, R. (1997) Molar Mass and Size of Suwannee River Natural Organic Matter Using Multi-Angle Laser Light Scattering. *Environ. Sci. Technol.* **31**, 937 -941

Wershaw, R. L. (1989) Sizes and Shapes of Humic Substances by Scattering Techniques. In *Humic Substances II. In Search of Structure* (ed. Hayes, M. H. B. et al.) p. 545-559. John Wiley & Sons

Wershaw, R. L. and Pickney, D. J. (1973) Determination of the Association and Dissociation of Humic Acid Fractions by Small Angle X-Ray Scattering Experiments. *J. Res. U. S. Geol. Survey* **1**, 701-701.

Zänker, H. Mertig, M. , Böttger, M., Hüttig, G., Pompe, S., Pompe, W., and Nitsche, H. (1999) Photon Correlation Spectroscopy and Scanning Force Microscopy of Humic Acid. Submitted to Geochim. Cosmochim. Acta.

Kim, J. I., Buckau, G., Li, G. H., Duschner, H., and Psarros, N. (1990) Characterization of humic and fulvic acids from Gorleben groundwater. *Fresenius J. Anal. Chem.* **338**, 245-252.

Kliduff, J. and Weber, W. J. (1992) Transport and Separation of Organic Macromolecules in Ultrafiltration Processes. *Environ. Sci. Technol.* **26**, 569-577.

Koppel, D. E. (1972) Analysis of Macromolecular Polydispersity in Intensity Correlation Spectroscopy: The Method of Cumulants. *J. Chem. Phys.* **57**, 4814-4820.

Magonov S.N., Elings, V., Whangbo, M.H. (1997) Phase imaging and stiffness in tapping-mode atomic force microscopy. *Surface Science* **375**, L385-391.

Mertig, M., Thiele, U., Bradt, J., Leibiger, G., Pompe, W., and Wendrock, H. (1997) Scanning Force Microscopy and Geometrical Analysis of Two-Dimensional Collagen Network Formation. *Surface and Interface Analysis* **25**, 514-521.

Muller, F. L. L. (1996) Measurement of electrokinetic and size characteristics of estuarine colloids by dynamic light scattering spectroscopy. *Anal. Chim. Acta* **331**, 1-15.

Murphy, E. M., Zachara, J. M., Smith, S. C., Phillips, J. L., and Wietsma, T. W. (1994) Interaction of Hydrophobic Organic Compounds with Mineral-Bound Humic Substances. *Environ. Sci. Technol.* **28**, 1291-1299.

Namjesnik-Dejanovic, K. and Maurice, P. A. (1997) Atomic force microscopy of soil and stream fulvic acids. *Coll. Surf. A: Physicochem. Eng. Aspects* **120**, 77-86.

Österberg, R. and Mortensen, K. (1992) Fractal dimension of humic acids. *Eur. Biophys. J.* **21**, 163-167.

Österberg, R. and Mortensen, K. (1994) The growth of fractal humic acids: cluster correlation and gel formation, *Radiat. Environ. Biophys.* **33**, 269-276.

Österberg, R., Szajdak, L., and Mortensen, K. (1994) Temperature-Dependent Restructuring of Fractal Humic Acids: A Proton-Dependent Process. *Environ. Int.* **20**, 77-80.

Österberg, R., Mortensen, K., and Ikai, A. (1995) Direct Observation of Humic Acid Clusters, a Nonequilibrium System with a Fractal Structure. *Naturwiss.* **82**, 137-139.

Pinheiro, J. P., Mota, A. M., d'Oliveira, J. M. R., and Martinho, J. M. G. (1996) Dynamic properties of humic matter by dynamic light scattering and voltammetry. *Anal. Chim. Acta* **329**, 15-24.

Provencher, S.W. (1982) A Constrained Regularization Method for Inverting Data Represented by Linear Algebraic or Integral Equations. *Comput. Phys. Commun.* **27**, 213-227.

Reid, P. M., Wilkinson, A. E., Tipping, E., and Jones, M. N. (1990) Determination of molecular weights of humic substances by analytical (UV scanning) ultracentrifugation. *Geochim. Cosmochim. Acta* **54**, 131-138.

Reid, P. M., Wilkinson, A. E., Tipping, E., and Jones, M. N. (1991) Aggregation of humic substances in aqueous media as determined by light-scattering methods. *J. Soil Sci.* **42**, 259-270.

Ren, S. Z., Tombacz, E., and Rice, J. A. (1996) Dynamic light scattering from power-law polydisperse fractals: Application of dynamic scaling to humic acid. *Physical Rev. E* **53**, 2980-2983.

Santschi, P. H., Balnois, E., Wilkinson, K. J., Zhang, J., and Buffle, J. (1998) Fibrillar polysaccharides in marine macromolecular organic matter as imaged by atomic force microscopy and transmission electron microscopy. *Limnol. Oceanogr.* **43**, 896-908.

Schimpf, M. E. and Petteys, M. P. (1997) Characterization of humic materials by flow field-flow fractionation. *Colloids Surfaces A: Physicochem. Eng. Aspects* **120**, 87-100.

Schimpf, M.E. and Wahlund, K.-G. (1997) Asymmetrical Flow Field-Flow Fractionation as a Method to Study the Behavior of Humic Acids in Solution. *J. Microcolumn Separations* **9**, 535-543.

Schmitz, I, Schreiner, M. Friedbacher, G. and Grasserbauer, M. (1997) Phase imaging as an extension to tapping mode AFM for the identification of material properties on humidity-sensitive surfaces. *Applied Surface Science* **115**, 190-198.

Schmitz, K. S. (1990) *An Introduction to Dynamic Light Scattering by Macromolecules*, Academic Press, Inc., p. 50.

Schurtenberger, P. and Newman, M.E. (1993) Characterization of Biological and Environmental Particles Using Static and Dynamic Light Scattering. In *Environmental Particles, IUPAC Series on Environmental Analytical and Physical Chemistry*, (ed. J. Buffle and H. P. van Leeuwen), Volume 2, pp. 37-116. Lewis Publishers.

Skytte Jensen, B., Halken, T., Jesting, I., and Jørgensen, D. (1996) The Role of colloids in the migration of radioelements. *European Communities Report EUR 16763 EN*, Risø National Laboratory, Roskilde, Denmark.

Annex 8

Complexation of Aquatic Humic Substances from the Bog "Kleiner Kraanichsee" with Uranium(VI)

(Schmeide et al., FZR/IfR)

2 nd Technical Progress Report

EC Project:

"Effects of Humic Substances on the Migration of Radionuclides: Complexation and Transport of Actinides"

Project No.: FI4W-CT96-0027

FZR/IFR Contribution to Task 1 (Sampling and Characterization) and Task 2 (Complexation)

Complexation of Aquatic Humic Substances from the Bog "Kleiner Kranichsee" with Uranium(VI)

Reporting period 1998

K. Schmeide, H. Zänker, G. Hüttig, K.H. Heise, G. Bernhard

Forschungszentrum Rossendorf e.V.
Institute of Radiochemistry
P.O. Box 510119
01314 Dresden
Germany

Contents

Abstract

As a contribution to Task 1 (Sampling and Characterization), we have characterized the Derwent Reservoir fulvic acid, provided by J.J.W. Higgo (BGS, UK), by means of FTIR spectroscopy and capillary zone electrophoresis and compared to Kranichsee humic and fulvic acid and Aldrich humic acid.

Our contribution to Task 2 (Complexation) consists of two parts. First, we studied the complexation of Kranichsee humic acid (HA) and fulvic acid (FA) with uranyl(VI) ions by laser-induced fluorescence spectroscopy at pH 4 and an ionic strength of 0.1 M ($NaClO_4$). The loading capacities were determined to be 14 ± 1 % and 13 ± 1 % for humic acid and fulvic acid, respectively. The complexation constants for Kranichsee humic acid and fulvic acid were found to be log ß = 6.35 ± 0.22 and log ß = 6.21 ± 0.20, respectively. These results were compared to the uranyl complexation behavior of other natural humic acids such as Aldrich HA and GoHy-573 HA. Second, we investigated original bog water of the mountain bog 'Kleiner Kranichsee' by ultrafiltration to determine the hydrodynamic particle size distribution, i.e., the 'apparent molecular weight' distribution of the organic substances in the bog water. Furthermore, the influence of uranyl complexation on this particle size distribution of humic colloids was investigated. No significant influence of the uranyl ions on the molecular weight distribution of the humic substances was found.

1 Introduction

The determination of the effect of humic substances on the migration behavior of actinides in natural aquifer systems is of great interest and allows to assess their impact on the long-term safety of abandoned uranium mines in Saxony and Thuringia, Germany. The speciation of radionuclides is a primary factor that influences their behavior in complex aqueous systems. The solubility of actinides can be increased by complexation with humic substances and, thus, their mobility in the geosphere can be enhanced. Complexation constants are used to quantify the interaction between radionuclides and humic substances. Therefore, we studied the complexation of site-specific humic substances with uranyl(VI) ions by laser-induced fluorescence spectroscopy and the influence of uranyl complexation on the particle size distribution of humic colloids.

2 Comparison of Derwent Reservoir Fulvic Acid with Kranichsee Humic and Fulvic Acid and Aldrich Humic Acid

2.1 IR Spectroscopy

The Derwent Reservoir FA (Derwent FA), isolated by Higgo et al. (1998), was investigated by FTIR measurements (SPECTRUM 2000, Perkin Elmer). This method is useful because IR spectroscopy of humic substances provides information on functional groups, especially on oxygen containing groups. The Derwent fulvic acid was a FA concentrate containing 4.1 g/L TOC (Total Organic Carbon). The solution was lyophilized and KBr pellets of the dry FA product were used for IR measurements. The results of the IR measurements of Kranichsee HA and FA and of Aldrich HA are already described in detail by Schmeide et al. (1998). However, to facilitate a comparison of all humic and fulvic acids, the IR spectrum of Derwent FA is shown in Fig. 1 together with the spectra of Kranichsee HA and FA, and Aldrich HA.

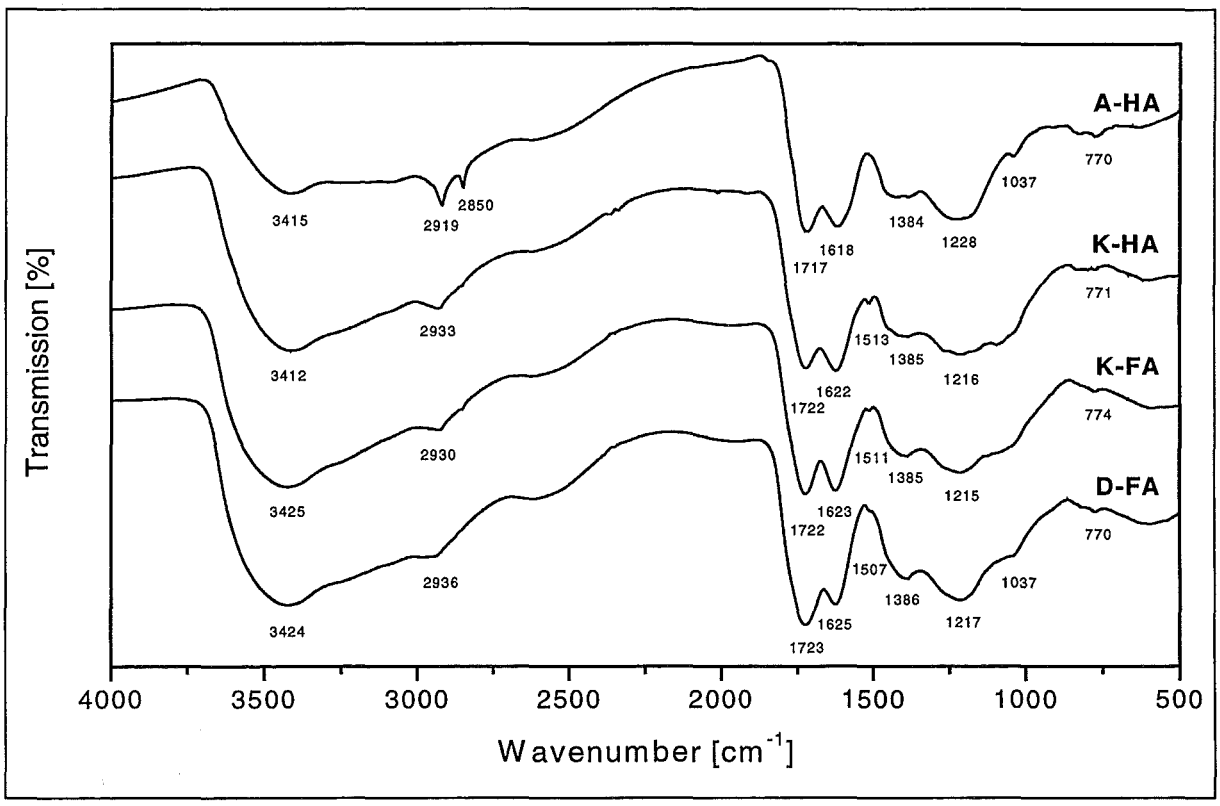

Figure 1: IR spectra of Kranichsee HA (K-HA), Kranichsee FA (K-FA) and Derwent FA (D-FA) compared to Aldrich HA (A-HA)

These spectra are very similar to each other and to typical IR spectra of humic and fulvic acids published in the literature (Schnitzer and Khan, 1972, MacCarthy and Rice, 1985).
The following differences of the Derwent FA compared to the other humic substances are remarkable:

- High intensity of the 1723 cm^{-1} band. This corresponds to the pronounced band at 1217 cm^{-1} and is attributed to a higher carboxylic group content which was determined as follows:

Derwent FA [1]	Kranichsee FA [2]	Kranichsee HA [2]	Aldrich HA [2]
5.0 meq/g	3.98 ± 0.25 meq/g	3.88 ± 0.41 meq/g	3.9 ± 0.1 meq/g

[1] Higgo et al. (1998) - determined by fitting of the pH titration curve to NICA-Donnan continuos distribution model.

[2] Schmeide et al. (1998) - determined radiometrically.

- In the case of Derwent FA, the 1723 cm^{-1} band is much more pronounced than the 1625 cm^{-1} band. Furthermore, the band at 1510 cm^{-1} is very small. It can be concluded that the Derwent FA has a lower content of aromatic structures compared to Kranichsee humic substances.

2.2 Capillary Zone Electrophoresis

The Derwent FA was investigated by capillary zone electrophoresis (P/ACE 2050, Beckman Instruments, Palo Alto, CA, USA). Again, the Derwent FA was applied in its lyophilized form. The separation conditions of the measurements were:
Buffer: 40 mM Na_2HPO_4, 20 mM H_3BO_3, pH 8.17; temperature 30 °C; separation voltage 15 kV, I: 84 µA; detection 214 nm; 15 s injection by means of pressure; fused silica capillary, 57 cm total length, 50 cm effective length, 75 µm inner diameter.

In Fig. 2 the electropherogram of the Derwent FA is depicted together with the electropherograms of Kranichsee HA and FA and Aldrich HA that are already discussed elsewhere (Schmeide et al., 1998). Comparing both FA's, it becomes evident that their peak shapes differ somewhat. The peak of the Derwent FA is much broader. This means that a larger distribution of the charge-to-size ratio exists. Thus, the molecule fraction of the Kranichsee FA shows a greater homogeneity than the Derwent FA. Furthermore, the

migration time of the Derwent FA is slightly larger indicating a somewhat smaller molecular size and/or a higher amount of charge carriers due to a higher COOH content.

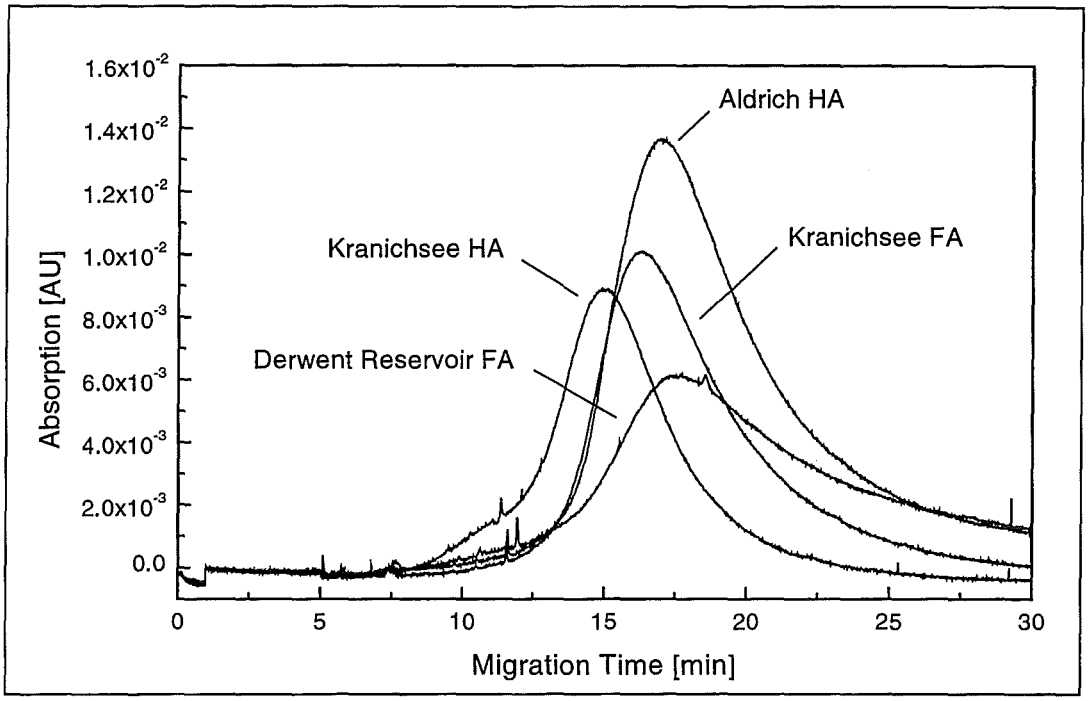

Figure 2: Electropherograms of Kranichsee HA, Kranichsee FA and Derwent FA compared to Aldrich HA.
Buffer: 40 mM Na_2HPO_4, 20 mM H_3BO_3, pH 8.17

3 Uranyl(VI) Complexation with Kranichsee Humic and Fulvic Acid at pH 4

The complexation of uranyl(VI) with Kranichsee humic acid and fulvic acid is studied by laser-induced fluorescence spectroscopy at pH 4 in 0.1 M $NaClO_4$.

The humic material used for this study was isolated from surface water of the mountain bog 'Kleiner Kranichsee' that is located in the vicinity of uranium mining sites at Johanngeorgenstadt (Saxony, Germany). The humic material was separated into humic and fulvic acid (Schmeide et al., 1998).

3.1 Experimental

Kranichsee Humic and Fulvic Acid

The isolation, purification and characterization of the Kranichsee humic and fulvic acid is described in detail by Schmeide et al. (1998). The proton exchange capacity (PEC) was determined potentiometrically for Kranichsee humic acid and fulvic acid as 4.83 ± 0.18 meq/g and 5.60 ± 0.12 meq/g, respectively.

Laser Spectroscopic Measurements

The measurements were performed in air at 20 °C at pH 3.96 ± 0.02 in 0.1 M $NaClO_4$. The fluorescence of uranyl(VI) ions was measured as a function of the total uranyl concentration at constant HA concentrations (5 mg/L). The uranyl concentration was varied from 0.5 to 5.1 µmol/L. The relative fluorescence signal as a function of the uranyl concentration was calibrated by means of solutions containing uranyl but no humic material. The uranyl concentration in these solutions was equal to the uranyl concentration of the uranyl humate solutions, and was determined by ICP-MS (Inductive Coupled Plasma-Mass Spectrometry, Mod. ELAN 5000, Perkin Elmer). The pH of the solutions was adjusted by addition of appropriate amounts of dilute $HClO_4$ or NaOH.

The experimental setup of the laser spectroscopic measurements is described in detail by Brachmann (1997). The fourth harmonic oscillation of the Nd:YAG laser (266 nm) was used for the excitation of uranyl fluorescence. The laser energy was about 500 µJ. Further experimental conditions were: delay time - 200 ns and gate time - 1000 ns. Ten spectra were always collected, each with 100 laser pulses, per sample. The spectra were deconvoluted by a non-linear least-square method using spectra of free uranyl (UO_2^{2+}) and of the first hydrolytic uranyl species (UO_2OH^+) and scattered laser light of the excitation laser pulse (second order) at 532 nm produced in the spectrograph. Thus, the contribution of the free uranyl ion to the fluorescence signal could be determined. The uranyl fluorescence intensity was integrated from 465 to 570 nm.

3.2 Results

The experimental data were evaluated by means of the metal ion charge neutralization model (Kim and Czerwinski, 1996). For the complexation reaction a charge neutralization of the metal ion is assumed, i.e., the uranyl ion occupies two proton exchanging sites of the HA molecule (Eq. (1)):

$$UO_2^{2+} + HA(II) \leftrightarrow UO_2HA(II) \tag{1}$$

where HA(II) represents the humic acid ligand and $UO_2HA(II)$ stands for uranyl humate. The complexation constant ß can be described by

$$ß = \frac{[UO_2HA(II)]}{[UO_2^{2+}]_{free} \cdot [HA(II)]_{free}} \tag{2}$$

ß - complexation constant; $[UO_2HA(II)]$ - uranyl humate concentration; $[UO_2^{2+}]_{free}$ - free uranyl ion concentration; $[HA(II)]_{free}$ - free HA concentration

It is assumed that only a fraction of the total complexing sites of the humic acid is available for the binding of uranyl ions. Thus, the loading capacity LC, defined as the maximum fraction of proton exchanging sites of the humic material that can be occupied by uranyl ions under the given experimental conditions, is introduced:

$$LC = \frac{[UO_2HA(II)]_{max}}{[HA(II)]_{total}} \tag{3}$$

$[UO_2HA(II)]_{max}$ is the maximum concentration of uranyl humate complex that can be formed under the given experimental conditions. $[HA(II)]_{total}$ is the total HA concentration. The free HA concentration ($[HA(II)]_{free}$) is given by

$$[HA(II)]_{free} = [HA(II)]_{total}\, LC - [UO_2HA(II)] \tag{4}$$

Thus, the loading capacity LC and the complexation constant ß can be determined by the following relation:

$$[UO_2^{2+}]_{free} = LC \frac{[HA(II)]_{total}\,[UO_2^{2+}]_{free}}{[UO_2HA(II)]} - \frac{1}{ß} \tag{5}$$

The loading capacities of Kranichsee humic and fulvic acid were determined graphically as shown in Fig. 3. In Tab. 1 and 2 the analytical data of the initial concentrations, data determined from spectroscopic measurements and the complexation constants derived from these data are given for the complexation of uranyl(VI) with Kranichsee HA and FA, respectively.

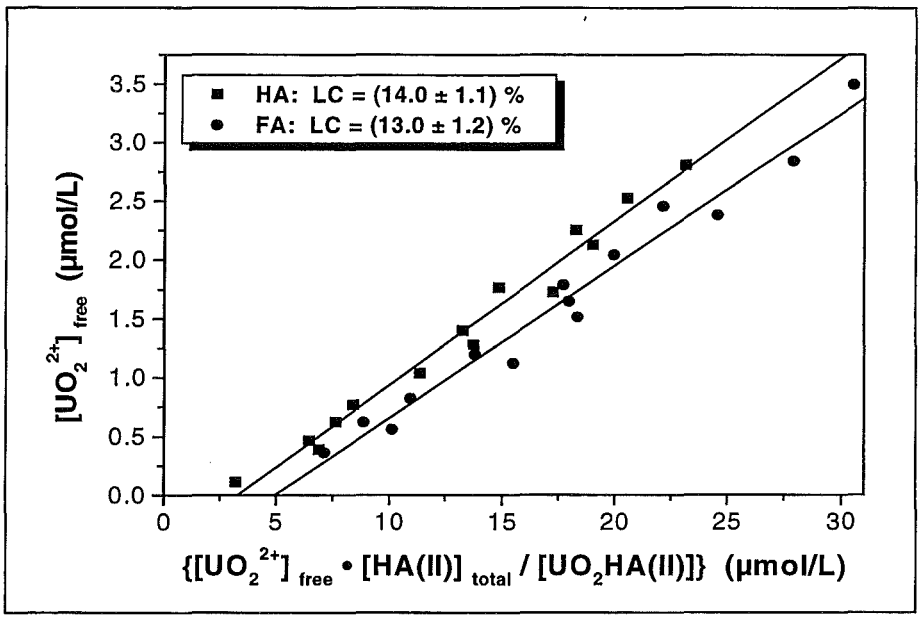

Figure 3: Graphical determination of the loading capacity (LC) for the complexation of UO_2^{2+} with Kranichsee humic substances

Table 1: Complexation of uranyl(VI) with Kranichsee HA. Analytical data of initial concentrations, data calculated from spectroscopic study and complexation constants log ß. PEC $_{\text{Kranichsee HA}}$ = 4.83 ± 0.18 meq/g; pH = 3.96 ± 0.02; I: 0.1 M $NaClO_4$; LC: 0.14 ± 0.01

$[UO_2^{2+}]_{total}$ (µmol/L)	$[HA(II)]_{total}$ (µmol/L)	$[UO_2^{2+}]_{free}$ (µmol/L)	$[HA(II)]_{free}$ (µmol/L)	$[UO_2$-HA(II)] (µmol/L)	log ß
0.53	12.08	0.11	1.26	0.42	6.48
1.07	12.08	0.39	1.00	0.68	6.24
1.33	12.08	0.46	0.82	0.87	6.36
1.60	12.08	0.62	0.70	0.98	6.35
1.87	12.08	0.77	0.58	1.10	6.39
2.13	12.08	1.03	0.58	1.10	6.26
2.40	12.08	1.28	0.56	1.12	6.19
2.67	12.08	1.40	0.41	1.27	6.34
2.93	12.08	1.73	0.48	1.21	6.17
3.20	12.08	1.77	0.25	1.44	6.52
3.47	12.08	2.12	0.34	1.35	6.28
3.74	12.08	2.25	0.20	1.49	6.52
4.00	12.08	2.52	0.20	1.48	6.46
4.27	12.08	2.81	0.22	1.46	6.37
				mean value:	6.35 ± 0.22

Table 2: Complexation of uranyl(VI) with Kranichsee FA. Analytical data of initial concentrations, data calculated from spectroscopic study and complexation constants log ß. PEC $_{\text{Kranichsee FA}}$ = 5.60 ± 0.12 meq/g; pH = 3.96 ± 0.02; I: 0.1 M $NaClO_4$; LC: 0.13 ± 0.01

$[UO_2^{2+}]_{total}$ (µmol/L)	$[FA(II)]_{total}$ (µmol/L)	$[UO_2^{2+}]_{free}$ (µmol/L)	$[FA(II)]_{free}$ (µmol/L)	$[UO_2$-FA(II)] (µmol/L)	log ß
1.07	14.0	0.36	1.10	0.71	6.25
1.33	14.0	0.56	1.04	0.77	6.12
1.60	14.0	0.62	0.83	0.98	6.28
1.87	14.0	0.82	0.76	1.05	6.22
2.13	14.0	1.12	0.80	1.01	6.05
2.40	14.0	1.19	0.60	1.21	6.23
2.67	14.0	1.51	0.66	1.16	6.07
2.93	14.0	1.65	0.53	1.29	6.17
3.20	14.0	1.79	0.40	1.41	6.30
3.47	14.0	2.04	0.38	1.43	6.26
3.74	14.0	2.38	0.46	1.36	6.10
4.00	14.0	2.45	0.26	1.55	6.38
4.27	14.0	2.84	0.39	1.43	6.11
5.10	14.0	3.50	0.21	1.60	6.34
				mean value:	6.21 ± 0.20

The complexation constants (log ß) and loading capacities (LC) of the uranyl complexation with Kranichsee humic substances are summarized in Tab. 3. The results indicate that there is only little difference between the complexation of UO_2^{2+} with humic acid and fulvic acid of the Kranichsee site.

Table 3: Complexation constants (log ß) and loading capacities (LC) of the uranyl(VI) complexation of Kranichsee HA and FA compared to Aldrich HA (Pompe et al., 1998) and GoHy-573 HA (Czerwinski et al., 1994)

	log ß	LC [%]	Validation (slope)
Kranichsee HA	6.35 ± 0.22 [a]	14.0 ± 1.1 [a]	0.84 ± 0.12
Kranichsee FA	6.21 ± 0.20 [a]	13.0 ± 1.2 [a]	0.77 ± 0.12
Aldrich HA [b]	5.86 ± 0.14 [a]	21.7 ± 2.1 [a]	
GoHy-573 HA [c]	6.16 ± 0.13	18.5 ± 0.3	

[a] $\pm 2\sigma$ [b] purified commercial product [c] isolated from Gorleben, Germany

Furthermore, comparing the complexation constants of the uranyl complexation of Kranichsee humic and fulvic acid with those of Aldrich HA (commercial product) (Pompe et al., 1998) and GoHy-573 HA (isolated from Gorleben, Germany) (Czerwinski et al., 1994) it turns out that the complexation behavior of the humic substances from different origin with U(VI) is comparable. This corresponds to the model applied which permits the determination of the complexation constants independently of the HA origin, the metal ion concentration, and the pH value (Kim and Czerwinski, 1996).

The loading capacities determined for the Kranichsee humic substances are lower than those of Aldrich HA and GoHy-573 HA. That means, fewer proton exchanging sites of the Kranichsee humic substances can be occupied by uranyl(VI) ions under the given experimental conditions.

For the graphical validation of the complexation reaction, Eq. (2) is rearranged to:

$$\log \frac{[UO_2HA(II)]}{[UO_2^{2+}]_{free}} = \log[HA(II)]_{free} + \log ß \qquad (6)$$

The slope of the function of Eq. (6) represents the metal ion to ligand ratio and is expected to be one. In Tab. 3 the results of the graphical validation of the uranyl complexation with

Kranichsee humic substances are given. The slopes are nearly one within the experimental error. Thus, the assumed complexation model is verified.

4 Colloid Characterization in the Kranichsee Bog Water After Addition of Varying Amounts of UO_2^{2+}

Continuing the experiments described by Schmeide et al. (1998), we characterized water samples from the Kranichsee bog by ultrafiltration. The samples were taken in Winter 1998. We applied Centricon type concentrators equipped with YM membranes (Amicon GmbH, Witten, Germany). Fig. 4 shows the filtration scheme. A prefiltration through a 5 µm Nuclepore filter was carried out and the ultrafiltrations were done in parallel. Both the filtrates and the retentates were investigated by UV-Vis detection (calibrated against TOC analysis). The results are given in Fig. 5. Decreasing amounts of humic material were passing through the ultrafilters with decreasing molecular weight cut-off. The sums of the filtrate and the retentate concentrations show that the recovery of the ultrafiltration procedure is reasonable (the poorest recovery was found for the 10 kD ultrafilter). From the differences between the filtrate concentrations an estimation of the fraction of humic substance in four molecular weight ranges can be made. Fig. 6 presents these fractions. Note that the 'molecular weights' determined by ultrafiltration are hydrodynamic particle sizes in reality. They are affected by considerable systematic errors due to the facts that ultrafilters are calibrated with substances quite different from humic acid and that the hydrodynamic diameter of polyelectrolyte molecules is dependent on solution conditions such as the ionic strength and the pH. However, relative measurements, i.e. comparisons, can be made on the basis of such 'apparent molecular weights' as long as the ambient conditions are kept constant. In the following we will discuss the influence of uranyl ions on the 'apparent molecular weight' of the Kranichsee humic acid.

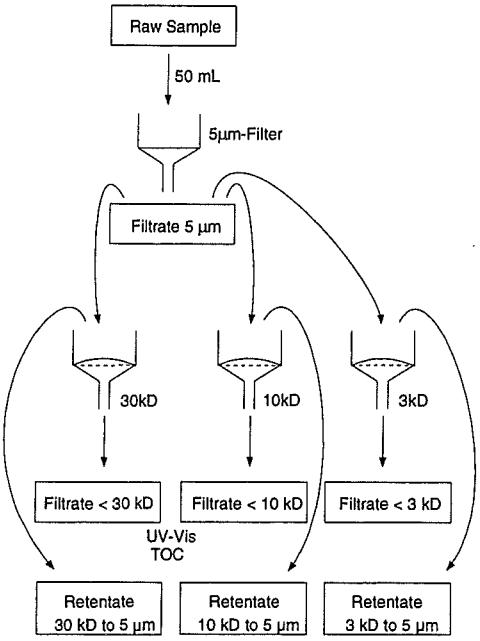

Figure 4: Scheme of Filtration. Application of a 5 µm Nuclepore filter and of Centricon type Amicon ultrafilters of varying molecular weight cut-off.

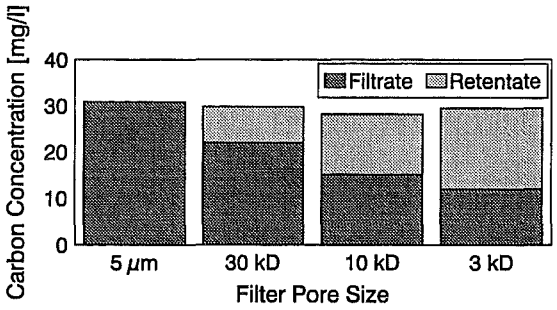

Figure 5: Carbon concentration in the sample fractions obtained from the filtration/ultrafiltration according to the scheme in Fig. 4.

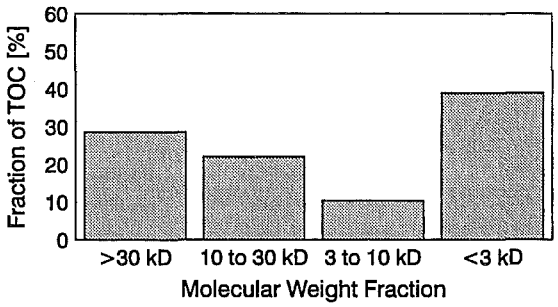

Figure 6: Molecular weight distribution of the organic substances in the bog water as derived from the ultrafiltration results.

6 References

Beckett, R., Bigelow, J. C., Zhang, J. and Giddings, J. C. (1989) Analysis of Humic Substances Using Flow Field-Fractionation. In *Influence of Aquatic Humic Substances on Fate and Treatment of Pollutants* (ed. P. Mac Carthy and I. H. Suffet), ACS Advances in Chemistry Series 219, Chapter 5, ACS, Washington DC.

Brachmann, A. (1997) *Zeitaufgelöste laserinduzierte Fluoreszenzspektroskopie zur Charakterisierung der Wechselwirkung des Uranylions mit Huminsäuren sowie Carboxylatliganden zur Simulation der Huminsäurefunktionalität.* Dissertation, TU Dresden.

Czerwinski, K.R., Buckau, G., Scherbaum, F. and Kim, J.I. (1994) Complexation of the Uranyl Ion with Aquatic Humic Acid. *Radiochim. Acta* ***65***, 111.

Higgo, J.J.W., Davies, J.R., Smith, B. and Milne, C. (1998) Extraction, Purification and Characterization of Fulvic Acid. In *First Technical Progress Report of the EC Project " Effects of Humic Substances on the Migration of Radionuclides: Complexation and Transport of Actinides"* . Project No. FI4W-CT96-0027 (ed. G. Buckau). Report FZKA 6124, Forschungszentrum Karlsruhe, 103.

Kim, J.I. and Czerwinski, K.R. (1996) Complexation of Metal Ions with Humic Acids: Metal Ion Charge Neutralization Model. *Radiochim. Acta* **73**, 5.

Klein, T. and Nießner, R. (1997) Characterization of Heavy Metal Containing Seepage Water Colloids by Flow FFF, Ultrafiltration, ELISA and AAS. *Microchim. Acta* **129**, 47-55.

MacCarthy, P. and Rice, J.A. (1985) Spectroscopic Methods (Other than NMR) for Determining Functionality in Humic Substances. In *Humic Substances in Soil, Sediment, and Water.* G.R. Aiken, D.M. McKnight, R.L. Wershaw and P. MacCarthy (eds.) John Wiley & Sons, New York, ch. 21.

Pompe, S., Brachmann, A., Bubner, M., Geipel, G., Heise, K.H., Bernhard, G. and Nitsche, H. (1998) Determination and Comparison of Uranyl Complexation Constants with Natural and Model Humic Acids. *Radiochim. Acta* **82**, 89.

Reid, P. M., Wilkinson, A. E., Tipping, E. and Jones M. N. (1990) Determination of molecular weights of humic substances by analytical (UV scanning) ultracentrifugation. *Geochim. Cosmochim.* Acta **54**, 131-138.

Schimpf, M. E. and Petteys, M. P. (1997) Characterization of humic materials by flow field-flow fractionation. *Colloids Surfaces A: Physicochem. Eng. Aspects* **120**, 87-100.

Schmeide, K., Zänker, H., Heise, K.H. and Nitsche, H. (1998) Isolation and Characterization of Aquatic Humic Substances from the Bog "Kleiner Kranichsee". In *First Technical Progress Report of the EC Project " Effects of Humic Substances on the Migration of Radionuclides: Complexation and Transport of Actinides"* . Project No. FI4W-CT96-0027 (ed. G. Buckau). Report FZKA 6124, Forschungszentrum Karlsruhe, 161.

Schnitzer, M. and Khan, S.U. (1972) *Humic substances in the environment.* (A.D. McLaren, ed.), Marcel Dekker, Inc., New York.

If one compares the results in Fig. 6 with those obtained on samples from Summer 1997 (Schmeide et al., 1998), a remarkable change becomes obvious. The 'molecular weight' distribution of the organic substances has significantly shifted toward the low molecular weight fraction (probably fulvic acid) in Winter 1998. The reason for this change is unknown.

After having determined the original colloid-chemistry of the bog water by ultrafiltration we added varying concentrations of uranyl ions to the water to elucidate the influence of uranyl complexation on the humic colloid particle size distribution. Conclusions on the colloid-facilitated uranium transport in humic-rich natural waters can be drawn from such interactions (size exclusion effects in aquifers, for instance, are dependent on the particle size of the colloids). Fig. 7 shows the particle size distribution of the organic matter (TOC analysis) and the uranium (ICP-MS) for three degrees of uranyl complexation. The calculation of these degrees was based on a humic proton exchange capacity (PEC) of 5 meq/g which is the average value for the humic and the fulvic acids of the Kranichsee bog water as determined after isolation of the humics (cf. Schmeide et al., 1998).

As can be seen from Fig. 7, there is no clear influence of the uranyl ions on the molecular weight distribution of the humics - at least at the humic and uranyl concentrations investigated. However, the distribution of the uranyl ions themselves depends on the uranium concentration. At low U concentration the uranyl is preferentially bound to the higher molecular weight fractions. When higher uranium concentrations are employed, a considerable amount of the uranium is bound to the low molecular weight fractions or remains uncomplexed. We intent to verify the molecular weight distributions found by ultrafiltration by means of field flow fractionation (FFF). FFF is less prone to artifacts such as the above-mentioned ones than ultrafiltration. Generally, FFF provides significantly smaller molecular weights for humic acids than does ultrafiltration (Beckett, 1989; Klein and Nießner, 1997; Schimpf and Petteys, 1997). FFF molecular weights are also in better agreement with humic acid molecular weights determined by ultracentrifugation (Reid, et al., 1990) than those found by ultrafiltration.

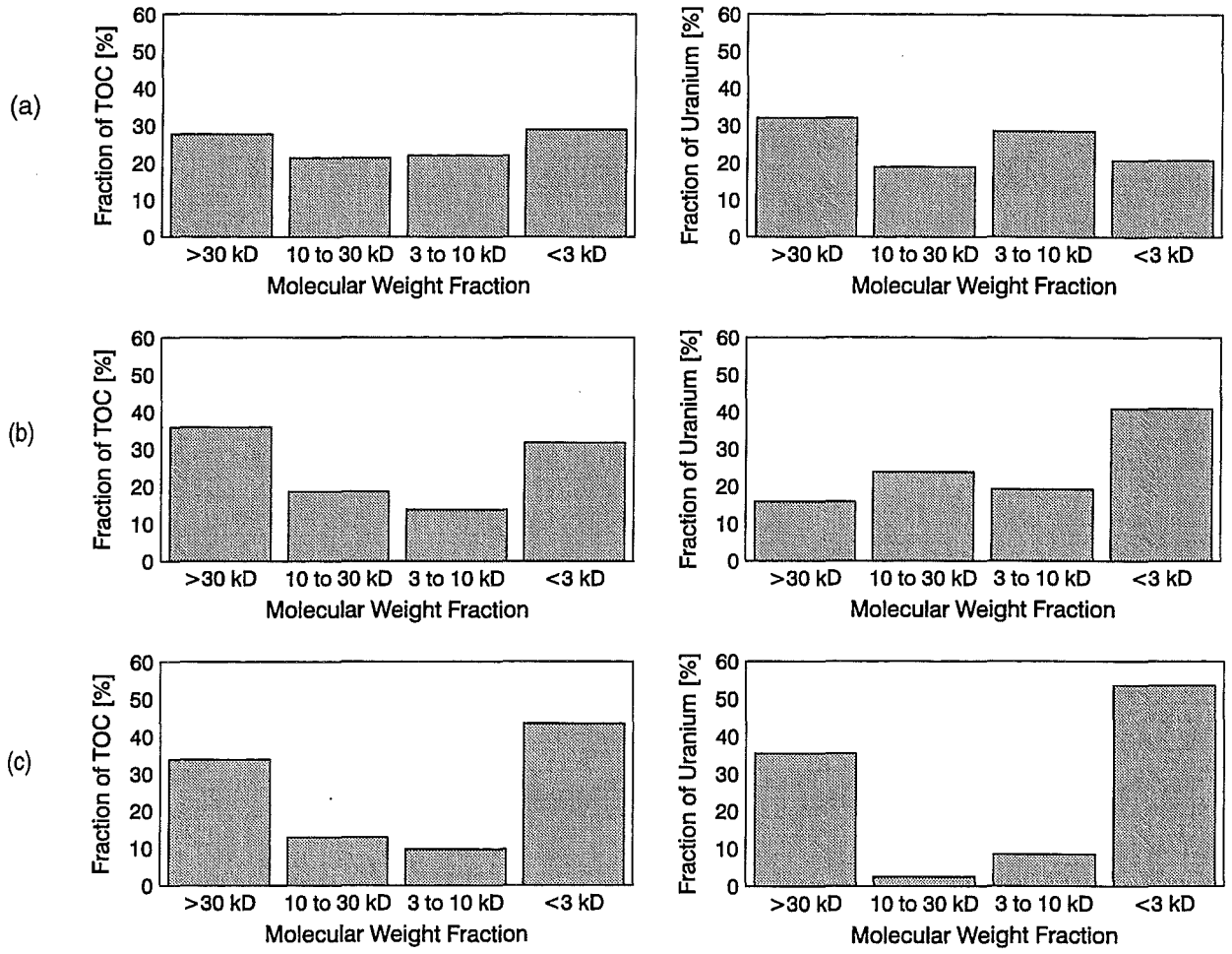

Figure 7: Humic substance and uranyl molecular weight distribution by ultrafiltration; uranyl addition corresponding to (a) 0.73% of PEC, (b) 11.9 % of PEC, and (c) 27.1 % of PEC.

5 Acknowledgment

This work was supported by Commission of the European Communities under contract no. F14W-CT96-0027.

Annex 9

Effect of Humic Substances on the Uranium(VI) Sorption onto Phyllite and its Mineralogical Constituents

(Schmeide et al., FZR/IfR)

2 nd Technical Progress Report

EC Project:

"Effects of Humic Substances on the Migration of Radionuclides: Complexation and Transport of Actinides"

Project No.: FI4W-CT96-0027

FZR/IFR Contribution to Task 3 (Actinide Transport)

Effect of Humic Acid on the Uranium(VI) Sorption onto Phyllite and its Mineralogical Constituents

Reporting period 1998

K. Schmeide, R. Jander, K.H. Heise, G. Bernhard

Forschungszentrum Rossendorf e.V.
Institute of Radiochemistry
P.O. Box 510119
01314 Dresden
Germany

Contents

Summary

The effect of humic acid (HA) on the uranium(VI) sorption onto phyllite and onto its individual main mineralogical constituents, muscovite, albite, and quartz was studied in air-equilibrated batch experiments in the pH range of 3.5 to 9.5. The uranyl(VI) and HA concentration was $1 \cdot 10^{-6}$ M and 5 mg/L, respectively. The ionic strength was held constant at 0.1 M ($NaClO_4$ solution). A size fraction of 63 to 200 µm of the solids was used, the mass loading was 12.5 g/L, and the experimental volume was 40 mL.

The rock material phyllite shows both the highest HA sorption over the entire pH range and the highest uranyl sorption in the neutral pH range compared to the pure mineral phases muscovite, albite and quartz. In contrast to the minerals the maximum of the uranium sorption on phyllite is not shifted to lower pH values but remains largely unchanged in the pH range from 6 to 7.8 when HA is present at 5 mg/L. This is attributed to ferrihydrite a secondary mineral phase formed during the sorption experiments.

The humic acid and uranyl sorption on the mineral surfaces of the constituents of phyllite decreased in the sequence: muscovite ≥ albite > quartz. Below pH 5, the uranium uptake is generally increased in the presence of HA. This is attributed to the fact that the HA is sorbed on the mineral surface thereby providing additional sorption sites due to their complexing ability and/or due to adsorption of uranyl humate complexes on the mineral surface. In the neutral pH range, the HA sorption decreases with increasing pH. The dissolved HA forms aqueous uranyl humate complexes thereby decreasing the uranyl uptake on the solids. At alkaline pH values, the HA has little or no effect on the amount of uranium sorbed by muscovite, albite and quartz. Inorganic carbonates with its high complexing ability towards uranyl ions predominate the influence of HA under the given experimental conditions. We conclude that the uranium sorption is determined by the kind of rock material or mineral and is strongly affected by both the pH and the presence of organic material.

In addition, the uranium adsorption on phyllite was studied as a function of the HA concentration (5 and 60 mg HA/L). Below pH 5.7, the uranium sorption is enhanced in the presence of 60 mg HA/L compared to experiments carried out with 5 mg HA/L. From pH 5.4 to 9.4, the uranium uptake, on a percentage basis, decreased as the humic acid concentration increased. Thus, a strong relationship between the initial humic acid concentration in solution and the amount of uranium adsorbed at a given pH was found.

1 Introduction

Abandoned mines and waste rock piles of the uranium mining areas of Saxony and Thuringia (Germany) represent a permanent reservoir and source of radioactive contaminants. Leaching of radionuclides, present in the waste rock, may occur and may introduce significant contamination to adjacent water bodies. However, spreading of uranium and of its decay products has to be minimized since the mines are located in densely populated areas. For safety assessment of uranium mining areas it is crucial to understand the interaction of uranium with site-specific rock material and furthermore, to know all processes and substances that may influence this interaction. Such processes are, for instance, potential chemical reactions inside a rock pile. Organic materials, such as humic and fulvic acids, may interact with dissolved inorganic contaminants and may affect the sorption behavior of such contaminants on geological materials. Due to complex formation reactions between radionuclides and humic substances the solubility of contaminants can be enhanced. The sorption of the thereby formed species can be either stronger or weaker than the sorption of the uncomplexed species. Thus, also the uranium migration in aquifers is affected. Consequently, it is necessary to quantify the influence of humic material on radionuclide sorption.

Phyllite was chosen as a site-specific rock material because it is quite common in the Western Erzgebirge in Saxony, Germany, and because it is closely associated with the uranium deposits of the uranium mining areas in East Germany. Phyllite is a low-grade metamorphic rock that is mainly composed of the minerals quartz, muscovite, chlorite, and albite.

Batch experiments were conducted in order to determine the effect of humic acid on the sorption behavior of uranium(VI) onto phyllite and onto its main mineralogical components muscovite, albite and quartz. Site-specific humic acid, isolated from the bog 'Kleiner Kranichsee' (Schmeide et al., 1998), was used for the experiments.

The effect of various humic substances on the uranium(VI) sorption onto different rock materials and minerals has been described in the literature (Beneš et al., 1998; Ho and Miller, 1985; Labonne-Wall et al., 1997; Payne et al., 1996; Payne et al., 1998; Ticknor et al., 1996).

2 Experimental

2.1 Materials

The light-colored phyllite, used for the sorption experiments, was obtained from the uranium mine 'Schlema-Alberoda' near Aue in Western Saxony (Germany). It was collected at a depth of 540 m. The phyllite is composed of 48 vol.% of quartz, 25 vol.% of chlorite, 20 vol.% of muscovite, 5 vol.% of albite, and 2 vol.% of brownish opaqueous material, identified as Ti- and Fe-oxides (Arnold et al., 1998a).

Furthermore, sorption experiments with quartz, muscovite, and albite as pure mineral phases were carried out. The quartz was a commercially available fine-grained quartz (Merck, p.a.) whereas the muscovite and the albite were geological specimens.

The 63 to 200 µm grain size fractions of the rock and the mineral samples were used for batch sorption experiments. The specific surface areas of the 63 to 200 µm fractions, determined by means of the BET method, are 0.2 m^2/g for quartz, 0.2 m^2/g for albite, 1.4 m^2/g for muscovite and 4.0 m^2/g for phyllite.

The humic acid used for the sorption experiments was isolated from surface water of the mountain bog 'Kleiner Kranichsee' that is located in the vicinity of uranium mining sites at Johanngeorgenstadt in Western Saxony, Germany (Schmeide et al., 1998).

2.2 Sorption experiments

The sorption experiments were conducted under atmospheric conditions. 20 mL of a 0.1 M $NaClO_4$ solution were added to 500 mg of the geomaterial (63 to 200 µm fraction) in 50 mL polypropylene centrifuge tubes (Cellstar). Then, the samples were aged for 24 h. After that, additional 18 mL of 0.1 M $NaClO_4$ solution were added. The desired pH was adjusted by addition of dilute $HClO_4$ or NaOH. For studies at pH values higher than 7, a calculated amount of $NaHCO_3$ was added to accelerate the equilibration process with atmospheric CO_2. In the following days the pH was readjusted until the pH was stable. Then 2 mL of a HA stock solution (100 mg HA/L, 0.1 M $NaClO_4$) was added to reach the final volume of 40 mL and a HA concentration of 5 mg/L. The HA/mineral contact time was 14 days. The pH was checked and adjusted every day. Then, the experiment was started by adding 84 µL of a $4.8 \cdot 10^{-4}$ M uranyl perchlorate stock solution, prepared in $5 \cdot 10^{-3}$ M $HClO_4$, to obtain a uranyl

concentration of $1 \cdot 10^{-6}$ M. The pH was readjusted immediately after the addition of the perchlorate solution. Then, the samples were rotated end-over-end at room temperature for about 60 hours. After this time, the final pH values were determined. Subsequently, the samples were centrifuged at 10000 rpm for 30 minutes. The supernatant was filtered using Minisart N membranes (Sartorius) with a pore size of 450 nm. To avoid contamination caused by conservation agents in the filter membranes the membranes were washed five times with 20 mL of MILLIQ water (Milli-RO/Milli-Q-System, Millipore).

The supernatant (non-filtered solution) and the 450 nm filtrate were analyzed by ICP-MS (Inductive Coupled Plasma-Mass Spectrometry, Mod. ELAN 5000, Perkin Elmer) for the final uranium concentration and by UV/Vis spectrophotometry (Mod. 8452A, Hewlett Packard) at 254 nm for the final HA concentration. It could be shown that there was no significant difference between the concentrations determined for the supernatant and the 450 nm filtrate.

In addition, the uranium sorption onto the wall of the centrifuge tubes was determined. Therefore, at first the empty tubes were washed three times with MILLIQ water and second 40 mL of 1 M HNO_3 were added to the tubes that were then shaken for 60 h. Subsequently, uranium was determined by ICP-MS and the amount of uranium in solution was attributed to sorption to the centrifuge tube walls. It reached values up to 8-13 % for albite and muscovite in the pH range of 5.5 to 7.5. For quartz, the sorption on the centrifuge tubes reached values up to 15-17 % in the pH range of 5.4 to 7.7. For phyllite, the effect was only about 2-3 % at pH 5 to 7.7. In the acid pH range, the vial wall sorption was 0.5 to 6 % for all minerals. At alkaline pH values the wall sorption was negligible.

The amount of uranium adsorbed to the mineral surface was calculated as the difference between the initial U(VI) concentration ($1 \cdot 10^{-6}$ M) and the sum of the final uranium concentration in the 450 nm filtrates and the amount of uranium adsorbed onto the wall of the experimental vials.

The difference between the initial HA concentration (5 mg/L) and the corresponding concentration in the 450 nm filtrates is attributed to HA sorption onto the mineral. The HA sorption onto the centrifuge tube walls was not determined.

2.3 Leaching experiments

The leaching of the rock material phyllite in a 0.1 M $NaClO_4$ solution was investigated as a function of pH. Batch experiments were carried out according to the procedure in paragraph 2.2 with the exception neither HA nor uranium was added. Seven pH values between pH 4.5 and pH 9.3 were investigated. The concentration of the following elements was determined in the leachates (450 nm filtrate): K, Ca, Mg, Fe, Al, Si, Mn, Ba, Sr, U. The content of the following anions was determined as well: Cl^-, F^-, CO_3^{2-}.

3 Results and discussion

3.1 Leaching of phyllite

The treatment of the rock material phyllite with 0.1 M $NaClO_4$ solution led to mineral dissolution and cation exchange reactions. For instance, mineral dissolution takes place on quartz. Si is dissolved from the mineral thereby forming silicic acid. In contrast to this, primarily cation exchange reactions take place on albite. Na is exchanged with H^+ forming a proton enriched surface layer thereby increasing the pH of the solutions. In smaller quantities also Ca and K are leached. These elements originate from anorthite and K-feldspar present as minor phases in albite. Mineral dissolution of muscovite and chlorite takes place predominantly on the edges (hk0). In case of muscovite mainly K is dissolved from the interfacial layers and in case of chlorite Mg and Fe are dissolved out of the brucite layer. The leaching of Si and Al is also possible for muscovite and chlorite. Additionally, amorphous and crystalline iron oxyhydroxides are formed as secondary mineral phases during the batch experiments with phyllite.

In the leachates mostly K, Ca, Mg and Si but also Mn, Al and Fe were identified. The amount of uranium naturally present in the rock material that can be leached ($\leq 10^{-8}$ mol/L) is far below the amount of uranium that will be added in the sorption experiments.

The objective of the leaching experiments was to determine whether the uranium speciation in solution as a function of pH is changed due to cations and anions leached from the phyllite in the course of the batch experiments. Therefore, at first, the uranium speciation in solution was determined for samples without phyllite and HA with the speciation modeling software EQ3/6 (Wolery, 1992) using the NEA data base (Grenthe et al., 1992). The results are shown as lines

in Fig. 1. The species distribution is dominated by UO_2^{2+} up to pH 5.5. $UO_2(OH)_{2(aq)}$ becomes predominant between pH 5.5 and 7.7, and $UO_2(CO_3)_3^{4-}$ predominates at higher pH values. Second, the quantitative composition of the leachate was included in the speciation calculation. The results shown in Fig. 1 (symbols) indicate that the uranium speciation is not altered significantly if the leached cations and anions are included.

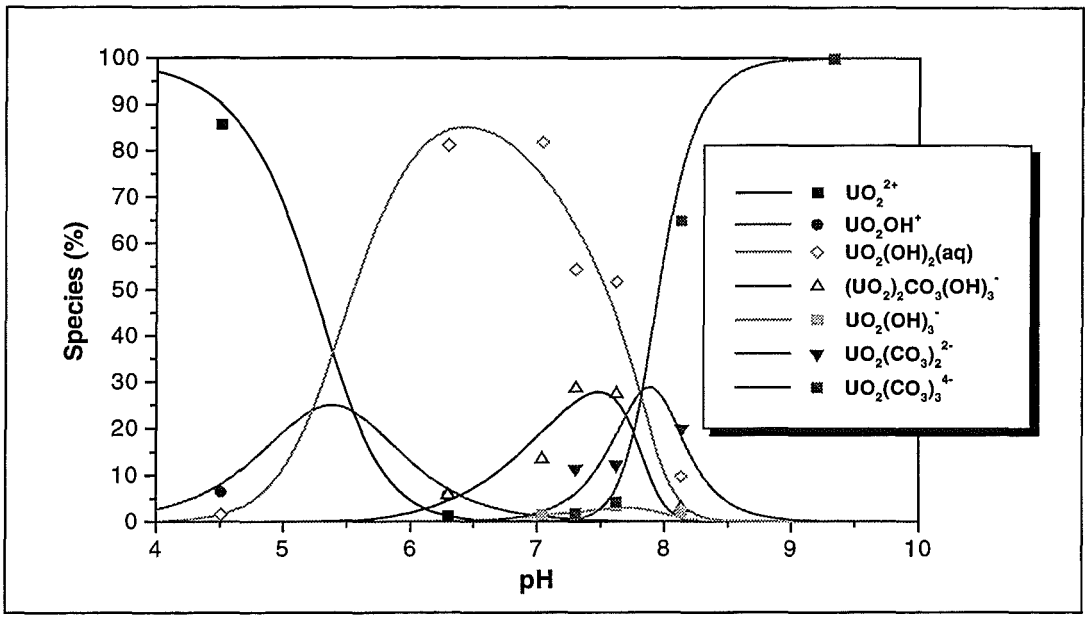

Figure 1: Uranium speciation in solution without phyllite (lines) and with phyllite (symbols)
$[UO_2^{2+}] = 10^{-6}$ M, [HA] = 0 mg/L, I = 0.1 M ($NaClO_4$), p_{CO2}: $10^{-3.5}$ atm
OECD/NEA data base, software: EQ3/6

The uranium speciation in the presence of HA (5 mg/L) was calculated using stability constants compiled in the NEA data base (Grenthe et al., 1992) and stability constants of the uranyl humic acid complexation published by Czerwinski et al. (1994) for $UO_2HA(II)$ and Zeh et al. (1997) for $UO_2OHHA(I)$. The uranium speciation in the presence of HA is different from the uranium speciation in the absence of HA. $UO_2HA(II)$ is predominating at acidic pH. The maximum of $UO_2OHHA(I)$ occurs at pH 5.7. $UO_2(CO_3)_3^{4-}$ is predominating at alkaline pH. In the neutral pH range, $UO_2(OH)_{2(aq)}$ dominates. The cations and anions leached from the phyllite could not be included in the speciation calculation because their complexation constants with HA as published in the literature were determined under different experimental conditions and evaluated by different models and thus, are not comparable with each other.

Furthermore, the influence of inorganic colloids originating from the rock material has to be considered when the sorption and migration behavior of radionuclides in complex systems is investigated. Colloid-chemical studies on a slurry of ground phyllite at pH 8.9 are in progress.

3.2 Uranium(VI) and humic acid sorption onto phyllite, muscovite, albite and quartz with an initial humic acid concentration of 5 mg/L

The results of the uranyl and HA sorption experiments onto phyllite and its constituents are compared to results from previously conducted experiments where the sorption of U(VI) onto phyllite and its constituents was studied in the absence of humic material (Arnold et al., 1998b). The experimental conditions for these experiments were the same as described in paragraph 2.2. The main results of these experiments can be summarized as follows: The sorption of uranium on phyllite and on the pure mineral phases, quartz, muscovite, albite, and chlorite, has its maximum at near neutral pH range. The maximum amount of uranium sorbed onto each individual mineral was different and ranged from 48 % of the initially added uranium for quartz to 58 % for albite, 70 % for muscovite and chlorite and 97 % for phyllite. None of the main mineralogical constituents of phyllite dominates the sorption behavior of uranium onto phyllite. However, a secondary iron mineral newly formed during the batch experiment, very likely ferrihydrite, significantly influences the uranium sorption onto phyllite.

In Fig. 2 the results of the batch sorption experiments carried out in the presence of 5 mg/L HA are depicted. The U(VI) and HA uptake by the solids phyllite, muscovite, albite and quartz is shown as a function of pH.

Fig. 2a shows the pH-dependent U(VI) and HA uptake onto phyllite. The uranium adsorption curve in the presence of HA is similar to the adsorption curve obtained for the experiments in the absence of HA. The strong uranyl sorption on phyllite (95 - 97 % in the absence of HA) is not changed by HA in the pH range from 6 to 7.8. However, in the pH range from 3.6 to 6, the uranium uptake on phyllite is slightly higher when HA is present. Above pH 8, the HA slightly reduces the uranyl sorption on phyllite. Furthermore, HA is strongly taken up from pH 3.6 to 7.7: 78 to 88 % of the HA are adsorbed. Above pH 8, the HA sorption decreases to 59 % at pH 9.5.

The results for muscovite are depicted in Fig. 2b. At pH values from 8 to 9.5, the uranium sorption on muscovite is not affected by HA. In the pH range from 5.8 to 8, the uranium sorption becomes smaller in the presence of HA. However, the uranium sorption is much stronger in the presence of HA below pH 5.8. That means, the maximum of the uranyl sorption is shifted from pH 6.3 (70 % without HA) to pH 5.5 (67 % with HA). The sorption of HA on muscovite strongly depends on the pH of the solution. At pH 8 to 9.5 the HA is not sorbed; below pH 8, the HA sorption increases with decreasing pH and has a maximum at pH 4.5 to 5 (~ 83 %).

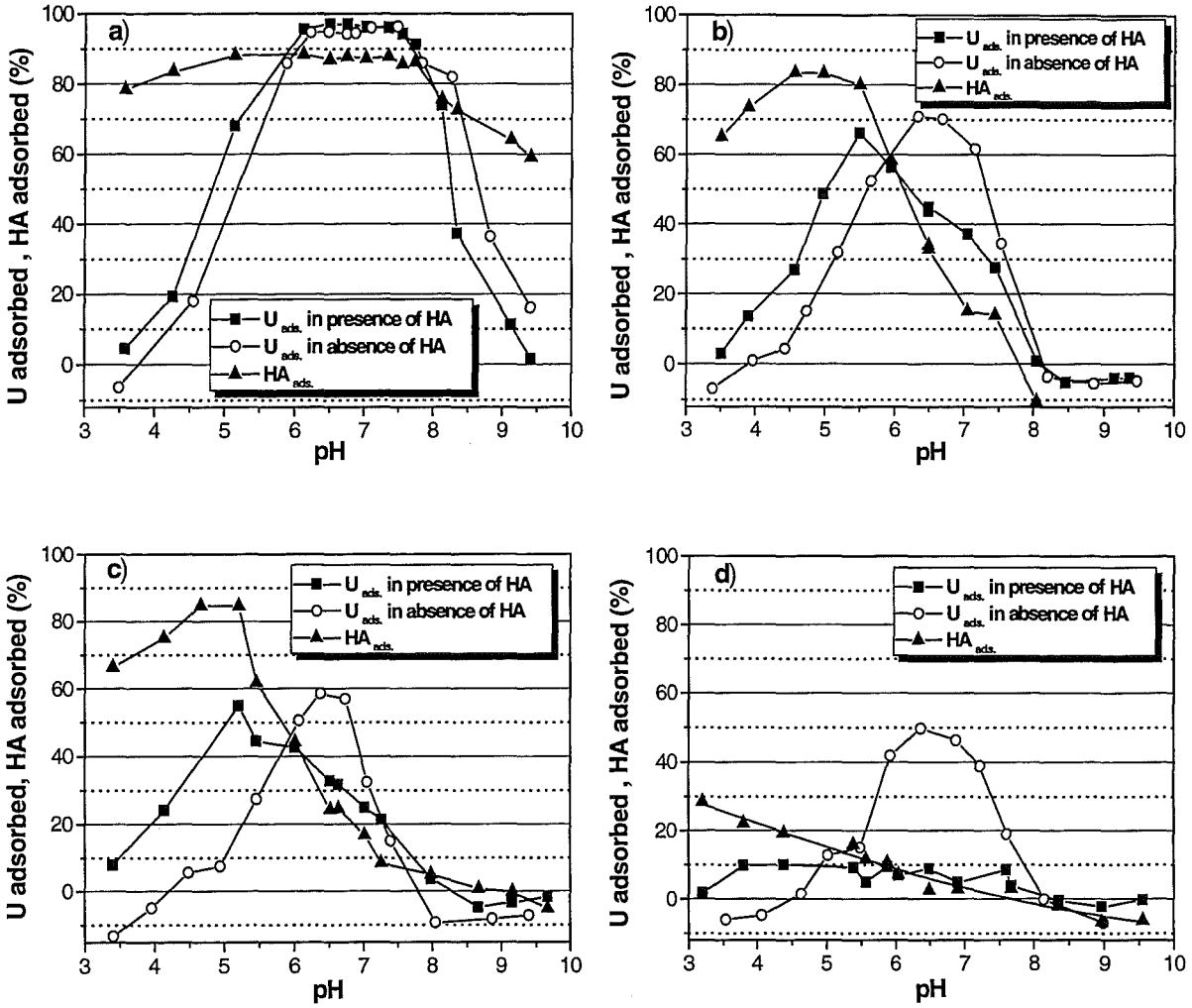

Figure 2: Uranium and HA uptake in experiments with added HA (5 mg/L) by the minerals: a) phyllite, b) muscovite, c) albite and d) quartz.
Data for uranium uptake in the absence of HA (Arnold et al., 1998b) are also shown.

The uranyl(VI) and HA adsorption curves for albite shown in Fig. 2c are similar to those for muscovite. The HA adsorption curve shows a maximum at pH 4.5 to 5. The maximum of the uranium uptake is shifted from pH 6.4 (58 % without HA) to pH 5.2 (55 % with HA).
The uranyl and HA uptake on quartz is depicted in Fig. 2d. There is little sorption of Kranichsee HA onto quartz. Essentially no HA is adsorbed at pH > 7.5. Below pH 7.5, the HA sorption increases with decreasing pH. In the absence of HA, the uranium sorption onto quartz mainly takes place in the pH range between 5 and 7.8 with a maximum of 48 % at pH 6.4. In this pH range, the uranyl sorption on quartz is strongly reduced to 5-10 % in the presence of HA. Below pH 4.8, the uranyl sorption in the presence of HA is higher than the uranyl sorption in the absence of HA.

When discussing the results of the sorption experiments, it has to be taken into account that the minerals were already contacted with HA for 14 days before uranium(VI) was added. That means, the mineral surfaces are likely to be coated with HA at the beginning of the sorption experiments. Thus, sorption sites of the solids may either be blocked by adsorbed HA from other aqueous species or the HA may provide additional sorption sites due to their complexing ability. The influence of HA on the uranyl sorption on muscovite, albite and quartz can be summarized as follows:
i) In the presence of HA, the uranium adsorption is generally increased in the pH range from 3.5 up to 5 (quartz) or to 5.7 (muscovite, albite). This may be attributed to the fact that the HA is sorbed on the mineral surface thereby providing additional sorption sites due to their complexing ability and/or due to adsorption of uranyl humate complexes on the mineral surface.
ii) In the neutral pH range, the HA sorption decreases with increasing pH. The dissolved HA forms aqueous uranyl humate complexes thereby decreasing the uranyl uptake on the solids. The HA sorption on quartz is substantially smaller than the HA sorption on muscovite and albite. Consequently, the uranium uptake on quartz, on a percentage basis, is reduced most strongly in the presence of HA.
iii) At alkaline pH values, the HA has little or no effect on the amount of uranium sorption. According to the speciation calculation considerable amounts of HCO_3^- are available to form complexes with uranyl ions ($UO_2(CO_3)_3^{4-}$, $UO_2(CO_3)_2^{2-}$). The inorganic carbonates have a

higher complexing ability towards uranyl ions compared to HA. Thus, the weakly sorbing uranyl carbonate complexes (Ticknor, 1994; Waite et al., 1994) predominate the influence of HA.

Phyllite shows the highest HA sorption compared to the minerals muscovite, albite and quartz over the entire pH range. This can not only be interpreted by its somewhat higher specific surface area which was determined by means of BET method as 4.0 m^2/g compared to 1.4 m^2/g for muscovite and 0.2 m^2/g for albite and quartz. Against that, we believe that ferrihydrite is responsible for the high HA adsorption onto phyllite. Ferrihydrite ($Fe_2O_3 \cdot 1.8$ H_2O) as secondary mineral phase is formed in the course of the sorption experiments (proved by Arnold et al., 1998b) and is visible as precipitation of a slight reddish-brownish color. It has a high specific surface area of 600 m^2/g and thus, it is expected to offer a significant sorption potential both to uranium and to HA. This assumption is supported by results found by Payne et al. (1996) who investigated the uranium adsorption on ferrihydrite in the presence of HA. They found that the HA uptake by ferrihydrite as a function of pH was generally strong (approx. 82 to 90 % between pH 3.5 to 9) and decreased only at pH values higher than pH 9. The very strong uranium adsorption on phyllite can also be attributed to the component ferrihydrite. Oxidic iron present in solution is known to form coatings on the surface of other minerals and to adsorb uranium well in composite minerals (Payne et al., 1994). Therefore, in contrast to the pure mineral phases, muscovite, albite and quartz, the maximum of the uranium sorption on phyllite is not shifted to lower pH values but remains unchanged in the pH range from 6 to 7.8 when HA is present at 5 mg/L.

We conclude that the influence of HA on the uranium sorption is affected by the pH of the solutions and depends on the kind of the rock materials or minerals.

3.3 Uranium(VI) and humic acid sorption onto phyllite with an initial humic acid concentration of 60 mg/L

In this series of batch experiments the HA concentration was increased to 60 mg/L. This concentration approximated to the organic material content of the original surface water of the mountain bog 'Kleiner Kranichsee' from which the HA was isolated. The results were com-

pared to results from the batch experiments conducted in the presence of 5 mg HA/L. Fig. 3 shows the influence of the HA concentration (5 and 60 mg HA/L) on the uranium and HA uptake by phyllite.

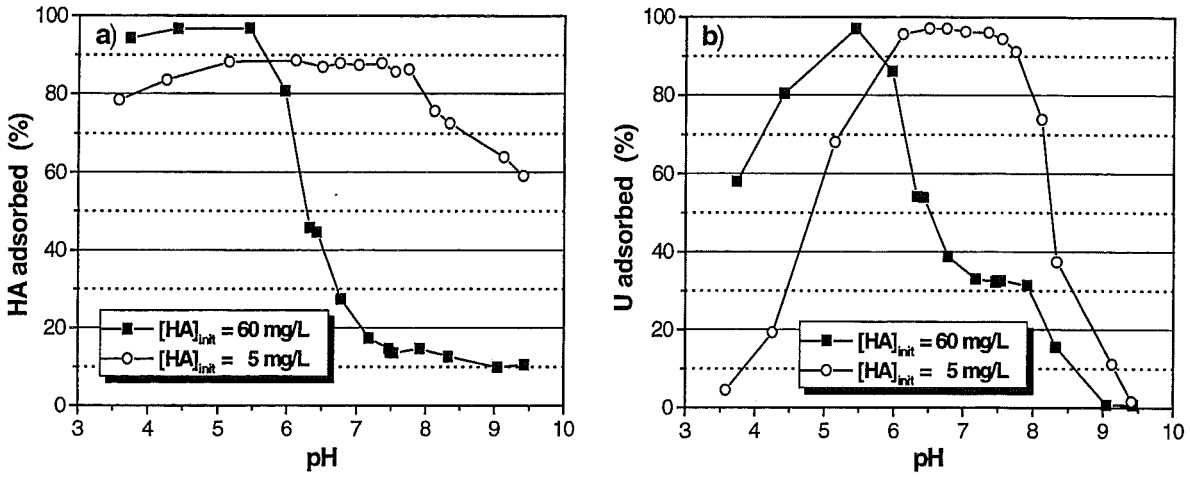

Figure 3: Effect of initial HA concentration (5 and 60 mg HA/L) on the uranium and HA uptake by phyllite

In contrast to experiments carried out with 5 mg HA/L where the HA strongly sorbed across a wide pH range, the HA sorption in experiments with 60 mg HA/L is strongly dependent on pH values (Fig. 3a). In the acid pH range (pH 3.7 to 5.4), the HA sorption is apparently very strong (94 to 97 %). However, the high HA sorption is caused most likely by an overlapping of sorption and precipitation of the HA. The uranium sorption is enhanced in the pH range up to pH 5.7 which leads to a shift of the maximum of the uranyl sorption (97 %) to pH 5.4 (Fig. 3b). This can be attributed either to the greater number of surface sorption sites that are provided by the HA or to coprecipitation of uranium with the HA. From pH 5.4 to 9.4, the amount of HA sorbed on the phyllite, on a percentage basis, decreases with increasing pH in the experiments carried out with 60 mg HA/L and is considerably lower than in experiments conducted with 5 mg HA/L. A decreasing HA sorption, on a percentage basis, with an increasing initial HA concentration has been observed by Tipping (1981), Norden et al. (1994), and Ticknor et al. (1996). The percentage of uranium adsorbed in the pH range 5.4 to 9.4 also decreases with increasing pH values and is significantly lower compared to the batch experiments carried out with only 5 mg HA/L. A decreasing uranium uptake with increasing HA concentration in solution was also reported by Ho and Miller (1985) for hematite. In the neutral pH range, the higher initial HA concentration leads to higher percentages of aqueous

uranyl humate complexes thereby strongly depleting the uranyl sorption onto phyllite. At high pH values, the effect of HA on the uranyl sorption is somewhat smaller than in the neutral pH range because there is a competition between uranium complexation by carbonate and uranium complexation by HA.

We conclude that there is a strong relationship between the initial HA concentration in solution and the amount of uranium adsorbed at a given pH.

4 Acknowledgment

This work was supported by Commission of the European Communities under contract no. F14W-CT96-0027.

5 References

Arnold, T., Zorn, T., Bernhard, G. and Nitsche, H. (1998a) Characterization of Phyllite with SEM/EDS, PIXE, and Thin Section Microscopy. In *FZR-218, Annual Report of Institute of Radiochemistry 1997* (ed. H. Nitsche). Forschungszentrum Rossendorf, 1.

Arnold, T., Zorn, T., Bernhard, G. and Nitsche, H. (1998b) Sorption of Uranium(VI) onto Phyllite. *Chemical Geology* **151**, 129.

Beneš, P., Kratzer, K., Vlcková, Š. and Šebestová, E. (1998) Adsorption of Uranium on Clay and the Effect of Humic Substances. *Radiochim. Acta* **82**, 367.

Czerwinski, K.R., Buckau, G., Scherbaum, F. and Kim, J.I. (1994) Complexation of the Uranyl Ion with Aquatic Humic Acid. *Radiochim. Acta* ***65***, 111.

Grenthe, I., Fuger, J., Lemire, R.J., Muller, A.B., Nguyen-Trung, C. and Wanner, H. (1992) *Chemical Thermodynamics of Uranium*, 1st ed., Elsevier Science Publishers, Amsterdam.

Ho, C.H. and Miller, N.G. (1985) Effect of Humic Acid on Uranium Uptake by Hematite Particles. *J. Colloid Interf. Sci.* **106**, 281.

Labonne-Wall, N., Moulin, V. and Vilarem, J.-P. (1997) Retention Properties of Humic Substances onto Amorphous Silica: Consequences for the Sorption of Cations. *Radiochimica Acta* **79**, 37.

Norden, M., Ephraim, J.H. and Allard, B. (1994) The influence of a fulvic acid on the adsorption of europium and strontium by alumina and quartz: effects of pH and ionic strength. *Radiochim. Acta* **65**, 265.

Payne, T.E., Davis, J.A. and Waite, T.D. (1994) Uranium Retention by Weathered Schists - The Role of Iron Minerals. *Radiochim. Acta* **66/67**, 297.

Payne, T.E., Davis, J.A. and Waite, T.D. (1996) Uranium Adsorption on Ferrihydrite - Effects of Phosphate and Humic Acid. *Radiochimica Acta* **74**, 239.

Payne, T.E., Shinners, S. and Twining, J.R. (1998) Uranium Sorption on Tropical Wetland Sediments. In *Uranium Mining and Hydrogeology II. Proceedings of the International Conference and Workshop. Freiberg, Germany, September 1998*, (ed. B. Merkel, C. Helling and St. Hurst), von Loga, Köln, pp. 298.

Schmeide, K., Zänker, H., Heise, K.H. and Nitsche, H. (1998) Isolation and Characterization of Aquatic Humic Substances from the Bog "Kleiner Kranichsee". In *First Technical Progress Report of the EC Project " Effects of Humic Substances on the Migration of Radionuclides: Complexation and Transport of Actinides"* . Project No. FI4W-CT96-0027 (ed. G. Buckau). Report FZKA 6124, Forschungszentrum Karlsruhe, 161.

Ticknor, K.V. (1994) Uranium Sorption on Geological Materials. *Radiochim. Acta* **64**, 229.

Ticknor, K.V., Vilks, P. and Vandergraaf, T.T. (1996) The effect of fulvic acid on the sorption of actinides and fission products on granite and selected minerals. *Applied Geochemistry* **11**, 555.

Tipping, E. (1981) The adsorption of aquatic humic substances by iron oxides. *Geochim. Cosmochim. Acta* **45**, 191.

Waite, T.D., Davis, J.A., Payne, T.E., Waychunas, G.A. and Xu, N. (1994) Uranium(VI) Adsorption to Ferrihydrite: Application of a Surface Complexation Model. *Geochim. Cosmochim. Acta* **58**, 5465.

Wolery, T.J. (1992) EQ3/6. *A software package for the geochemical modeling of aqueous systems.* UCRL-MA-110662 Part I. Lawrence Livermore National Laboratory, California, USA.

Zeh, P., Czerwinski, K.R., and Kim, J.I. (1997) Speciation of Uranium in Gorleben Groundwaters. *Radiochim. Acta* **76**, 37.

Annex 10

Investigation of the Migration Behavior of Uranium in an Aquifer System Rich in Humic Substances: Laboratory Column Experiments

(Pompe et al., FZR/IfR and FZK/INE)

2nd Technical Progress Report

EC Project:

"Effects of Humic Substances on the Migration of Radionuclides: Complexation and Transport of Actinides"

Project No.: FI4W-CT96-0027

FZR/IFR and FZK/INE Contribution to Task 3 (Actinide Transport)

Investigation of the Migration Behavior of Uranium in an Aquifer System Rich in Humic Substances: Laboratory Column Experiments

Reporting period 1998

S. Pompe[1], R. Artinger[2], K. Schmeide[1], K. H. Heise[1], J. I. Kim[2], G. Bernhard[1]

[1]Forschungszentrum Rossendorf e.V., Institut für Radiochemie
P.O. Box 510119, 01314 Dresden, Germany

[2]Forschungszentrum Karlsruhe, Institut für Nukleare Entsorgungstechnik
P.O. Box 3640, 76021 Karlsruhe, Germany

CONTENTS

ABSTRACT

The migration behavior of uranium in a sandy aquifer system rich in humic substances was studied in laboratory column experiments. For the investigations we used a Pleistocene aeolian quartz sand and groundwater GoHy-532 from the Gorleben site (Germany). The column experiments were performed in a glove box under anaerobic conditions (Ar + 1 % CO_2). $^{232}U(VI)$ was used as a tracer. The migration behavior of uranium was investigated as a function of the uranium/groundwater equilibration time before injection into the column, the groundwater flow velocity and the column length.

From the breakthrough curves one can conclude that a part of the injected uranium migrates slightly faster than groundwater. The observed migration behavior is attributed to the association of a part of uranium with humic colloids, which move faster due to size exclusion processes. Depending on the experimental conditions the recovery of humic colloid-bound transported uranium amounts to 0.4 up to 7.6 %. The recovery of non-retarded colloid-borne uranium increases with increasing uranium/groundwater equilibration time before injection into the column. Beyond it, the recovery of humic colloid-borne uranium decreases with decreasing groundwater flow velocity and increasing column length, which corresponds to an increasing residence time in the column.

The results refer to the fact that the migration behavior of uranium is strongly influenced by kinetically controlled interaction processes of uranium with humic colloids.

1 INTRODUCTION

The investigation of the migration behavior of actinides in natural aquifer systems is absolutely necessary to develop strategies for long-term risk assessment in the regions of the former uranium mines in Saxony and Thuringia and also for potential nuclear waste repositories. The migration behavior of actinide ions in natural aquifer systems is strongly influenced by the prevailing natural conditions. Humic substances as ubiquitous, organic complexing agents may play a decisive role for the migration and immobilization of actinide ions.

Laboratory flow through column experiments contribute essential knowledge to understand the influence of humic substances on the migration behavior of actinide ions. There is the possibility to investigate the migration behavior of actinides depending on different parameters, e.g., groundwater flow velocity and column length.

There are some publications which describe flow through column experiments for the investigation of the migration behavior of radionuclides in geological formations. Investigations regarding the migration behavior of Am(III) [1], Eu(III), Np(IV)/(V) and Pa(IV)/(V) [2] belong to it. Up to now, the migration behavior of uranium was studied by Kim et al. by means of column experiments [3, 4]. Migration experiments with a sediment/groundwater (GoHy-2227) system from the Gorleben site (Germany) were performed. The investigations were carried out under inert gas conditions (Ar + 1 % CO_2) with columns of 25 cm length and 5 cm inner diameter.

The present study [5] focuses on flow through column experiments to investigate the migration behavior of uranium in a sandy humic colloid-rich aquifer system, i.e., in the system sediment/groundwater GoHy-532 from Gorleben. We investigated the uranium migration behavior as a function of uranium/groundwater equilibration time before injection into the column, groundwater flow velocity and column length. Ultrafiltration experiments were used for the determination of the uranium size distribution.

2 EXPERIMENTAL

Experimental set-up

The experiments were performed in a glove box under inert gas conditions (Ar + 1 % CO_2, 22 ± 2 °C). The columns were tightly packed with sand and equilibrated with groundwater over several months. The sediment and groundwater characterization was described by Artinger et al. [1, 6]. The groundwater has a dissolved organic carbon content (DOC) of about 30 mg C/L, a pH value of 7.2 ± 0.1 and a Eh value of - 220 mV. The monitoring of the experiments and the recording of the experimental data was performed on-line by a personal computer. The experimental set-up is shown in Fig. 1.

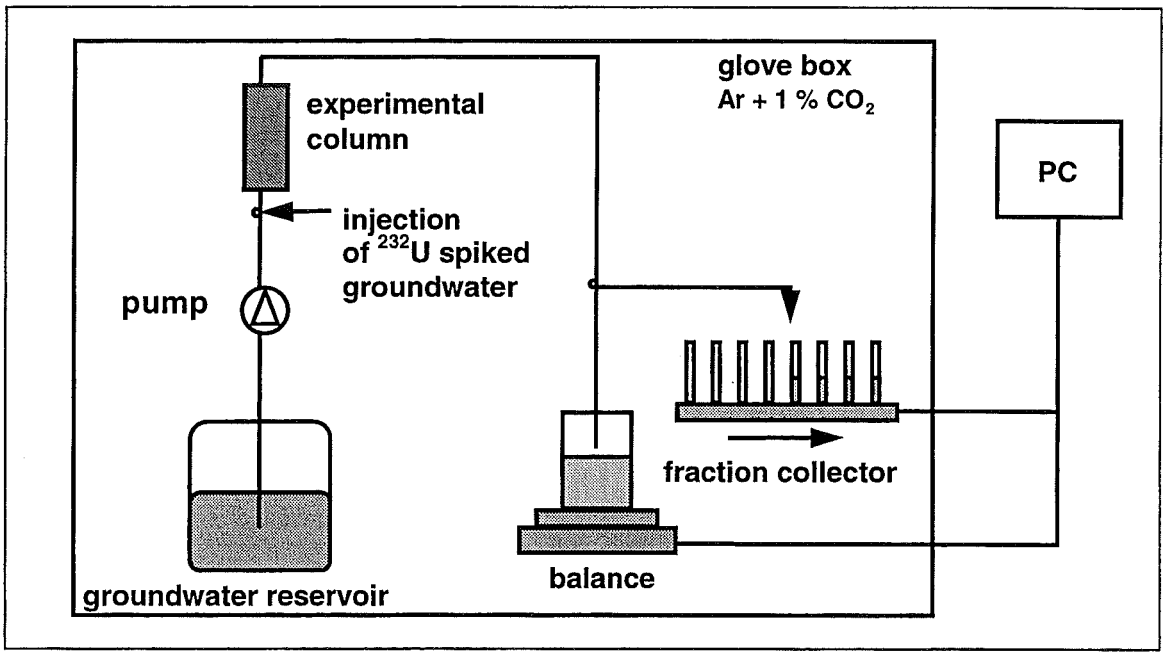

Figure 1: Experimental set-up of the column experiments.

Tracers

The uranium isotope Uranium-232 ($t_{1/2}$ = 72 years) in form of $^{232}UO_2Cl_2$ (Isotopendienst M. Blaseg GmbH, Waldburg, Germany) was applied because of its high specific activity. The ^{232}U stock solution showed a specific activity of 841 kBq/mL which corresponds to a uranium concentration of $4.6 \cdot 10^{-6}$ mol/L. Furthermore, tritiated water (HTO) was used as a conservative tracer to determine the hydraulic properties of the columns.

Procedure

The column experiments were performed in dependence on:

- ^{232}U/groundwater pre-equilibration time before the injection into the column,
- groundwater flow velocity and
- column length.

Prior to the experiments ^{232}U spiked groundwater solutions were prepared by allowing aliquots of the ^{232}U stock solution to react with the groundwater corresponding to the studied pre-equilibration time. Different pre-equilibration times from 1 hour to 82 days were investigated. The groundwater flow velocity was varied from 0.04 m/d to 2.03 m/d. The column length was varied between 25 cm and 75 cm. The experimental parameters and the hydraulic properties of the columns are summarized in Tab. 1.

For all experiments 1 mL of the ^{232}U spiked initial solution and 200 µL HTO were simultaneously injected into the column. The eluted water was collected in a polypropylene flask. In addition to this, fractions of the eluate were collected by a fraction collector at certain times during the experiment. The eluate, the eluate fractions and the initial solutions were analyzed for their ^{232}U and HTO concentrations by liquid scintillation counting. Additionally, alpha-spectroscopy was applied to determine the concentration of ^{232}U daughter nuclides. Thus, it was possible to correct the alpha-activities determined by liquid scintillation counting with regard to the alpha-activity contributed by the daughter nuclides. The breakthrough curves for HTO and ^{232}U result from the ^{232}U and HTO concentration in the eluate fractions.

Furthermore, investigations regarding the size distribution of uranium in the initial solutions and in different eluate fractions were performed by ultrafiltration. Ultrafilters with molecular weight cutoffs of 1 kD to 1000 kD (MICROSEP, Filtron, Northborough, MA, USA) were applied.

Table 1: Experimental conditions for the column experiments.

Experiment number	^{232}U/groundwater equilibration time [d]	Column length [cm]	Uranium concentration [mol/L]	Darcy velocity v_D [m/d]	Pore water flow velocity v [m/d]	Effective porosity ε	Longitudinal dispersion coefficient D_L [cm^2/s]
1	0.04	25	$5.1 \cdot 10^{-7}$	0.321	0.970	0.331	$8.64 \cdot 10^{-5}$
2	0.63	25	$4.5 \cdot 10^{-7}$	0.314	0.949	0.331	$3.73 \cdot 10^{-5}$
3	11	25	$4.9 \cdot 10^{-7}$	0.312	0.943	0.331	$3.70 \cdot 10^{-5}$
4	82	25	$4.2 \cdot 10^{-7}$	0.310	0.934	0.332	$3.34 \cdot 10^{-5}$
5	5	25	$4.4 \cdot 10^{-7}$	2.030	6.078	0.334	$2.14 \cdot 10^{-4}$
6	6	25	$4.7 \cdot 10^{-7}$	0.038	0.114	0.333	$1.58 \cdot 10^{-5}$
7	5	50	$4.1 \cdot 10^{-7}$	0.241	0.724	0.333	$2.55 \cdot 10^{-5}$
8	5	75	$4.3 \cdot 10^{-7}$	0.239	0.697	0.343	$3.24 \cdot 10^{-5}$

^{232}U species distribution

Species calculations for the groundwater GoHy-532 ([UO_2^{2+}]: 5• 10^{-7} mol/L, pH 7.2 ± 0.1, 1 % CO_2) were performed to determine the distribution of uranium species in the investigated groundwater/sediment system. The calculations based on complex formation constants compiled by Grenthe et al. [7] (NEA data base) and stability constants for the complex formation of UO_2^{2+} with humic acid published by Czerwinski et al. (UO_2HA(II)) [8] and Zeh et al. (UO_2OHHA(I)) [9]. Two calculations were performed at Eh = 800 mV and Eh = -220 mV, respectively. Uranium(VI) occurs at Eh = 800 mV and pH 7.2 to about 72 % as $UO_2(CO_3)_2^{2-}$, 21 % as $UO_2(CO_3)_3^{4-}$, 2 % as $UO_2(OH)_{2(aq)}$ and only to about 3 % as UO_2OHHA(I) complex. Under consideration of the experimentally determined redox potential of the groundwater of –220 mV uranium shows a totally different species distribution. Assuming thermodynamic equilibrium, U(VI) is completely reduced to U(IV) and occurs solely as $U(OH)_{4(aq)}$ complex. Possibly occurring U(IV) humate complexes were not considered because there are no reliable thermodynamic data, although it is known from literature that tetravalent actinides like Th(IV) show a strong interaction with humic substances [10].

In contrast to the calculated species distributions, ultrafiltration experiments of the ^{232}U labelled groundwaters showed for uranium roughly the size distribution of the humic substances in the groundwater [6]. Fig. 2 shows the ^{232}U size distribution in different initial solutions (alpha-activity contribution by daughter nuclides ≤10 %). From this one can conclude that the colloid-bound ^{232}U is mainly associated with humic colloids. Approximately 85 - 90 % of ^{232}U are associated with colloids greater than 1000 D and about 20 - 30 % occur in form of ionic species, probable carbonato complexes.

Up to now it can not definitely be stated whether and to what extent the humic colloid-bound uranium is present in the reduced tetravalent state. From neptunium experiments performed recently [11] it is known that the oxidation state has an essential influence on the neptunium size distribution. The reduction of Np(V) causes a decrease of ionic NpO_2^+ species in solution. Np(IV) is almost quantitatively associated to humic colloids. From that one may expect that the reduction of U(VI) to U(IV) also influences the uranium size distribution. However, no significant changes in the ^{232}U size distribution were observed. Therefore, one may conclude that there is no significant uranium reduction in the initial solutions.

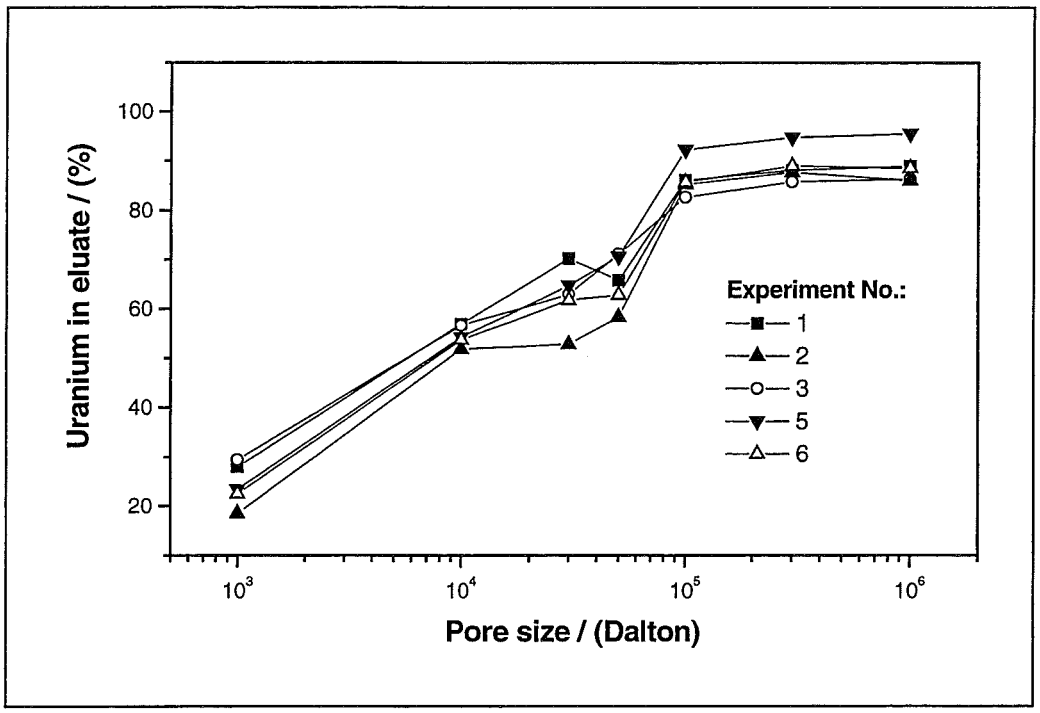

Figure 2: ^{232}U size distribution in initial solutions (GoHy-532, 1 % CO_2, [U]: $4.4 \cdot 10^{-7}$–$5.1 \cdot 10^{-7}$mol/L, activity contribution of daughter nuclides ≤10 %).

3 RESULTS AND DISCUSSION

3.1 Comparison of ^{232}U and HTO breakthrough curves

From the breakthrough curves of ^{232}U and HTO one can conclude how far the ^{232}U migration differs from the groundwater flow.

The migration behavior is characterized by the retardation factor, R_f [Eq. (1)], where V represents the volume of the eluate and V_P stands for the effective pore volume of the column.

$$R_f = \frac{V}{V_P} \qquad (1)$$

$R_f > 1$ indicates a retarded transport of an injected metal ion through the column in comparison to that of the conservative tracer with a retardation factor of one, whereas $R_f < 1$ means an accelerated migration.

As example, the ^{232}U and HTO breakthrough curves of experiment No. 7 are depicted in Fig. 3. These curves are typical for the experiments carried out under varied experimental

conditions. In addition, a ^{241}Am breakthrough curve is shown in Fig. 3, that was measured under comparable conditions [1].

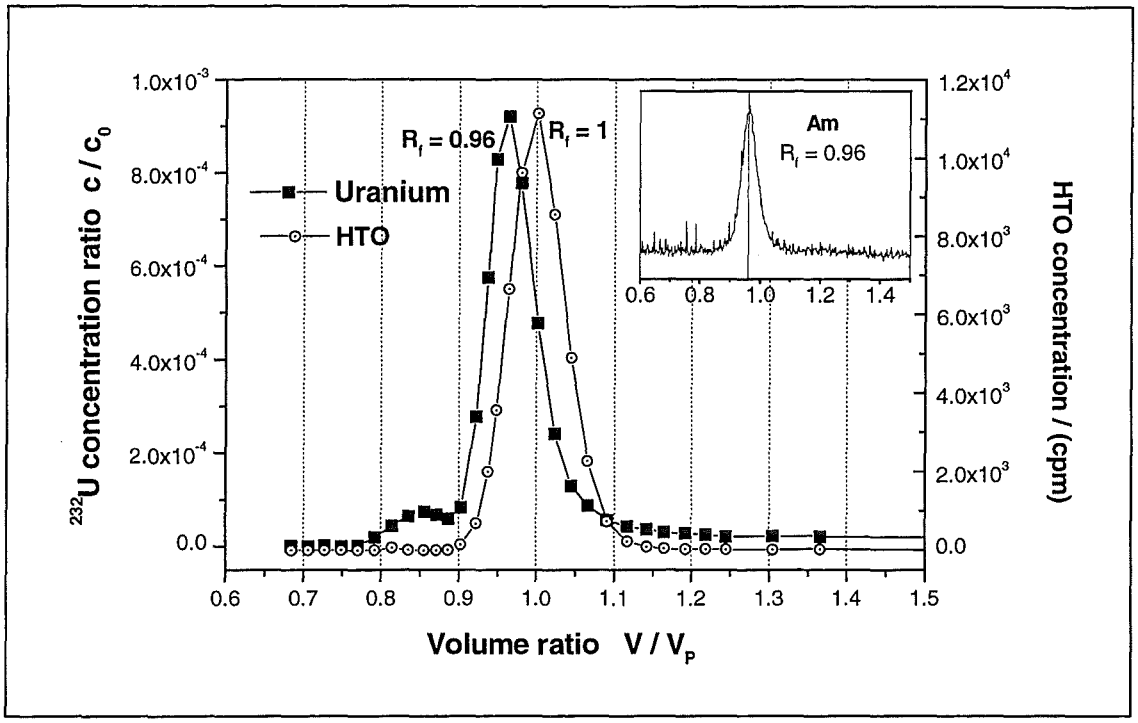

Figure 3: ^{232}U and HTO breakthrough curves in comparison to a ^{241}Am breakthrough curve determined under comparable conditions [1].

Fig. 3 shows that a fraction of ^{232}U is eluted with the retardation factor $R_f = 0.96$. That means that this part of uranium is transported slightly faster than the groundwater. This accelerated transport is attributed to the association of uranium with humic colloids, which move faster due to size exclusion processes.

The humic colloid-borne transport is confirmed by ultrafiltration experiments. Fig. 4 shows exemplary for experiment No. 7 the size distribution of uranium in fraction 13, eluted at $R_f = 0.92$. In this fraction ^{232}U shows roughly the size distribution of the DOC in the groundwater [6]. No significant fraction of ionic uranium species was obtained.

In addition, the R_f value of 0.96 for humic colloid-borne ^{241}Am confirms the humic colloid-borne transport of uranium.

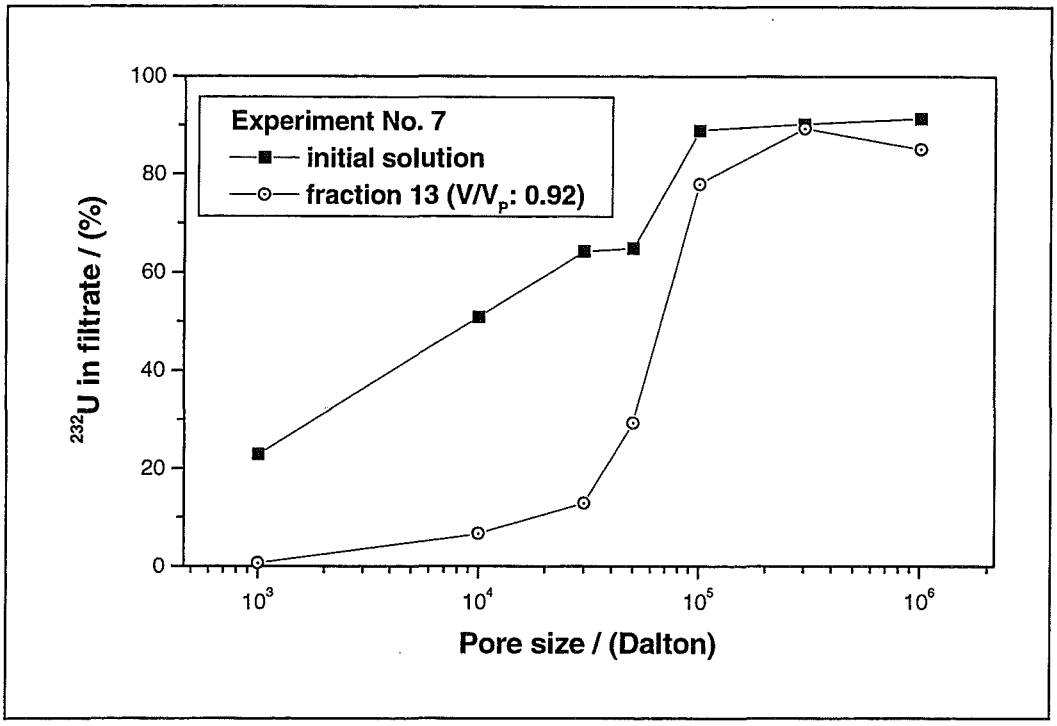

Figure 4: Size distribution of ^{232}U in fraction 13, experiment No. 7.

Furthermore, the ^{232}U breakthrough curves show the elution of a smaller fraction of ^{232}U at R_f = 0.84, which was not observed for the americium migration experiments and a different strong pronounced tailing after the breakthrough maximum (Fig. 3). The early eluted uranium fraction at R_f = 0.84 is attributed to the association of uranium with larger colloids, that was shown by filtration experiments. For example, in experiment No. 4 about 50 % of ^{232}U and its daughter nuclides eluted from 0.78 to 0.88 pore volumes are bound to colloids >450 nm. Merely 20 % of the nuclides are associated with colloids smaller than 10^6 Dalton, which is typical for humic colloids. Whether this transport is mediated by enlarged coagulated humic substances, inorganic colloids, and eventual microorganisms, is not known up to now.

There are some indications that the uranium transport with larger colloids is in connection with a reduction of U(VI) to U(IV). An example for this is the enhancement of the ^{228}Th/^{232}U isotope ratio in the early eluted fraction at R_f = 0.84. Breakthrough curves of ^{228}Th, which was formed during the experiments with concentrations between 10^{-10} and 10^{-9} mol/L because of the radioactive decay of ^{232}U, were determined for two experiments by means of alpha-spectrometry. As illustrated in Fig. 5 the maximum of the ^{228}Th breakthrough curves occurs at a R_f value of about 0.9. This thorium fraction migrates distinctly faster through the column

than the humic colloid-bound non-retarded ^{232}U fraction at $R_f = 0.96$. This points to the fact that the tetravalent ^{228}Th migrates with larger colloids.

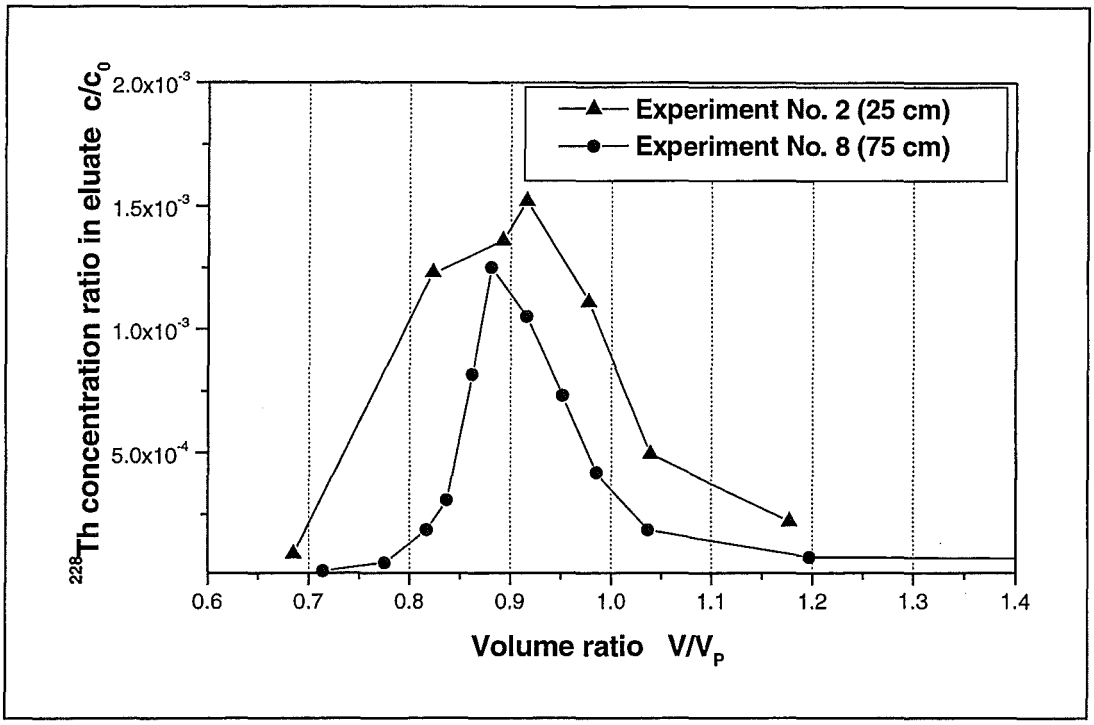

Figure 5: ^{228}Th breakthrough curves determined by alpha-spectrometry.

Another indication for the possible accelerated transport of U(IV) gives experiment No. 4 with the highest ^{232}U/groundwater pre-equilibration time of 82 days. At this the uranium fraction with $R_f = 0.84$ is especially pronounced (cf. Fig. 7), which points to a stronger migration of ^{232}U with larger molecules.

3.2 Determination of the ^{232}U recovery

As mentioned before, colloid-borne ^{232}U is not only eluted with $R_f = 0.96 \pm 0.01$ (mean value of all experiments) but also earlier at $R_f = 0.84$. Beyond it, a different strong pronounced tailing is observed after the breakthrough maximum. To be able to compare the recovery of humic colloid-borne uranium with $R_f = 0.96 \pm 0.01$ of all experiments, a Gaussian distribution with $R_f = 0.96 \pm 0.01$ as center, and a dispersion derived from the HTO migration was taken as a basis. As second component a Gaussian distribution with $R_f = 0.84 \pm 0.01$ (exception

experiment No. 8: R_f = 0.88) as center was fitted. Up to now it is not clear, whether this earlier eluted uranium fraction migrates associated with larger humic colloids, inorganic colloids or eventual with microorganisms. As example, Fig. 6 shows the analysis of the breakthrough curves regarding the recovery of humic colloid-borne ^{232}U for experiment No. 4.

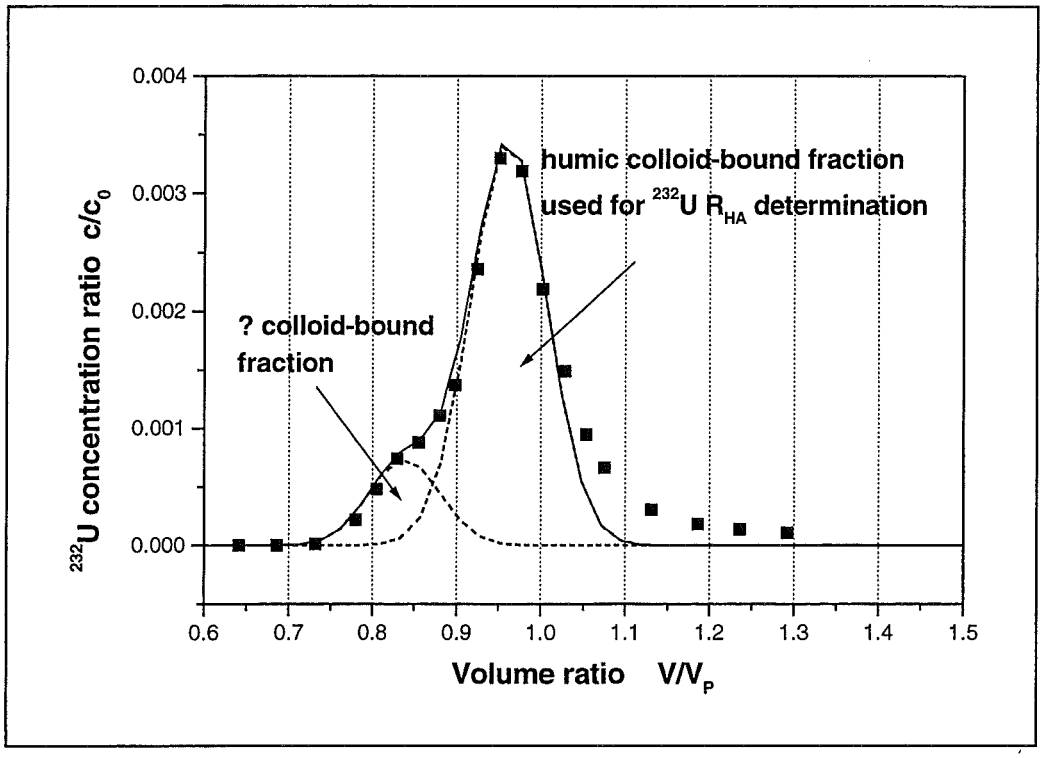

Figure 6: Determination of the humic colloid-borne ^{232}U fraction.

Furthermore, we determined the total recovery of ^{232}U after about 5 pore volumes, which includes the recovery on colloid-borne uranium fractions with R_f values of 0.84 and 0.96 as well as the recovery of retarded ^{232}U in the tailing. It is calculated according to Eq. (2):

$$R = \frac{U_{eluted}}{U_{injected}} \bullet 100\% \qquad (2)$$

where U_{eluted} represents the eluted uranium after about 5 pore volumes and $U_{injected}$ stands for the injected uranium. The total recoveries (R_{tot}) and the recoveries of humic colloid-borne ^{232}U (R_{HA}), which includes only the fraction eluted at $R_f = 0.96 \pm 0.01$ are summarized in Tab. 2 for all experiments.

Table 2: Recovery of ^{232}U in column experiments.

Experiment number	Pre-equilibration time [d]	Darcy velocity v_D [m/d]	Column length [cm]	Total ^{232}U recovery R_{tot} [%]	Humic colloid-borne ^{232}U recovery R_{HA} [%]	Retardation of humic colloid-borne ^{232}U R_f (± 0.01)
Variation of pre-equilibration time						
1	0.04	0.321	25	2.0 ± 0.5	0.4 ± 0.1	0.97
2	0.63	0.314	25	3.5 ± 0.9	1.4 ± 0.3	0.97
3	11	0.312	25	5.2 ± 1.3	3.3 ± 0.8	0.96
4	82	0.310	25	14.2 ± 3.6	7.6 ± 1.9	0.96
Variation of Darcy velocity						
5	5	2.030	25	9.1 ± 2.3	6.5 ± 1.6	0.95
3	11	0.312	25	5.2 ± 1.3	3.3 ± 0.8	0.96
6	6	0.038	25	6.0 ± 1.5	1.5 ± 0.4	0.97
Variation of column length						
3	11	0.312	25	5.2 ± 1.3	3.3 ± 0.8	0.96
7	5	0.241	50	3.5 ± 0.9	2.4 ± 0.6	0.96
8	5	0.239	75	6.4 ± 1.6	2.0 ± 0.5	0.96

3.3 The influence of the pre-equilibration time on the migration behavior of uranium

Fig. 7 depicts the ^{232}U breakthrough curves for the experiments, which were performed applying different ^{232}U/groundwater pre-equilibration times before injection into the column. The ^{232}U recoveries are summarized in Tab. 2.

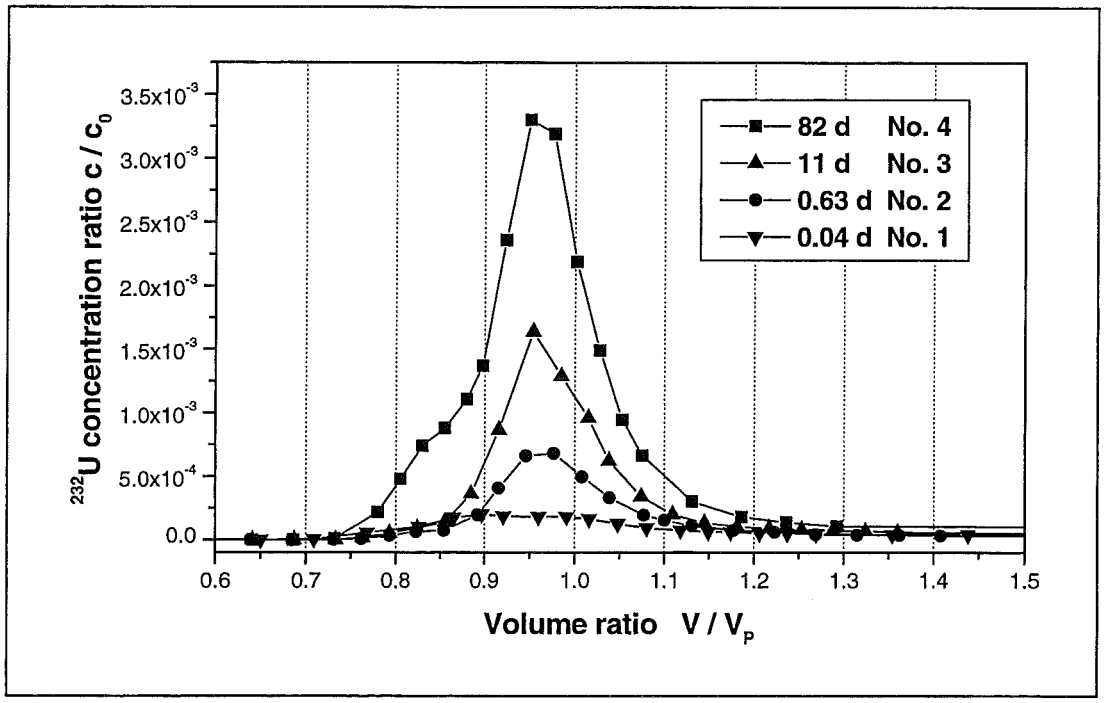

Figure 7: ^{232}U breakthrough curves in dependence on the ^{232}U/groundwater equilibration time before injection into the column.

Fig. 7 shows that with increasing ^{232}U/groundwater pre-equilibration time before injection into the column a significant increase of the humic colloid-bound ^{232}U fraction occurs. These observations are confirmed by the recoveries summarized in Tab. 2. Comparing the recovery of colloid-borne uranium and the total recovery after about 5 pore volumes in dependence on the pre-equilibration time it is obvious that both recoveries increase with increasing pre-equilibration time. This fact suggests that uranium binding onto humic colloids becomes stronger with increasing equilibration time. Consequently, uranium becomes less available for an interaction with the sediment surface during the migration through the column. Comparable results were found for americium [1]. In addition, Rao et al. [12] studied the interaction between Eu(III) and humic acids using cation exchange. They described a time-

dependent stronger binding of trivalent metal ions with humic substances. However, the cause of this phenomenon is not known up to now.

The relatively large fraction of ^{232}U eluted at $R_f = 0.84$ after an equilibration time of 82 days (experiment No. 4) can possibly be attributed to the reduction of uranium(VI) to uranium(IV). The fact that the breakthrough curve of the tetravalent uranium daughter nuclide thorium shows a maximum at $R_f \sim 0.9$ (cf. paragraph 3.1) represents possibly a reference for that. Nevertheless, an experimental proof for a reduction of uranium(VI) does not exist.

3.4 The influence of groundwater flow velocity and column length on the migration behavior of uranium

Variations in the groundwater flow velocity and the column length cause variations in the residence time of the colloid-bound uranium in the column.

Fig. 8 shows the ^{232}U breakthrough curves obtained with different groundwater flow velocities.

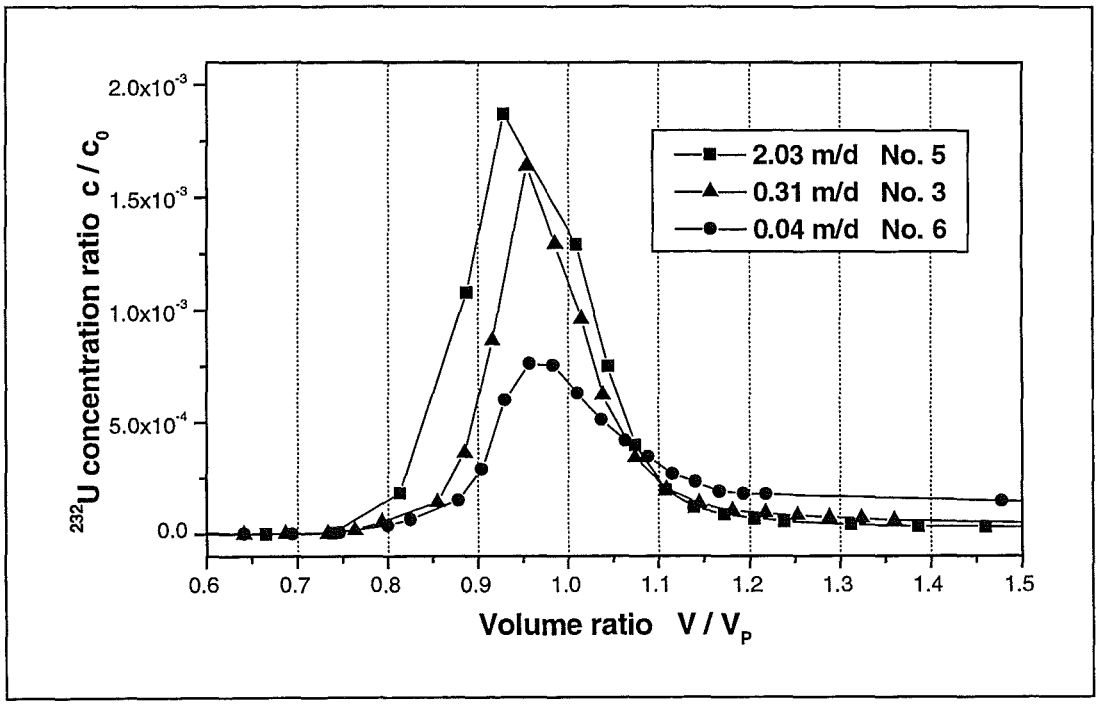

Figure 8: ^{232}U breakthrough curves in dependence on the groundwater flow velocity.

Increasing the groundwater flow velocity from 0.04 m/d to 2.03 m/d, an increase of the recovery of colloid-bound ^{232}U from 1.5 % to 6.5 % was obtained (Tab. 2). A similar tendency was found for Am(III) [1].

Furthermore, with increasing column length a decrease in the recovery of colloid-borne uranium was observed (Tab. 2).

Fig. 9 depicts the recovery of non-retarded colloid-borne ^{232}U depending on its residence time in the column. The results consist of the data obtained by varying the groundwater flow velocity and the column length. The recovery of non-retarded colloid-bound transported uranium decreases continuously with increasing residence time in the column, which points to a time-dependent stronger interaction of uranium with the sediment surface. This dependence may be explained by a time-dependent dissociation of uranium from the colloids followed by an interaction with the sediment surface.

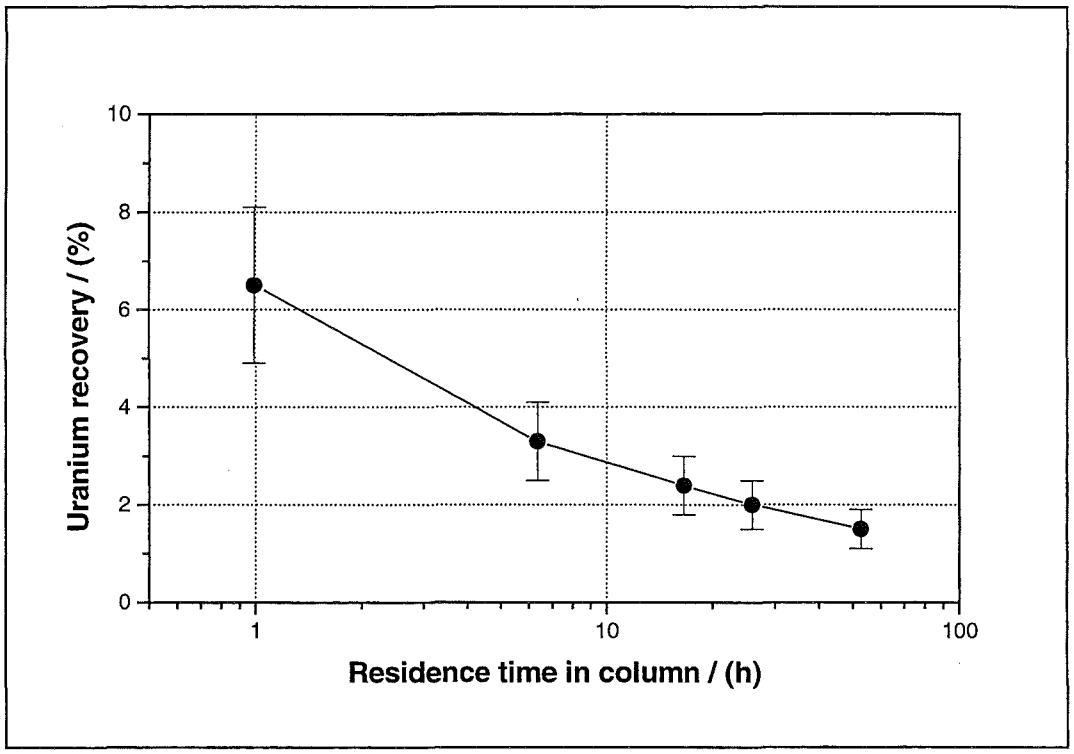

Figure 9: Recovery of humic colloid-borne ^{232}U ($R_f = 0.96 \pm 0.01$) in dependence on the residence time in the column. The pre-equilibration time is constant.

In contrast to this fact, the total recovery of eluted ^{232}U shows no distinct trend depending on the migration period (Tab. 2). This may be due to the different strong tailing and the varying amount of the colloid-borne uranium fraction at $R_f = 0.84$. From Fig. 8 one can gather that the

tailing of the breakthrough curves is increased with increasing migration time, that means the interaction of uranium with the sediment shows an increasing influence on the uranium migration.

4 CONCLUSIONS

The results of the migration experiments in a sandy humic colloid-rich groundwater/sediment system show that depending on the experimental conditions 0.4 up to 7.6 % of the injected uranium migrates non-retarded colloid-bound. Due to size exclusion effects the migration velocity of the colloid-borne uranium is up to about 15 % faster than the groundwater flow velocity, whereby the maximum of the humic colloid-borne uranium fraction is eluted about 5 % earlier than the groundwater. Up to now it is not known which kind of colloids causes the transport of the early eluted uranium fraction at $R_f = 0.84$.

The migration behavior of uranium is strongly influenced by kinetically controlled processes. The recovery of non-retarded humic colloid-bound transported uranium depends on the uranium/groundwater equilibration time before injection into the column. The recovery increases with increasing pre-equilibration time, which is attributed to a time-dependent, different strong binding of uranium onto the humic colloids. Furthermore, the recovery of uranium depends on the residence time of humic colloid-borne uranium in the column, which is determined by the groundwater flow velocity and the column length. With increasing residence time a decreasing recovery of humic colloid-borne uranium was observed. These observations are due to a time-dependent dissociation of uranium from the humic colloids followed by an interaction of uranium with the sediment. Up to now it is not known how far U(VI) is reduced to U(IV) during the experiments. First indications were found, which point to the reduction of uranium and a colloid-borne transport of U(IV).

^{228}Th, which was formed from ^{232}U by radioactive decay during the migration experiments, also migrates colloid-bound through the groundwater/sediment system. The mean migration velocity of the colloid-borne thorium fraction is about 10 % higher than the groundwater flow velocity.

The results can be summarized as follows: The column experiments reveal important kinetic effects controlling the humic colloid-borne migration of uranium. These kinetic effects are

comparable to those found for the migration behavior of Am(III). Consequently one can conclude that the K_D concept, which is based on thermodynamic equilibrium, is not suitable to describe the humic colloid-borne uranium migration. Therefore, the uranium migration experiments provide a first basis to describe and to predict the subsurface migration of colloidal uranium in natural aquifers. Additional experiments further improving this understanding are necessary, especially experiments investigating the influence of the uranium reduction to the tetravalent oxidation state on the migration behavior of uranium.

5 REFERENCES

1. Artinger, R., Kienzler, B., Schüßler, W., Kim, J.I.: Effects of Humic Substances on the ^{241}Am Migration in a Sandy Aquifer: Column Experiments with Gorleben Groundwater/ Sediment Systems. J. Contam. Hydrol. **35**, 261 (1998).
2. Kim, J.I., Delakowitz, B., Zeh, P., Klotz, D., Lazik, D.: A Column Experiment for the Study of Colloidal Radionuclide Migration in Gorleben Aquifer Systems. Radiochim. Acta **66/67**, 165 (1994).
3. Kim, J.I., Zeh, P., Runde, W., Mauser, C., Paskalidis, B., Kornprobst, B., Stöwer, C.: *Nuklidmigration (^{99}Tc, ^{237}Np, ^{238}Pu, ^{241}Am) im Deckgebirge und Salzstsock des geplanten Endlagers Gorleben.* RCM-Report 01495, TU München, 1995.
4. Kim, J.I., Delakowitz, B., Zeh, P.: Migration Behaviour of Radionuclides. In: *Colloid migration in groundwaters: geochemical interactions of radionuclides with natural colloids.* Final report, EUR 16754EN, 1996, p. 63.
5. Pompe, S., Heise, K.H., Bernhard, G.: BMWi-Forschungsvorhaben: *Einfluß von Huminstoffen auf das Migrationsverhalten radioaktiver und nicht radioaktiver Stoffe unter naturnahen Bedingungen - Synthese, radiometrische Bestimmung funktioneller Gruppen, Komplexierung (contract number 02E 8815).* Final report, in preparation.
6. Artinger, R., Kienzler, B., Schüßler, W., Kim, J.I.: Sampling and Characterization of Gorleben Groundwater/Sediment Systems for Actinide Migration Experiments. In: *Effects of Humic Substances on the Migration of Radionuclides: Complexation and Transport of Actinides.* First Technical Progress Report (G. Buckau, ed.). Forschungszentrum Karlsruhe, Wissenschaftliche Berichte, FZKA 6124, Karlsruhe 1998, p. 23.

7. Grenthe, I., Fuger, J., Konings, R.J.M., Lemire, R.J., Muller, A.B., Nguyen-Trung, Cregu, C., Wanner, H.: *Chemical Thermodynamics of Uranium*, 1st ed., Elsevier Science, Amsterdam (1992).
8. Czerwinski, K.R., Buckau, G., Scherbaum, F., Kim, J.I.: Complexation of the Uranyl Ion with Aquatic Humic Acid. Radiochim. Acta **65**, 111 (1994).
9. Zeh, P., Czerwinski, K.R., Kim, J.I.: Speciation of Uranium in Gorleben Groundwaters. Radiochim. Acta **76**, 37 (1997).
10. Choppin, G. R.: Humics and radionuclide migration. Radiochim. Acta **44/45**, 23 (1988).
11. Artinger, R., Seibert, A., unpublished.
12. Rao, L., Choppin, G. R., Clark, S. B.: A Study of Metal-Humate Interactions using Cation Exchange. Radiochim. Acta **66/67**, 141 (1994).

Annex 11

Studies on the Reduction of Tc(VII) and the Formation of Tc-Humic Substance Complexes in Synthetic and Natural Systems

(Maes et al., KUL)

2nd Technical Progress report

EC project

K.U.Leuven contribution to task 2 (complexation)

Effects of humic substances on the migration of radionuclides: complexation and transport of actinides

Studies on the Reduction of Tc(VII) and the formation of Tc-Humic Substance Complexes in Synthetic and Natural Systems

A. Maes, J. Van Cluysen, K. Geraedts

K.U.Leuven

Departement Interfasechemie
Laboratorium voor Colloïdchemie
Kardinaal Mercierlaan 92, B-3001 Heverlee

Content

1. Introduction

There is still a great concern that over long periods of time radionuclides may enter aquifers upon disposal of high level nuclear waste in a geological barrier. Since humic substances are a potential carrier of metal ions and radionuclides, the goal of this paper is to determine the particular role played by tem.

The present research is focussed on the behaviour of ^{99}Tc in a reducing medium, which may be encountered in geological disposal conditions. Two different geologicalal environments (Gorleben,Germany and Boom Clay, Belgium) were under study.

The objective of this contribution is threefold

1. Study of the kinetics of TcO_4^- reduction in a) homogeneous solution and b) in presence of different surfaces (clay minerals, pyrite, FeS,$FeCO_3$) able to create reducing conditions and/or to stimulate the TcO_4^- reduction.
2. Once a suitable surface is found (pyrite in this case) it is further used to study the influence of humic substances on the reduction kinetics. Humic substances from Boom clay and Gorleben are used. The Tc distribution data at equilibrium are used to calculate the Tc-humic substance interaction constant.
3. Derive the Tc-humic substance complexation from measurements of the Tc distribution in a real system such as the reducing Boom clay sediment.

2. General experimental set-up

All experiments were carried out at ambient temperature (22°C) in a controlled atmosphere glovebox flushed with a mixture of N_2 (95%) and H_2(5%) to minimise the intrusion of oxygen into the reaction vessels. The box atmosphere was circulated over a catalytic converter (Pt) in order to remove excessive oxygen. The mean concentration of O_2 in the glovebox throughout the experiments was below 2 ppm.

All chemicals used were of analytical grade and the water used was deionized, filtered by a Water Purification System (Milli-Q) and finally boiled out to obtain oxygen-free water. ^{99}Tc was purchased from Amersham in 0.1 M NH_4OH aqueous solution. TcO^-_4 solutions in $NaClO_4$ (10^{-2} M) were prepared by diluting aliquots of a stock solution.

Typical experiment

Typically, experiments were conducted in neutral to slightly alkaline solutions in the presence of different Fe(II)-containing minerals and clay minerals and 10^{-2} M $NaClO_4$ (if not stated otherwise e.g. 10^{-2}M $NaHCO_3$). The reaction is followed as a function of time by preparing different polypropylene vials, containing 100 (± 2) mg of the minerals (if not stated otherwise) and 20 ml volumes of a pertechnetate solution. The final TcO^-_4 concentration was usually about $5x10^{-6}$ M. The vials were turned slowly head over head to ensure good mixing. After certain

periods of time the minerals and solutions were separated by centrifugation (30 min, 18000 tpm) before being analysed.

The centrifuged samples were analysed for ^{99}Tc in a Packard Liquid Scintillation Analyser using Ultima Gold Liquid Scintillation Cocktail (Packard).
The pH measurements were made by a Portatest 655 and a WTW SenTix 50 glass electrode, and the redox potentials were monitored by a combined redox Toledo Mettler P14805-DXK-S8/120 electrode connected to the Portatest 655.
The total Fe-concentration in solution was determined by a calorimetric method at 508 nm using o-phenantroline and sodiumacetate.

The presence of reduced Tc species (e.g. $TcO(OH)_2$) in solutions was determined by extracting an aliquot of the solution three times with equal volumes chloroform containing 0.001 mol dm^{-3} tetraphenyl arsonium chloride. TcO^-_4 is extracted in the organic phase. The concentration of reduced species is calculated by difference between the TcO^-_4 concentration in the starting and equilibrium solutions.

Separation of the TcO^-_4/Tc-humic fraction was determined by gel exclusion chromatography. This was carried out by eluting a 1 ml sample over a glass column (30x1 cm), filled with Superdex 30 Prep Grade gel (Pharmacia Biotech). The eluent was a saline NaCl solution (0.15 M containing 0.002% NaN_3). The U.V.-absorbance (at 254 nm) was measured continuously and the collected fractions were β-monitored radiometrically for their Tc-levels.

Minerals

Glauconite was obtained from a local deposit in Kessel-Lo. It was used as found and was also washed with deionized water.
Silver Hill Illite was obtained from the Source Clay Minerals Repository. The fraction <0.2 mm was separated after crushing
Siderite, pyrite and phlogopite were purchased from a mineral shop. Small sized fractions of the minerals were obtained by crushing the solids in the glovebox using an Agate mortar and pestle, and sieving to < 100 μm, 100-200 μm and 200-250 μm fractions.

Influence of Humic Substances

Unpurified organic matter from potential disposal sites were used. The first organic matter sample was Gorleben humic substance containing groundwater (Gohy 2227), which was used as supplied by FZK(Karlsruhe,Germany). The second kind of organic matter (Boom Clay Extract) used was obtained by four fold extraction of a Boom Clay sample with $2x10^{-2}$ M $NaHCO_3$ (S/L = 1/5) supplied by SCK/CEN (Mol,Belgium). After each extraction step, the sample was centrifuged for 45 minutes at 12000 rpm. The extract was one more time centrifuged.

The solutions used in the experiments to investigate the effect of humic substances contained in the case of Gorleben HS 19 ml Gorleben Water to which 1 ml of 10^{-2} M $NaHCO_3$ and 10^{-4} M TcO^-_4 was added. The used $NaHCO_3$ concentration was close to the real concentration in Gorleben Water (≅ $8x10^{-3}$ M, Gohy-2227, see Artinger *et al.*, 1998. In the case of Boom Clay HS 19 ml of B.C. Extract and 1 ml Synthetic Clay Water (S.C.W.) with 10^{-4} M TcO^-_4 was used. The S.C.W. has the following composition: $1.08x10^{-3}$ M $MgCl_2.6H_2O$, $3.35x10^{-3}$ M KCl, $2.11x10^{-3}$ M Na_2SO_4, $6.84x10^{-3}$ M NaCl, $1.3927 x10^{-2}$ M $NaHCO_3$, 10^{-6} M $FeCl_2$ and saturated

in $CaCO_3$. The Boom Clay sample was supplied by SCK in the frame of the TRANCOM project.

A reference experiment to investigate the reduction of TcO^-_4 in absence of Humic Substances was made in S.C.W., and served as a reference for both Gorleben and Boom Clay Humic Substances.

3. Results and discussion

3.1 Reduction of pertechnetate in presence of Fe^{2+}: influence of pH

In a previous paper (Maes and Capon, 1998) it was observed that $Fe(OH)_2$ precipitate can reduce pertechnetate, whereas Fe^{2+} as a free ion in solution can not exhibit this reduction. To verify the previous observation the reduction of TCO_4^- was studied as a function of pH under reducing conditions induced by the presence of Fe^{2+}.

Under reducing conditions, TcO^-_4 may precipitate as $TcO_2.nH_2O$. The removal of Tc, added as pertechnetate ($^{99}TcO^-_4$) in aqueous solutions under reducing conditions was therefore measured after centrifugation. The experiment was conducted in a background solution of 10^{-2} M $NaClO_4$ in which $2x10^{-3}$ M Fe^{2+} and $5x10^{-6}$ M pertechnetate were present. However only 24 hours of equilibration were allowed.

The reduction of pertechnetate was examined in the pH range from 4 to 10.25 (table 1). Only in the case of a pH > 7.80 a significant reduction of pertechnetate was noticed after 24 hours. At these high pH's, the redoxpotential lowered to values -200 to -300 mV (SHE). Thus redoxpotentials were sufficiently low to expect a reduction of TcO^-_4. Beyond pH 7.8, only 5 % of the initial Fe-concentration remained in solution as free Fe^{2+}, due to a precipitation of $Fe(OH)_2$. The measured Fe^{2+} concentration agrees with the solubility product of $Fe(OH)_2$ (K_{sp} = $8x10^{-16}$) (Vandegraaf *et al.*, 1984).

The observations are explained as a surface catalysed reduction of TcO^-_4 to Tc(IV) onto freshly precipitated $Fe(OH)_2$. Fe^{2+} in solution is not reacting, or at least very slowly, with the pertechnetate anion. The results are in agreement with observations of Cui and Eriksen (1996a,b).

Sample	pH	Eh (mV)	$[Fe^{2+}]$ (M)	$[TcO^-_{4\,(24h)}]/[TcO^-_{4\,(in)}]$ (%)
1	4.05	98	10^{-3}	92
2	4.25	63	10^{-3}	99
3	4.32	13	10^{-3}	90
4	4.67	-45	10^{-3}	94
5	7.80	-189		**6**
6	10.25	-309	$4.13x10^{-5}$	**2**

Table 1. Experimental conditions and results after 24h of equilibration of $5x10^{-6}$ M TcO^-_4 in $2x10^{-3}$ M Fe^{2+} and 10^{-2} M $NaClO_4$.

3.2 Reduction of pertechnetate in presence of clay minerals

Illite

Previous findings (Maes and Capon, 1998) showed no reduction of pertechnetate in presence of illite and illite to which a small concentration of Fe^{2+} ($3.5x10^{-5}$ M) was added.

The reduction of pertechnetate was therefore examined in presence of illite saturated with Fe^{2+}. The Fe^{2+}-saturated illite was prepared by using dialysis membranes which were filled with illite (>75 mesh, < 0.2 mm) and repeatedly equilibrated with solutions containing $2x10^{-2}$M $FeCl_2.4H_2O$.

Although Fe^{2+} was sorbed on the illite surface and active sites were present, 100 % of the added Tc ($\cong 6x10^{-6}$ M) was found back in the equilibrium solution (see figure 1). However, this equilibrium solution contained 15% of undefined reduced Tc compounds as determined by the solvent extraction method. During the whole experiment the solution was slightly acidic (pH = 6) and redoxpotentials were well below those necessary for reduction of TcO^-_4 (Eh = -100 mV, vs. H_2).

Glauconite

The influence of glauconite on the reduction of pertechnetate was conducted in absence and presence of Fe^{2+} (10^{-4} M). In both cases no Tc was reduced up to more than 40 days. The pH of the solution was slightly acidic during the whole of the experiment. In the experiment without Fe^{2+} redoxpotentials (-100 to -200 mV, vs. H_2) were always below those necessary for TcO^-_4 reduction. In presence of Fe^{2+}, redoxpotentials were much higher and 50% of the initial Fe^{2+} adsorbed on the mineral.

The same results were obtained irrespective of whether glauconite was used as sampled or was prewashed.

Phlogopite

Similar experiments as with glauconite were also made with phlogopite and also showed almost no removal of Tc. However the solvent extraction method indicated the presence of about 20% reduced Tc species in solution.

It can be concluded that the studied clay minerals have a very low tendency to reduce pertechnetate. Although the clay minerals contained bound Fe^{2+} and although the redox conditions were favourable, no reduction of TcO^-_4 was observed. Even in presence of additional Fe^{2+} (free and adsorbed) no reduction was measured.

Only small amounts of reduced Tc-species were detected in solution as deduced from the solvent extraction method. But the nature of these species is unknown and is highly uncertain. In view of the hydrolysis behaviour of Tc(IV), their presence is very unlikely. Therefore the solvent extraction method is at present believed to be unreliable, in other words artefacts are probably interfering.

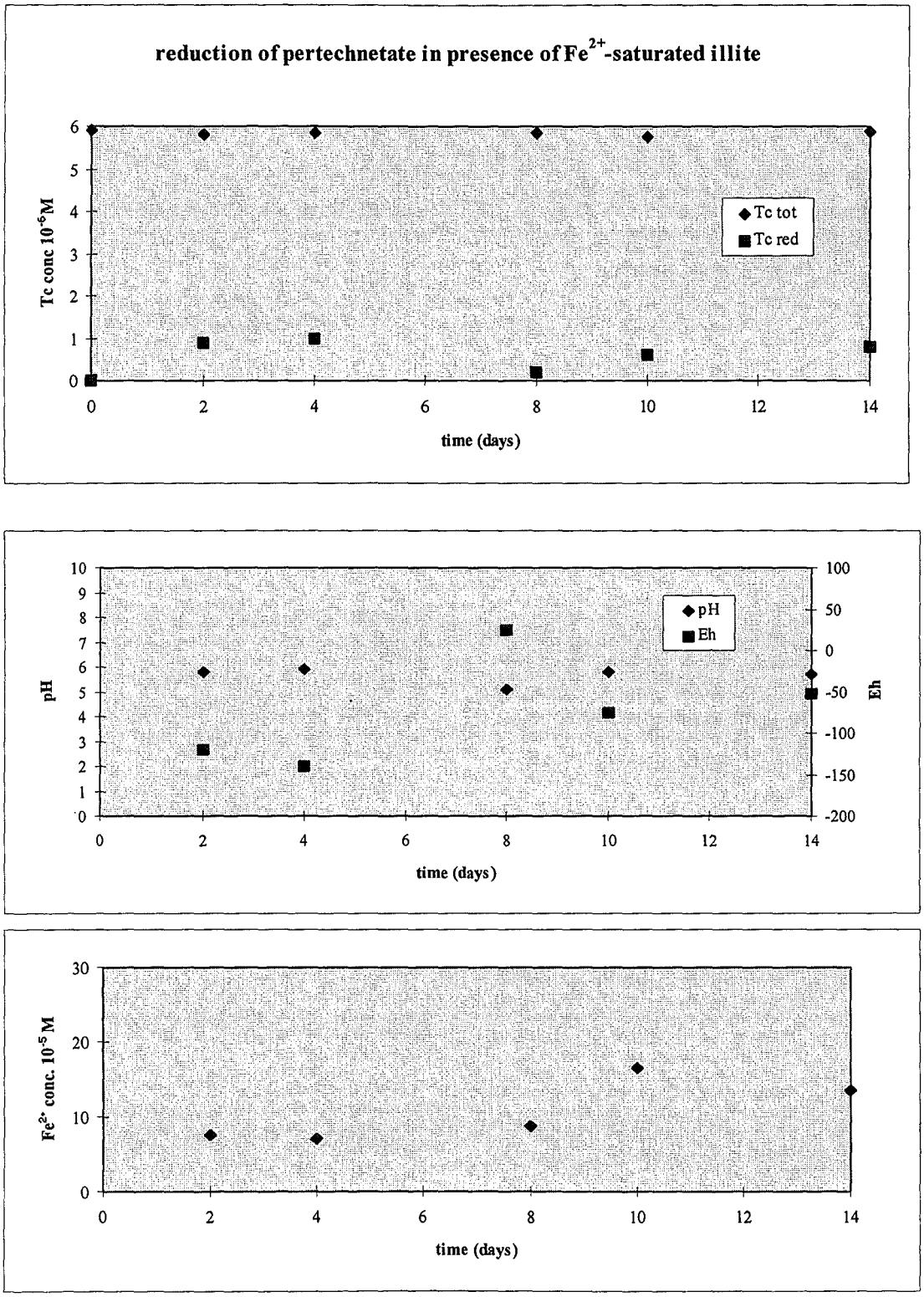

Figure 1. *Reduction of pertechnetate in presence of Fe^{2+}-saturated illite*

3.3. Reduction of pertechnetate in presence of Fe-containing minerals

Previous experiments (Capon and Maes, 1998) have already shown that Fe-containing minerals such as FeS and FeS2 are capable to efficiently reduce pertechnetate. We proceeded with these experiments to further investigate the influence of the size of pyrite particles. Also siderite was investigated.

Pyrite

In a previous contribution (Capon and Maes, 1998), coarse pyrite particles (>0.84 mm) were only able to fully reduce TcO^-_4 after 22 days of reaction. In the present experiment much smaller pyrite particles (100mg FeS_2, >160 mesh, < 0.1 mm) were investigated.

The variation of [Tc], pH and Eh as a function of time is shown in figure 2. Within 24 hours all Tc ($\cong 6x10^{-6}$ M) was removed from solution. Comparison with the earlier results (experiments conducted with coarser pyrite), indicates that the redox reaction kinetics increases with decreasing particle size and thus with increasing number of surface functional groups.

Also, the influence of ionic strength (0.1, 0.01 M) and the amount of pyrite (100-200 mg) on the reaction kinetics were examined for the case of pyrite <0.1 mm. No Tc remained in solutions after 150 minutes at both ionic strengths and for both amounts of pyrite (not shown).

Siderite

In another series of experiments $FeCO_3$ (>160 mesh, < 0.1 mm) was used as Fe-containing mineral. Similar to the case of pyrite (<0.1 mm) a quick reduction occurred as judged from the absence of Tc remaining in the supernatant solution after 24 hours equilibration (see figure 3). The solution remained neutral to slightly alkaline and the redoxpotential was about -200 mV (vs. H_2). Also about 10^{-5} M Fe^{2+} was found in solution, due to the dissolution of $FeCO_3$.

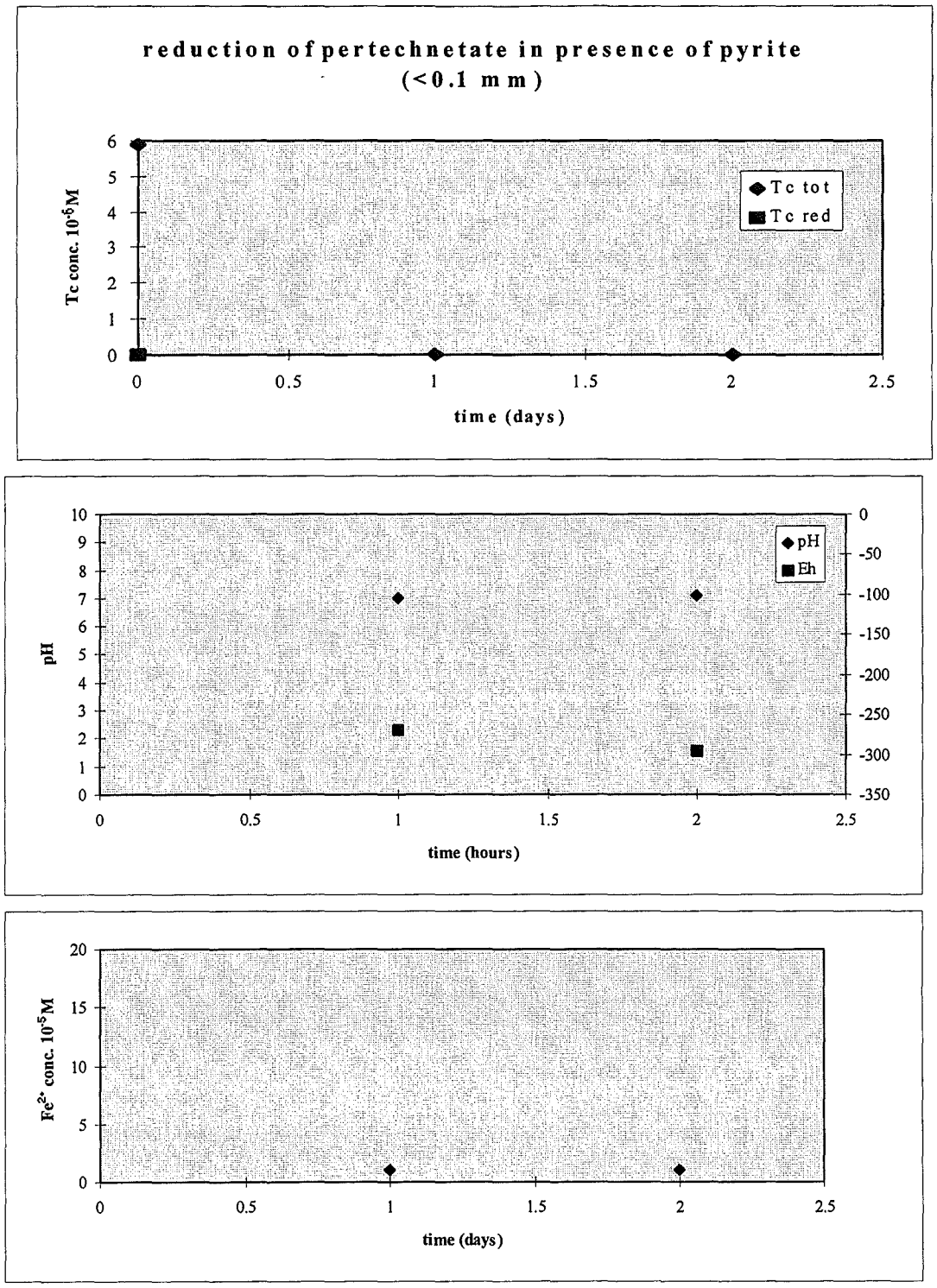

Figure 2. *Reduction of pertechnetate($6.10^{-6}M$ in $10^{-2}M$ $NaClO_4$) in presence of pyrite (100mg,<0.1 mm)*

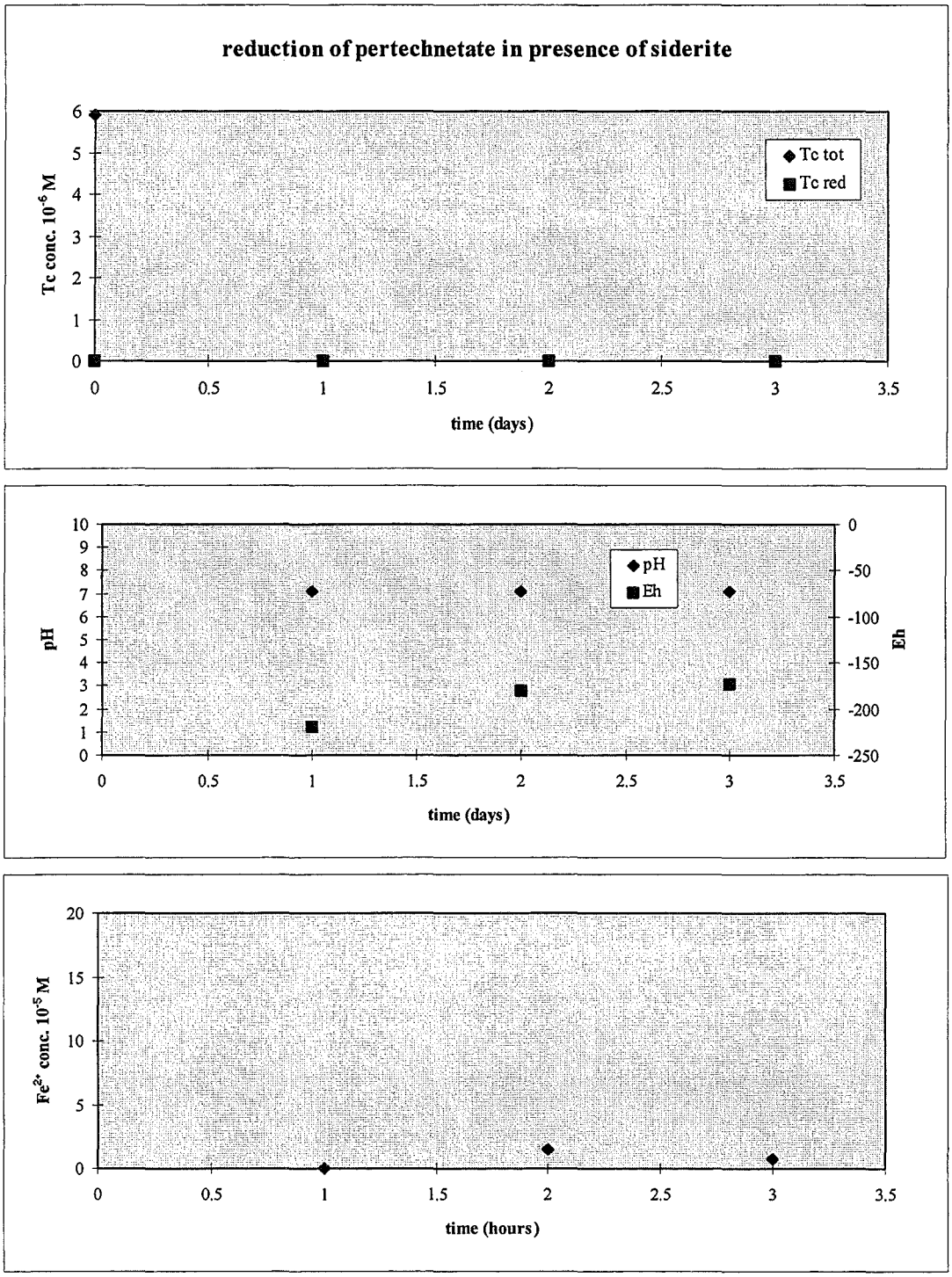

Figure 3. *Reduction of pertechnetate ($6.10^{-6}M$ in $10^{-2}M$ $NaClO_4$) in presence of siderite (100mg,<0.1 mm)*

It is concluded from the foregoing results that surfaces play a significant enhancing role in the reduction of pertechnetate. Fe-containing minerals such as pyrite and siderite can speed up the reduction of pertechnetate. (Cui and Ericksen 1996a;1996b) reported surface induced reduction in presence of magnetite. Comparing clay minerals with Fe-containing minerals reveals that TcO_4^-
reduction is favoured when Fe is present as co-ordinated Fe^{2+} in the surface phase. Exchangeable Fe^{2+} is much less effective in TcO_4^- reduction.

3.4 Suitable reaction conditions in presence of pyrite and $NaHCO_3$.

Pyrite was chosen to be studied further in detail.

In order to find appropriate conditions, by which the reduction of pertechnetate can be followed in a reasonable time span of a few hours to days, different TcO_4^- concentrations were equilibrated with different amounts and different size fractions of pyrite in presence of 10^{-2}M $NaHCO_3$. 10^{-2}M $NaHCO_3$ instead of 10^{-2}M $NaClO_4$ was used in order to work in a more relevant environmental medium.

Figure 4 shows TcO_4^- remaining in solution in function of time for an initial concentration of 10^{-4}M TcO_4^- in presence of 50 mg pyrite (<50μm). Figure 5 shows results for an initial concentration of 5.10^{-6}M Tc and 50 mg of < 100μm and <100-200> μm pyrite. Analysis of these results showed that those reactions are ruled by a combination of first order kinetic constants.

Comparison of figure 4 and 5 demonstrates that the reaction kinetics depends on the total TcO_4^- concentration and the particle size and should be further investigated. Efforts to measure the specific surface area failed for unknown reasons. A method for measuring the available number of functional groups would be more appropriate and should be developed.

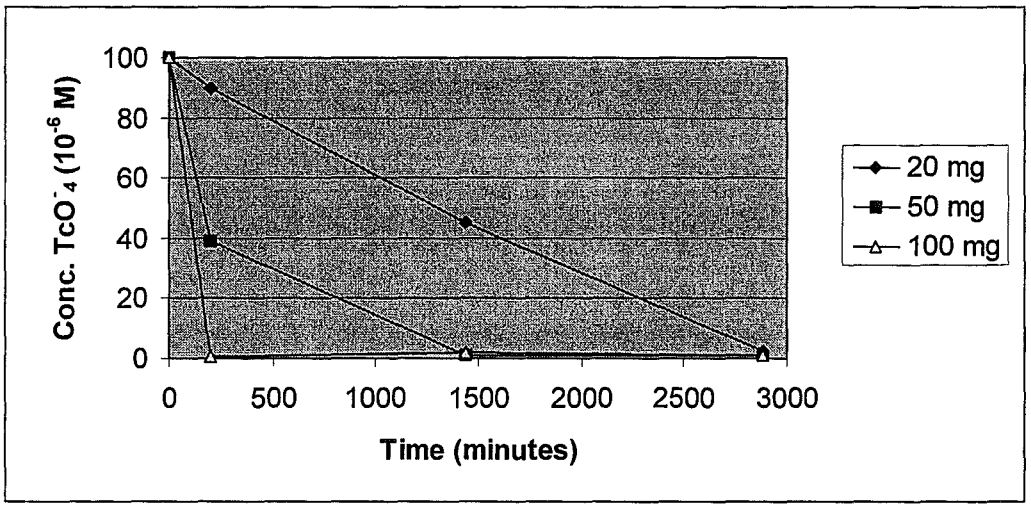

Figure 4. *Pertechnetate remaining in solution in presence of pyrite (50mg,<50μm). Initial* $TcO_4^- = 10^{-4}M$ *in* $10^{-2}M\ NaHCO_3$

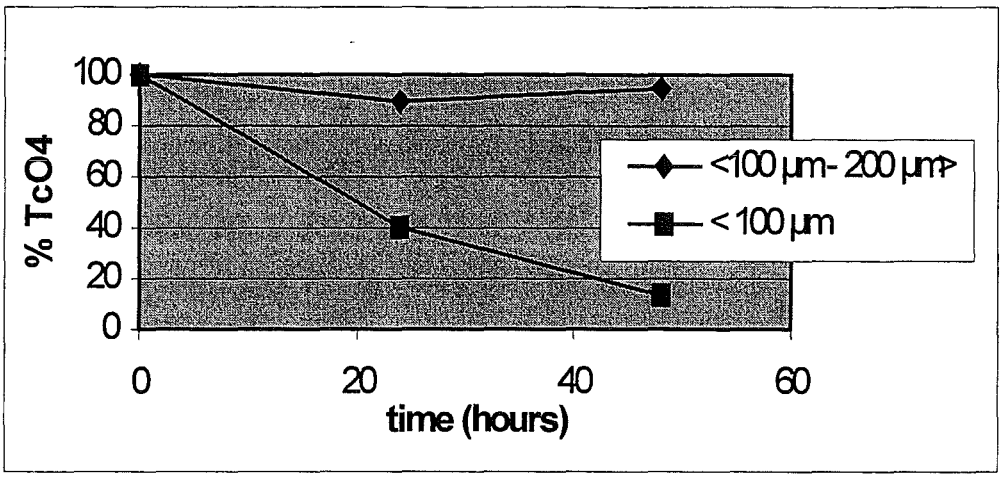

Figure 5. *Percentage of $5.10^{-6}M$ pertechnetate in $10^{-2}M$ $NaHCO_3$ remaining in solution in presence of 50mg of different sizes of pyrite (<100µm-200µm) and (<100µm).*

3.5 Influence of humic substances on the reduction of technetium

In order to examine the effect of humic substance on the reduction of TcO_4^-, 50 mg FeS_2 (<100µm) was equilibrated for different periods of time with 20 ml of a solution containing humic substances. Natural waters were used with the aim to approach the natural redox conditions. Two types of humic substances, an extract from Boom Clay and Gorleben groundwater, were used.

Gorleben Humic Substances

- TcO^-_4 reduction with pyrite

Figure 6 shows that the initial Tc concentration of $5x10^{-6}$ M decreased to approximately $2x10^{-6}$M within 24 hours in presence of 50 mg FeS_2. Gel Permeation Chromatography showed that no pertechnetate was left in solution. All the Tc present in the solutions was associated with the organic matter. The speciation is given in table 2.

n°	Medium	Sorbent Amount/ size	C_{Tc} (M) initial	pH	Eh (mV)	Tc-speciation i in equilibrium solution
1	$NaClO_4$ - 10^{-2} M	illite 100 mg	$6x10^{-6}$	6	-100	85% TcO^-_4 15% reduced Tc(IV) ?
2	$NaClO_4$ - 10^{-2} M	glauconite 100 mg	$6x10^{-6}$	6	-100	100% TcO^-_4
3	$NaClO_4$ - 10^{-2} M	phlogopite 100 mg	$6x10^{-6}$	9	-200	80% TcO^-_4 20% reduced Tc(IV) ?
4	$NaClO_4$ - 10^{-2} M	pyrite 100 mg/<0.1mm	$6x10^{-6}$	7	-270	no Tc left in solution
5	$NaClO_4$ - 10^{-2} M	siderite 100mg/<0.1 mm	$6x10^{-6}$	7	-200	no Tc left in solution
6	$NaHCO_3$ - 10^{-2} M	pyrite 100 mg/<50 µm	$1x10^{-4}$	8.3	-200	/
	$NaHCO_3$ - 10^{-2} M	pyrite 50 mg/<50 µm	$1x10^{-4}$	8.3	-200	/
	$NaHCO_3$ - 10^{-2} M	pyrite 20 mg/<50 µm	$1x10^{-4}$	8.3	-200	/
7	$NaHCO_3$ - 10^{-2} M	pyrite 50 mg/<100 µm - 200 µm>	$5x10^{-6}$	8.3	n.d.	n.d.
	$NaHCO_3$ - 10^{-2} M	pyrite 50 mg/<100 µm	$5x10^{-6}$	8.3	n.d.	n.d.
8	Gorleben	pyrite 50 mg/<100 µm	$5x10^{-6}$	9.5	-270	100% Tc-HS
9	Gorleben	pyrite 50 mg/<100 µm	$5x10^{-6}$	9.4	-270	n.d.
	Gorleben / 2	pyrite 50 mg/<100 µm	$5x10^{-6}$	9.2	-270	n.d.
	Gorleben / 9.5	pyrite 50 mg/<100 µm	$5x10^{-6}$	9.0	-270	n.d.
10	S.C.W.	pyrite 50 mg/<100 µm	$5x10^{-6}$	8.7	-200	100% TcO^-_4
	B.C. extract	pyrite 50 mg/<100 µm	$5x10^{-6}$	8.8	-200	36% Tc-HS 64% TcO^-_4
11	S.C.W.	pyrite 50 mg/<100 µm	$5x10^{-6}$	8.9	-200	n.d.
	B.C. extract	pyrite 50 mg/<100 µm	$5x10^{-6}$	9.0	-200	n.d.

Table 2. Experimental conditions and Gel Permeation Chromatographic results for all the experiments

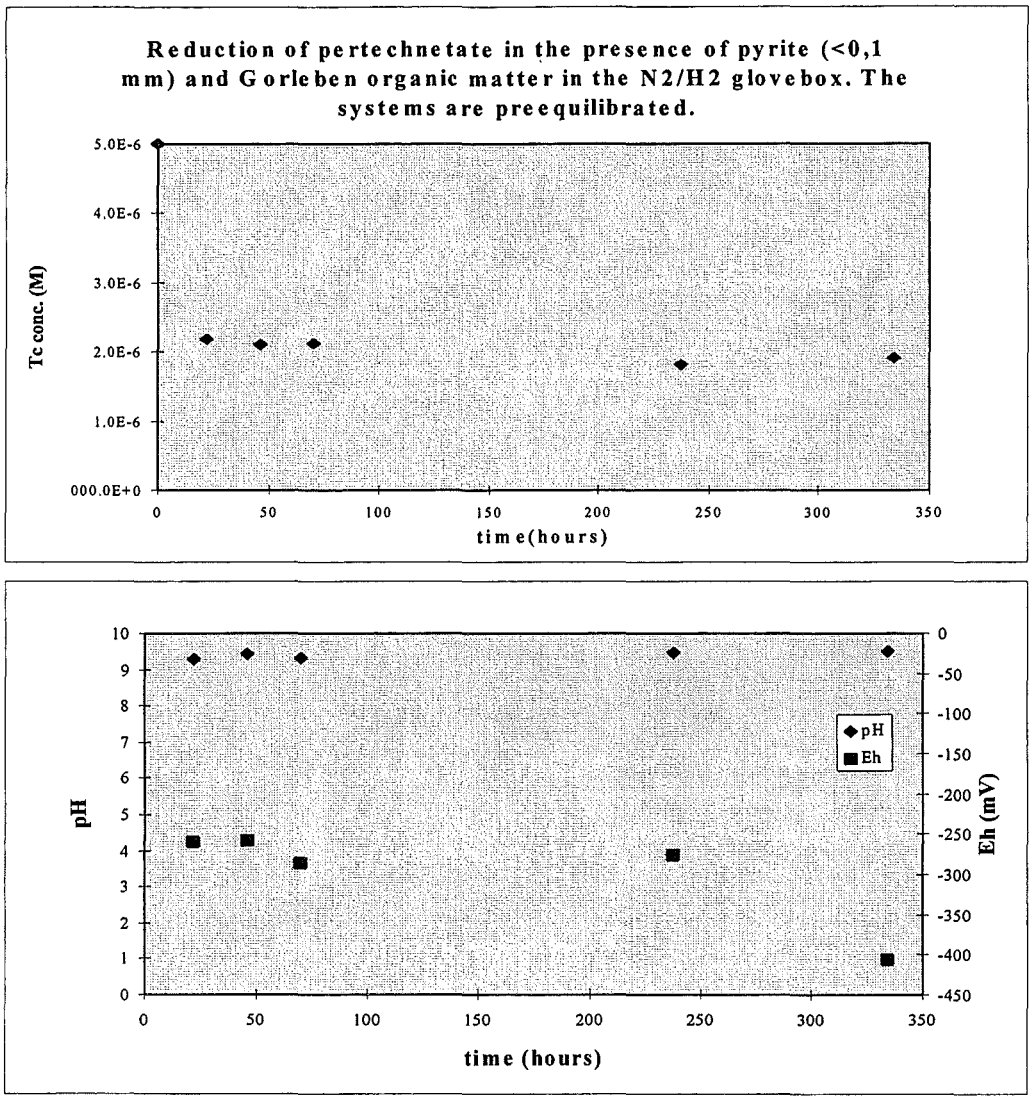

Figure 6. *Reduction of pertechnetate (5.10^{-6}M) in presence of pyrite (50 mg, <0.1 mm) and Gorleben groundwater (organic matter*

- TcO^{-}_4 reduction: influence of Gorleben HS-concentration

If humic substances do associate with reduced Tc species by way of a complexation reaction it can be predicted that varying the HS concentration will lead to different equilibrium Tc concentrations. This is verified by the experimental results of [Tc], pH and Eh versus time in figure 7. The experimental conditions are similar to those with original Gorleben water. Varying HS concentrations were obtained by diluting the Gorleben Water with 10^{-2} M $NaHCO_3$.
Another conclusion drawn from figure 7 is that the time for reaching equilibrium tends to slow down for smaller humic substances concentrations.

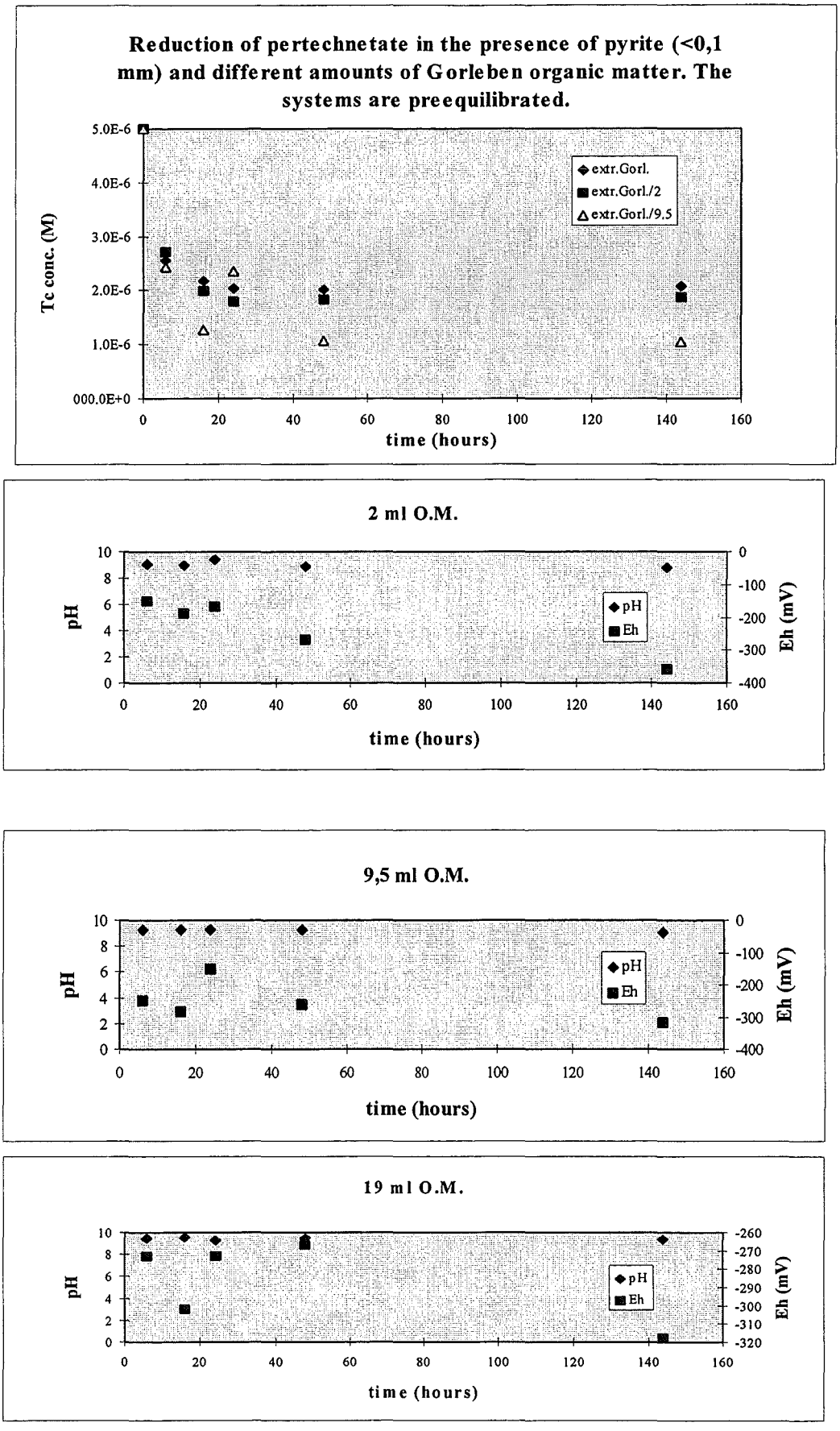

Figure 7.: *Influence of Gorleben HS concentration on the reduction of 5.10^{-6}M pertechnetate in presence of 50 mg pyrite (<100µm)*

Boom Clay Humic Substances

The kinetics of TcO^-_4 reduction was investigated in presence of a Boom Clay extract in Synthetic Clay Water and in pure Synthetic Clay Water (SCW) as a reference. In order to investigate the role played by the time of equilibration of pyrite with the S.C.W. the above experiment was executed without preequilibration of pyrite and after a preequilibration period of one week.

- TcO^-_4 reduction without preequilibration of pyrite

The experimental data shown in figure 8 correspond to TcO_4^- reduction experiments in presence and absence of organic matter.

In the system with Synthetic Clay Water alone the Tc reduction was completed after about 150 hours, due to the reducing activity of pyrite. The pH remained stable around 8.7 and the Eh varied between 0 and -300 mV. We assume that TcO_2 is precipitated.

The presence of humic substances in the Boom Clay Extract resulted in a slower reaction, which however tends to come to an equilibrium. Gel permeation chromatograms of the equilibrium solution showed that 36% Tc was associated with the HS phase. It is probable that the reduction was not complete after 180 hours. During this experiment the pH was about 9 and the Eh varied between +125 en -250 mV.

- *TcO^-_4 reduction with preequilibration of pyrite

The systems with a preequilibration of pyrite do not differ much from the previous systems. Only the Tc equilibrium level in this case seems to be higher (see figure 9).

The foregoing observations are explained as follows: if no organic matter is available all the reduced Tc will precipitate or adsorb on the pyrite and hence is removed from the solution. In presence of humic substances the Tc equilibrium solubility is enhanced due to an association of Tc with HS. The association is considered to be due to a complexation reaction between reduced Tc and the available organic matter. (The interaction constant is calculated in a later section.)

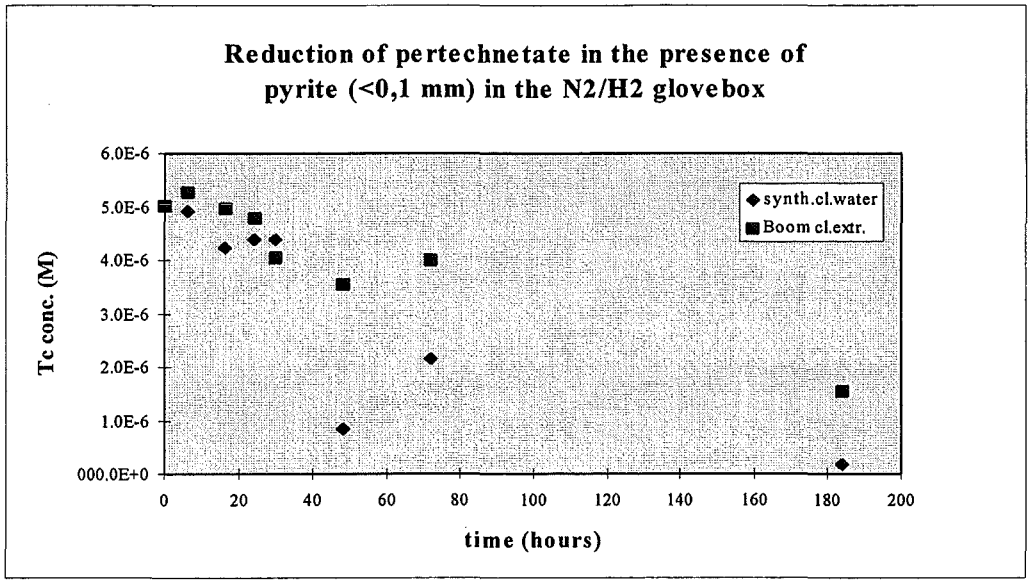

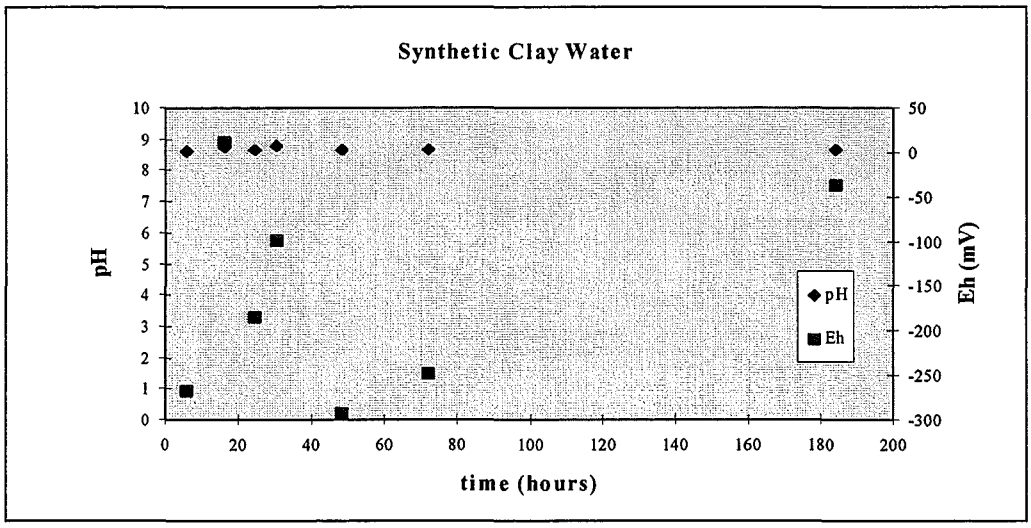

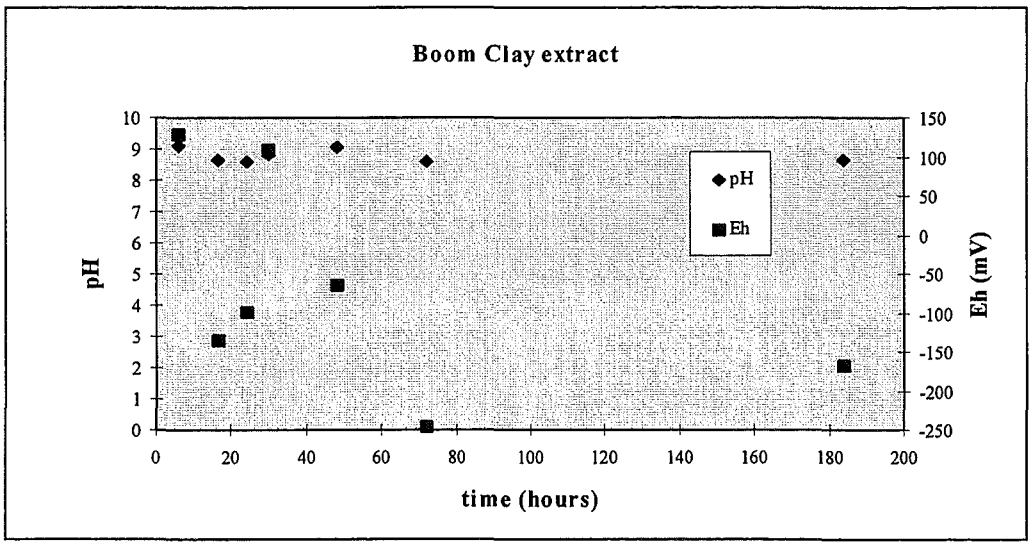

Figure 8. *Reduction of pertechnetate in presence of 50 mg pyrite (<100μm). The systems were not preequilibrated in S.C.W.*

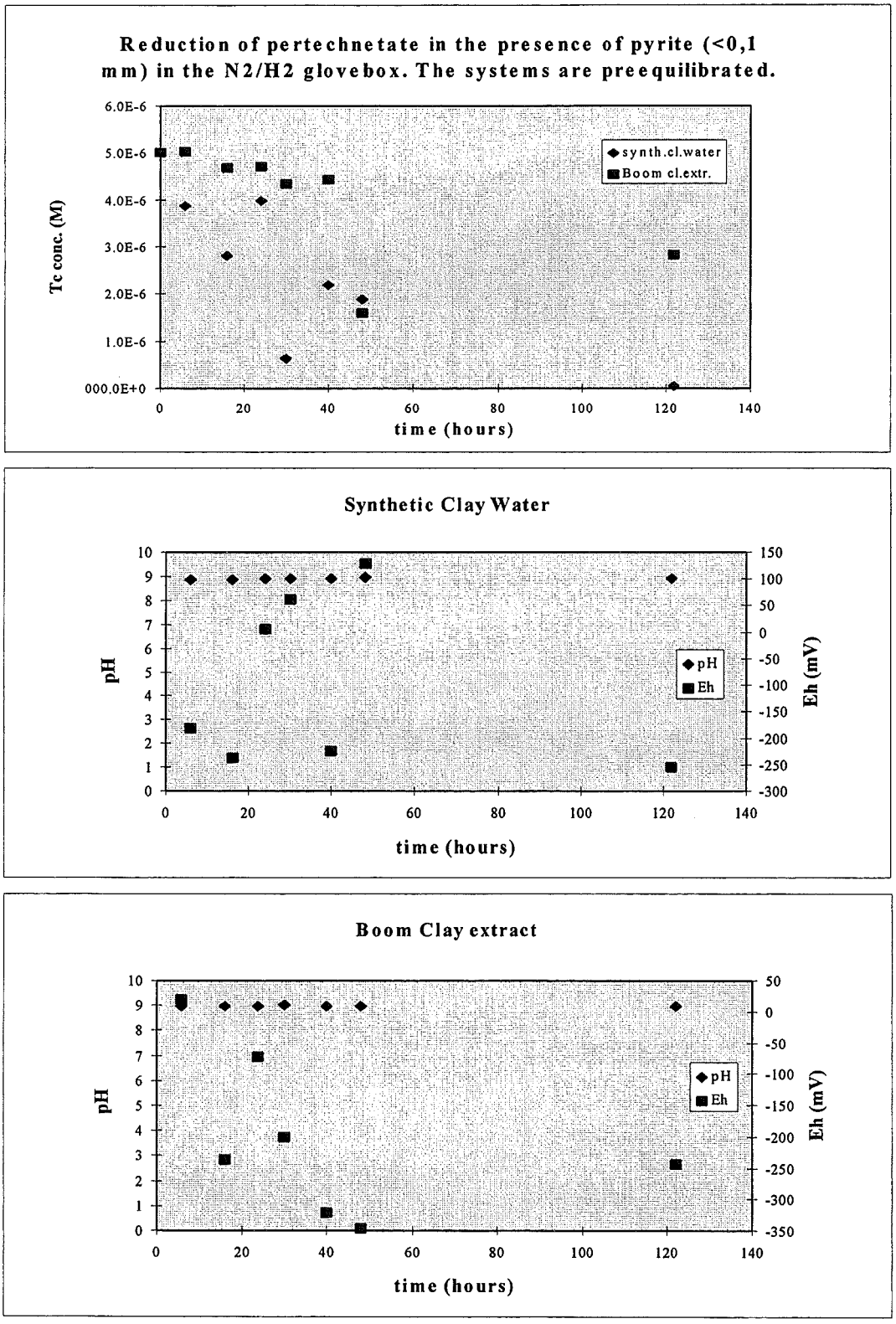

Figure 9. *Reduction of pertechnetate in the presence of 50 mg pyrite (<100 μm). The systems are preequilibrated in S.C.W. during 6 days.*

3.6 Conclusions

Reduction of pertechnetate in presence of Fe-containing minerals is favoured when Fe^{2+} is present as co-ordinatively bound Fe^{2+}, such as is the case in presence of pyrite and siderite.

In absence of humic substances the reduction of pertechnetate can be fully accomplished with an active surface such as pyrite. Hence technetium will be precipitated. At present we suppose that $TcO_2.nH_2O$ is formed although we have no definite proof of it. The solubility of TcO_2 is very low and therefore almost no Tc will be present in solution.

In presence of humic substances, TcO^-_4 reduces to Tc(IV) and the formation of $TcO_2.nH_2O$ precipitate will also occur. The solubility of the reduced Tc species is much higher due to an interaction (complexation) of Tc with the available humic substances.

4. Calculation of Tc-Humic Substance interaction constant

4.1 Solubility of Tc(IV) in absence of humic substances

The solubility of Tc(IV) at sufficiently low redox potentials (~ - 200 mV) and in equilibrium with TcO_2 precipitate can be calculated from the following hydrolysis equilibria:

$$TcO^{2+} + H_2O \overset{10^{-1.14}}{\Leftrightarrow} TcO(OH)^+ + H^+$$

$$TcO^{2+} + 2\,H_2O \overset{10^{-3.3}}{\Leftrightarrow} TcO(OH)_2 + 2\,H^+$$

$$2\,TcO^{2+} + 4\,H_2O \overset{10^{-0.13}}{\Leftrightarrow} (TcO(OH)_2)_2 + 4\,H^+$$

$$TcO^{2+} + 3\,H_2O \overset{10^{4.23}}{\Leftrightarrow} TcO_2.2H_2O\,(am) + 2\,H^+ \qquad (1)$$

The total solubility of Tc in absence of humic substances will be:

$$Tc_{TOT} = [TcO^{2+}] + [TcO(OH)^+] + [TcO(OH)_2] + [(TcO(OH)_2)_2] \qquad (2)$$

$$= [TcO^{2+}](1 + 10^{-1.14}/[H^+] + 10^{-3.3}/[H^+]^2 + 10^{-0.13}\,[TcO^{2+}]/[H^+]^4) \qquad (3)$$

$[TcO^{2+}]$ can be calculated from equation (1):

$$[TcO^{2+}] = 10^{-4.23} \times [H^+]^2$$

The total solubility of Tc therefore only depends on the pH. For example at a pH of 8.3, Tc_{TOT} = $3.21x10^{-8}$ M. This agrees with the previous results (see section 5.5) which demonstrated that in absence of humic substances almost no Tc was found in solution.

4.2 Solubility of Tc(IV) in presence of humic substances: calculation of the interaction constant

The results from the previous section 3.5 revealed that the redox reactions of technetium in presence of organic matter finally lead to an equilibrium. In addition all of the Tc in solution was associated with the available organic matter. Therefore it is possible to calculate interaction constants K^{HS}.

In presence of humic substances, the reducing circumstances induced by pyrite, will also reduce the pertechnetate to TcO^{2+} and other hydrolysis species and to TcO_2 which precipitates. At present we do not know which Tc(IV)-species interacts with the available humic substances. However we will assume that TcO^{2+} forms complexes with humic substances according to the following complexation reaction:

$$TcO^{2+} + HS\ (\text{Humic Substances}) \overset{K^{HS}}{\Leftrightarrow} TcO^{2+} - HS \qquad (4)$$

with equilibrium constant K^{HS}:

$$K^{HS} = [TcO^{2+}\text{-}HS]/(TcO^{2+}][HS]$$

In presence of HS the Tc solubility is enhanced by the formation of TcO^{2+}-HS. Equation (2) then extends to:

$$Tc_{TOT} = [TcO^{2+}] + [TcO(OH)^{+}] + [TcO(OH)_2] + [(TcO(OH)_2)_2] + [TcO^{2+}\text{-}HS]$$

The results from gel permeation chromatography showed that Tc in solution was associated with the available organic matter. Therefore the solubility of technetium is experimentally equal to $[TcO^{2+}$-HS] because the other Tc(IV) species are very low in concentration.

In presence of Gorleben humic substances equilibrium was reached and complete association of Tc with OM was observed. In presence of Boom Clay organic matter equilibrium was not completely reached. By way of approximation the experimental Tc-HA is used in the calculations.

All data used to calculate K^{HS} are given in table 3.

Humic Substances	Tc equil. Conc. (M)	[HS] (M)	pH	K^{HS}	K^{HS}_{TOT}
Gorleben	$2x10^{-6}$	$6x10^{-4}$	9.5	**$5.6\ 10^{20}$**	$1.04\ 10^{5}$
Gorleben	$2.1x10^{-6}$	$6x10^{-4}$	9.4	**$3.75\ 10^{20}$**	$1.09\ 10^{5}$
Gorleben	$1.9x10^{-6}$	$3x10^{-4}$	9.2	**$2.7\ 10^{20}$**	$1.97\ 10^{5}$
Gorleben	$1.1x10^{-6}$	$6x10^{-5}$	9.0	**$3.1\ 10^{20}$**	$5.71\ 10^{5}$
B.C. extract	$3.7x10^{-6}$	$1.88x10^{-4}$	8.8	**$1.33\ 10^{20}$**	$6.13\ 10^{5}$
B.C. (*)	$4.8x10^{-7}$	$3.3x10^{-4}$	8.2	**$6.2\ 10^{17}$**	$4.53\ 10^{4}$

(*) *from previous results (Maes and Capon, 1998)*

Table 3. Calculation of the interaction constant of TcO^{2+} with humic substances

The complexation constant of Tc(IV) with HA has a value of the order of $\mathbf{K^{HS} = 10^{20}}$.

Important note:

If an interaction between all the soluble Tc(IV)-species (instead of solely TcO^{2+})and the humic substances is assumed an interaction constant K^{HS}_{TOT} is obtained, which is of the order of 10^5 (see table 3).

5. Alternative method to measure Tc-Humic Substances interaction constant in a real system

Boom Clay is used as a natural reducing environment. According to the previous results TcO^{2+} is expected to complex with humic substances. If sufficiently small Tc concentrations(or sufficiently high HS concentration) are used, TcO_2 formation can be avoided. If only Tc-HS complexes are formed Tc will then distrubute between the dissolved organic matter and solid organic matter as for example in a Boom clay suspension. The methodology developed by Maes *et al.*(1992) for determining the complexation constant with dissolved organic matter in a sediment or soil will be used. For this purpose the Tc solid/liquid distribution in different successive extracts will be used to determine the Tc-interaction constant with Boom Clay organic matter.

5.1 Experimental set-up

A polypropylene vial containing 8.79 g of Boom Clay and 25 ml S.C.W. was allowed to stand for 5 days with regular gentle mixing. Then 25 ml of S.C.W. with a ^{99}Tc spike ($4x10^{-7}$ M) was added. This system was 7 days end over end shaken before phase separation by centrifugation (2 hours - 27200 g). A 20 ml sample of the supernatant is taken and monitored for optical density, concentration of ^{99}Tc, pH and Eh. The sediment is used for a further equilibrium by adding 20 ml S.C.W.. After manual resuspension using a vortex, the tube is again shaken end over end during one week. The same procedure of centrifugation and analysing of a new 20 ml sample is applied. This procedure was repeated 7 times.

5.2 Results

The experimental variation of the Log K_D versus absorbance is shown in figure 10 and table 4. Increasing organic matter concentrations lead to smaller K_D values due to increasing competition of the Tc complexation with dissolved organic matter.

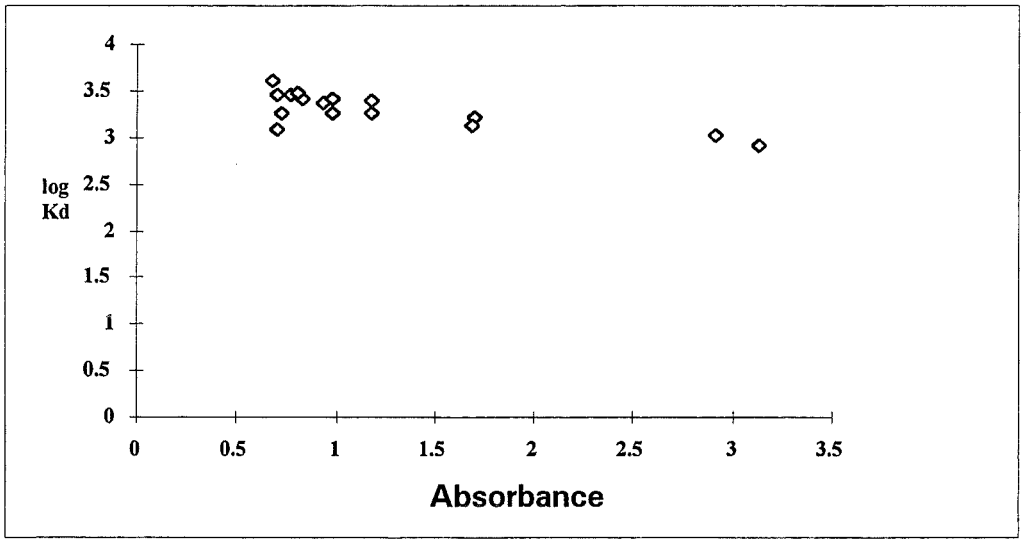

Figure 10. *Variation of Log K_D for Tc with absorbance obtained for successive extractions of BoomClay with Synthetic Clay Water.*

5.3 Interpretation by Schubert like approach: calculation of K^{HS}

The aforementioned competition can be used for the determination of the conditional complexation constant using the methodology developed by Maes et al. (1992). For this purpose Boom clay solid phase was considered to act as a Tc adsorption sink, which competes with dissolved Boom Clay organic matter for Tc. The method is thus similar to Schubert's ion exchange method. The determination of the conditional complexation constant thus only refers to the dissolved part of the Boom Clay organic matter, which is in equilibrium with the solid organic matter.

Assuming the complexation reaction (4) to occur then the well known Schubert equation can be written as:

$$(K^{\circ}_D/K_D - 1) \cdot A = K^{HS}\,[HS]$$

or $$\text{Log}\,(K^{\circ}_D/K_D - 1) = \text{Log}\,K^{HS} - \text{Log}[HS] + \log A$$

where $K°_D$ and K_D are distribution coefficients in the absence and presence of Boom Clay Humic Substances; K^{HS} is the conditional complexation constants of TcO^{2+} with HS. A is the side reaction coefficient.

The application of the aforementioned modified Schubert approach necessitates a value for the distribution coefficient $K°_D$ in absence of organic matter in solution. $K°_D$ was obtained by extrapolation to zero Humic Substance concentration from a plot of Log K_D versus absorbance as shown in figure 10.

Figure 11 shows Log($K°_D/K_D$ -1) versus Log L. All data points satisfy the previously obtained relationship. The slope is close to unity.

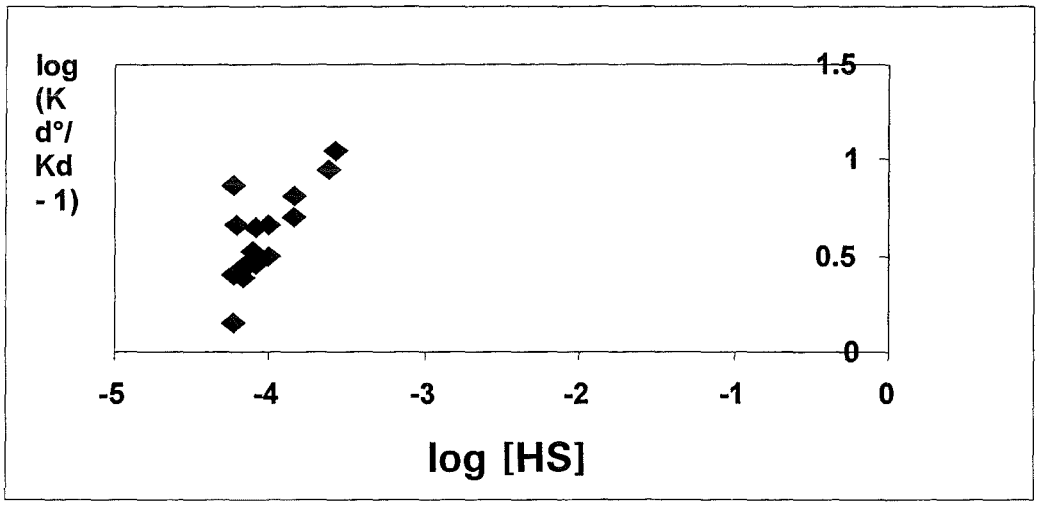

Figure 11. *Schubert plot. Variation of Log ($K_D/K°_D$ - 1) with organic matter concentration for successive extraction of Tc from Boom Clay.*

The conditional complexation constants K^{HS} were calculated by applying the foregoing equation to the individual data points (see table 4).

The side reaction coefficient A accounts for the presence of all complexes other than those with humic substances. In this case no other complexation reactions than hydrolysis reactions are expected and A can therefore be calculated from the total solubility of technetium in absence of organic matter and in absence of TcO_2 formation. Equation (2) can be rewritten as:

$$Tc_{TOT} = [TcO^{2+}] \times (\text{side reaction coefficient A})$$

At a pH of 8.3 the side reaction coefficient will be $10^{13.3}$.

The obtained K^{HS} values range from 17.70 to 18.40 and are somewhat smaller than the K values determined in presence of pyrite as reducing solid surface.

Important note:

If we assume that **all** the soluble Tc-species in solution are directly associated with the humic substances then the interaction constant K^{HS}_{TOT} of about $10^{4.6}$ is obtained (see table 4), and is close to the previously obtained values in presence of pyrite.

pH	O.D. (Abs) 280 nm	Log K_D	Log(K°_D/K_D-1)	OS (eq/l)	Log K^{HS}	Log K^{HS}_{TOT}
8.30	2.9100	3.0055	0.9481	0.000243	**17.86**	4.56
8.31	3.1250	2.9119	1.0511	0.000261	**17.93**	4.63
8.29	1.7000	3.2188	0.7026	0.000142	**17.85**	4.55
8.30	1.6850	3.1266	0.8110	0.000141	**17.96**	4.66
8.29	1.1800	3.3865	0.4923	0.000099	**17.80**	4.50
8.28	1.1750	3.2569	0.6566	0.000098	**17.96**	4.66
8.26	0.9775	3.4123	0.4578	0.000082	**17.85**	4.55
8.26	0.9775	3.2629	0.6493	0.000082	**18.04**	4.74
8.25	0.9400	3.3670	0.5178	0.000079	**17.92**	4.62
8.28	0.8325	3.4178	0.4504	0.000070	**17.91**	4.61
8.30	0.7760	3.4473	0.4099	0.000065	**17.90**	4.60
8.30	0.8040	3.4684	0.3804	0.000067	**17.85**	4.55
8.34	0.7090	3.0749	0.8702	0.000059	**18.40**	5.10
8.30	0.7040	3.4510	0.4048	0.000059	**17.94**	4.64
8.34	0.7230	3.2543	0.6597	0.000060	**18.18**	4.88
8.34	0.6840	3.6159	0.1527	0.000057	**17.70**	4.40

Table 4. Detailed experimental data on the distribution of Tc in Boom Clay extracted successively with Synthetic Clay Water (Log A= 13.3)

6. General Conclusion

- Tc(VII) reduction to probably Tc(IV) is enhanced in presence of Fe^{2+} containing minerals such as pyrite and siderite
- The kinetics of Tc(VII) reduction depends on the reducing capacity of the available surfaces.
- Two methods were developed to measure Tc-Humic Substances interaction constants. The following reaction mechanism was assumed: $TcO^{2+} + HS \Leftrightarrow TcO^{2+}$ - HS.

  *Method 1: in presence of TcO_2 precipitate the enhanced solubility of Tc(IV) associated with HS is used to calculate the K^{HA}_{Tc}. The method was demonstrated for individual geochemical components (FeS_2).

  *Method 2: The complexation constant of Tc(IV) with HS was determined from the competition for complexation between dissolved organic matter and precipitated organic matter (method of Maes *et al.* 1992). The method was demonstrated for Boom clay sediment.
  Both methods lead to an interaction constant of the order of **10^{18} to 10^{20}**.
- The assumed reaction mechanisms and K values are based on the assumption that TcO_2 precipitates. However TcS_2 can also precipitate. The reaction mechanisms should therefore be further verified and elucidated.

7. References

Maes, A., Capon, L. Reduction of Technetium in Solution: Influence of Ferrous Iron, Minerals Phases and Organic Matter. In: Effects of Humic Substances on the Migration of Radionuclides: Complexation and Transport of Actinides, First technical progress report of the EC-project No.: F14W-CT96-0027 Report FZKA 6124, Ed. G.Buckau, August 1998.

Vandergraaf, T.T., Ticknor, K.V., George, I.M. Geochemical behavior of disposed radioactive waste, chapter 2: 27-43. ACS Symposium Series 26. Eds. Barney, G.S.; Navratil, J.D.; Schulz, W.W. American Chemical Society (1984).

Cui, D., Eriksen, T.E. Reduction of pertechnetate by ferrous iron in solution: Influence of sorbed and precipitated Fe(II). Environ. Sci. Technol., 30:2259-2262 (1996a).

Cui, D., Eriksen, T.E. Reduction of pertechnetate in solution by heterogeneous electron transfer from Fe(II)-containing mineral. Environ. Sci. Technol., 30:2263-2269 (1996b).

Maes, A., van Herreweghen F., Van Elewijck F. and Cremers A. Behaviour of trace cadmium in Boom clay reducing sediment I. Complexation with in situ dissolved humic acids. The Science Total Env. 117/118, 463-473, 1992.

Artinger, R., Kienzler, B., Schüβler, W., Kim, J.I. Sampling and Characterization of Gorleben groundwater/Sediment Systems for Actinide Migration Experiments. Effects of Humic Substances on the Migration of Radionuclides: Complexation and Transport of Actinides, First technical progress report of the EC-project No.: F14W-CT96-0027 (1998).

Baeyens B;, Maes, A., Cremers, A. In situ physico-chemical characterization of Boom clay. In Radioactive Waste Management and the nuclear Fuel Cycle. Harwood Academic Publishers. 391-408, 6(3-4), (1985)

Annex 12

A Study of Metal Complexation with Humic and Fulvic Acid: The Effect of Temperature on Association and Dissociation

(King et al., LBORO and RMC-E)

2nd Technical Progress Report

EC Project:

"Effect of Humic Substances on the Migration of Radionuclides:

Complexation and Transport of Actinides"

LBORO Contribution to Task 2 (Complexation)

A Study of Metal Complexation with Humic and Fulvic Acid: The Effect of Temperature on Association and Dissociation

Reporting period 1998

S.J. King [1], P. Warwick [1] and N. Bryan [2,3]

[1] Department of Chemistry, Loughborough University, Loughborough, Leicestershire, LE11 3TU, UK

[2] RMC Ltd, Suite 7, Hitching Court, Abingdon Business Park, Abingdon, Oxfordshire, OX14 1RA

[3] Department of Chemistry, University of Manchester, Oxford Road, Manchester, M13 9PL

1.0 Introduction

The main objective of the project is to determine the influence of humic substances on the migration of radionuclides. One of the first steps taken in order to deepen this understanding was to investigate the complexation of Eu^{3+} and $UO_2^{2+}$with humic substances (Task 2).

There is concern that after disposal in underground repositories radionuclides may eventually come into contact with groundwaters containing humic substances at elevated temperatures. Investigations have therefore been undertaken to determine the temperature dependence of the stability constants for europium and uranium binding to humic and fulvic acid by a series of batch experiments. The rate at which these complexes dissociate may be a significant factor in understanding the radionuclide transportation in the environment and has been investigated over a range of environmental parameters.

The derived binding strengths, enthalpies and entropies of reaction and dissociation rate constants have been used for the mechanistic modelling of metal-humate interactions by Bryan *et al* in this volume.

2.0 Batch experiments

Batch studies to determine the effect of temperature on Europium binding to fulvic acid

Similar experiments as to those performed with humic acid have now been completed with fulvic acid. In the batch procedure Eu III solutions (1.0×10^{-6}, 1.1×10^{-7}, 2.4×10^{-8} mol dm^{-3}) containing radioactive tracer quantities of Eu-152, were equilibrated with 0.004g (± 0.0001g) of dry conditioned resin (Dowex 50x4, 100-200 mesh cation exchange resin). The resin was completely converted to the sodium form before use by washing successively with HCl (2 mol dm^{-3}), distilled H_2O, NaCl (3 mol dm^{-3}), distilled H_2O, NaOH (0.1 mol dm^{-3}), distilled H_2O and finally with the appropriate pH solution before air drying at 40°C.

Experiments were performed in acid washed polysulfone centrifuge tubes with non-buffered $NaClO_4$ solution (0.1 mol dm^{-3}) at pH=4.5, in the presence or absence of purified fulvic acid (5.09, 10.19, 15.28 and 20.37mg dm^{-3}). The fulvic acid used was provided and characterised (Task 1) by Jenny Higgo, at BGS. Samples were then left to equilibrate at temperatures between 20°C and 60°C for one week. During this time samples were shaken at frequent intervals.

Batch studies to determine the effect of temperature on Uranium binding to humic/fulvic acid

In the batch procedure purified U-233 solutions (1.0×10^{-6}, 7.5×10^{-7}, 5.0×10^{-7} 2.5×10^{-7} and

1.0 x10^{-7} mol dm^{-3}) were equilibrated with 0.08g (± 0.001g) of dry conditioned resin (Dowex 50x4, 100-200 mesh cation exchange resin). The U-233 was first separated from the decay daughters by separation on a U/TEVA spec column. The experiments were performed in acid washed polysulfone centrifuge tubes with non-buffered $NaClO_4$ solution (0.1 mol dm^{-3}) at pH=4.5, in the presence or absence of purified fulvic acid (extracted from Derwent reservoir) at 10.19mg dm^{-3} or humic acid (Aldrich Chemical Co.) 5mg dm^{-3}. Samples were then left to equilibrate at temperatures 20°C, 40°C and 60°C for one week.

Afterwards the activity of each supernatant solution was determined by removing $3cm^3$ aliquot which was mixed with $17cm^3$ of EcoscintA (National Diagnostics) liquid scintillation cocktail. The sample was then counted for 10 minutes using an LKB (Wallac) 1215 RackBeta Counter.

2.1 Derivation of Stability constants

The stability constants were derived by three different approaches.

a) The Schubert method[1] where the metal concentration remains fixed. The stability constants derived at Eu concentrations of 1.1 x10^{-7} and 2.4 x10^{-8} mol dm^{-3} were averaged at each temperature studied. These are shown in Table 1.

b) The Scatchard approach[2] and the Charge neutralisation model[3], where the humic acid concentration remains fixed. In both cases the results were first interpreted by the Ardakani and Stevenson approach[4]. The average stability constants for EuHS over the humic substance concentration range at each temperature are shown in Table 1. The stability constants derived for EuHA in the previous reporting period[5] are included for comparison. The derived stability constants for UO_2HS are shown in Table 2.

2.1.1 Changing Metal Concentration

This batch procedure was based on the Ardakani and Stevenson modification of the Schubert Method[4]. In the batch procedure metal solutions, containing radioactive tracer, were equilibrated with cation exchange resin in the absence (controls) and presence of humic substance (HS). Plots of log [M]res against log [M]soln were constructed, at each temperature, both for the controls and the solutions containing the HS. These plots were used to deduce the amounts of MHS present in each sample. This data was then interpreted further by two approaches, the Scatchard Method and the Charge Neutralisation Model.

Table 1: Logarithmic stability constants, logK, for EuHA and EuFA complex derived at different temperatures.

Temperature	Schubert	CN Model	Scatchard	
°C	logK	logK	$logK_1$	$logK_2$
	10^{-7}-10^{-8} M	10^{-6}-10^{-8} M	10^{-7}-10^{-8} M	10^{-6}-10^{-7} M
Humic Acid				
20	5.28 ± 0.22	7.57 ± 0.08	8.20 ± 0.07	7.34 ± 0.09
25	6.39 ± 0.27	7.69 ± 0.05	8.27 ± 0.05	7.47 ± 0.06
30	6.38 ± 0.01	7.91 ± 0.08	8.52 ± 0.08	7.68 ± 0.09
40	6.77 ± 0.11	8.15 ± 0.05	8.77 ± 0.05	7.91 ± 0.06
50	6.82 ± 0.23	8.06 ± 0.28	8.67 ± 0.27	7.83 ± 0.29
60	7.74 ± 0.45	8.42 ± 0.08	9.07 ± 0.08	8.18 ± 0.09
Fulvic Acid				
20	6.26 ± 0.87	7.70 ± 0.04	8.33 ± 0.03	7.48 ± 0.03
40	7.54 ± 0.08	8.20 ± 0.04	8.83 ± 0.04	7.97 ± 0.05
60	6.75 ± 0.41	8.40 ± 0.13	9.05 ± 0.13	8.18 ± 0.15

Scatchard Approach

The simple Scatchard approach is often used as it assumes a reaction stoichiometry of 1 cation to 1 site. This approach also does not require knowledge of the humic substance concentration. A plot of [MHS]/[M] versus [MHS] has a slope of -K. Stability constants for the humic substance binding of metal over the metal concentration range used were then estimated from fitting straight lines to plots of the experimental data. Scatchard plots in this case were found to be curved, as they invariably are for humic substances. Therefore, two lines were fitted to the experimental data.

Table 2: Logarithmic stability constants, logK, for UO_2HA and UO_2FA complex derived at different temperatures.

Temperature	Schubert	CN Model	Scatchard	
°C	logK	logK	$logK_1$	$logK_2$
	10^{-6} M	10^{-6}-10^{-7} M	10^{-7}-$5x10^{-7}$ M	$5x10^{-7}$-10^{-6} M
Humic Acid				
20	7.36	7.85	8.26	7.58
40	6.37	7.61	8.04	7.34
60	5.53	7.42	7.84	7.17
Fulvic Acid				
20		7.54	7.84	7.23
40		7.50	7.78	7.21
60		7.35	7.58	7.08

Charge Neutralisation Model

The Charge Neutralisation Model as proposed by Kim and Czerwinski[3] is based on the concept of metal ion charge neutralisation upon complexation to humic acid functional groups. Only a fraction of the total sites present on the humic acid are available for reaction under a given set of conditions. Hence the effective concentration of humic acid ($[HA(z)]_{eff}$) is calculated from its proton exchange capacity (PEC), metal ion charge (z) and loading capacity of the humic (LC), which changes as a function of pH, ionic strength and metal ion charge. It is defined as:

$$[HA(z)]_{eff} = \frac{(HA)(PEC)(LC)}{z} = [HA(z)]_t(LC) \qquad (1)$$

where (HA) is the concentration of humic acid in g/l, $[HA(z)]_t$ in mol/l and PEC in eq/g. The proton exchange capacity for Aldrich Humic acid and Derwent fulvic acid has been determined to be 5.43 ± 0.20 meq/g[6] and 5.00 meq/g[7] (under Task 1, at BGS).

It can be shown that

$$[M^{Z+}]_f = LC\left(\frac{[M^{Z+}]_f[HA(z)]_t}{[MHA(z)]}\right) - \frac{1}{K} = LCxF - \frac{1}{K} \qquad (2)$$

In the absence of knowledge of the loading capacity (LC) of HA under given conditions the stability constant K and LC can be determined from a plot of $[M^{Z+}]_f$ versus F has a slope of LC and a y intercept -1/K. It can be seen that these plots yielded curves. The model was used in the traditional manner and the best straight line fitted to this curve to determine a single stability constant.

2.1.2 Changing Ligand Concentration

Schubert Method

The original Schubert method was also investigated for the determination of MHS stability constants [1]. In this method the metal ion is regarded as the central group. This is only true when the concentration of metal ions is much smaller than that of the ligand.

The distribution coefficients of metal ions between resin and solution in the presence of humic acid (D) and absence of humic substance (D_O) are given by

$$D = \frac{[M]_{RESIN}}{[M]_{AQ} + [ML]} \qquad (3)$$

$$D_O = \frac{[M]_{RESIN}}{[M]_{AQ}} \qquad (4)$$

As the distribution coefficient in the absence of HS (D_O) and in the presence of HS (D) is related to the concentration of HS (mol dm^{-3}) and the stability constant K

It follows that

$$\log\left(\frac{D_o}{D} - 1\right) = \log K + m\log[HA] \qquad (5)$$

Plots of log D_O/D-1 versus log [HS] were used to derive the stability constant logK and m from the intercept and slope of the line.

2.2 Derivation of thermodynamic parameters

The thermodynamic parameters, ΔH, ΔG and ΔS were calculated from the stability constants determined from each of the three different model approaches. The enthalpy of the complexation reaction of M and HS is given by

$$-\frac{\Delta H}{R} = \frac{d \ln K}{d(1/T)} \tag{6}$$

The Gibbs free energy and the entropy of the complexation reaction were determined from

$$\Delta G = -RT \ln K \tag{7}$$

and

$$\Delta S = (\Delta H - \Delta G)/T \tag{8}$$

2.3 Discussion

The stability constants derived for EuHA and EuFA complexation were observed to increase as temperature increased. While those for UO_2HA and UO_2FA were observed to decrease. However, the change in stability constant was not very significant, over the temperature range 20°C to 60°C. The enthalpy changes under standard atmospheric pressure were deduced from the slopes of the plots of logK against 1/T in accordance with equation (6). The plots were found to be linear and are shown in Figures 1, 1a, 2, 3 and 4. The values for ΔG and ΔS were obtained using the equations (7) and (8). The thermodynamic parameters, ΔG, ΔS and ΔH derived at 298K are shown in Table 3. There is good agreement between the ΔH and ΔS values derived by CN model and Scatchard approach. However, the values derived by the Scatchard approach are slightly larger.

The EuHS complexation reaction overall was found to be endothermic. The values indicate spontaneous changes (ΔG negative) with a large favourable entropy change (ΔS positive). In contrast the complexation reaction for UO_2HS was found to be exothermic overall with a less favourable entropy than that derived for EuHS. The values of ΔG and ΔS derived a very similar HA and FA for both metals studied. By comparison to literature data (Table 3) the thermodynamic parameters derived for EuHS are of a similar order of magnitude to those derived for ThHS[8] complexation and UO_2HS are of a similar order of magnitude to other divalent metal ions, SrHA[9], NiHA[10] and UO_2HA[11]. It has been suggested that the entropy increase results from the release of co-ordinated water molecules during complexation[9]. Bryan *et al* [19] have produced a mechanistic model for the metal-humate interaction (this volume). The experimental entropies reported have been used to test this model.

Table 3:Thermodynamic Parameters of Metal HA complexes at 298K.

COMPLEX	ΔG	ΔH	ΔS	Model approach
	kJ eq^{-1}	kJ eq^{-1}	J $T^{-1}eq^{-1}$	
Sr(HA)	-15.0±1.1	-1.5±1.0	45.3± 7.0	Schubert[8]
$Sr(HA)_2$	-26.7±1.4	-13.3±4.4	45.0±16.1	
Ni(HA)	-34.4±0.8	-12.4±9.8	75.0±33	
$UO_2(HA)$	-29.2±0.1	-2.7±0.4	89±33	Schubert[9]
$UO_2(HA)_2$	-51.0±0.2	+8.0±4.0	200±13	
Th(HA)	-63.56±0.1	32.6±3.2	323±12	Schubert[10]
$Th(HA)_2$	-92.23±0.2	42.7±3.3	453±12	
Th(FA)	-55.90±0.2	18.9±4.2	251±44	Schubert[10]
$Th(FA)_2$	-76.97±0.3	46.4±8.4	414±30	
EuHA	-44.1	35.5	267	CN Model
K_1	-47.5	37.2	287	Scatchard
K_2	-42.8	35.1	264	Scatchard
	-35.1	89.1	417	Schubert
EuFA	-44.7	32.8	260	CN Model
K_1	-43.5	34.1	276	Scatchard
K_2	-48.3	32.8	256	Scatchard
UO_2HA	-44.4	-20.0	81.9	CN Model
K_1	-46.7	-26.2	68.8	Scatchard
K_2	-42.9	-20.1	56.0	Scatchard
UO_2FA	-43.0	-8.7	115.0	CN Model
K_1	-44.7	-12.0	109.6	Scatchard
K_2	-41.3	-6.9	98.2	Scatchard

Figure 1: Temperature dependence of the stability constants of EuHA as derived by the Scatchard Approach and the Charge Neutralisation Model.

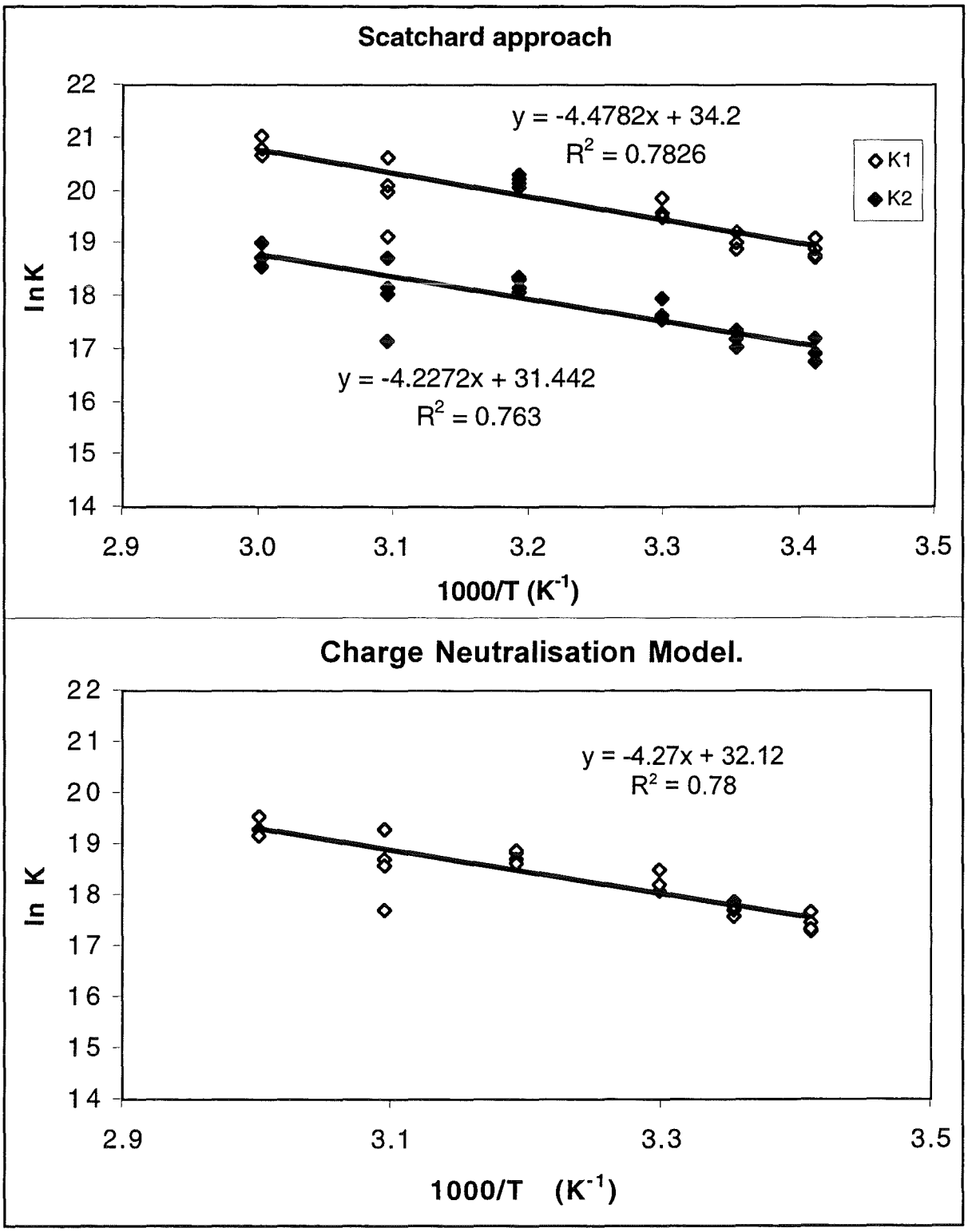

Figure 1a: Temperature dependence of the stability constants of EuHA as derived by the Schubert Approach.

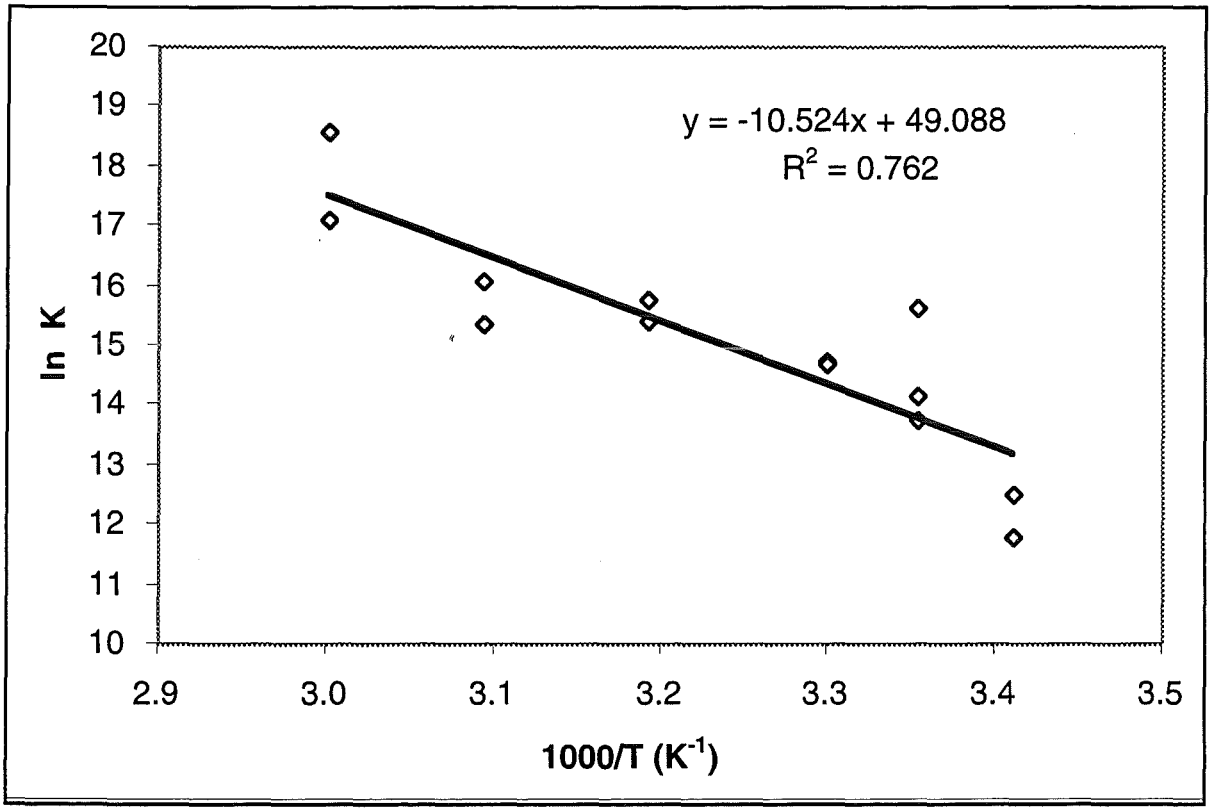

Figure 2: Temperature dependence of the stability constants of EuFA as derived by the Scatchard Approach and the Charge Neutralisation Model.

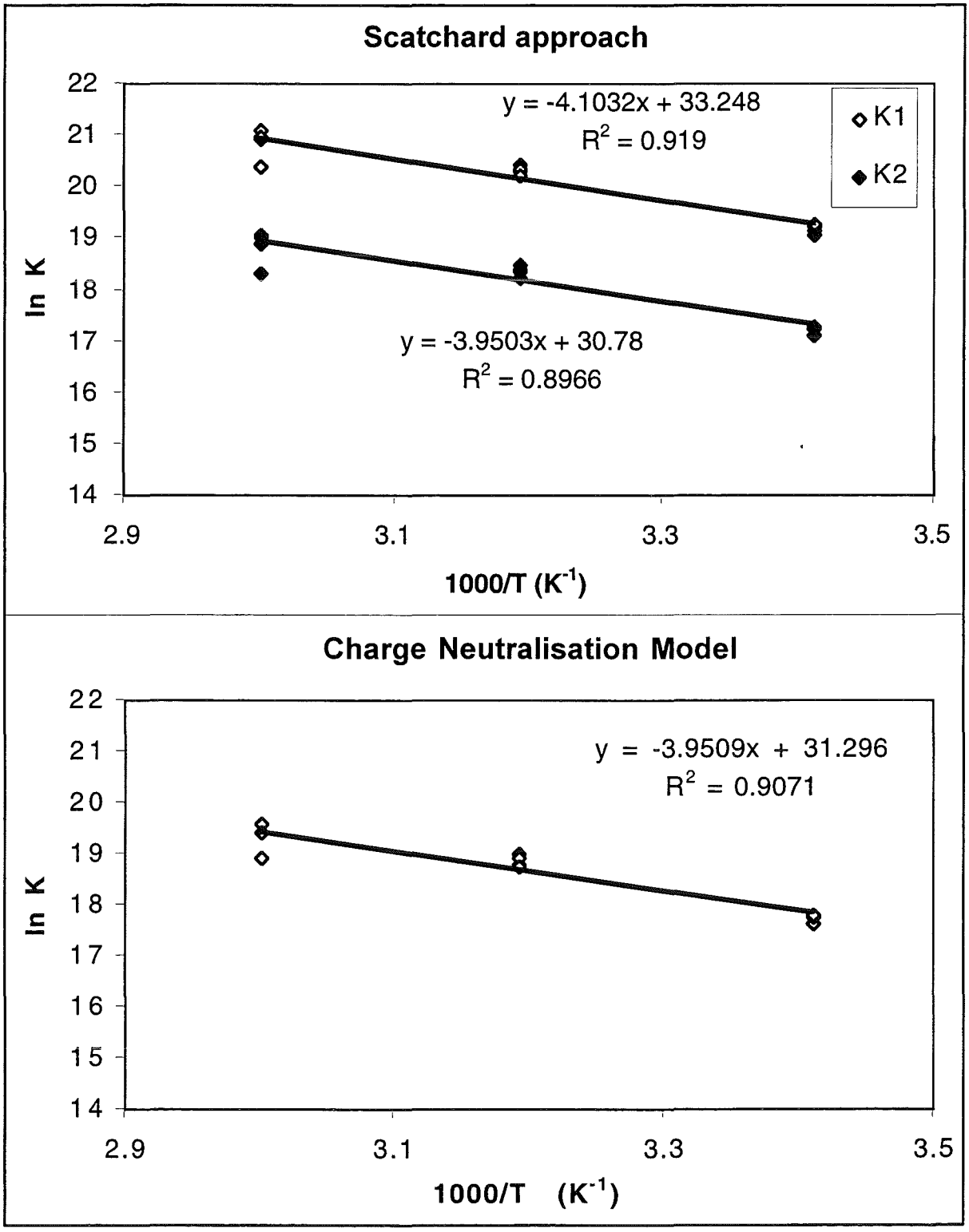

Figure 3: Temperature dependence of the stability constants of UO_2HA as derived by the Scatchard Approach and the Charge Neutralisation Model.

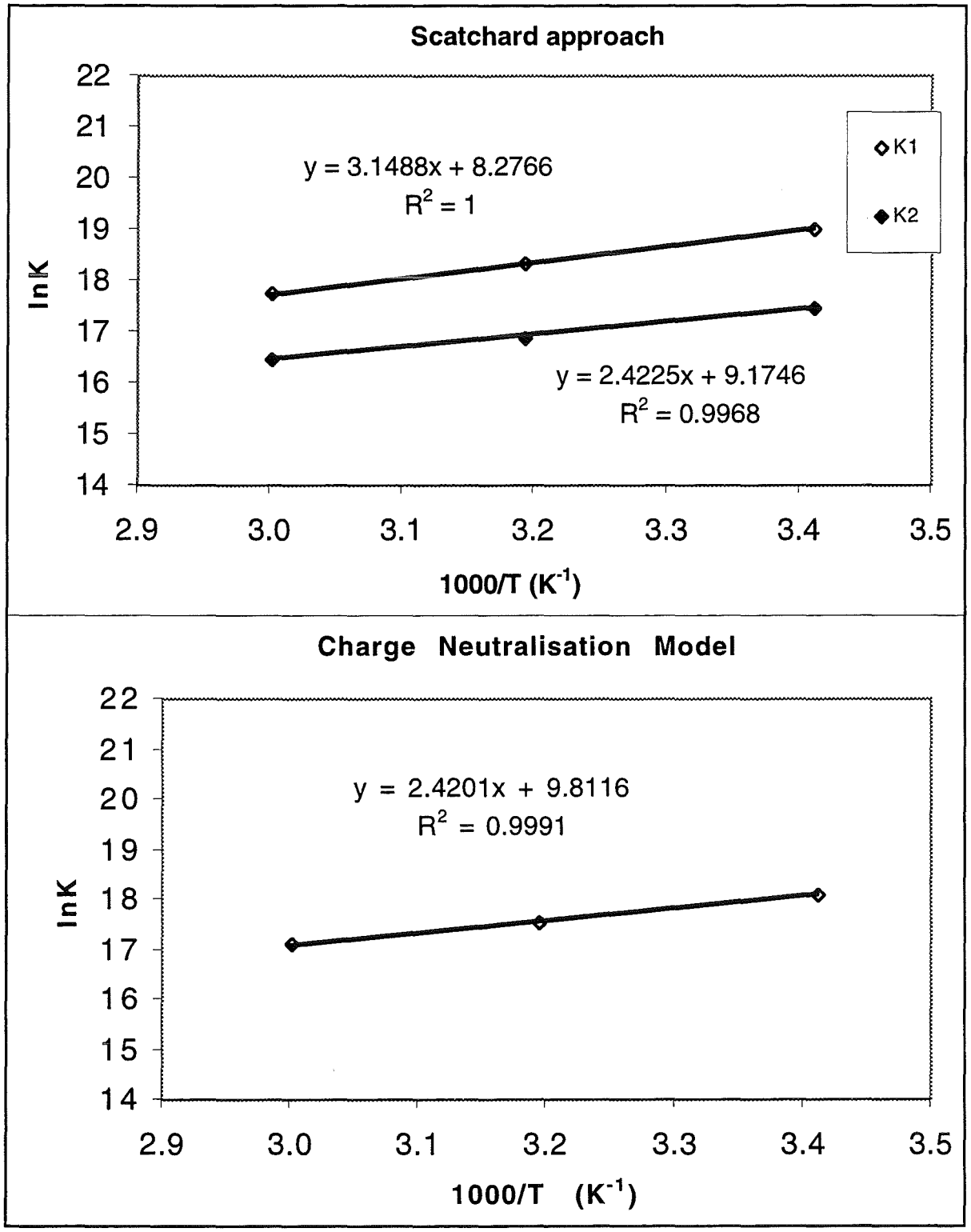

Figure 4: Temperature dependence of the stability constants of UO_2FA as derived by the Scatchard Approach and the Charge Neutralisation Model.

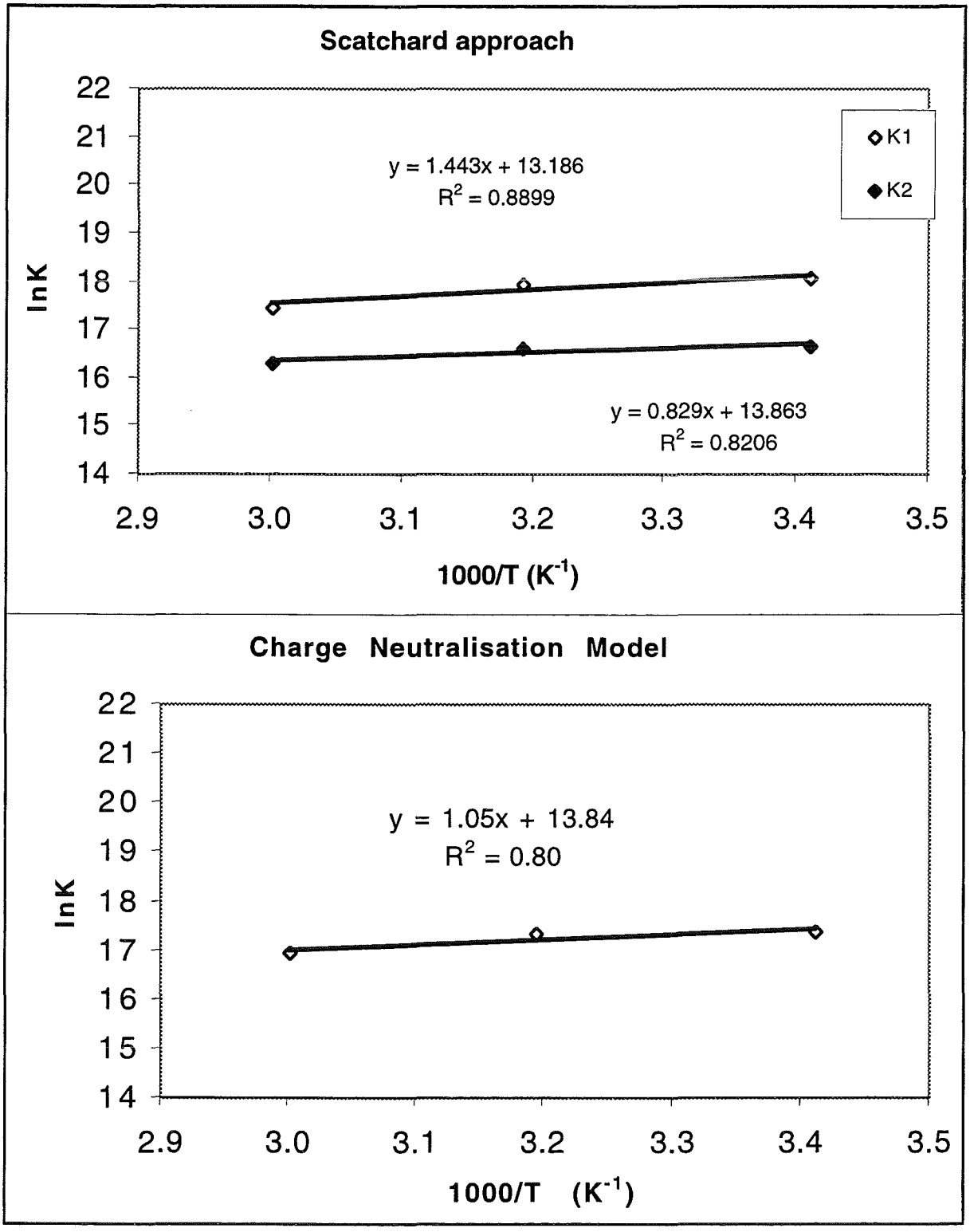

3.0 Kinetic Batch experiments

The stability constants of many metal ions to humic substances is high. Another important factor in determining the effect of HS on the migration of the metal ion in the environment is the rate at which they dissociate. Insight into metal ion interactions with HS can be obtained from studies of dissociation kinetics. Various schemes have been developed and applied to the study of metal HS dissociation kinetics such as; ion exchange[12,13] competing ligand technique[14,15,16] anoidic stripping voltametry[17] and ion selective electrodes[18]. A method of studying the dissociation kinetics of EuHS has been developed using Dowex cation exchange resin. It allows the dissociation kinetics to be studied over long dissociation times, at trace metal concentrations and different temperatures.

3.1 Method Development

The reaction between a metal humic substance complex MHS and resin can be expressed as

$$MHS + Resin = MRes + HS \quad (9)$$

When the resin is present in excess the rate of formation of MRes is determined by the rate of dissociation of MHS. The rate of MRes association was investigated at pH=4.5 and 6.5. For a resin weight of 0.5g the rate of Eu binding to the resin was found to be sufficiently fast, after 2 minutes >99% bound at pH=4.5 and >98% bound at pH=6.5.

In the batch procedure Eu III solutions (1.14×10^{-7} mol dm^{-3}) containing radioactive tracer quantities of Eu-152, were equilibrated with 10.0 mg dm^{-3} fulvic acid. Prior to this step the fulvic acid was filtered through a 0.45μm membrane to remove any microbes present. The experiments were performed in duplicate in acid washed polysulfone centrifuge tubes with non-buffered $NaClO_4$ solution (0.1 mol dm^{-3}) at pH=4.5, with a total volume of 15ml. The samples were left to equilibrate at 20°C for 26 days. In order to ensure the reaction was first order or pseudo first order various weights (0.5, 1.0, 1.5, 2.0 and 2.5g) of dry conditioned resin (Dowex 50x4, 100-200 mesh cation exchange resin) were added. The experiments were performed in duplicate. The samples were then laid on their side in a thermostated shaking water bath. At specific times the tubes were stood upright for 1 minute and the resin allowed to settle. A 0.5ml aliquot of the supernatant was then removed and counted for 1 minute in a clean vial. In order to investigate the effect of removing aliquots, hence changing concentration of resin, for one of the samples to which 1.5g of resin was added the aliquot was replaced immediately after counting. The pH of solutions was checked regularly and any solution with greater than 0.5 of pH unit drift was discarded from the final results.

The Eu-152 activity remaining in solution can be used to calculate the concentration of EuFA

present at a specific time. The stability constant for EuFA formation under these experimental conditions has been determined to be of the order of 10^8. The percentage of free europium at the time the resin is added is therefore assumed to be negligible. A plot of [EuFA]/ $[EuFA]_0$ versus time can be seen in Figure 5.

The results show that as the resin weight is increased the rate of dissociation decreases. At the higher resin weights of 2.0 and 2.5g, however, the kinetics of dissociation are not effected by resin weight. The data from this study and those mentioned in the following section have been used in a kinetic modelling study by Bryan *et al* [19] in this volume.

It can be seen in Figure 5 that the removing of an aliquot had no effect on the dissociation kinetics. In future studies after the first day of removing aliquots the sample was replaced in order to conserve the volume and hence allow studies to be extended to longer time periods. Experiments were performed using a resin weight of 2.5g. In addition no Eu was observed to sorb to the vials for counting and no HA/FA was observed to sorb to the resin.

Figure 5: Experimental data for EuFA dissociation with different resin weights (26 days, pH=4.5, T=20°C).

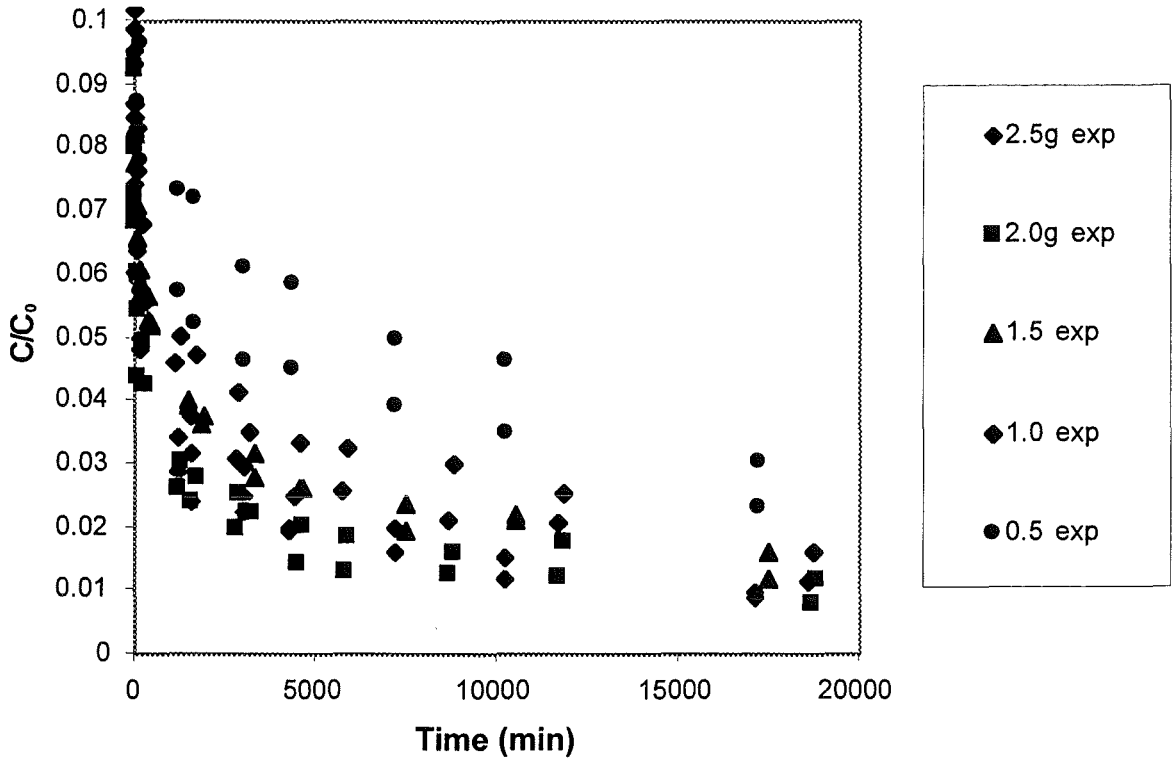

The effects of temperature, filtering, pre dissociation equilibration time, pH, Eu concentration, FA concentration and humification (HA) have been investigated.

3.2 Results and Discussion

The simplest interpretation of the results showed that the dissociation of Eu from humic acid occurred by three first order pathways. For the results obtained using 2.5g of resin the majority of the Eu (90%) underwent a fast dissociation step with a rate constant k_1=0.22min^{-1}. Further dissociation occurred by two slower steps 4% with a rate constant k_2=0.00716 min^{-1} and 3.2% with a rate constant k_3=0.000072 min^{-1}. It is the rate and the percentage of Eu undergoing this latter very slow dissociation step that is important to the transport of metal ions by natural organic ligands in the environment. The following investigations will therefore be largely discussed in terms of the effect of a change in the environmental parameters on this fraction $[Eu]_{FIX}$ and the rate constant k_3. The results are shown in Table 4. It is interesting to note that the effect of resin weight did not effect the rate of this very slow dissociation step.

Table 4: The Eu concentration available for slow dissociation, $[Eu]_{FIX}$, and corresponding dissociation rate, k_3.

[HS] (mg dm^{-3})	$[Eu]_T$ (mol dm^{-3})	Prequil time (days)	$[Eu]_{FIX}$ (mol dm^{-3})	k_3 (min^{-1})
20°C, pH=4.5				
10 (FA)	1.14x10^{-7}	9	5.29x10^{-9}	1.5x10^{-5}
60 (FA)	1.14x10^{-7}	9	1.99x10^{-8}	8.5x10^{-6}
10 (HA)	1.14x10^{-7}	9	1.10x10^{-8}	1.5x10^{-5}
10 (FA)	1.14x10^{-7}	26	3.40x10^{-9}	7.2x10^{-5}
10 (FA)	1.14x10^{-7}	35	4.19x10^{-9}	2.9x10^{-5}
20°C, pH=6.5				
10 (FA)	1.14x10^{-7}	9	3.62x10^{-8}	1.4x10^{-5}
60 (FA)	1.14x10^{-7}	9	1.01x10^{-7}	3.5x10^{-6}
10 (HA)	1.14x10^{-7}	9	8.28x10^{-8}	1.4x10^{-5}

Table 4 cont/d: The Eu concentration available for slow dissociation, $[Eu]_{FIX}$, and corresponding dissociation rate, k_3.

[HS] (mg dm^{-3})	$[Eu]_T$ (mol dm^{-3})	Prequil time (days)	$[Eu]_{FIX}$ (mol dm^{-3})	k_3 (min^{-1})
40°C, pH=4.5				
10 (FA)	$1.14x10^{-7}$	8	$3.36x10^{-9}$	$1.2x10^{-4}$
60 (FA)	$1.14x10^{-7}$	12	$1.65x10^{-8}$	$5.8x10^{-5}$
10 (HA)	$1.14x10^{-7}$	8	$1.45x10^{-8}$	$1.1x10^{-4}$
10 (FA)	$1.14x10^{-7}$	2	$2.90x10^{-9}$	$7.2x10^{-5}$
10 (FA)	$1.14x10^{-7}$	12	$3.16x10^{-9}$	$8.2x10^{-5}$
10 (FA)	$1.14x10^{-7}$	41	$4.33x10^{-9}$	$7.8x10^{-5}$
40°C, pH=6.5				
10 (FA)	$1.14x10^{-7}$	3	$3.69x10^{-8}$	$2.9x10^{-5}$
10 (FA)	$1.14x10^{-7}$	8	$3.95x10^{-8}$	$2.7x10^{-5}$
10 (FA)	$1.14x10^{-7}$	64	$3.63x10^{-8}$	$3.1x10^{-5}$
10 (FA) UF	$1.14x10^{-7}$	64	$3.64x10^{-8}$	$3.0x10^{-5}$

3.2.1 Equilibration time

The amount of time the europium ($1.14x10^{-7}$ mol dm^{-3}) was in contact with fulvic acid (10mg dm^{-3}) prior to dissociation was varied. It can be seen in Table 4 that at pH=4.5 as the pre dissociation equilibration time increases the amount of europium remaining bound to the fulvic acid, $[Eu]_{FIX}$, increases. The rate of increase in $[Eu]_{FIX}$ was found to be similar for temperatures of 40°C and 60°C, $3.57x10^{-11}$ and $3.72x10^{-11}$ mol dm^{-3} Eu per day, respectively. This shows that equilibrium has not been reached after 60 days. However, no clear effect at the temperature 20°C was observed. At pH=6.5 and 40°C no effect of equilibration time prior to dissociation was observed on $[Eu]_{FIX}$. The rate of dissociation (k_3) was also unaffected by the pre equilibration time at both pH values studied.

Table 4 cont/d: The Eu concentration available for slow dissociation, $[Eu]_{FIX}$, and corresponding dissociation rate, k_3.

[HS] (mg dm^{-3})	$[Eu]_T$ (mol dm^{-3})	Prequil time (days)	$[Eu]_{FIX}$ (mol dm^{-3})	k_3 (min^{-1})
60°C, pH=4.5				
10 (FA)	$1.14x10^{-7}$	8	$1.70x10^{-9}$	$6.1x10^{-5}$
60 (FA)	$1.14x10^{-7}$	8	$8.01x10^{-9}$	$4.8x10^{-5}$
10 (HA)	$1.14x10^{-7}$	8	$1.12x10^{-8}$	$6.1x10^{-5}$
10 (FA)	$1.14x10^{-7}$	15	$2.18x10^{-9}$	$4.1x10^{-5}$
10 (FA)	$1.14x10^{-7}$	61	$3.76x10^{-9}$	$5.3x10^{-5}$
10 (FA)	$6.84x10^{-7}$	7	$8.02x10^{-9}$	$5.9x10^{-5}$
10 (FA)	$1.28x10^{-6}$	7	$1.74x10^{-8}$	$4.0x10^{-5}$
60 (FA)	$6.84x10^{-7}$	8	$4.53x10^{-8}$	$5.7x10^{-5}$
60 (FA)	$1.28x10^{-6}$	8	$8.23x10^{-8}$	$4.0x10^{-5}$
10 (HA)	$1.28x10^{-6}$	7	$7.09x10^{-8}$	$4.9x10^{-5}$
60°C, pH=6.5				
10 (FA)	$1.14x10^{-7}$	7	$2.57x10^{-8}$	$9.5x10^{-5}$
10 (FA)	$1.28x10^{-6}$	7	$1.96x10^{-7}$	$9.8x10^{-5}$
60 (FA)	$1.14x10^{-7}$	9	$7.72x10^{-8}$	$6.8x10^{-5}$
60 (FA)	$6.84x10^{-7}$	8	$3.39x10^{-7}$	$7.1x10^{-5}$
10 (HA)	$1.14x10^{-7}$	8	$7.35x10^{-8}$	$8.2x10^{-5}$

3.2.2 Filtering

In order to assess whether microbes have a significant effect on the dissociation kinetics an experiment was performed where the fulvic acid was not passed through 0.45μm membrane filter. It can be seen in Table 4 that at 40°C and an pre equilibration time of 64 days that no effect was observed. If any microbes were present they are not having an effect.

3.2.3 pH

The effect of pH was investigated for Eu ($1.14x10^{-7}$ mol dm^{-3}) equilibrated with 10mg dm^{-3} FA, 60mg dm^{-3} FA and 10mg dm^{-3} HA (Aldrich). The amount of europium available for dissociation by the very slow pathway $[Eu]_{FIX}$ was found to increase with increasing pH. At 20°C this was found to be similar for 10mg dm^{-3} FA, 60mg dm^{-3} FA and 10mg dm^{-3} HA which increased by a factor of 7.0, 5.2 and 6.7, respectively. This could be expected due to the increase in pH increasing the humic substance acid functional groups degree of deprotonation. This results in an increase in the charge density which expands the macromolecule via electrostatic repulsion. Changes in the rate constant showed no consistent trends and more data is required.

The effect of temperature on $[Eu]_{FIX}$ for 10mg dm^{-3} HA had no effect at pH=4.5 and 6.5. However, for 10mg dm^{-3} and 60mg dm^{-3} FA increasing temperature decreased $[Eu]_{FIX}$ at both pH=4.5 and 6.5, slightly less at the higher pH. This had the effect that at 60°C the increase $[Eu]_{FIX}$ was not found to be similar for 10mg dm^{-3} FA, 60mg dm^{-3} FA and 10mg dm^{-3} HA which increased by a factor of 15.1, 9.6 and 6.6, respectively.

3.2.4 Fulvic acid concentration

The effect of fulvic acid concentration was investigated for Eu ($1.14x10^{-7}$ mol dm^{-3}) equilibrated with 10mg dm^{-3} and 60mg dm^{-3} FA over a range of temperatures. At pH=4.5 the effect of increasing the FA concentration by a factor of six increased $[Eu]_{FIX}$ by a factor of 3.8, 4.9, and 4.7 at temperatures of 20°C, 40°C and 60°C, respectively. At pH=6.5 the effect of increasing the concentration of FA was a slightly lower, 2.8 and 3.0 at temperatures of 20°C and 60°C, respectively. The observed increase in $[Eu]_{FIX}$ is consistent with the increased number of sites available for binding with increasing fulvic acid concentration. The effect of increasing the fulvic acid concentration was to decrease the rate of dissociation at both pH values.

3.2.5 Humic acid

The effect of composition in the humic substance was investigated for Eu ($1.14x10^{-7}$ mol dm^{-3}) equilibrated with 10mg dm^{-3} FA and HA over a range of temperatures. At pH=4.5 the effect of increasing molecular weight increased of $[Eu]_{FIX}$ by a factor 2.38, 4.32 and 6.59 at temperatures of 20°C, 40°C and 60°C respectively. At pH=6.5 an increase of a factor of 2.3 and 2.9 was observed at temperatures of 20°C and 60°C, respectively. The observed increase in $[Eu]_{FIX}$ is consistent with the increased number of possible hindered sites available for binding with increasing molecular weight. No effect on rate of dissociation at either pH.

3.2.6 Metal Loading

The effect of increased metal loading was investigated at 60°C over the Eu concentration range $1.14x10^{-7}$, $6.84x10^{-7}$ and $1.28x10^{-6}$ mol dm^{-3}. The proton exchange capacity (PEC) can be used to calculate the concentration of COOH groups, hence, the operational concentration of humic substance. The PEC for Aldrich humic acid and Derwent fulvic acid have been determined to be 5.43meq/g[6] and 5.00meq/g[7], respectively. The metal loading was determined by the ratio of total concentration of Eu added ($[Eu]_{TOTAL}$) to the concentration of [HS] determined from the PEC. The effect increasing the Eu concentration on the ratio of $[Eu]_{FIX}/[Eu]_{TOTAL}$ can be seen in Table 5.

Table 5: The effect of metal loading on $[Eu]_{FIX}$ and k_3.

[HS] (mg dm^{-3})	[HS] (eq dm^{-3})	Metal loading range [Eu]/[HS] %	C/Co
pH=4.5			
10 (FA)	$5.00x10^{-5}$	0.23-2.56	0.013 ± 0.002
60 (FA)	$3.00x10^{-4}$	0.04-0.43	0.067 ± 0.003
10 (HA)	$5.43x10^{-5}$	0.21-2.36	0.077 ± 0.030
pH=6.5			
10 (FA)	$5.00x10^{-5}$	0.23-2.56	0.19 ± 0.05
60 (FA)	$3.00x10^{-4}$	0.04-0.43	0.59 ± 0.13

At pH=4.5 the ratio of $[Eu]_{FIX}/[Eu]_{TOTAL}$ is constant for both 10mg dm^{-3} and 60mg dm^{-3} FA over the metal loading range studied. This suggests that the sites on the fulvic acid available for long retention of Eu are not yet saturated. However, an increase in the Eu concentration decreased the ratio $[Eu]_{FIX}/[Eu]_{TOTAL}$ for 10mg dm^{-3} HA (pH=4.5) and 10mg dm^{-3} and 60mg dm^{-3} FA (pH=6.5) by a factor of 0.56, 0.68 and 0.73, respectively. No significant effect on the rate of dissociation was observed by increasing the concentration of Eu. More experimental data are required in order to investigate the effect of metal loading under these conditions.**4.0**

Conclusion

The EuHS complexation reaction overall was found to be endothermic. The values indicate spontaneous changes (ΔG negative) with a large favourable entropy change (ΔS positive). In contrast the complexation reaction for UO_2HS was found to be exothermic overall with a less favourable entropy than that derived for EuHS. The values of ΔG and ΔS derived are very similar for HA and FA for both metals studied. There is good agreement between the values reported here and with those in the literature. However, research has all been performed in the pH range 4 to 5. Experiments with Eu at pH=6.5 are therefore underway, in order to investigate the effect of pH on the thermodynamics of complexation.

An ion exchange technique has been developed to study the effect of changing environmental parameters on the dissociation kinetics of EuHS. The results have shown that the dissociation occurred by three first order pathways. The slowest pathway, which is the most important step when considering radionuclide transport, has a half-life of the order 200 hours. The concentration of europium remaining to undergo this slow dissociation step is increased with increasing pH, pre equilibration time prior to dissociation, fulvic acid concentration and humification (i.e. HA>FA). The factors effecting the rate of dissociation require further investigation. Experiments are underway in order to provide a full data set for detailed analysis and comparison with the literature. Additional experiments into the effect of MES buffer and competing cations on the dissociation kinetics of EuHS are also planned.

It does appear, however, that Eu transport by humic substances may occur with Eu in the kinetically controlled fraction. If this occurs the Eu transport will be governed by the humic substance transport. In which case the kinetics of humic substance sorption and desorption with solid surfaces is very important. Experiments have been designed to investigate the rate of exchange of labelled humic material between aqueous solution and minerals surfaces.

5.0 Acknowledgement

The European Community is thanked for funding this work.

6.0 References

[1] J. Schubert. The use of ion exchangers for the determination of physical-chemical properties of substances, particularly radio tracers in solution. Theoretical. J. Phys. Colloid Chem. 52, 340-350, (1948).

[2] J. Buffle. Complexation Reactions in Aqueous Systems. Ellis Horwood, Chichester, U.K. (1988).

[3] J.I. Kim and K.R. Czerwinski. Complexation of Metal Ions with Humic Acid: Metal Ion Charge Neutralisation Model. Radiochimica Acta, 73, 5-10, (1996).

[4] M.S. Ardakani and F.J Stevenson. A Modified Ion Exchange Technique for the Determination of Stability Constants of Metal Soil Organic Matter Complexes. Soil Sci. Soc. Amer. Proc. 36, 884-890, (1972).

[5] S.J. King and P. Warwick. Studies of Metal Complexation with Humic and Fulvic Acid. In Effects of Humic Substances on the Migration of Radionuclides: Complexation and Transport of the Actinides. pp 217-244 Ed. G. Buckau. Wissenschaftliche Berichte (FZKA 6124, ISSN 0947-8620), Forschungszentrum Karlsruhe Technik and Umwelt, Karlsruhe, Germany (1998).

[6] J.I. Kim, G. Buckau, E. Bryant and R. Klenze. Complexation of Americium(III) with Humic Acid. Radiochimica Acta, 48, 135-143, (1989).

[7] J.J. Higgo *et al*.. Extraction, Purification and Characterization of Fulvic Acid. In Effects of Humic Substances on the Migration of Radionuclides: Complexation and Transport of the Actinides. pp 103-128 Ed. G. Buckau. Wissenschaftliche Berichte (FZKA 6124, ISSN 0947-8620), Forschungszentrum Karlsruhe Technik and Umwelt, Karlsruhe, Germany (1998).

[8] K.L. Nash and G.R. Choppin. Interaction of Humic and Fulvic Acids with Th(IV). J. Inorg. Nucl. Chem., 42, 1045-1050, (1980).

[9] M. Samadfam, Y. Niitsu, S. Sato and H. Ohashi. Complexation Thermodynamics of Sr(II) and Humic Acid. Radiochimica Acta, 73, 211-216, (1996).

[10] P. Warwick, A. Hall, S.J. King, J.Zhu and J. Van der Lee. Thermodynamic aspects of nickel humic acid interactions. Radiochimica Acta, 81, 215-222, (1998).

[11] P.M. Shanbhag and G.R. Choppin. Binding of Uranyl by Humic Acids. J. Inorg. Nucl. Chem., 43, 3369-3372, (1981).

[12] J.C. Rocha, I.A.S. Toscano and P. Burba. Lability of heavy metal species in aquatic humic substances characterised by ion exchange with cellulose phosphate. Talanta, 44, 69-74, (1997).

[13] C.L. Chakrabarti, Y. Lu, D.C. Gregoire, D.C. Back and W.H. Schroeder. Kinetic studies of metal speciation using Chelex cation exchange resin: Application to cadmium, copper and lead speciation in river water and snow. Environ. Sci. Technol., 28, 1957-1967, (1994).

[14] W.P. Cacheris and G.R. Choppin. Dissociation kinetics of Thorium-Humate complex. Radiochimica Acta, 42, 185-190, (1998).

[15] G.R. Choppin. and S.B.Clark. The kinetic interactions of metal ions with humic acids. Marine Chemistry, 36, 27-38, (1991).

[16] A.W. Rate, R.G. McLaren and R.S. Swift. Response of copper(II)-humic acid dissociation Kinetics to factors influencing complex stability and macromolecular conformation. Environ. Sci. Technol., 27, 1408-1414, (1993).

[17] H.K.J. Powell and R.M. Town. Interaction of humic substances with hydrophobic metal complexes: a study by stripping voltammetry and spectrophotometry. Analytica Chimica Acta, 248, 95-102, (1991).

[18] H.M.V.M. Soares and M.T.S.D. Vasconcelos. Study of the lability of copper(II)-fulvic acid complexes by ion selective electrodes and potentiometric stripping analysis. Analytica Chimica Acta, 293, 261-270, (1994).

[19] N.D. Bryan, D. Jones, D. Griffin, L. Regan, S.J. King, P. Warwick, L. Carlsen and P. Bo. Combined Mechanistic and Transport Modelling of Metal Humate Complexes. Effects of Humic Substances on the Migration of Radionuclides: Complexation and Transport of the Actinides. pp (this volume) Ed. G. Buckau. Wissenschaftliche Berichte (FZKA, ISSN), Forschungszentrum Karlsruhe Technik and Umwelt, Karlsruhe, Germany (1999).

Annex 13

Combined Mechanistic and Transport Modeling of Metal Humate Complexes

(Bryan et al, RMC-E, LBORO and NERI)

2nd Technical Progress Report

EC Project:

"Effects of Humic Substances on the Migration of Radionuclides:
Complexation and Transport of the Actinides"

RMC-Environmental Contribution to Task 4, (Model Development and Testing)

Combined Mechanistic and Transport Modelling of Metal Humate Complexes.

Reporting period 1998

Bryan N.D.[1,2], Jones D.[2], Griffin D.[1], Regan L.[1], King S.[3], Warwick P.[3], Carlsen L.[4] and Bo P.[5]

[1]RMC Ltd, Suite 7, Hitching Court, Abingdon Business Park, Abingdon, Oxfordshire, OX14 1RA

[2]Department of Chemistry, University of Manchester, Oxford Rd., Manchester, M13 9PL

[3]Department of Chemistry, Loughborough University, Loughborough, Leicestershire, LE11 3TU, UK

[4]National Environmental Research Institute, Department of Environmental Chemistry, DK-4000, Roskilde, Denmark

[5]P.Bo Programming, Haraldsborgvej 54, DK-4000, Roskilde, Denmark

INTRODUCTION

Natural organic matter plays a crucial role in the environmental behaviour of metals (Livens 1991). The presence of dissolved humic substances will affect the solubility of metallic elements, and hence affect their migration through the environment (Jones and Bryan 1998). Many of the radioactive isotopes found in radioactive waste are metallic, including the radiologically significant actinide elements. Hence, the presence of humic substances around proposed repository sites may have a significant effect upon the risk of exposure, both of the environment, and also of the general public. For this reason, there is a great deal of interest in understanding, and being able to model, the interaction of metals, in particular the actinides, with natural organic matter.

The aim of this on-going work is to develop models which are capable of describing the interaction of metallic elements with humic substances, and also predict the effect upon the transport of radionuclides. The final goal is to produce a model, which may be used in radiological performance assessment studies of proposed repositories. To this end, the work described here may be divided into two distinct parts. The first, mechanistic modelling, concerns the investigation of metal-humate interactions at the microscopic level, such as enthalpies and entropies of reaction, overall binding strength and dissociation rate constants. The second area concerns transport modelling. Here, the aim is to simulate the macroscopic behaviour of radionuclide/humate complexes. Models have been developed which are able to predict the migration behaviour of radionuclides in laboratory column experiments. They have been tested against a large set of experimental data from both pulsed and up/downflooding column experiments.

MECHANISTIC MODELLING

Thermodynamic Modelling

There are many models in the literature which are designed to simulate the behaviour of humic substances (Jones and Bryan 1998). However, although many are based on assumptions and parameters which have some theoretical connection with reality, they are all largely empirical. Certainly, all of them are based on binding constants of one form or another, which

are altered, along with other parameters, in order to obtain the best possible fit between experiment and model. None of them address questions such as, why does a given metal bind to a humic substance with a given strength, whilst another binds with a different one ? Similarly, most current models contain some method for accounting for the change in binding with ionic strength, I, but the methods are very empirical. Therefore, the thermodynamic modelling undertaken here is not designed to produce a model which will have the best possible fit to the observed data. Rather, it is an attempt to explain the observed behaviour in terms of the underlying mechanisms. In this way, it is hoped that it will increase the understanding of these processes, assist in extending modelling studies to systems which are not yet fully understood and build confidence in the reliability of environmental predictive modelling.

The thermodynamic modelling has two parts: the first is the modelling of the electrostatic effects, and the second concerns the chemical nature of the binding mechanism.

Electrostatics

There are several methods for including electrostatic effects in humic modelling. Some models use entirely empirical parameters in order to obtain a best fit (Tipping and Hurley 1992), whilst others use Debye-Huckel, Gouy-Chapman or Donnan models (Falck 1991; Kinniburgh et al 1996). The last three models types are all approximations to Poisson-Boltzmann theory, based upon different simplifying assumptions regarding the nature of humics and their complexes. These more simple models are used, because the Poisson-Boltzmann equation has no analytical solution, and must be solved numerically for each set of conditions; a computationally costly process. However, regardless of the problems in it's application, full Poisson-Boltzmann theory was selected as the model for this work.

There are two basic conceptual models of humics: firstly, the impermeable model, which treats the humic as a hard rigid sphere, and secondly, the penetrable model in which small ions and solvent molecules are able to penetrate into the humic structure. Initially, investigations were conducted with the two models, but it soon became clear that the penetrable model was

the most realistic and flexible description of the system. The penetrable conceptual model is shown in figure 1.

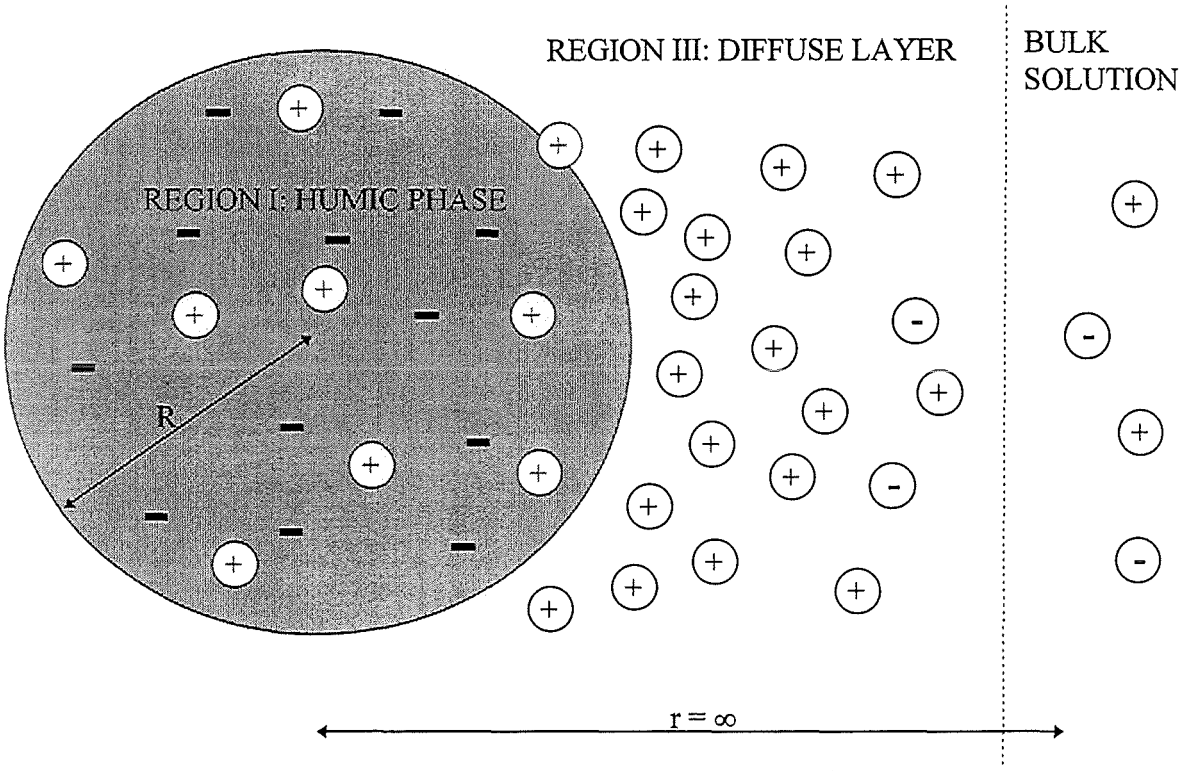

Figure 1: Conceptual model of penetrable humic substances

The model developed considers all of the various thermodynamic contributions associated with the neutralisation of the charge on the humic acid. There are three major components:

(1) The electrical free energy of the humic molecule, arising from the fact that the humic, which will have a large negative charge, finds itself in a region of negative potential, and which will be **positive**;

(2) The electrical free energy of the counterions which will be negative for the cations and positive for the anions. But, since the total cation concentration in the double layer is greater than that of the anion, overall this will be **negative**;

(3) The statistical free energy of the small ions in the double layer, which will be positive for the cations and negative for the anions, and once again, since cations dominate the double layer, the overall contribution is **positive**.

When the double layer relaxes, all of these terms will tend to zero, and hence, the respective contributions to the total free energy change will be:

(1) Exothermic enthalpy change;
(2) Endothermic enthalpy change;
(3) Positive entropy change.

The first stage in calculating these terms is to calculate the shape of the field generated by the humic particle before and after charge neutralisation. The potential at a point, r, from the centre of the humic particle, ψ_r, will be given by,

$$\nabla^2 \psi_r = -\frac{1}{\varepsilon}\left[\rho_{HUMIC}(r) + \beta N_A e\left(\sum_{i=1}^{N_{ions}} z_i [X_i^{z_i}]_{BULK} \exp^{-\left(\frac{\psi_r z_i e}{kT}\right)}\right)\right]$$

where: e is the electronic charge; k is the Boltzmann constant; T is the absolute temperature; ε is the permittivity; β_r is the fraction of space available for the solvent and small ions at r, which will be a constant (< 1) within the humic particle and equal to one outside; $\rho_{HUMIC}(r)$ is the humic particle charge density, a constant within the humic particle, and zero elsewhere, N_{ions} is the number of small ion types, X_i; z_i is the charge number of ion i; $[X_i^{zi+}]_{BULK}$ is the bulk concentration of ion i. The boundary conditions used to solve this equation are given by (Bartschat et al 1992),

$$\left(\frac{\partial \psi}{\partial r}\right)\Bigg|_{r=0} = 0 \qquad \text{and} \qquad \psi_r \rightarrow 0 \;\; as \;\; r \rightarrow \infty$$

Once the potential versus r curve has been calculated, the free energy contributions may be calculated. The electrical free energy of the humic particle, $G_{el,HUMIC}$, will be given by,

$$G_{el,HUMIC} = \int_{r=0}^{R} \rho_{HUMIC}(r)\,\psi_r\, 4\pi r^2\, dr$$

where R is the radius of the humic. The electrical free energy of the small ions, $G_{el,DL}$, will be given by,

$$G_{el,D.L.} = \int_{r=0}^{\infty} \left(\sum_{i=1}^{N_{IONS}} z_i e[X_i^{z_i+}]_{BULK} \exp^{-\left(\frac{\psi_r z_i e}{kT}\right)} \right) \beta_r N_A \psi_r 4\pi r^2 dr$$

where N_A is Avogadro's number, and the entropic contribution, S_{DL}, via,

$$S_{DL} = \frac{4\pi e \beta_r}{T} \int_{0}^{\infty} \left(\sum_{i=1}^{N_{IONS}} z_i [X_i^{z_i+}]_r \right) \psi_r r^2 dr$$

By calculating the magnitude of the three components, before and after the addition of a metal ion, the electrostatic contribution to metal binding may be obtained.

Chemical Contributions

The electrostatics cannot be the only contribution to binding, since it depends only upon the magnitude of the charge on the binding cation, and there is evidence that the chemistry of the metal ion plays a significant part (Jones and Bryan 1998). The chemical contribution will have two components; enthalpic and entropic. The first will derive mostly from bond breaking and formation, whilst the latter will come from the dehydration of the metal ion. It has been shown (King et al this volume) that metal humate complexation reactions have small but positive, endothermic, enthalpies, and very large entropy changes.

Enthalpies

Estimates of the chemical contribution to the enthalpy of reaction were obtained by using the enthalpies of reaction of simple carboxylates with metals: this is because there is a great deal of evidence that, in most cases, these are the co-ordinating groups (Jones and Bryan 1998). It was found that the predicted enthalpies were endothermic, as expected, but when these contributions were compared with those from the double layer, it was found that variations in the double layer contribution, arising from uncertainties in molecular weight distribution and molecular volume, greatly outweighed the chemical contribution. The final conclusion was that the overall reaction enthalpies could be expected to be small and endothermic, but that it would not be possible to predict their magnitude precisely. However, since they are only a very minor contribution to the overall free energy change, this is not a severe problem.

Entropies

The chemical contribution to the overall reaction entropy derives mostly from the dehydration of the metal ion. However, there are a number of measures of this quantity available. Three were studied as part of this work: ΔS^{o}_{solv}, the entropy change upon taking a naked ion from the gas phase to aqueous solution; $\overline{S}^{0}_{CONV}$, the conventional molar entropy, relative to a value for the proton of 0; $\overline{S}^{0}_{ABS}$, the absolute molar entropy, which has $\overline{S}^{0}_{ABS}(H^{+})$=-22.2 J K^{-1} mol^{-1}. In theory, ΔS^{o}_{solv} should be the best measure to use, however, it was found that, because of the large errors incurred during it's calculation, the partial molar entropies provided the most reliable measure of the contribution of dehydration.

Comparison with experiment

The combined mechanistic model, electrostatics plus chemistry, was tested against experimental data. The first exercise was to test whether the model was capable of predicting metal binding strengths. It is very difficult to quantify the binding strength of a metal with humic substances, since there are many assumptions involved in any such parameter. However, the K_{MHA} parameter of Tipping's Model V was selected, since this model has been widely applied, and K_{MHA} values are available for a wide range of metals. Figure 2 shows the correlation between the model predicted entropy change, $-(\overline{S}^{0}_{ABS}) + \Delta S_{DL}$, and the log of K_{MHA}.

The correlation coefficient for these data is 0.94, which is a very encouraging result given that the model does not contain any fitting parameters.

The model was also compared with some experimentally observed entropies, although only a very few such data are available. The result is shown in figure 3.

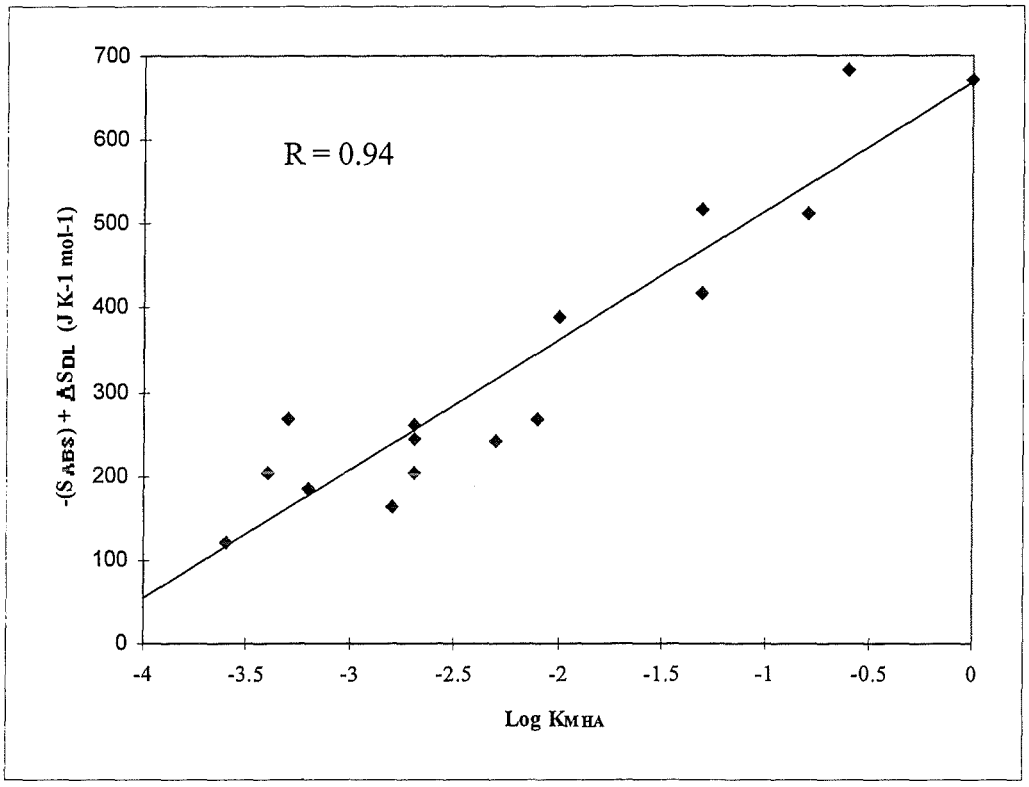

Figure 2: Correlation between mechanistic model and the Model V K_{MHA} parameter.

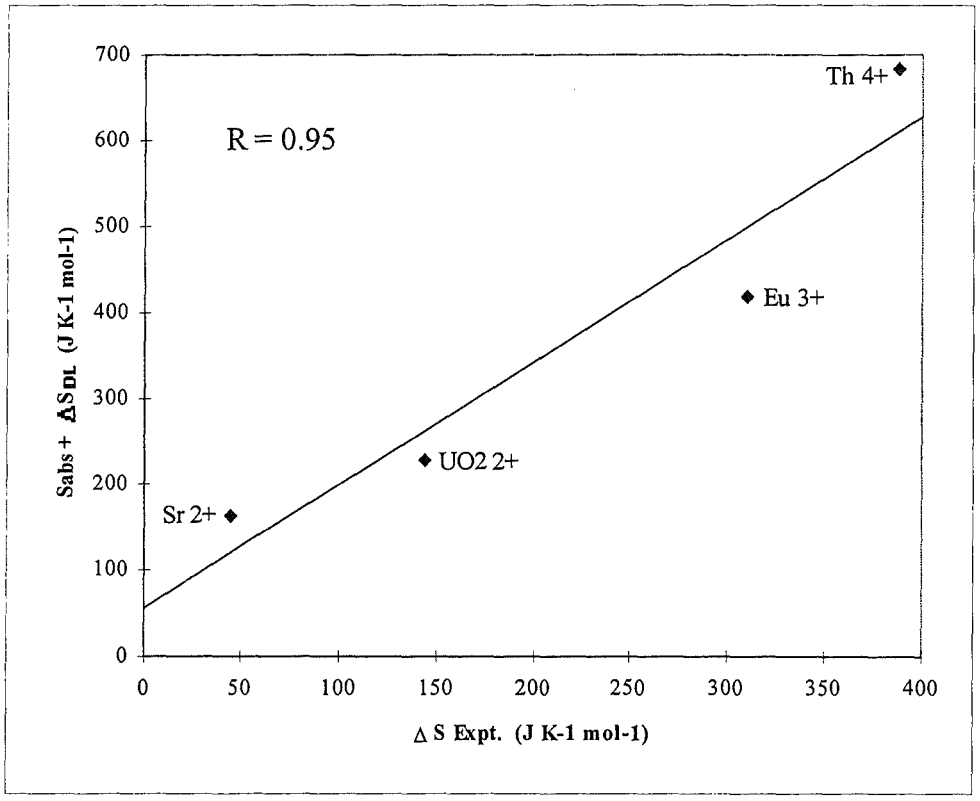

Figure 3: Correlation between mechanistic model and experimental entropies of reaction.

Once again there appears to be a good correlation, although there too few data to make any conclusions regarding the shape of the curve.

In a specific test of the electrostatic model, an attempt was made to predict the change in binding strength with ionic strength. This is of interest more generally, since many of the existing predictive models do not perform well at higher ionic strengths (Bryan 1998). Several data sets were examined: as an example, the results for some Cu^{2+} data are shown in figure 4. The experimental data and model predictions are shown as the ratio of the binding constant at an ionic strength, I, relative to that observed at I=8.

The tests outlined above, and those not reported here, indicate that the model is a realistic description of the microscopic processes which accompany metal-humate binding.

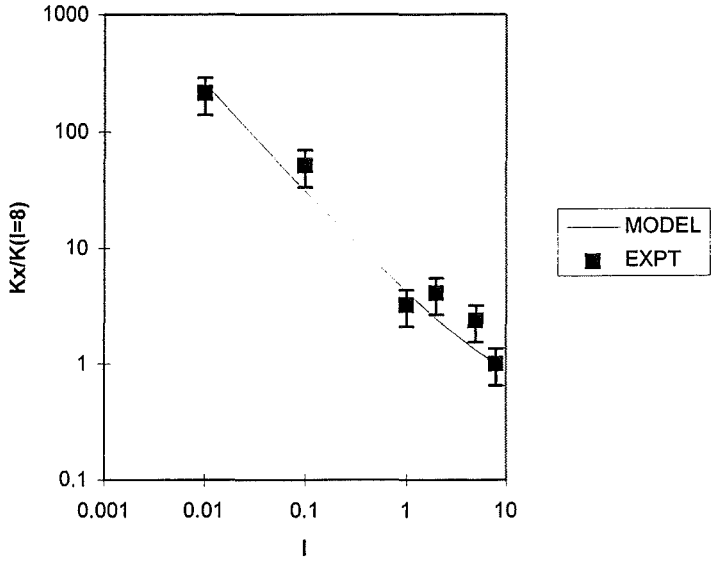

Figure 4: Comparison of experimentally observed and model predicted ionic strength dependency.

Kinetic Modelling

Observations

The University of Loughborough has conducted an extensive series of batch resin competition kinetic experiments which are described in King et al in this volume. Slow desorption

kinetics are crucial in controlling the migration of metal-humate complexes. Therefore, these data have been used in a kinetic modelling study, which is an attempt to elucidate the slow desorption kinetics observed.

It was found that the desorption of Eu from the humic and fulvic acids could be modelled by an equilibrium component and a series of first order rate equations, i.e., the amount of Eu remaining bound to the humic at time t, $Eu_B(t)$, is given by,

$$Eu_B(t) = Eu_{EQM} + \sum_{i=1}^{N_{Comp}} Eu_{FIX,i}\, e^{-k_i t}$$

where: Eu_{EQM} is the equilibrium component, which remains constant with time and depends upon the mass of resin used in the desorption experiment; N_{comp} is the number of first order components; $Eu_{FIX,i}$ is the amount of component i at t=0; and, k_i is the dissociation first order rate constant for component i. Figure 5 shows data and model fit from a series of dissociation experiments at pH 4.5 and 20°C (plotted as bound Eu concentration over the initial concentration versus time), where different masses of resin have been used. The model curves were calculated using three first order components, and an equilibrium component which was calculated using a single equilibrium constant. Note, the values of $Eu_{FIX,i}$ and k_i for the three components used to calculate the model curves were the same across the resin mass range. Given the complexity of the system, the fit obtained with such a simple model is very encouraging.

From the graph, it is clear that the experiments using different resin weights appear to be approaching different end points. This is due to the different contributions of the equilibrium component, which becomes progressively smaller as the mass of resin increases. It can be seen that after the mass of resin passes 1.5g, the result is independent of the resin mass. This is because, Eu_{EQM} is effectively zero for higher resin masses, and $Eu_{FIX,i}$ and k_i are independent of the mass used.

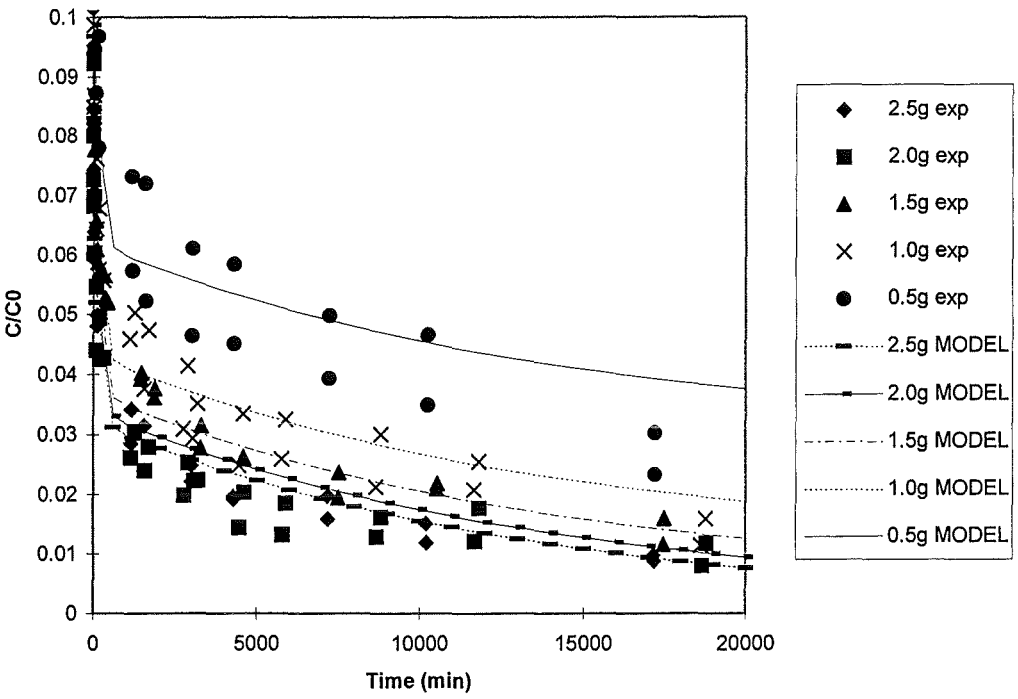

Figure 5: Eu/FA desorption experimental data and model curves for different competing resin weights (pH 4.5. T=20°C).

The values of k_i used to model these data were: k_1=0.22 min^{-1}; k_2=0.0072 min^{-1}; k_3=7.2x10^{-5} min^{-1}. In the environment, the first two components will be sufficiently fast that they may be considered as exchangeable. It is the longer lived, most slowly dissociating component, which is the most interesting fraction for this work. Therefore, data from a series of dissociation experiments under a variety of different conditions were examined, in order to determine the effect upon the amount of the slowest dissociating component present at the start of desorption, $Eu_{FIX,3}$ and the dissociation constant, k_3. The results are listed in table 4 of King et al in this volume. The most surprising result is that, for the majority of the experiments performed, a single first order component was able adequately to account for the observed Eu dissociation in the range 1,000 - 20,000 minutes. An example of typical behaviour, plotted as the natural log of bound Eu concentration over initial concentration versus time, along with the model line is shown in Figure 6.

When examining the data, the first significant result is that for both fulvic and humic acid, and all conditions, $Eu_{FIX,3}$ increases as the pre-equilibration time increases, and reaches a constant value after a number of days. This result is expected, since, as the pre-equilibration time increases, the bound Eu will have more time to access the kinetically controlled fraction. Another important observation is the difference in behaviour at the two different pH values; 4.5 and 6.5. At pH 4.5, for fulvic and humic acids, both $Eu_{FIX,3}$ and k_3 are both insensitive to changes in temperature. By contrast, at pH 6.5, although there is still very little effect upon $Eu_{FIX,3}$, k_3 now does have a significant dependence upon temperature.

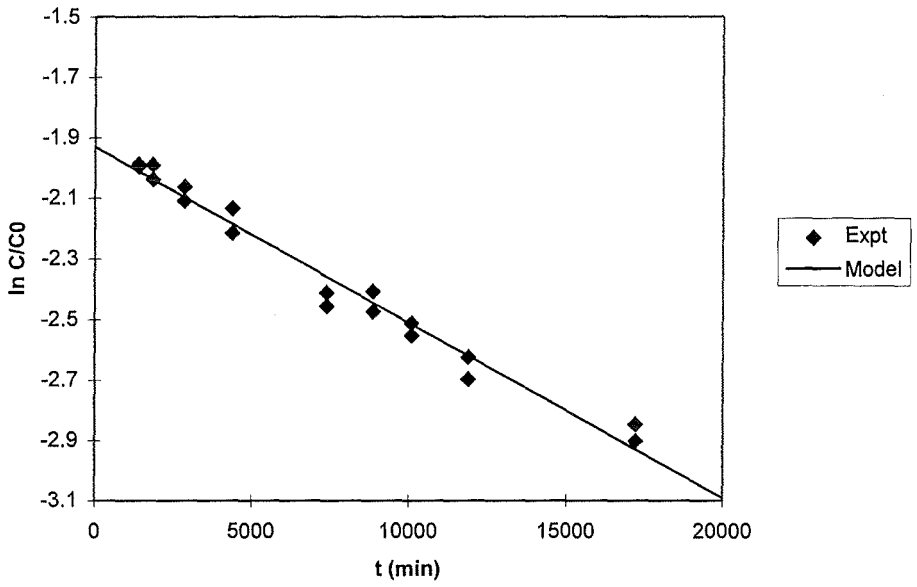

Figure 6: Long term desorption of Eu from humate complexes, experiment and model fit.

At T=20°C, k_3 at pH 6.5 is less than that observed at pH 4.5, but at T=60°C, there is very little difference in k_3 between pH 6.5 and 4.5. Changing the ratio of Eu to humic substance does not have a significant effect upon the observed value of k_3. But, by increasing the amount of Eu present in the solution during pre-equilibration, whilst keeping the humic substance concentration constant, the observed value of $Eu_{FIX,3}$ increases significantly. Although, it is important to note that the amount of Eu in the kinetically hindered fraction at equilibrium always represents a minority component of the total Eu in the system.

Interpretation

Activation Energies and Entropies

Considering first the effect of temperature upon the rate constants, it is possible to calculate the magnitude of the activation energy from the dependence of the k upon T using the Arrhenius equation:

$$k = Ae^{\frac{-E_a}{RT}}$$

where k is the rate constant, E_a is the activation energy, and A is the pre-exponential factor. Hence, a plot of ln k versus 1/T will result in a straight line of slope $-E_a/R$ and intercept ln A. In the case of the pH 6.5 data, there is a significant temperature dependence and it is possible to calculate an activation energy: the data for 10ppm fulvic acid, pH 6.5 and $[Eu]_T=1.14\times10^{-7}$ M are plotted in figure 7.

The slope of the line in figure 7 is -4640 K^{-1}, which gives an activation energy of 38.6 kJ mol^{-1}, and the intercept is 0.46 (=ln A). Hence, A has a value of 1.6, although due to the fairly narrow range of temperature over which data were taken, this value carries a large uncertainty.

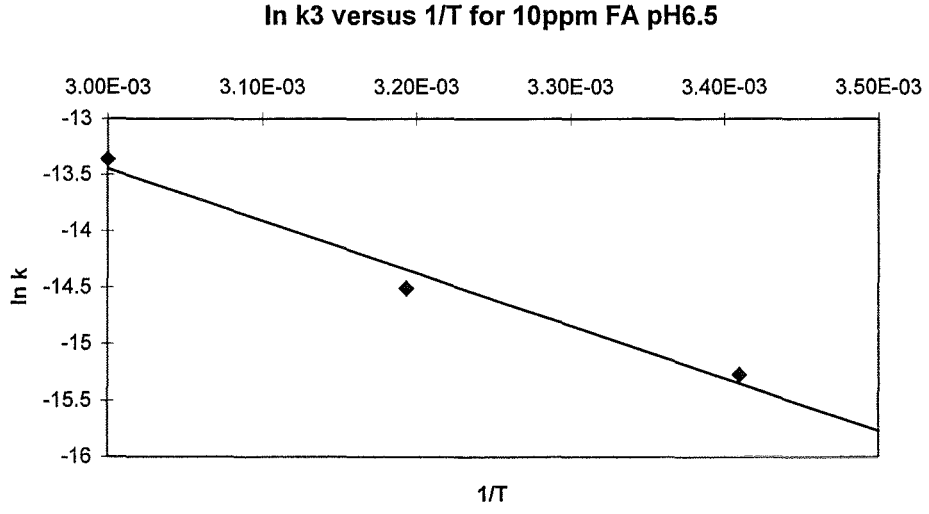

Figure 7: Arrhenius plot

For a first order reaction, the activation entropy, $\Delta S^{\ddagger}$, is related to A via the equation,

$$A = e\frac{RT}{N_A h}e^{\frac{\Delta S^{\ddagger}}{R}}$$

Hence, this leads to an activation entropy of -250 J K^{-1} mol^{-1}.

In the case of the pH 4.5 data, there is no systematic temperature dependence, and so the enthalpic contribution to the activation barrier must be negligible. Hence, the barrier must be entirely entropic in origin. A plot of ln k versus 1/T is a horizontal straight line for any reaction with a zero enthalpic contribution to the activation barrier. Therefore, A, which is given by the intercept of the Arrhenius plot, will have the same magnitude as the rate constants themselves. The value of A obtained in this way varies slightly according to the data set chosen, however, $1.2x10^{-6}$ s^{-1} is a typical value, which corresponds to an activation entropy of ~ -370 J K^{-1} mol^{-1}. At pH 4.5, this is the only contribution to the activation barrier. Therefore, the corresponding height of the activation barrier will be given by $T\Delta S^{\ddagger}$, or, 108 kJ mol^{-1} at 20°C.

There are probably several reasons for this difference in behaviour, which are matched by differences in $Eu_{FIX,3}$; greater at pH 6.5 than at pH 4.5. Lower pHs are known to suppress overall metal binding to humics, and this would appear to be mirrored in the amount of metal able to access the kinetically controlled fraction. The precise reasons for the change in activation thermodynamics with pH are probably very complex. However, the physical state of the humic substance is likely to be very different at the two pH values: at pH 4.5, the humic would be expected to have a much reduced charge compared to pH 6.5. Adopting the penetrable gel model of humic substances discussed above, the humic would be expected to much more 'open' at higher pH. Another explanation for the difference is that at a pH of 4.5, there will be significant competition for carboxylate groups by protons. Therefore, any Eu-carboxylate bonds broken during the course of the transition from the kinetically controlled fraction to the exchangeable fraction, might well be immediately replaced by carboxylate-H^+ bonds. This would not be the case at pH 6.5.

Total Free Energy Changes

In addition to the size and nature of the activation barrier, these experiments have also provided a great deal of insight into the nature of the free energy difference between the exchangeable and kinetically controlled fractions. To gain information on the nature of this difference, we must look at the $Eu_{FIX,3}$ values. The first significant piece of information is that at both pH 4.5 and 6.5, the temperature does not seem to have any very significant effect upon the amount of Eu remaining in the kinetically controlled fraction. This would imply that there is no significant enthalpic contribution to the free energy difference, and that in common with the free energy change associated with initial, exchangeable binding, this free energy difference is entropic in nature. However, the most significant result is provided by the experiments conducted at different Eu:humic substance ratios. In the initial experiments conducted at a fulvic acid concentration of 10ppm and $[Eu]_T=1.14x10^{-7}M$ it was observed that the very slowly desorbing fraction accounted for a minority of the total Eu bound. This could have been due to two reasons. Firstly, it could have been because there is a significant reduction in free energy involved, but only a very limited amount of kinetically controlled sites, which become quickly filled up. The other explanation is that there are vacant sites where further metals could become trapped, but that the free energy change is not favourable. The fact that the amount of Eu trapped in the kinetically controlled fraction increases with the total amount of Eu in the system, while the humic substance concentration remains constant, shows that the latter explanation is correct, since by adding further Eu it is possible to push more metal into the kinetically controlled component. If the results are observed, then it is clear that the amount of metal which desorbs slowly is always a minor fraction of the total, and hence the free energy change in going from the exchangeable to the kinetically controlled is small but **positive**.

The data also allow the estimation of the magnitude of the free energy change. Assuming that the exchange between the equilibrium and kinetically controlled fractions is first order in both the forward and backward directions:

$$M_{Eq} \underset{k_b}{\overset{k_f}{\rightleftarrows}} M_{FIX}$$

then the equilibrium constant will be given by $[M_{FIX}]/[M_{Eq}]$. At pH 4.5, this leads to a value of ~ 0.07, and ~ 0.5 at pH 6.5. Hence, the associated free energy changes at 20°C are +6.6 kJ mol^{-1} at pH 4.5 and +1.7 kJ mol^{-1} at pH 6.5, which correspond to entropy changes of -20 and -6 J K^{-1} mol^{-1} respectively. Further, given the equilibrium constant, it is possible to calculate approximate values for the forward rate constants, which are $1x10^{-7}$ s^{-1} at pH 4.5 and $2.4x10^{-7}$ s^{-1} at pH 6.5.

Table 1 shows tabulated values for k_f and k_b for these Eu resin experiments and also analogous values for Am determined by FZK-INE (Schussler et al 1998), and Co determined during transport modelling (see below).

Table 1: sorption and desorption rate constant for several metals

	k_f (s^{-1})	k_b (s^{-1})
LBORO Eu^{3+} pH 4.5, 20°C	-	$1.2x10^{-6}$
LBORO Eu^{3+} pH 4.5, 40°C	$1x10^{-7}$	$1.4x10^{-6}$
LBORO Eu^{3+} pH 6.5, 40°C	$2.4x10^{-7}$	$5.0x10^{-7}$
BGS Co^{2+}	$2.9x10^{-7}$	$1.3x10^{-6}$
FZK Am^{3+}	$5.9x10^{-7}$	$1.1x10^{-6}$

The most significant feature about these rate constants is that they are remarkably similar, despite the fact that they are for very different metals, determined by different sorts of experiment and in different laboratories. This behaviour is in marked contrast to that observed for initial binding to the exchangeable sites. There, the observed binding strengths are very dependent upon the identity of the metal ion. Therefore, whatever the origin of this effect it would appear to be virtually independent of metal ion chemistry. Indeed, these results are indicative of some physical process.

TRANSPORT MODELLING

Previous Work

Virtually all transport models are based on the assumption that all chemical processes are fast compared to the rate of flow of the solution phase. In that case, all chemical processes may be described by simple equilibrium constants. This equilibrium assumption has many numerical advantages, not least of which is that such models are very economical with computer resources. However, previous column modelling work has shown that the transport behaviour of radionuclides in the presence of humic acid could not be modelled by a model based on the assumption of local equilibrium (Bryan 1998). It had also become clear that a particular fraction of the bound metal was very slow to desorb from the humic acid, which resulted in a much faster transport than would otherwise be expected. Hence, new transport models, k1D and COLUMN3, have been developed which are able to account for slow chemical processes.

k1D Transport Model

Although some of the important chemical processes controlling the behaviour of the radionuclides in the column experiments are clearly kinetically controlled, many more are very rapid, and can be assumed to be at equilibrium. It is possible to simulate fast processes using rate constants, however it is very inefficient in terms of computing time. For this reason, the k1D model has been written so that it is able to use equilibrium constants to simulate those processes which are at equilibrium and rate constants to describe those which are kinetically hindered. Therefore, the new transport model uses three different sets of equations to solve for the chemistry of the system.

(1) Mass balance equations: the total mass of an element at any given time and place will be sum of the free form, plus the mass included in any complexes. For example, considering a component C, the total concentration of that element, $[C]_T$, will be given by,

$$[C]_T = [C] + \sum_{i=1}^{N} x.[(C_x L_n)_i]$$

where, [C] represents the concentration of the free element, $[(C_xL_n)_i]$ the concentration of species i, and x is the stoichiometry of element C in that species.

(2) Equilibrium equations: Considering a generalised equilibrium reaction,

$$A + B \leftrightarrow C + D$$

the concentrations [A], [B], [C] and [D] obey an equilibrium law:

$$[C] = K\frac{[A].[B]}{[D]}$$

where, K is the equilibrium constant.

(3) Kinetic or Rate equations: Once again, considering a generalised kinetically controlled reaction

$$A + B \underset{\leftarrow}{\overset{\rightarrow}{}} C + D$$

The rates of change of the chemical concentrations will be controlled by kinetic reactions, e.g.

$$\frac{d[C]}{dt} = k_f[A].[B] - k_b[C].[D] \qquad or \qquad \frac{d[A]}{dt} = k_b[C].[D] - k_f[A].[B]$$

where k_f and k_b are forward and backward rate constants respectively.

During the initial pre-equilibration of the column and solutions, at zero time, only the mass balance and equilibrium equations are solved, by standard Newton-Raphson iteration. Elsewhere, the rate equations must also be solved. This is done separately to the equilibrium equations: preliminary studies used a method where the equilibrium and rate equations were solved simultaneously as a single set, however, this proved to be prone to numerical instability. In the final version of the model, at each time step, the equilibrium equations are solved first followed by the rate equations. In order to prevent the rate equations from significantly disturbing the balance of the equilibrium equations, the model may re-equilibrate the system using the equilibrium equations at any point during the time step. Although this method is less numerically elegant, it is significantly more robust, and has therefore been selected.

The transport of the chemical species is described by a simple 1-dimensional advection/dispersion model. The transport equation takes the form,

$$\omega\left(\frac{\partial X_i}{\partial t} - \frac{\partial S_i}{\partial t}\right) = \frac{\partial}{\partial x}\left(qX_i - D\frac{\partial X_i}{\partial x}\right)$$

where ω is the porosity (dimensionless), $q\,(m\ s^{-1})$ is the Darcy flux, $D\,(m^2\ s^{-1})$ is the dispersion coefficient, $X_i\,(mol\ m^{-3})$ is the concentration of the i^{th} species and $\partial S_i/\partial t\ (mol\ m^{-3}\ s^{-1})$ is the rate of change in concentration due to chemistry. For each time step, the model iterates between the chemical and transport calculations until convergence is achieved and the model proceeds to the next step.

Up/Downflooding Column Experiments

The k1D model was tested using a set of up/downflooding column experiments provided by the University of Loughborough. In these experiments, the packing material in the columns was first equilibrated with humic acid solution (10 mg l^{-1}) before the introduction of the radionuclide. The radionuclide (^{152}Eu) and stable Eu carrier were introduced at the top of the column in a solution of humic acid (10 mg l^{-1}). The concentration of Eu emerging from the bottom of the column was monitored throughout the experiments. When the outflow Eu concentration, c, had reached that of the feed solution, c_0, the Eu was removed from the feed solution, and the column eluted, or downflooded, with humic acid solution, also 10 mg l^{-1}. Silica colloids were also present in all of the solutions. However, previous experiments in the absence of humic acid had shown that the behaviour of the Eu was dominated by the humic acid. In fact, it was possible adequately to model the experiments, ignoring the presence of the inorganic colloidal material.

Because of the nature of these experiments, it is not possible to derive any information regarding the interaction of the humic acid with the mineral surface, since the system was in equilibrium with the humic acid throughout the migration of the Eu. Indeed, it was found that a relatively simple set of equations was able to account for the behaviour in the columns, and these are shown in figure 8.

The mechanistic modelling work had already shown the existence of several fractions of bound metal. In order to model the column experiments, it was found that 2 fractions of bound metal were required. The first, M_{eq}, represents the exchangably bound metal, i.e. that which may be readily removed from the humic acid. The formation of this fraction may be described by an equilibrium constant, K_{Eq}. The second, kinetically hindered fraction, M_{Fix}, is related to the exchangeable fraction via two rate constants, k_5 and k_6. From the experiments, it was possible to fix a value for k_5, however it was found that the results were relatively insensitive to k_6, provided that it was small. The reason for this would seem to be that this process effectively does not take place during the course of the column experiment. In the case of the interaction of the metal with the mineral surface, it was found that a single surface site was required in order to simulate the observed behaviour, but that it was necessary to describe the interaction using rate constants. Note: the sorption step is very fast, but the desorption step is significantly hindered. This result may seem surprising, since the interaction of metals with mineral surfaces are often modelled with equilibria. However, in this case, the mineral surface will have been significantly modified by the sorption of humic acid. Therefore, the exact physicochemical nature of the surface site and the surface bound metal, M_S, is unclear, and the slow desorption step may well reflect the influence of sorbed humic substances.

The results obtained for two different Eu concentrations, with the numerical system shown in figure 8, are shown in figures 9 and 10.

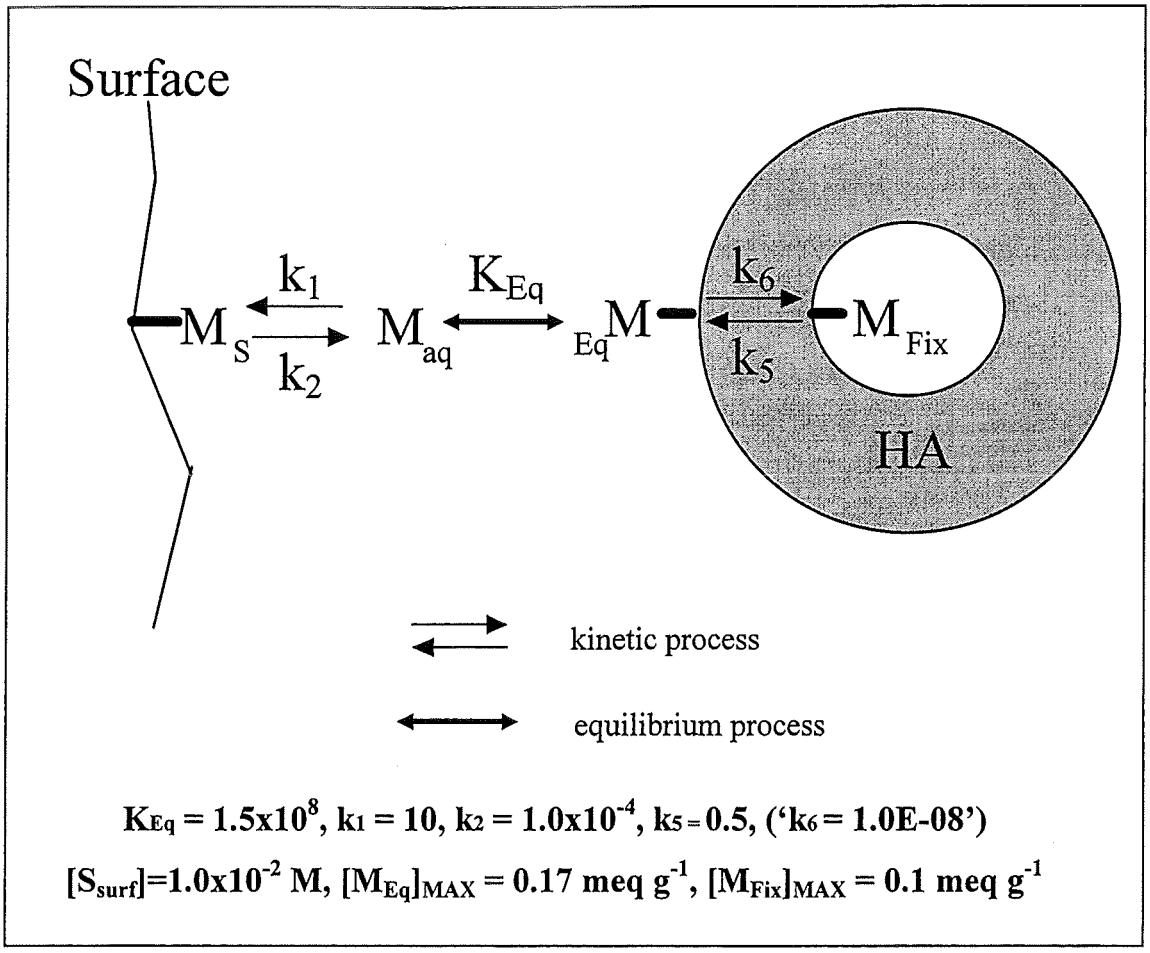

Figure 8: System of equations, and values of constants used to model the Loughborough up/downflooding experiments.

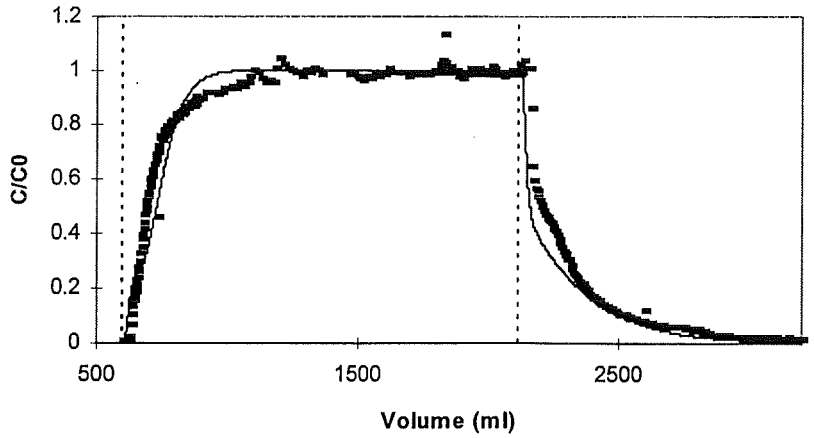

Figure 9: Loughborough Up/Downflooding Experiment (symbols, -) with k1D Model Prediction (line); $[Eu]_T = 1x10^{-7}$ M

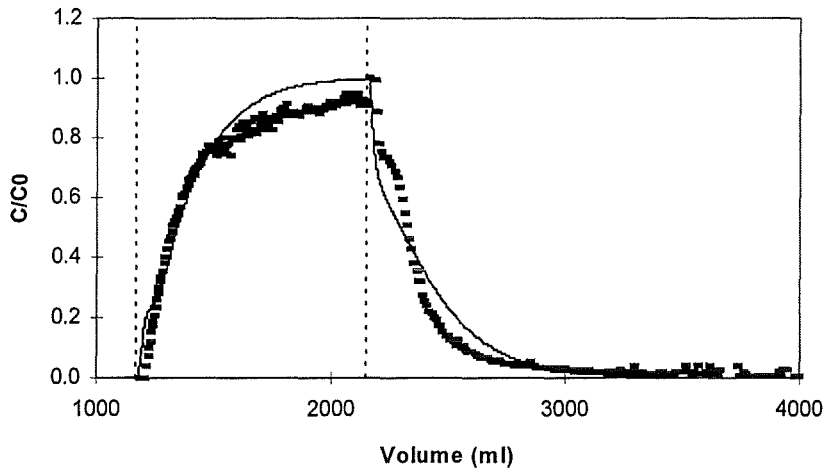

Figure 10: Loughborough Up/Downflooding Experiment (symbols, -) with k1D Model Prediction (line); $[Eu]_T = 1x10^{-6}$ M

In the previous, 'equilibrium only', modelling it had only ever been possible to obtain good fits to the up and downflooding sections of the experiments separately, using different parameters. However, with the new k1D model, it is now possible to fit both sections simultaneously. In addition, using codes based on the assumption of local equilibrium, it was impossible to reproduce the correct shapes of the experimental curves, and in particular the long tail of the downflooding section. The introduction of kinetics has resulted in a significant increase in the improvement of fit. This is demonstrated in figure 11, which shows the downflooding section of a column experiment and the best fit modelling results obtained with k1D and with an 'equilibrium only' approach. The k1D result is not only closer, but also reproduces the shape of the curve much more effectively.

Pulsed Column Experiments

k1D Modelling Results

In addition to the Loughborough columns, the k1D code was also tested against a set of pulsed injection column experiments provided by the BGS, Keyworth. These experiments are different to the up/downflooding experiments, in that the metal, this time Co, is injected as a single short pulse. Also, the columns were not pre-equilibrated with humic acid solution. This, coupled with the fact that the outflow concentrations of both the Co and the humic were recorded, means that it was possible to gain some information about the interaction of the humic with the sand packing. Since the humic/mineral interaction was also included, this time the system of processes and associated equations are apparently more complex: see figure 12.

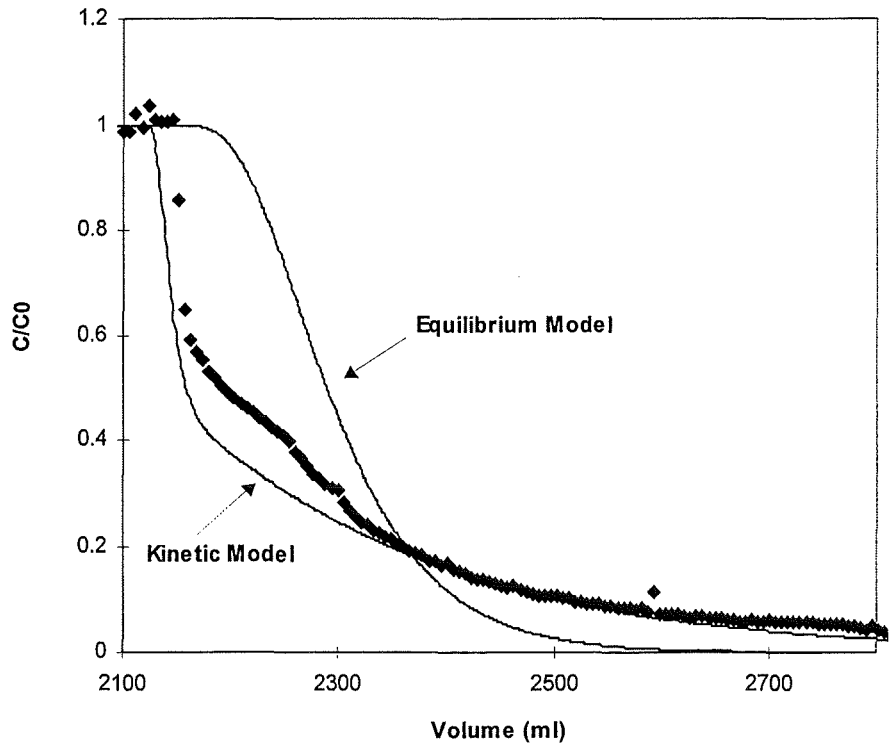

Figure 11: Comparison of equilibrium kinetic models

Although the BGS system looks very much more complex than that used for the Loughborough columns, in fact, only one extra process has been introduced, the sorption of

the humic molecule to the mineral surface, which is described with a single equilibrium constant, $K_{HA,S}$. In these experiments, it was possible to describe the interaction of the humic with an equilibrium constant. However, in the environment this may not be the case, since there, the mineral surfaces will be in equilibrium with the ambient concentration of humic substances. Note, the model assumes that humic molecules sorbed to the mineral surface interact with the metal in the same manner as those in solution. In reality, the immobilisation of the humic on the surface must have some effect upon the humic/metal behaviour. However, any such effects would not appear to affect the migration of the Co in these experiments. This is probably due to the fact that in these experiments, unlike the Loughborough columns, the movement of the metal is almost entirely dominated by the kinetically hindered site, and hence any effect of immobilisation on the exchangeable site would not be observed.

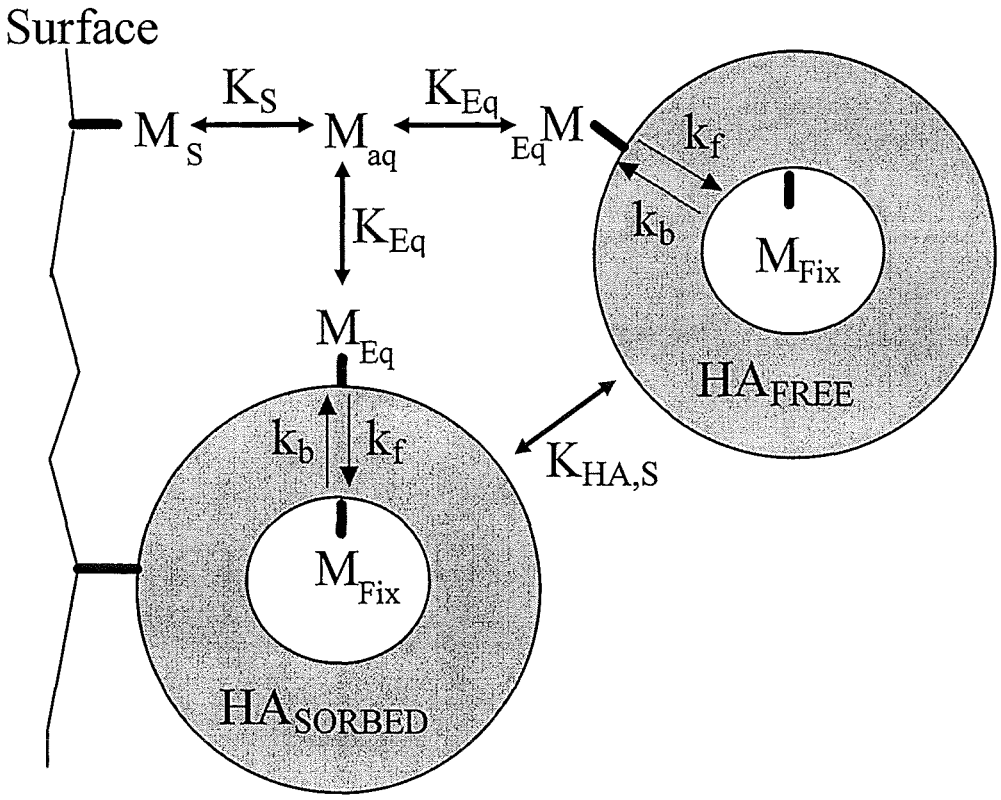

K_S= 1.0E7; $K_{HA,S}$= 10.0; K_{EQ}= 5.0E8; k_f= 0.029; k_b= 0.041

$[HA_{EQ}]$=1 mmol/g; $[HA_{FIX}]$=0.31 mmol/g; [S]=0.1

Figure 12: System of equations, and values of constants used to model the BGS pulsed injection experiments.

In the case of the Loughborough experiments, it was not possible to obtain a value for the association rate constant. However, in these experiments, it was possible to define values for the both the dissociation, k_b, and association, k_f, rate constants. This was possible because different pre-equilibration times had been used for the various Co/humic substance injection solutions. It was found that the amount of Co emerging from the column depended mainly upon the length of time which the Co was allowed to equilibrate with the humic: the longer the solution was left, the more Co entered the kinetically hindered fraction and the more Co was able to migrate through the column. This is further evidence of the crucial importance of kinetics to humate mediated transport.

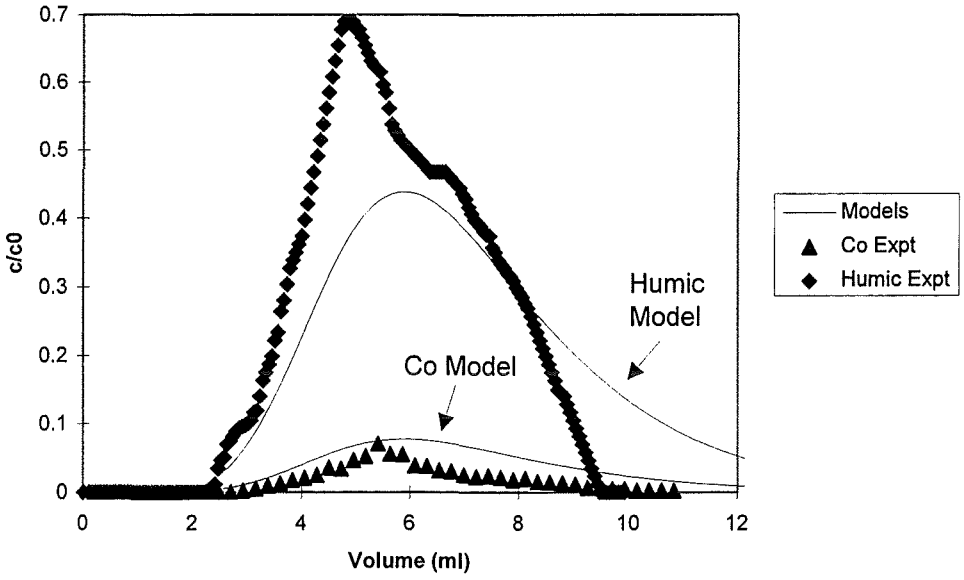

Figure 13: Example of BGS pulsed injection column

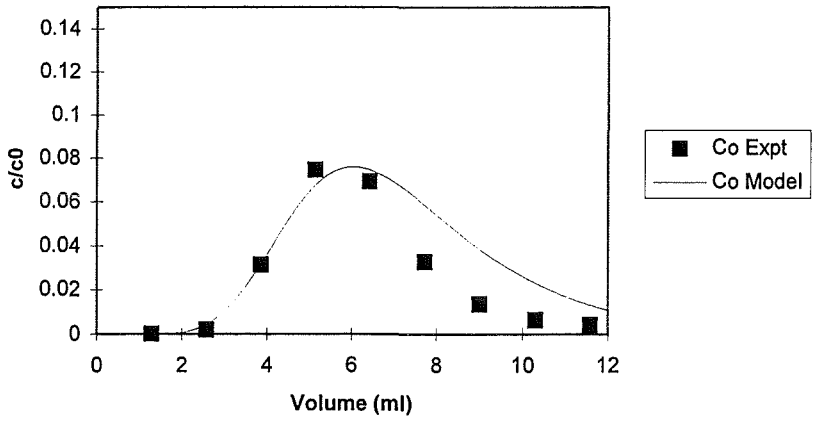

Figure 14: Example of BGS pulsed injection column

Examples of the k1D results obtained for the BGS columns are shown in figures 13 and 14. From these figures, it is clear that this relatively simple model is able to simulate both the Co and the humic substance behaviour very effectively. Previous attempts using an equilibrium only approach were able to predict the movement of the humic substance, but not the Co: the predicted Co elution peaks were usually of the wrong height and displaced slightly in their position. The improvement is shown in figure 15.

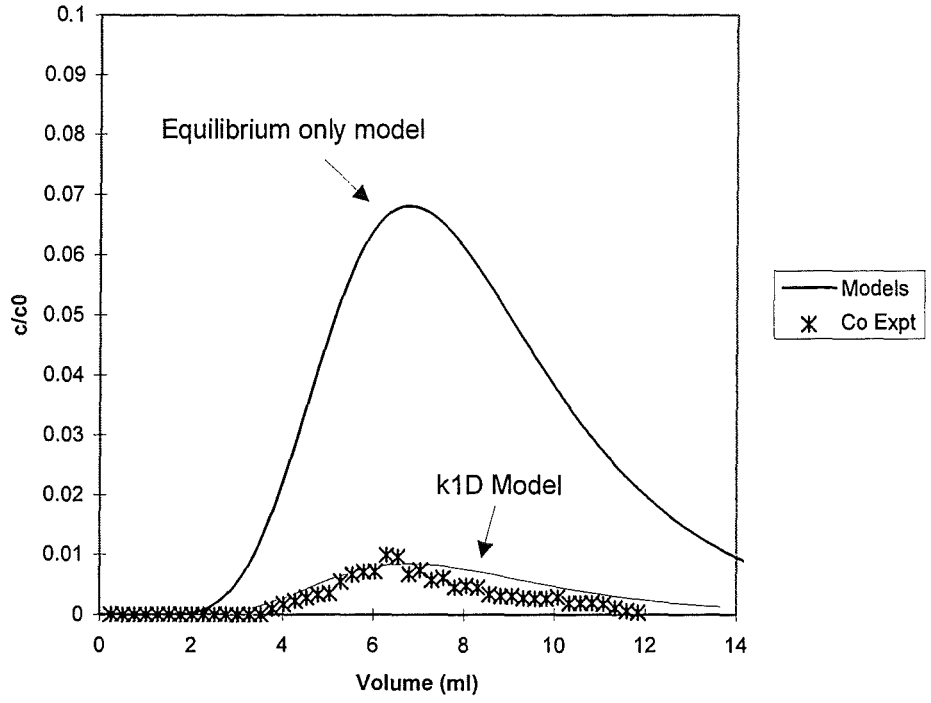

Figure 15: Comparison of equilibrium only and combined equilibrium/kinetic models for a BGS pulse injected column

COLUMN3 Modelling

The COLUMN3 transport model has been developed recently (Carlsen and Bo unpub; Carlsen et al 1999a,b) as a user friendly tool for simulating the transport of pollutants. It is an improvement upon the earlier COLUMN2 code (Nielson et al 1985), and is able to model sorption into or onto solid phases and solution phase chemical reactions of first and higher orders. COLUMN3 solves the one dimensional transport equation,

$$\partial c_i / \partial t = (D_i / R_f(i))\partial^2 c_i / \partial x^2 - (V / R_f(i))\partial c_i / \partial x + F(c_i, t)$$

where c_i, D_i and $R_f(i)$ are the concentration, the dispersion coefficient and the retention factor of component i, respectively, and V is the water velocity. Thus, the two first segments of the equation account for dispersion and convection processes, respectively. Through the term $F(c_i,t)$ possible chemical and physico-chemical reactions can be taken into account.

$$F(c_i,t) = \frac{\sum_r (k_r n_{i,r} \cdot \prod_i c_i^{n_{i,r}})}{R_f(i)}$$

where k_i is the rate constant of the ith reaction of reactant r, $n_{i,r}$ the stoichiometric coefficient. Thus, COLUMN3 uses essentially the same one dimensional advection dispersion equation as the k1D model, and can also cope with equilibrium and non-equilibrium, or kinetic, processes. Another similarity between k1D and COLUMN3 is that both use the same theoretical kinetic equations and rate constants to simulate slow processes. However, the two codes differ in the way in which they treat equilibrium processes: k1D uses equilibrium constants to account for fast chemical processes, whilst COLUMN3 defines a retention factor, R_f for each species. R_f is related to the dimensionless distribution coefficient, K_D, and the porosity, ω, via,

$$R_f = 1 + \frac{1-\omega}{\omega} K_D$$

The set of equations used to simulate the BGS columns differ from those used in k1D. The COLUMN3 modelling defines two surface sites, SolidSite and FixedSite: the former accounts for slow reversible sorption of fulvic acid and metal-fulvate complexes, and the second accounts for irreversible sorption of fulvic acid. In the k1D modelling, two fulvate bound Co fractions were used, whereas here, only one, kinetically hindered fraction is defined. A further difference is that the COLUMN3 modelling takes into account the binding of trace metals present in the groundwater, from which the injection solutions were made up. For the purposes of the modelling, all of the trace metals, other than Co, where considered to behave identically, and were treated as the single species X. All calculations were performed in relative molar concentrations, the initial concentrations being: [FA]=1; [Co]=0.01; [X]=20; [SolidSite]=100; [FixedSite]=1. The inorganic Co was assumed to behave as a retained

species with an R_f value of 3600. The following kinetically controlled reactions and rate constants were used to simulate other chemical processes.

Cobalt - Fulvic acid complex formation:

$[Co] + [FA] \rightarrow [CoFA]$; $k_1 = 50.0$

$[CoFA] \rightarrow [Co] + [FA]$; $k_{-1} = 0.05$

Competing complex formation with metal ions in the ground water:

$[X] + [FA] \rightarrow [XFA]$; $k_2 = 50.0$

$[XFA] \rightarrow [X] + [FA]$; $k_{-2} = 0.1$

Slow sorption/desorption processes:

$[FA] + [SolidSite] \rightarrow [FASolidSite]$; $k_3 = 0.003$

$[FASolidSite] \rightarrow [FA] + [SolidSite]$; $k_{-3} = 0.175$

$[CoFA] + [SolidSite] \rightarrow [CoFASolidSite]$; $k_4 = 0.003$

$[CoFASolidSite] \rightarrow [CoFA] + [SolidSite]$; $k_{-4} = 0.175$

$[XFA] + [SolidSite] \rightarrow [XFASolidSite]$; $k_5 = 0.003$

$[XFASolidSite] \rightarrow [XFA] + [SolidSite]$; $k_{-5} = 0.175$

Irreversible sorption reactions:

$[FA] + [FixedSite] \rightarrow [FAFixedSite]$; $k_6 = 0.025$

$[XFA] + [FixedSite] \rightarrow [FAFixedSite] + [X]$; $k_{-6} = 0.025$

Note, first order rate constants have units of min^{-1} whilst second order constants have units of ml min^{-1} relative mol^{-1}.

Figures 16 and 17 show the COLUMN3 results obtained for two BGS columns: one slow flow rate experiment (0.22 cm min^{-1}) and one fast flow (1.07 cm min^{-1}). Figure 16 shows the total fulvic acid elution profiles both experimental and COLUMN3 predicted. In addition, the profiles which would be obtained if a model excluding slow sorption/desorption were used are shown as dashed lines. Figure 17 shows the analogous Co elution profiles. It is clear that the inclusion of slow chemical processes is crucial in achieving a good description of these column experiments. The same conclusion that was reached independently during the k1D modelling work. At two different flow rates, the COLUMN3 model has achieved very good

fits to the experimental data, both in terms of the elution volume and of the shapes of the elution curves. In addition, the model was also able to reproduce the integrated recoveries of Co and fulvic acid at the two different flow rates (cf. Table 2).

Table 2. Experimentaly and calculated recoveries of fulvic and cobalt containing species.

	slow flow		high flow	
	exp. recovery	calc. recovery	exp. recovery	calc. recovery
Fulvic acid containing species	61	62	70	86
Co-57 containing species	1.3	2.5	9.0	6.7

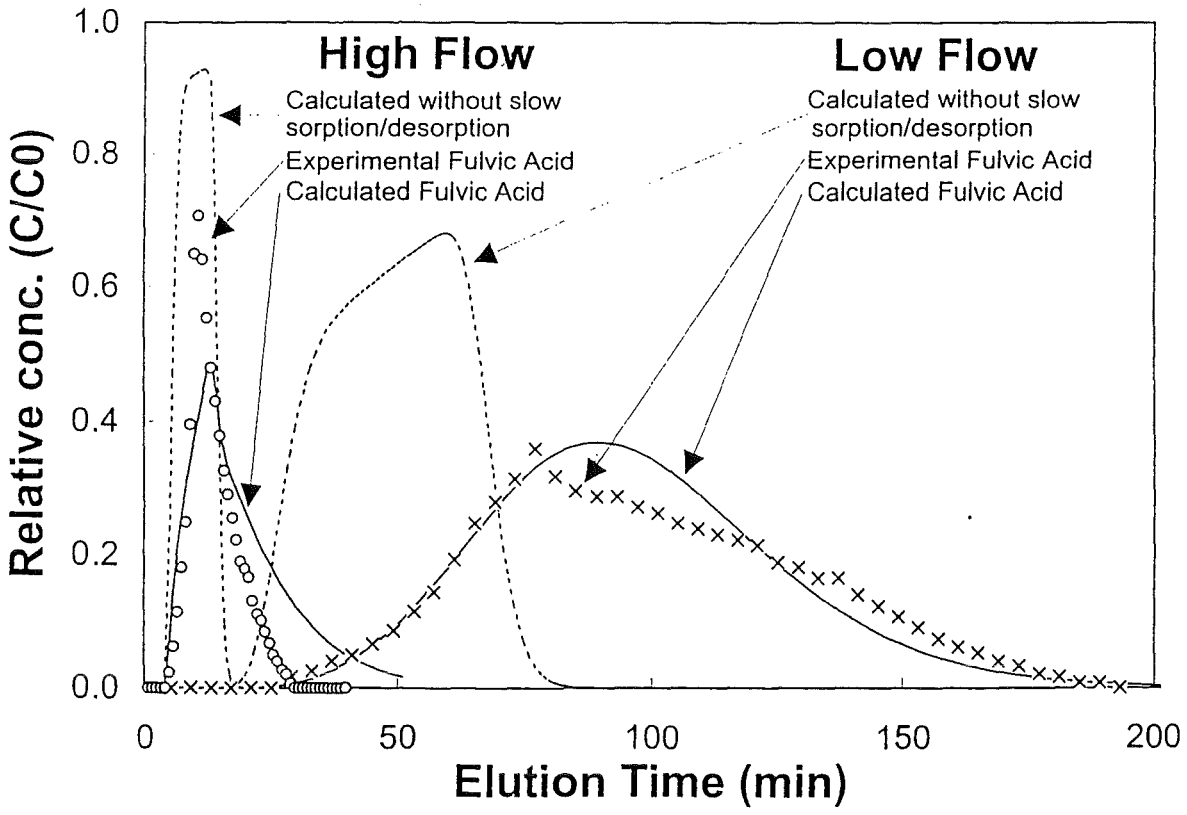

Figure 16: Fulvic acid elution profiles, experimental and calculated, for slow and fast flow rates.

It can be noted that the recoveries, not surprisingly, are generally significantly higher in the case of high flow through the column than in the case of low flow, which obviously, in agreement with the above discussion, can be explained in terms of sorption kinetics. Thus, the slow as well as the irreversible sorption processes will operate to a lower extent at higher flow rates. Analogously, the cleavage of the FA-Co complex, leading to strong sorption of the free Co will be less pronounced.

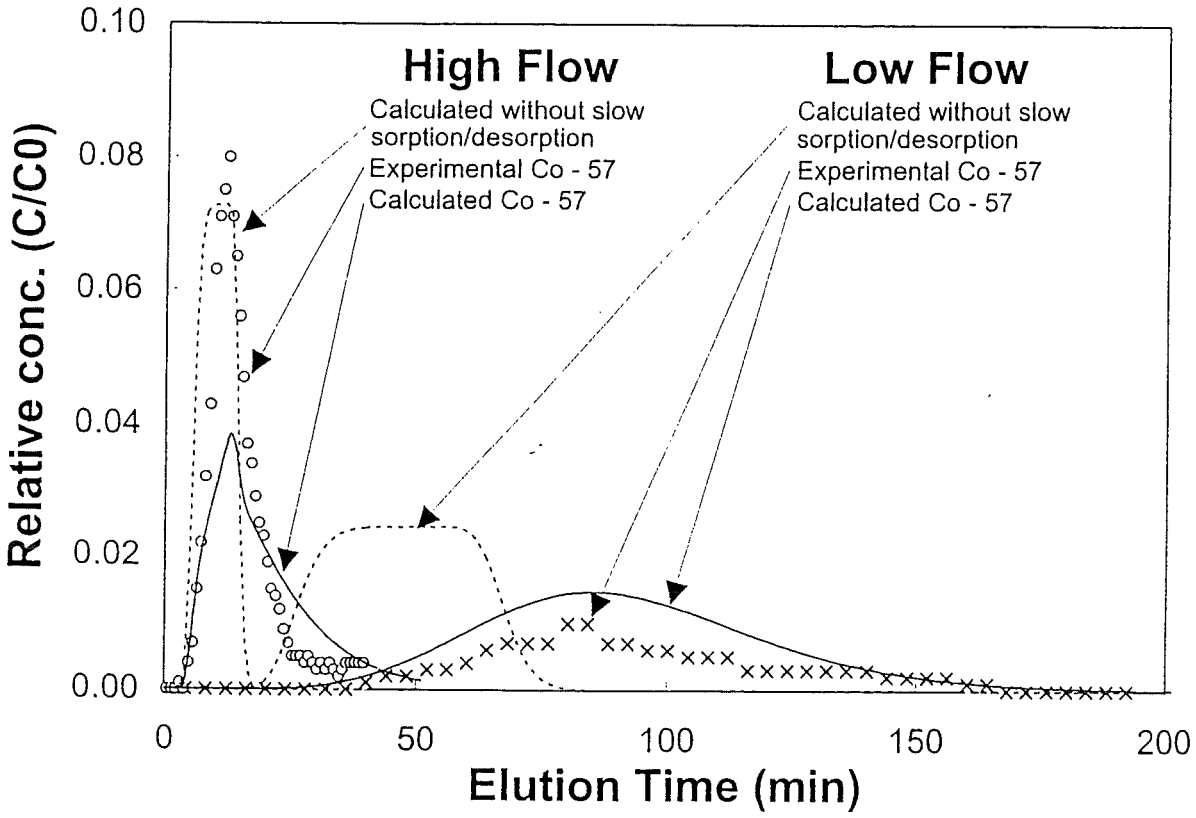

Figure 17: Cobalt elution profiles, experimental and calculated, for slow and fast flow rates.

Comparison of k1D and COLUMN3 Modelling

Both models have achieved good fits to the BGS column experiments, but using two different sets of equations. However, if the two equation sets are examined more closely, then it becomes clear that the two treatments, although formulated in different ways, are effectively very similar. COLUMN3 has used a large retention factor for the inorganic Co, whilst k1D has used a large equilibrium constant, K_S. K_S is larger than the Co retention factor, but this is because the k1D modelling defines an exchangeable site on the fulvic acid with a moderately

high equilibrium constant which competes with the surface. The reason that the two codes were able to obtain good fits with and without the exchangeable fraction is that, regardless of whether it exists in the columns or not, virtually all of the Co observed in the elution profile is accounted for by the kinetically controlled CoFA fraction. Hence it is possible, to achieve good fits to the experiment with or without the exchangeable site. Therefore, on the essential point, the two models are in agreement: the migration of the Co through the column is facilitated by the kinetically controlled binding site on the fulvic, and hence only a model which can take into account chemical kinetics may adequately simulate these column experiments.

CONCLUSIONS

It is clear that a great deal of information has been gained about the nature of the binding mechanisms of metals to humic substances. The mechanistic modelling has shown that the uptake of metals into the exchangeable fraction may be explained in terms of the dehydration of the cation and the relaxation of the humic double layer. The model predicts that the reaction is driven almost entirely by the entropy change associated with the loss of water molecules, and also with the release of cations from the double layer. This seems to fit well with the observed large entropies of reaction. In addition, the model predicts that the reaction enthalpies will be small and endothermic but otherwise unpredictable, which again would appear to agree with observation. The kinetic modelling has been able to reproduce the behaviour observed in long term desorption experiments, and has enabled the determination of activation energies and entropies, and also the free energy change associated with the conversion from the exchangeable to the kinetically controlled fractions. This work means that we now have a complete thermodynamic and kinetic description of the interaction of metals with humic substances. Figure 18. shows an energetics diagram illustrating the various processes and free energies studied in this project. The figure shows the progression, starting from free metal and humic to the final state with the metal locked away inside the humic acid structure: there is an initial sharp drop in free energy, corresponding to the relaxation of the double layer and the dehydration of the metal ion. Between the exchangeable and the fixed, kinetically controlled, states there is a large activation barrier which is largely entropic in

nature, although there is an enthalpic component, which becomes more important as pH increases. Although some metal does reach the final hindered state, it is a minority of the total metal, and hence there is a small but positive free energy change associated with going from the exchangeable to the fixed.

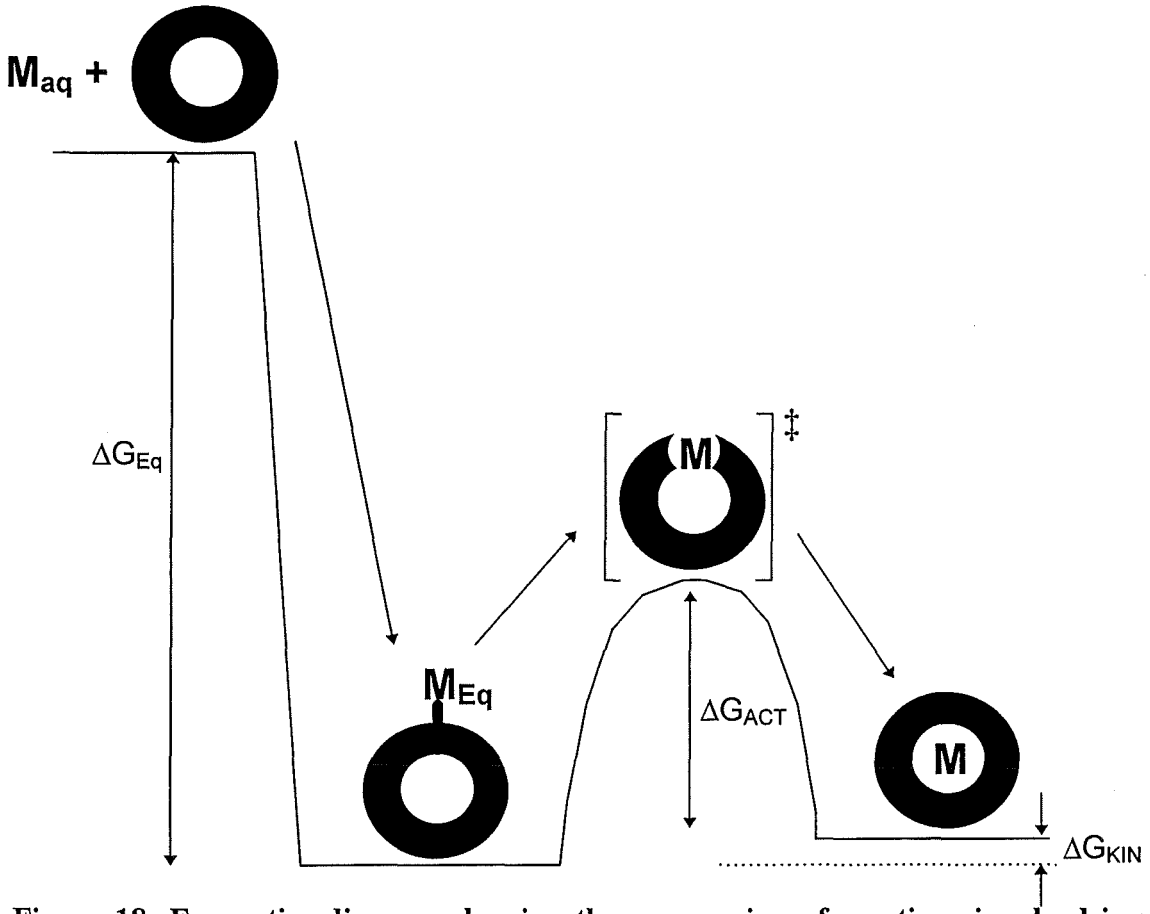

Figure 18: Energetics diagram showing the progression of reactions involved in metal humate binding.

The transport modelling has built upon the mechanistic work, and the result is that there are now two separate codes which are able to replicate the behaviour observed in column experiments. This is a significant improvement compared to the situation prior to this work. A number of column experiments have been modelled by both codes, including both up/downflooding and pulsed injection. The goodness of fit to both the humic substance and the metal behaviour is very encouraging.

The next stage will be to apply the results obtained here to performance assessment studies, so that this increased knowledge of the interaction of humic substances with radionuclides may be applied to radiological risk assessment studies.

REFERENCES

Bartschat B.M., Cabaniss S.E. and Morel F.M.M. Oligoelectrolyte Model for cation binding to humic substances *Environmental science and Technology*, **26**, 284-294, (1992)

Bo P. and Carlsen L. (unpub) COLUMN3: A computer code for modelling transport and distribution of complex mixtures.

N.D. Bryan A Modelling study of humate mediated metal transport. In *Effects of Humic Substances on the Migration of Radionuclides: Complexation and Transport of the Actinides.* pp 245 - 262 Ed. G. Buckau. Wissenschaftliche Berichte (FZKA 6124, ISSN 0947-8620), Forschungszentrum Karlsruhe Technik und Umwelt, Karlsruhe, Germany (1998).

Carlsen L., Bo P., Higgo J.J.W. and Davis J.R. Transport and distribution of complex mixtures: Influence of chemical and physicochemical reactions on the migration of pollutants (submitted) (1999a).

Carlsen L., Bo P. and Higgo J.J.W. Modelling of humic acid mediated migration of cobalt (submitted) (1999b)

Falck W.E. Multisite binding equilibria and speciation codes: incorporation of the electrostatic interaction approach into PHREEQE. *Computers and Geosciences*, **17**, 1219-1234, (1991).

Jones M.N. and Bryan N.D. Colloidal Properties of Humic Substances *Advances in colloid and interface science*, **78**, 1-48, (1998).

Kinniburgh D.G., Milne C.J., Benedetti M.F., Pinheiro J.P., Filius J., Koopal L.K. and Van Riemsdijk W.H. Metal ion binding by humic acid: Application of the NICA-Donnan Model. *Environmental Science and Technology*, **30**, 1687-1698, (1996).

Livens F.R. Chemical reactions of metals with humic materials *Environmental Pollution*, **70**, 183-208, (1991).

Nielson O.J., Carlsen L. and Bo P. COLUMN2 - A computer program for simulation of migration. Risø-R-514, Risø National Laboratory, Roskilde (1985).

Schussler W., Artinger R., Kienzler B. and Kim J.I. Modelling of Humic Colloid Mediated Transport of Amercium(III) by a kinetic approach. In *Effects of Humic Substances on the Migration of Radionuclides: Complexation and Transport of the Actinides.* pp 245 - 262 Ed. G. Buckau. Wissenschaftliche Berichte (FZKA 6124, ISSN 0947-8620), Forschungszentrum Karlsruhe Technik und Umwelt, Karlsruhe, Germany (1998).

Tipping E. and Hurley M.A. A unifying model of cation binding by humic substances. *Geochimica et Cosmochimica Acta*, **56**, 3627-3641, (1992).

Annex 14

Implications of Humic Chemical Kinetics for Radiological Performance Assessment

(Bryan et al., RMC-E)

2nd Technical Progress Report

EC Project:

"Effects of Humic Substances on the Migration of Radionuclides:
Complexation and Transport of the Actinides"

RMC-E Contribution to Task 5 (Performance Assessment)

Implications of Humic Chemical Kinetics for Radiological Performance Assessment

Reporting period 1998

Bryan N.D.[1,2], Griffin D.[1], Regan L.[1]

[1]RMC Ltd, Suite 7, Hitching Court, Abingdon Business Park, Abingdon, Oxfordshire, OX14 1RA

[2]Department of Chemistry, University of Manchester, Oxford Rd., Manchester, M13 9PL

INTRODUCTION

Models have been developed which can describe the behaviour of humic substances and radionuclides in laboratory column experiments (Bryan et al this volume). Previously, the results of these experiments could not be modelled satisfactorily using the existing local equilibrium assumption codes. The major modelling advance, therefore, has been the realisation that the humic/radionuclide complex behaviour is dominated by kinetics and rate constants, and not by equilibria and stability constants.

The next stage is to consider the models, and determine the implications for radiological performance assessment studies. There are two possible aspects to this problem. The first is the generic case, where we consider the general effect which humics would be expected to produce at any given site. The second considers the effect on migration at specific sites of interest, for example, Gorleben. However, before embarking upon a detailed site specific study, it is first necessary to consider the general implications of the column and mechanistic modelling to radiological performance assessment. This document describes a mathematical study of the implications of slow humic kinetics to field scale migration studies. The effect of the magnitude of the reaction rate constants is investigated, along with the issue of reversible/irreversible sorption of humic substances to mineral surfaces. Suggestions are made for simplifying the models developed during column modelling work for application in the field. Also, several important areas of uncertainty are highlighted.

UP-SCALING ISSUES

In P.A. studies conducted so far, humics have either been completely ignored, or have been included at the most basic level, for example with very simple, local equilibrium, 'Kd-type' parameters. This is primarily because the controlling reactions and processes were not understood. Following recent advances, the next stage is to produce a set of instructions, which would enable humics to be included effectively in a P.A. exercise.

One important aspect is to appreciate the problems which the recent mechanistic and column modelling work (Bryan et al this volume; Bryan 1998; Schussler et al 1998) has presented to performance assessors. P.A. studies are for the most part carried out using Kd values to describe the sorption of radionuclides to surfaces. However, it has been demonstrated that humic reactions are often very slow, and hence there is bound to be some incompatibility with a local equilibrium assumption approach. Modelling work has shown that rate constants are the most effective way to describe humic behaviour (Bryan et al this volume). However, the use of rate constants is expensive in terms of computing time, and so wherever possible performance assessors will want to use equilibria to describe these reactions. More than this, all current P.A. models are based solely upon equilibria. Therefore, one major contribution would be to determine the limits of the validity of an approach based upon equilibria. So that, for a given set of conditions, one could determine the range of rate constants where a simple equilibrium assumption would still be valid, and also, the likely errors and uncertainties which would be incurred. For a Kd code, for example, it should also be possible to determine the 'best Kd' to use.

In order to be useful to P.A. studies, it is not sufficient merely to produce a model and a set of parameters which can describe column experiments. It is necessary to explore the specific implications which this model has for the field scale migration of radionuclides. Given that we now know how humics behave, the next question to be answered is what will be the effect of that behaviour upon P.A. calculations. Will humic substances make a difference, and how big a difference will that be? What is the best way to include humics in P.A.: is it essential to use a mathematical model which includes chemical kinetics, or can a reasonable approximation be obtained with an equilibrium code? What will be the uncertainties in the final prediction, and how can they be minimised?

The first step in this process is to consider the chemical model of humic substances, which has been developed. The evidence from experiment is that humics have several different levels of binding, ranging from instantly exchangeable to very kinetically hindered, almost irreversible. Hence, we envisage the humic as having a series of successively more kinetically hindered binding sites (Figure 1).

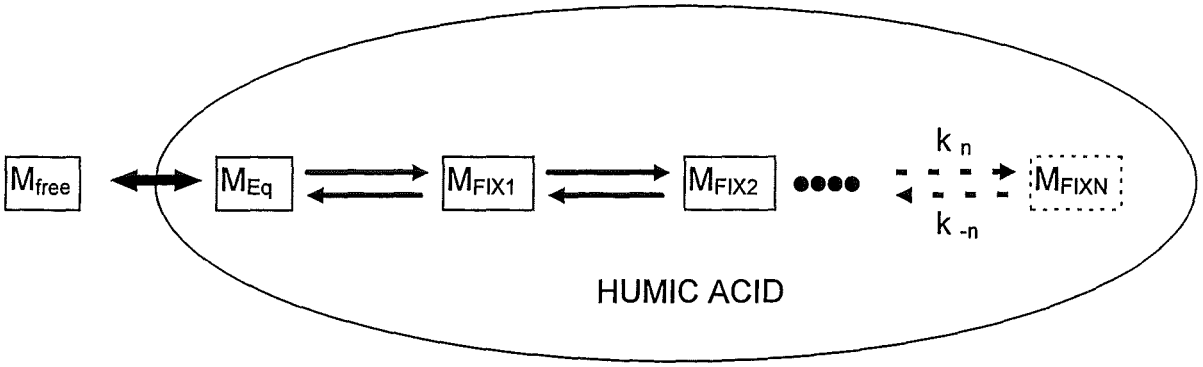

FIGURE 1: CONCEPTUAL MODEL OF HUMIC ACID

This model looks deceptively simple. However, to calculate the occupancy of each box with time is actually mathematically complex and computationally expensive. Such a model could not presently be included into a P.A. model. Therefore, one task is to examine the conceptual model above and to determine how it could be simplified, without the introduction of significant inaccuracy. The most obvious avenue for simplification lies in examining the values of the rate constants. The distinction between equilibrium and kinetic reactions is always artificial, since it depends upon the time scale of the observation: a reaction which is 'equilibrium' over periods of hours, may well be slow on the time scale of seconds. Given the physical conditions of the P.A. exercise, e.g. flow rate, distance travelled and total time of interest, it will be possible to reduce the series of reactions in the conceptual model to just three groups:

(1) Those reactions which are sufficiently fast to be treated as equilibria.
(2) Those which are sufficiently slow that they effectively do not take place.
(3) Those reactions which can only accurately be described via the use of rate equations.

This will be true regardless of the number of binding sites in the series, and will also hold true if the binding sites are not in series, as shown above.

Uncertainties in the model parameters, specifically the values of the rate constants, will also need to be taken into account.

The realisation of the importance of kinetics may well have a significant impact upon predictions, compared to the previous complete equilibrium. Although humics have a high affinity for metals, the vast excess of surface sites means that in an equilibrium calculation, any radionuclide would not be expected to travel very far before being sorbed onto a surface. However, if the desorption of the metal from the humic site is kinetically controlled, then the number and affinity of surface sites is no longer sufficient to prevent the movement of the radionuclide: the critical factor becomes the time available for desorption to take place. If there is time for the metal to desorb, then it will not migrate, but, for example, if the flow rate is sufficiently fast, then it will.

Another important factor is the initial state of the humic/radionuclide complex, i.e., what is the initial occupancy of each of the metal binding sites ? When modelling a column experiment, this information is provided by the pre-equilibration time. In a P.A. exercise, this will not be easy to estimate, but will have a large influence on the final prediction. It will depend crucially upon whether or not humic substances are able to penetrate into the near field and carry radionuclides out into the far field Or, will radionuclides only encounter humics at the boundary of the near and far fields; the 'local field'? This is likely to be one of the largest sources of uncertainty.

Although more is now known about the behaviour of humics towards radionuclides, one significant area of uncertainty is the interaction of the humic substances with the mineral surface. In the past, this area has been given less attention, since, in the case of an equilibrium description of metal binding, it has little effect upon the outcome of the prediction. However, if a metal is hidden inside the humic structure, then for transport purposes it will behave like a humic, and hence it becomes much more important to know how the humic will behave. In the case of the BGS columns, the behaviour of the humic was described with an equilibrium constant. However, the situation in column experiments is always artificial, and it is not certain how humics will behave in situ. One important difference between the column experiments and the field is that, in the environment, all of the surfaces will be in equilibrium with the ambient concentration of humic material. Is that interaction an equilibrium? Once the surface has reached maximum sorption, is any further humic material ignored, or does it

replace material already on the surface ? This distinction is potentially important, since it will make the difference between the kinetically hindered nuclide being retarded, or being transported effectively as a conservative tracer.

The advantage of a rigorous generic study is that it will make any subsequent site specific study relatively straightforward. In theory at least, if a set of instructions has been produced for the inclusion of humics in P.A., then to perform the site studies should be a matter of applying the results.

CALCULATIONS

Some calculations have been made, based upon the parameters determined during the modelling of Co migration in column experiments performed by the BGS The system used to model the BGS columns is shown in Figure 2.

The concentrations and flow rates etc. used in the column experiments are higher than one might expect in the field, and therefore, a set of typical conditions have been selected for this exercise. In the lab experiments, a total fulvic concentration of 32.5 ppm was used. However, in these examples, 2.58 ppm has been used, corresponding to a TOC measurement made upon the groundwater from where the column packing sediment was taken. A linear flow rate of 1.0E-5 m/s was selected as a typical flow rate through sand. A total upper boundary Co concentration of 1.0E-10 M was chosen, as a realistic environmental concentration of a metallic pollutant. Finally, the total distance over which the migration was calculated was increased from 6 cm to 100 m, and a total run time of 5E06 s was selected, since even a conservative tracer would not have reached the end of the column in that time. Apart from this, the parameters obtained form the column modelling were used to predict the movement of the Co. Figure 3 shows the Co profile obtained after 5E06 s of continual injection. Prior to contact with the sand, the model predicted that virtually 100% of the Co was bound to the fulvic, and for this initial calculation, it was assumed that the (single) kinetically hindered site had had sufficient time to come into equilibrium with the exchangeable site: the effect of this assumption is investigated later.

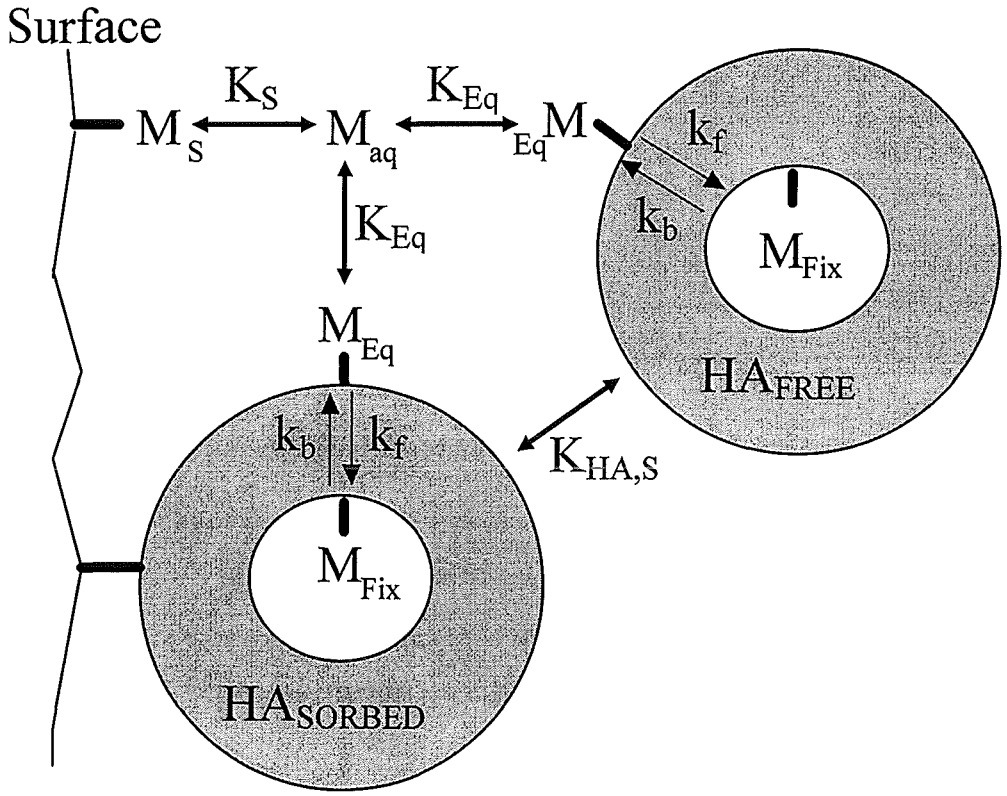

K_S= 1.0E7; $K_{HA,S}$= 10.0; K_{EQ}= 5.0E8; k_f= 0.029; k_b= 0.041

$[HA_{EQ}]$=1 mmol/g; $[HA_{FIX}]$=0.31 mmol/g; [S]=0.1

FIGURE 2: SYSTEM USED TO MODEL BGS COLUMNS

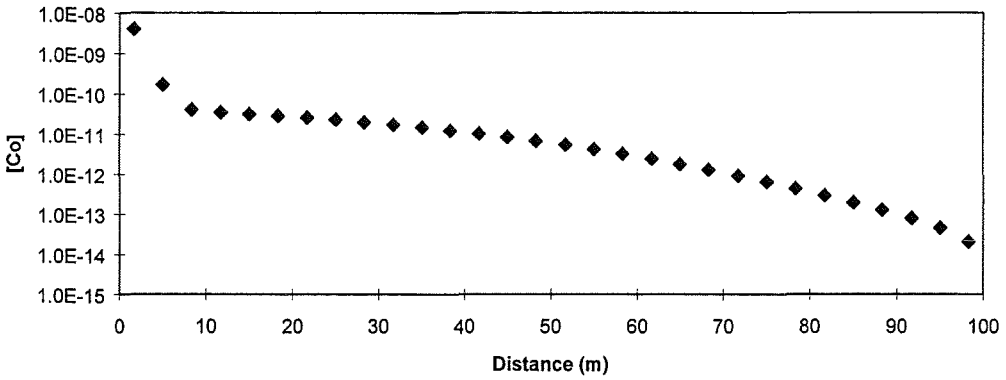

FIGURE 3: [CO] PROFILE OBTAINED USING BGS MODELLING PARAMETERS

From Figure 3, the two distinct types of Co behaviour are clearly discernible. The Co held in the exchangeable site is very easily removed by the sand. This is responsible for the sharp fall in the Co concentration at short distances. Hence, the vast majority of the metal has not moved past the top of the column (note the log scale in Figure 3). However, it is clear that the kinetically hindered metal fraction has been transported much further down the column: this is responsible for the long shallow curve in the profile at medium to long distances. For the purposes of their migration, it is possible to treat the two fractions as essentially independent, once they are exposed to the sand surface. In the case of Co, humic kinetics are clearly having an effect. What is of interest is the extent of this effect if the rate constants for the kinetically hindered site were higher or lower.

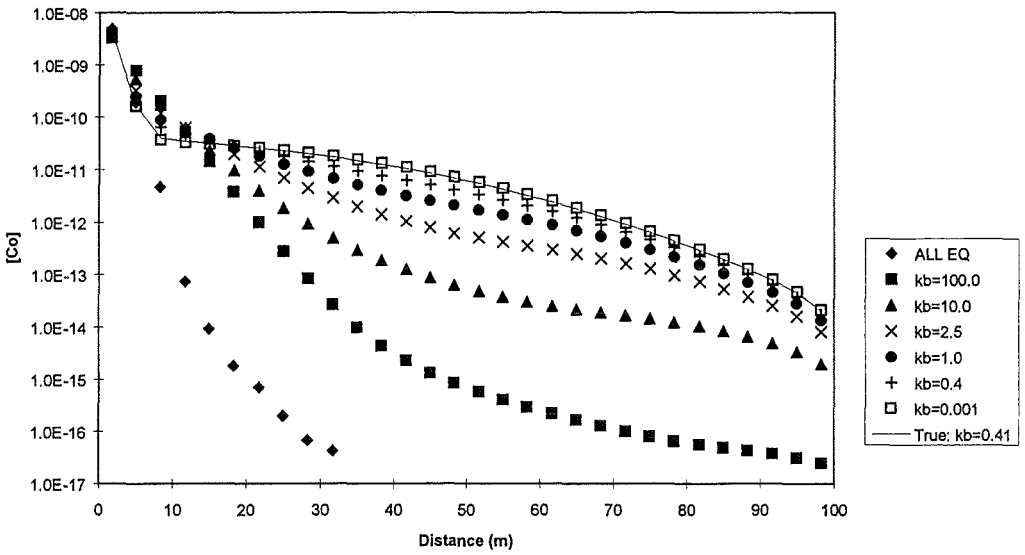

FIGURE 4: EFFECT OF CHANGING DESORPTION CONSTANT ON THE CO PROFILE

To investigate, a series of calculations were performed keeping all other parameters constant, but varying the values of k_f and k_b. Rather than changing the two constants simultaneously, and at random, which would have led to misleading and confusing results, the values were varied so that the ratio between the two remained constant. In this way, the upper boundary equilibrium concentration of the hindered site remained constant. Figure 4 shows the profiles

obtained: the 'true' behaviour, or that achieved with the column experiment derived parameters, is shown as a line.

As expected, as the rate constant, k_b, for the desorption reaction increases, the extent of Co migration decreases, and as k_b falls the behaviour seems to tend to some limit. Note that the true value (0.041) produces virtually identical behaviour to that with k_b=0.001. In order to understand the behaviour being shown by the kinetically hindered site, it is revealing to compare its behaviour down the column in isolation from the exchangeable fraction. Figure 5 shows ratio plots for the different values of k_b, that is, the distribution of the hindered site Co down the column, expressed as a ratio of the concentration at the top of the column: this enables comparison with other species. In addition to the hindered site, the behaviours of a conservative tracer, the exchangeable Co and the humic are also shown. These are three limiting behaviours which are useful when considering the behaviour of the hindered metal fraction.

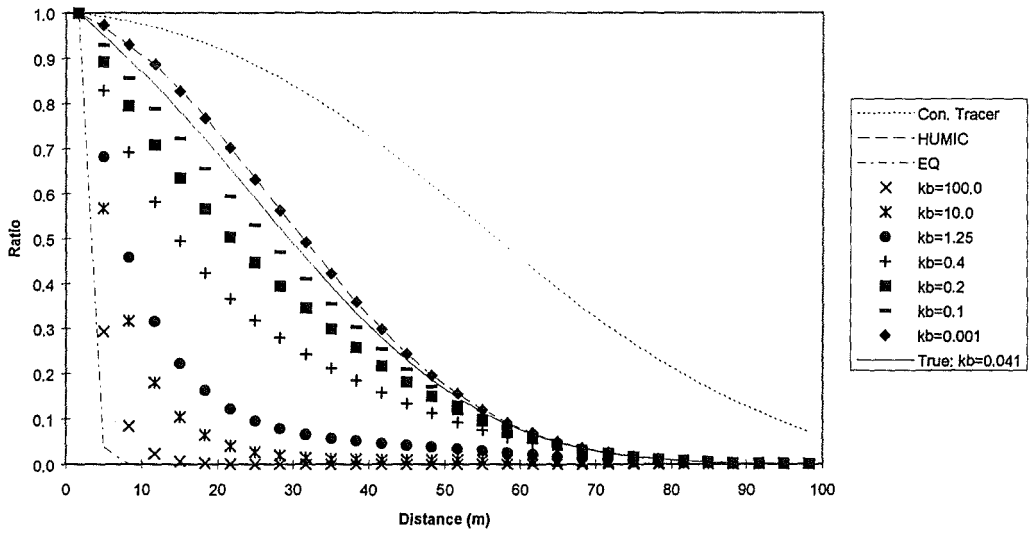

FIGURE 5: RATIO PLOT SHOWING BEHAVIOUR OF THE KINETICALLY HINDERED CO FRACTION

From this graph, it is clear that as k_b increases, the 'kinetic Co' behaves increasingly like the exchangeable Co. Indeed, for $k_b > 10$, the kinetic Co can be considered identical to the exchangeable fraction. Conversely, as k_b decreases, its behaviour tends towards that of the

humic itself. In this case, the true values of the desorption rate constants result in behaviour almost identical to the humic, and that certainly for k_b=0.001, the 'kinetic Co' behaves identically to the humic. Note, the Co can never migrate faster than the humic.

These observations are significant, since both the exchangeable Co and the humic migration may be described by equilibrium constants. Hence, for this case, humic desorption rate constants greater than 10 may be described via the exchangeable Co equilibrium constant, and those less than 0.05 may be described using the humic sorption constant. In fact, the 'true' plot shows that for the experimentally derived parameters, essentially the same result could have been obtained using $K_{HA,S}$. Only in the range $10 > k_b > 0.05$ is it necessary to use rate constants. It is important to bear in mind that this range is dependent upon physical conditions. To demonstrate this fact, the above calculations were repeated, but using a linear flow rate of 1.0E-6 m/s, and an increased total study time of 5.0E7 s: the results are shown as a kinetic Co ratio plot in Figure 6. At the reduced flow rate, the range over which the behaviour cannot be described using equilibria has become $1>k_b>0.005$. Interestingly, as a result, the 'true' behaviour no longer approximates to the humic limiting behaviour.

These calculations have been based upon the assumption that the hindered site was fully occupied at the start of migration. Another interesting question to ask is, what would happen if the Co did not have chance to fill the site before contact with the sand ? Reverting to flow rate of 1.0E-05 m/s and a total time of 5.0E06, the calculations were repeated, but with the kinetically hindered site initially empty: the profiles obtained are shown in Figure 7. As would be expected, there is in general less migration than for the initial case (see Figure 4). However, whereas before, the change in the profile was fairly simple, this time it is much more complex. The maximum migration is obtained for k_b=1.0. This is because both the forward and backward rate constants increase and decrease together. Initially, as k_b falls from 100 the rate of desorption falls, and the kinetic Co is able to travel slightly further. However, as k_b continues to fall, so does the forward reaction rate, and hence the Co finds it increasingly difficult to get into the hindered site. The profile is a result of a balance between these two, producing a maximum migration for k_b=1.

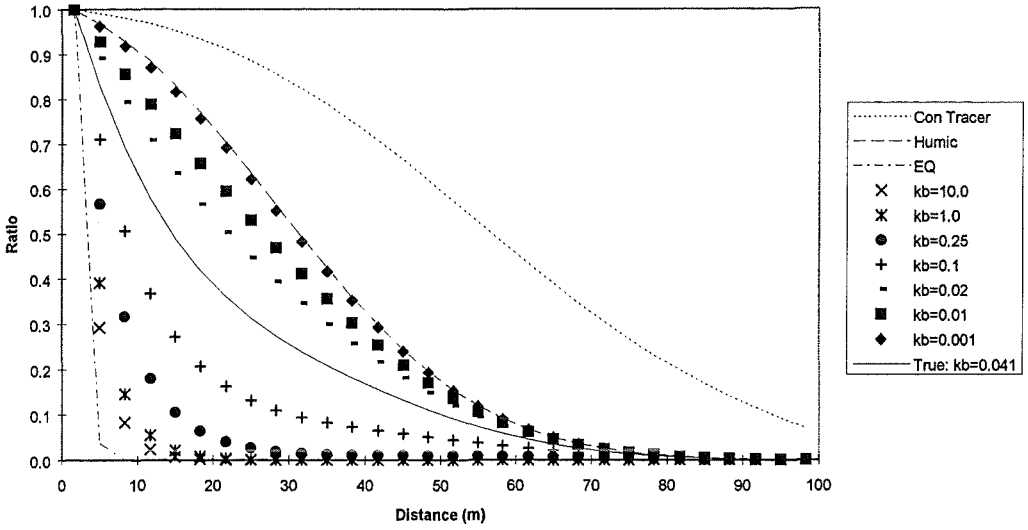

FIGURE 6: EFFECT OF FLOW RATE ON THE MIGRATION OF CO

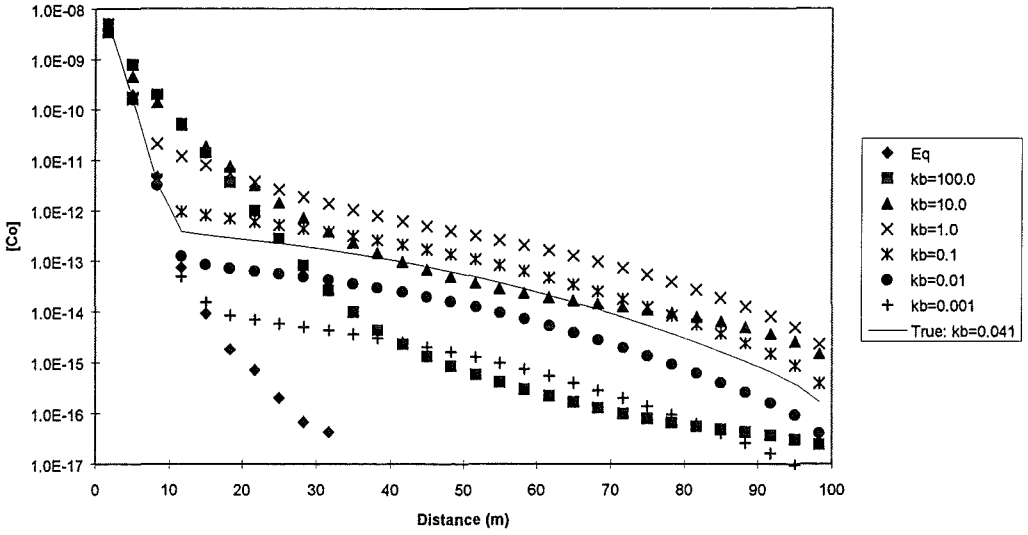

FIGURE 7: CO PROFILES OBTAINED WITH KINETICALLY HINDERED SITE INITIALLY EMPTY

The calculations performed so far have been calculated on the basis that the humic sorption reaction is a strict equilibrium. In the column experiments, this was the case, since the solid phase had not equilibrated with the concentration of humic used in those experiments. In the environment however, the solid phase will have been exposed to the ambient concentration of humics for a very long time. Therefore, it is possible that if the humic sorption process itself

is kinetically controlled, the humic and its metal complexes will not be retarded to the same extent as during the laboratory experiments. To investigate this, another series of calculations were conducted in which the humic sorption reaction was gradually changed from fast exchange to slow. Hence the reaction scheme shown in Figure 2 has been adapted to that shown in Figure 8. Note, during these calculations the values of k_f and k_b were kept fixed at the true values; 0.02 and 0.041 respectively.

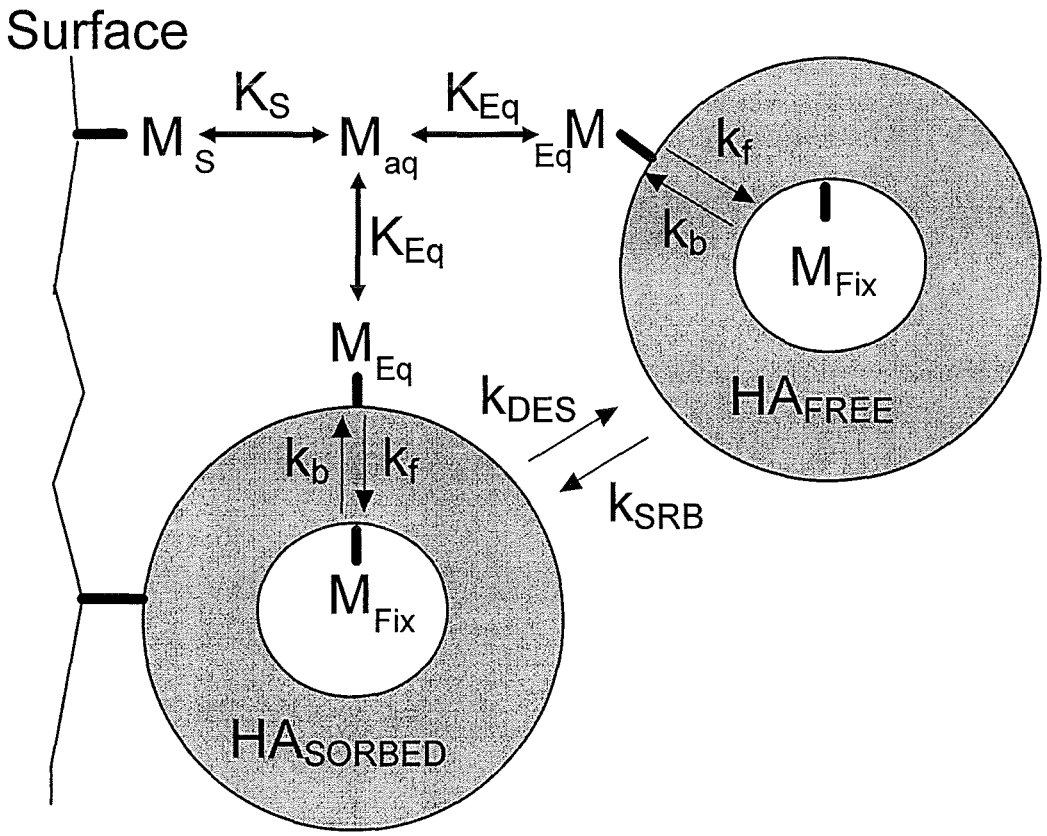

FIGURE 8: SYSTEM OF EQUATIONS WITH A KINETICALLY SLOW HUMIC SORPTION REACTION

As before, the values of k_{SRB} and k_{DES} were changed together to maintain the same effective equilibrium constant. The profiles obtained are shown in Figure 9. As the humic sorption reaction becomes slower, the extent of migration increases, once again, converging to a limit.

To understand this behaviour, the ratio plot should be examined (Figure 10). The ratio plot shows that, as k_{SRB} decreases, the kinetic Co behaviour does tend to some limit, but that this does not correspond to the conservative tracer limiting behaviour. This is because, even though the humic itself is moving as a conservative tracer, the kinetically hindered Co does not, because the Co desorption step is sufficiently fast that it is still retarded to some extent.

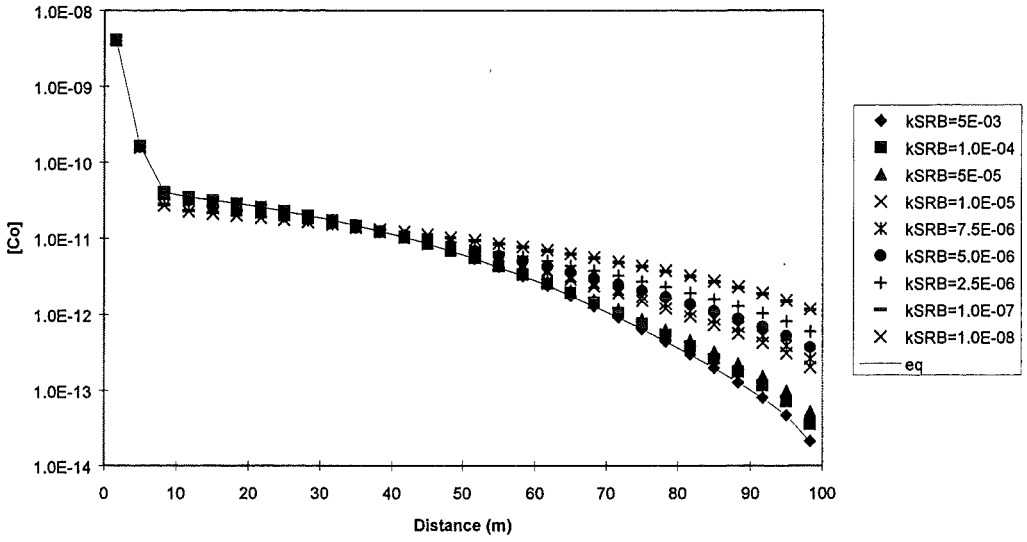

FIGURE 9: EFFECT OF SLOW HUMIC SORPTION ON CO PROFILE

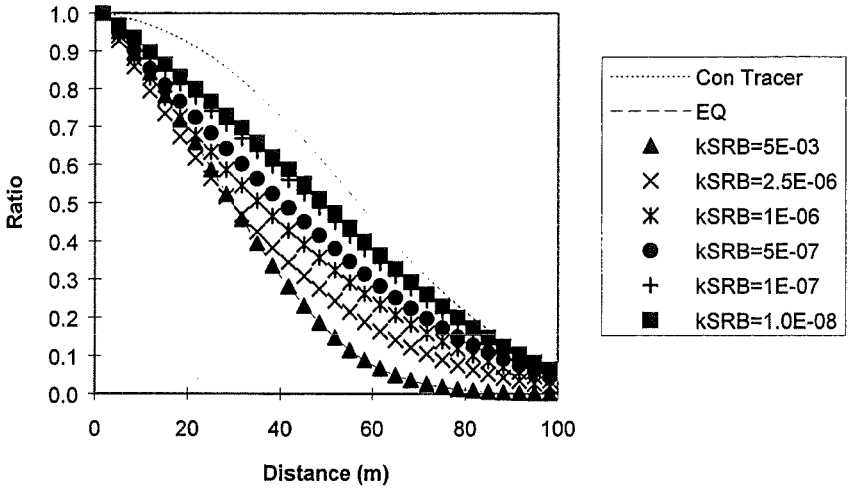

FIGURE 10: EFFECT OF SLOW HUMIC SORPTION ON KINETIC CO

As a final study, a series of calculations was carried out with k_{SRB} =1.0E-08, but once again changing the vales of k_f and k_b. The ratio plot is shown in Figure 10.

The behaviour in Figure 10 is similar to that displayed in Figure 5. The difference is that the kinetic Co is no longer limited by the humic sorption process and instead tends towards the behaviour of a conservative tracer as k_b decreases. Therefore, in the case of no significant retardation of the humic molecules, the range of values which need a rate equation to be described precisely is $10 > k_b > 0.02$. Above k_b=10, the kinetically hindered fraction may be described with the exchangeable fraction equilibrium constant, and below k_b=0.02, the behaviour approximates to that of a conservative tracer.

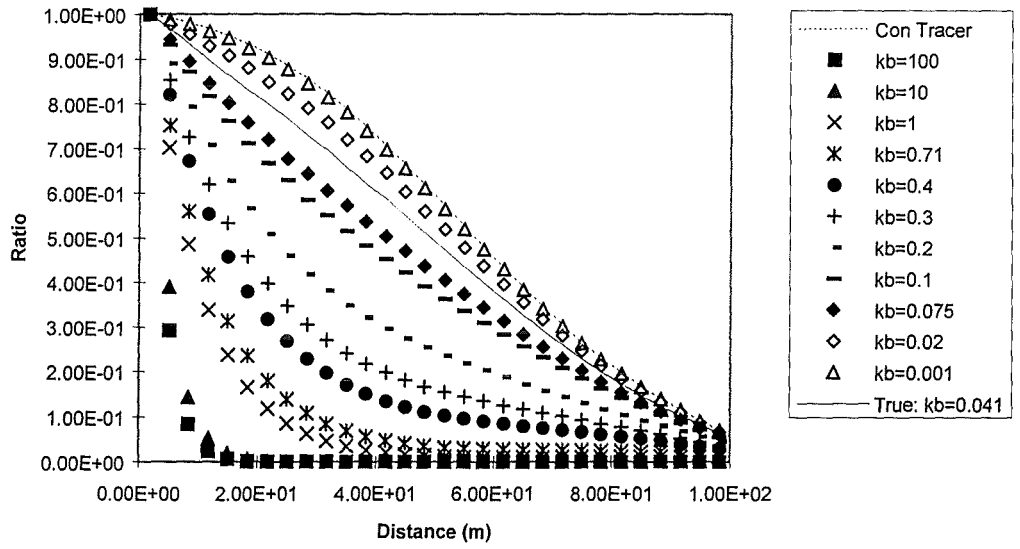

FIGURE 11: EFFECT OF k_b ON KINETIC CO BEHAVIOUR FOR SLOW HUMIC SORPTION

CONCLUSIONS

Although chemical kinetics are crucially important in metal-humate chemistry, these preliminary calculations show that it is not always necessary to use rate equations in order to predict the transport of humic bound radionuclides. Indeed, these calculations offer hope that it may well be possible to obtain realistic migration predictions using very simple transport

models. Further work is required in order to produce a set of instructions for the inclusion of humic substances in radiological performance assessment.

Several areas of uncertainty have been identified. The nature of the binding of humic substances to natural surfaces will be crucial. Whether or not the exchange between sorbed and solution phase humic molecules is rapid is likely to have a significant influence upon the migration of the kinetically hindered metal fraction. At present, these sorption processes are poorly understood, and more work is required to address this problem. Another significant source of uncertainty is expected to be the initial state of the humic metal complex as it enters the far field. This is likely to be a more difficult problem, since it will depend upon the nature of the near field and the interface between the near and far fields.

REFERENCES

N.D. Bryan A Modelling study of humate mediated metal transport. In *Effects of Humic Substances on the Migration of Radionuclides: Complexation and Transport of the Actinides.* pp 245 - 262 Ed. G. Buckau. Wissenschaftliche Berichte (FZKA 6124, ISSN 0947-8620), Forschungszentrum Karlsruhe Technik und Umwelt, Karlsruhe, Germany (1998).

Schussler W., Artinger R., Kienzler B. and Kim J.I. Modelling of Humic Colloid Mediated Transport of Amercium(III) by a kinetic approach. In *Effects of Humic Substances on the Migration of Radionuclides: Complexation and Transport of the Actinides.* pp 245 - 262 Ed. G. Buckau. Wissenschaftliche Berichte (FZKA 6124, ISSN 0947-8620), Forschungszentrum Karlsruhe Technik und Umwelt, Karlsruhe, Germany (1998).

Annex 15

Sorption of Humic Acids to Kaolinite and Goethite

(Carlsen et al., NERI)

SORPTION OF HUMIC ACIDS TO KAOLINITE AND GOETHITE

Lars Carlsen[1], Pia Lassen and Mai-Britt Volfing

National Environmental Research Institute, Department of Environmental Chemistry, DK-4000 Roskilde, Denmark

1) (Corresponding author e-mail: LC@DMU.DK)

Abstract

The sorption of humic acids to kaolinite and goethite has been investigated as function of the humic acid:mineral ratio. In both cases significant sorption of the humic material to the minerals was noted, the sorption to goethite, however, being significantly more pronounced than to kaolinite. Sorption of humic acids to kaolinite was apparently controlled by interaction between the humic material and the edges of the mineral particles whereas the sorption to goethite probably involves the entire mineral surface. Sorption to kaolinite apparently took place over the full size range of the humic material, whereas indications of a preference for the larger size fractions was noted in the case of sorption to goethite.

Introduction

It is well known that humic substances interact with polyvalent metal ions and organic pollutants thereby altering the migration and sorption properties of the ions and pollutants (Carlsen, 1989, 1992; Randall et al., 1996). Further the interaction between humic substances and mineral surfaces may also play a crucial role in determining the fate of pollutants in e.g. the soil/ground water system due to significant changes in surface characteristics as a consequence of the surface coating with organic material (Haas and Horowitz, 1986; Keoleian and Curl, 1989; Takahashi et al., 1996; Kretzschmar et al., 1997). These interactions can be described by the following reactions:

$$\mathbb{S} + \text{DOM} \rightleftharpoons \mathbb{S}\text{-DOM}$$

$$\mathbb{S} + \text{Me} \rightleftharpoons \mathbb{S}\text{-Me}$$

$$\text{DOM} + \text{Me} \rightleftharpoons \text{DOM/Me}$$

$$\mathbb{S} + \text{DOM/Me} \rightleftharpoons \mathbb{S}\text{-DOM/Me}$$

$$\mathbb{S}\text{-DOM} + \text{Me} \rightleftharpoons \mathbb{S}\text{-DOM/Me}$$

$$\mathbb{S}\text{-Me} + \text{DOM} \rightleftharpoons \mathbb{S} + \text{DOM/Me}$$

$$\mathbb{S}\text{-DOM/Me} + \text{DOM} \rightleftharpoons \mathbb{S}\text{-DOM} + \text{DOM/Me}$$

where DOM is dissolved organic matter, e.g. humic substances, Me is a metal pollutant or an organic contaminant and $\mathbb{S}$ a binding site on a solid surface such as on a mineral or clay surface etc. The above equations represent a complex chemical system and in order to simplify this system, usually, only one or a maximum of two of the above equations are experimentally investigated at a time.

We have previously studied the interaction between humic acids and alumina (Carlsen et al., 1995a, 1995b; Lassen et al., 1996). The present paper describes analogous investigations on the sorption of humic acids on Na-kaolinite and goethite focussing on the possible influence of the humic acid:mineral ratio. The possible size fractionation during the sorption process is discussed.

Experimental

Preparation of Na-kaolinite:
Kaolinite on Na-form was prepared by washing kaolinite with 1 M NaCl for 1 hour. The kaolinite was subsequently isolated by centrifugation and washed with 10^{-3} M NaCl 4 x 1 h corresponding to equilibrium (i.e. no chance in the aqueous concentration), isolated by centrifugation and filtration. The final product was air-dried and stored in a closed container.

Preparation of goethite:
A solution of 1 M $Fe(NO_3)_3$ was added 5 M KOH (ratio 1: 1.8) under stirring. The solution was diluted approximately 5 times with water and left for a minimum of 60 h at 70°C. During this period ferrihydrite was converted to goethite. The precipitate was isolated by centrifugation and washed with water until the supernatant was colourless. The goethite was isolated by centrifugation and air dried. The final product was the pulverised and stored in a closed container.

Humic acid solutions:
Stock solution of humic acids: 1.000 mg/L humic acids (obtained as sodium salt form Aldrich Co.) were dissolved in water and filtered through a 0.45 µm filter. pH was adjusted to a pH of 6 with 0.1 M HCl.

Humic acid solutions, in the concentrations: 0 to 1000 ppm, were made by dilution of the stock solution of the humic acid in 0.01 M NaCl, pH 6.

The concentrations in the humic acid solutions after adsorption to mineral surfaces were determined by electronic absorption spectroscopy at 400 nm.

Sorption of humic acids to kaolinite:

The effect of humic acid concentration on the sorption of humic acid:
Solution of humic acids in 0.01 M NaCl at pH 6 were prepared in the following concentrations: 5, 10, 25, 50, 100, 150, 200, 300, 400 500, 600, 700, 800, 1000 mg/L. 10 mg kaolinite were added to 5 mL of the various humic acid solutions. The solutions were shaken over night, centrifuged and filtered through a 0.45 μm filter. The resulting concentration of humic acids in the solutions were determined by electronic absorption spectroscopy (400 nm).

The effect of the kaolinite amount on the sorption of humic acid:
Solutions of humic acids in 0.01 M NaCl at pH 6 were prepared in the following concentrations: 200 and 500 mg/L HA. 25, 200 and 600 mg kaolinite were added to 5 mL of the 200 mg/L humic acid solution, and 10, 25, 50, 100, 200, 300, 400, 500, 600, 700, 800, 900 and 1000 mg kaolinite were added to 5 mL of the 500 mg/L humic acid solution. The solutions were shaken over night, centrifuged and filtered through a 0.45 μm filter. The resulting concentration of humic acids in the solutions were determined by electronic absorption spectroscopy (400 nm).

Molecular weight distribution of humic acid after sorption:
0, 50, 100, 200, 300 and 400 mg kaolinite were added to 5 mL of a humic acid solution containing 500 mg/L. The solutions were shaken over night. After sorption the supernatants were filtered through a 0.45 μm filter and subjected to GPC using Sephadex G-25M, which was eluted with 0,05 M NaCl at a flowrate of 10 mL/h. The column eluents were continuously monitored by UV absorption at 280 nm.

The effect on pH and E4/E6 of the sorption of humic acid on various amounts of kaolinite:
0, 25, 200, and 600 mg/5 mL kaolinite were added a humic acid solution containing 200 mg/L in 0.01 M NaCl at pH 6. The solutions were shaken over night, centrifuged and filtered through a 0.45 μm filter. The solution were analysed by electronic absorption spectroscopy absorptions at 465 and 665 nm as well as pH being determined.

Sorption of humic acids to goethite:
The effect of humic acid concentration on the sorption of humic acid:
Solution of humic acids in 0.01 M NaCl at pH 6 were prepared in the following concentrations: 200, 300, 400 500, 600, 700, 800, 1000 mg/L HA. 10 mg and 25 mg goethite, respectively, were added to 5 mL of the various humic acid solutions. The solutions were shaken over night, centrifuged and filtered through a 0.45 μm filter. The resulting concentration of humic acids in the solutions were determined by electronic absorption spectroscopy (400 nm).

The effect of the goethite amount on the sorption of humic acid:
Solutions of humic acids in 0.01 M NaCl at pH 6 were prepared in the following concentrations: 200 and 500 mg/L. 25, 200 and 600 mg Goethite were added to 5 mL of the 200 mg/L humic acid solution, and 25, 50, 75 and 100 mg goethite were added to 5 mL of the 500 mg/L humic acid solution. The solutions were shaken over night, centrifuged and filtered through a 0.45 μm filter. The resulting concentration of humic acids in the solutions were determined by electronic absorption spectroscopy (400 nm).

Kinetics of sorption of humic acids:
25 mg goethite/5 mL was added a humic acid solution containing 500 mg/L in 0.01 M NaCl at pH 6. The sorption was measured by extracting samples of supernatant, between 0.5 to 48 hours after the addition of goethite. The samples were filtered through a 0.45 μm filter and analysed by electronic absorption spectroscopy (400 nm). The vials were shaken during the reaction.

The effect on pH and E4/E6 of the sorption of humic acid on various amounts of goethite:
10, 25, 50, 75 and 100 mg/5 mL goethite were added a humic acid solution containing 500 mg/L in 0.01 M NaCl at pH 6. The solutions were shaken over night, centrifuged and filtered through a 0.45 μm filter. The solution were analysed by electronic absorption spectroscopy absorptions at 465 and 665 nm as well as pH being determined.

Results and Discussion

Sorption of humic acids to the minerals Na-kaolinite and goethite has previously been investigated (Parfitt et al., 1977; Day et al., 1994; Kaiser and Zech, 1997; Varadachari et al., 1997). In the present study the sorption of humic acids to the minerals Na-kaolinite and goethite was studied for varying humic acid:mineral ratios, the humic acids were applied in concentrations higher than in the previous studies. Thus, experiments conducted include sorption of humic acids in varying concentrations to a fixed amount of the mineral and sorption of humic acids in a fixed concentration to increasing amounts of the mineral, respectively. Further, in the latter type of experiments, the possible size fractionation of the humic acids during the sorption process was elucidated through monitoring the E4/E6 ratio.

The sorption of increasing concentrations of humic acids to kaolinite (10 mg/5 mL) disclosed a somewhat confusing picture. Obviously, an increasing sorption with increasing humic acid concentration was noted as visualized in Fig. 1 using average data for 7 individual experiments. However, the variation within the single sets of experiments are rather large as seen from the figures in Table 1, giving the average values as well as the standard deviations for the equilibrium concentrations of the humic acids in solution and on the solid phase, respectively.

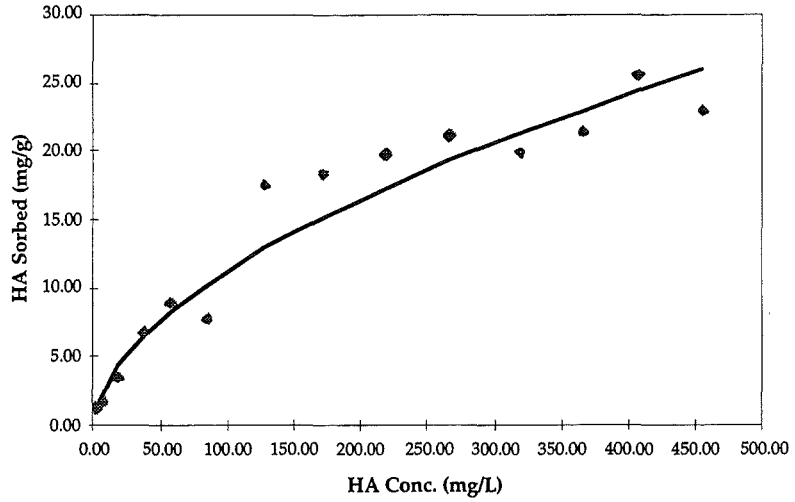

Figure 1. Sorption of humic acids to a fixed amount (10 mg/5 mL) of kaolinite. The experimental values are average values of 7 individual experiments. The solid line visualizes the Freundlich isotherm.

Table 1. Average values and standard deviation for humic acid concentrations in solution and on kaolinite at equilibrium

Humic acid Conc. in solution (mg/L)	Standard deviation	Humic acid Conc. on kaolinite (mg/g)	Standard deviation
2.16	1.37	1.42	0.69
6.45	1.98	1.78	0.99
17.86	5.54	3.57	2.77
36.34	8.44	6.83	4.22
56.93	13.13	9.04	6.57
84.44	9.90	7.78	4.95
127.15	26.07	17.60	8.61
170.17	25.55	18.41	10.60
217.03	26.85	19.85	11.01
265.40	27.83	21.23	10.16
317.40	30.71	19.95	13.08
364.09	32.53	21.47	14.62
406.05	35.51	25.64	16.30
453.91	40.86	23.04	20.43

It is immediately seen that the sorption isotherm is non-linear. The isotherm can best be modelled with a Freundlich type isotherm

$$C_{kaolinite} = 0.9 \, x \, C_{sol}^{0.55} \qquad (1)$$

In previous investigations on the sorption of humic acids on alumina have showed that the sorption of humic acid on alumina reach an equilibrium approximately 10 times higher (within the humic acid concentration range of 0-500 mg/L) (Lassen et al. 1996). The apparently lower

sorption capacity of kaolinite may, however, be explained in form of fewer sorption sites available on kaolinite compared to alumina.

Sorption sites is in the present context used as a general term reflecting the amount of humic material bound per gram solid material. Several research groups have found that the sorption mechanism for the interaction of humics with kaolinite and alumina primarily can be explained as ligand exchange. Although no exact values concerning the available number of sorption sites available for ligand exchange, the larger amount of humics sorbed to alumina relative to kaolinite can be elucidated by the difference of structure and site densities of the hydroxylated sites on the two solid materials.Thus, metal oxides and hydroxides like alumina typically exhibit octahedral sheet structure, whereas the class of phyllosilicate minerals like kaolinite ($[Si](Al_4)O_{10}(OH)_8$) exhibit a layered structure of tetrahedral and octahedral sheets. This structure shields most of the aluminol groups, thus leaving only aluminal groups at the edges of the layered silica sheets available for sorption by ligand exchance, where further steric hinderance may limit the humic acid sorption. In contrast to this the hydroxylated sites in alumina are more evenly distributed across the mineral surface leaving a higher number of sites available for humic sorption.

It should be emphasized that pH of the humic acid - kaolinite solution was around 6.8 virtually unaffected by the humic acid:mineral ratio. Thus, pH is more than 2 unit above the pH_{pzc} for kaolinite (4.6, cf. Schwarzenbach et al., 1993). This would a priori suggest that the negatively charged humic acids should not be sorbed to the kaolinite as the surface would be negatively charged at pH 6.8. However, since the sorption is controlled by alumina-like moieties at the edges it can be assumed that a pH_{pzc} for alumina, i.e. 8.5 (Schwarzenbach et al., 1993) prevails at a microscopic level for these sites leaving them positively charged or neutral and as such available for the humic acid molecules.

The rather high uncertainties in establishing the humic acid concentrations following sorption to kaolinite most probably reflect the problems associated with the variations in the small (10 mg) samples af kaolinite. Visual inspection by microscopy of the kaolinite particles disclosed significant variations in size and shape. As the sorption apparently is controlled by sites available at the edges of the individual particles (vide supra), the variations observed simply reflects variations in the number of available sites in the single preparations.

This assumption gains further support in the second set of experiments where increasing amounts of kaolinite are brought into equilibration with a solution of humic acid with a fixed concentration (2.5 mg/5 mL). The results are visualized in Fig. 2, the significant variations at low amounts of kaolinite (cf. Fig. 2B) apparently being cancelled in the cases where larger amounts of kaolinite are used. In the latter case the available number of edges being averaged.

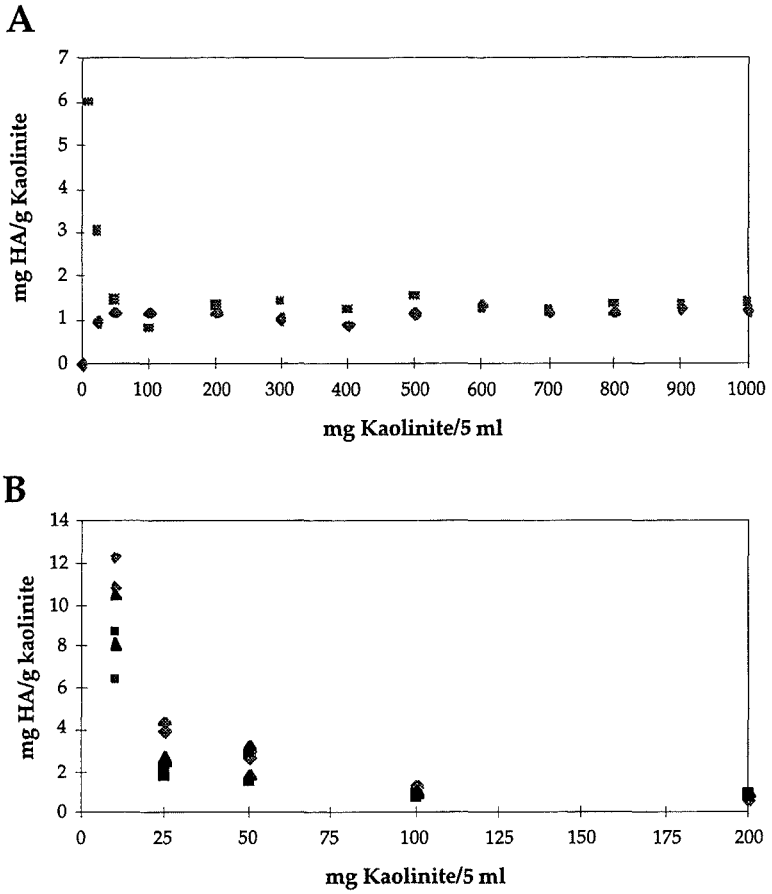

Figure 2. Sorption of humic acids to kaolinite as function of amount kaolinite (A: 0-1000 mg; B: 0-200 mg) brought into contact with 5 mL of a 500 mg/L humic acid solution.

It is noted (Fig. 2) that for increasing amounts of kaolinite an equilibrium is achieved corresponding to approximatly 1.1 mg humic acid pr. gram kaolinite.

In our previous study on the sorption of humic acids to alumina (Lassen et al., 1966) it was unambiguously demonstrated that a certain size fractionation of the humics was obtained. Thus, apparently alumina exhibits a certain preference for the smaller molecular size fractions of the humic acids. In the present study we monitored the E4/E6 ratio in the series of sorption experiments summarized in Fig. 2A. In Fig 3 the measured E4/E6 ratios of function of the amounts of kaolinite added to the 5 mL humic acid solution (500 mg/L) are depicted.

It is seen (Fig 3) that the E4/E6 ratio, which varies from approx. 5.8 (10 mg kaolinite) to approx. 5.4 (1000 mg kaolinite), virtually is constant throughout the investigated range of kaolinite. Thus, it can be concluded that only very minor, if any, size fraction takes place in favour of the smaller size fractions.

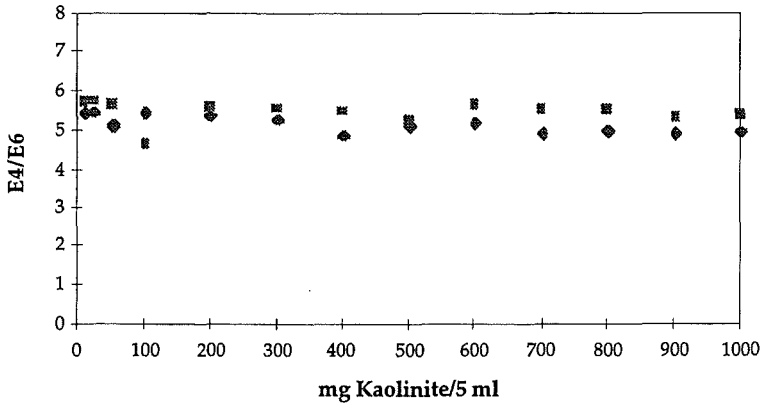

Figure 3. E4/E6 ratios as function of the amount of kaolinite added to 5 mL of a 500 mg/L humic acid solution.

This is further substantiated by analyzing the humic acid solutions following contact with varying amounts of kaolinite by size exclusion chromatography. In Fig. 4 the chromatographic traces of the resulting humic acid solutions are given. In our previous study (Lassen et al., 1966) the preference of alumina to sorb the smaller size fractions were unambiguously demonstrated through the chromatographic analysis. On the other hand the present chromatographic analysis (Fig. 4) obviously verified the apparent lack of any significant size fractionation by sorption of humic acids to kaolinite.

Turning to goethite a similar set of experiments has been conducted. The sorption of humic acids to goethite has previously been studied by Day et al. (1994), however, at rather low humic concentrations. In the present study we have investigated the sorption in the range up to 1000 mg/L humic acids.

In agreement with the previous study (Day et al., 1994), we found that the sorption of humic acids to goethite was rather rapid and probably finalized within minutes after bringing the mineral into contact with the humic acid solution. Since pH_{pzc} for goethite is 7.5 (Schwarzenbach et al., 1993) the surface bears a net positive charge at the pH value prevailing in the present study (6.5-7) and thus being subject to sorption of humic acids.

The sorption of humic acids to goethite has been described as ligand exchange (Parfitt et al., 1977). Day et al. (1994) suggested that the sorption of humic acids to goethite followed a Langmuir type isotherm. We studied the sorption process using different amounts of goethite. In Fig. 5 the sorption isotherms for 10 and 25 mg goethite, respectively, are shown.

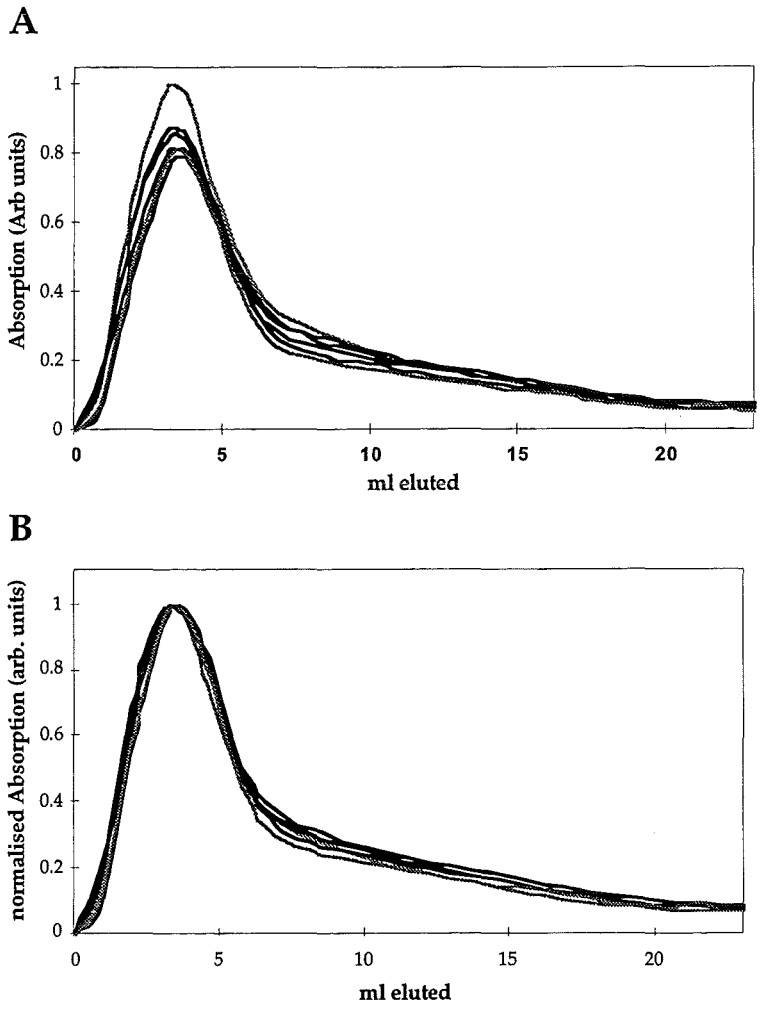

Figure 4. Chromatographic traces (A: as obtained, B: normalized to the peak eluted after ca. 4 min) of a 500 mg/L humic acid solution following contact with varying amounts of kaolinite.

At the lower humic acid concentrations, i.e. up to approx. 400 mg/L, the sorption may well proceed following a Langmuir type isotherm as elucidate for the sorption of humic acids to 25 mg goethite (Fig. 5B) the Langmuir isotherm being given by

$$C_{goethite} = 42 \times 0.0275 \times C_{sol}/(1+0.0275 \times C_{sol}) \qquad (2)$$

However, it appears that the sorption of humics increases dramatically by a further increase of the humic acid concentration. The latter three points in Fig. 5 correspond to nominal humic acid concentrations of 700, 800 and 1000 mg/L. This may be a result of significant changes in the surface characteristics upon sorption of the humics. Thus, after the surface initially are covered completely by a humic acid layer different sorption mechanisms seem to operate. This subject is not further pursued in the present study.

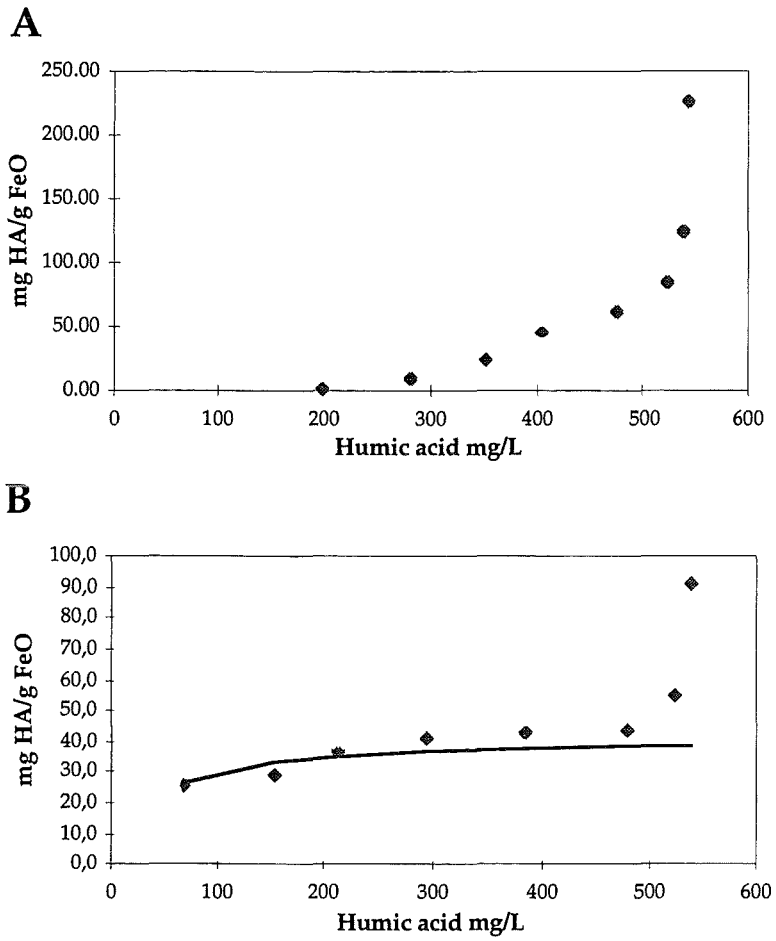

Figure 5. Sorption of humic acids to a fixed amount (A: 10 mg/5 mL, B: 25 mg/L) of goethite. The given results are results of single experiments. The solid line in Fig. 5B visualizes the Langmuir isotherm.

The second set of experiments, i.e. the sorption of humic acids to goethite from a solution of fixed concentration is visualized in Fig. 6. These experiments have been conducted using two different humic acid solutions. Thus, the sorption to goethite from a 200 mg/L humic acid solution was studied for goethite in the range from 10-600 mg/5mL (Fig. 6A) and from a 500 mg/L solution in the range of 10-100 mg of goethite (Fig. 6B).

As disclosed above in the case of kaolinite, the amount sorbed decreased with increasing amounts of goethite. In the case of sorption from the 200 mg/L solution (Fig. 6A) the equilibrium solution seems to level out around 1.7 mg humic acid pr. gram goethite at approx. 600 mg of goethite/5mL solution. However, this is simply a result of a virtually complete removal of the humic acids from the solution. Consequently a second experiment was carried out using a 500 mg/L humic acid solution. Obviously an analogous trend are noted (Fig. 6B). However, in the latter case the highest amount of goethite used was 100 mg. The total amount of humic acids

sorbed at 100 mg goethite amounts to 2 mg corresponding to 80% of the humic acids available, unambiguously demonstrating the very efficient sorption of humics to goethite.

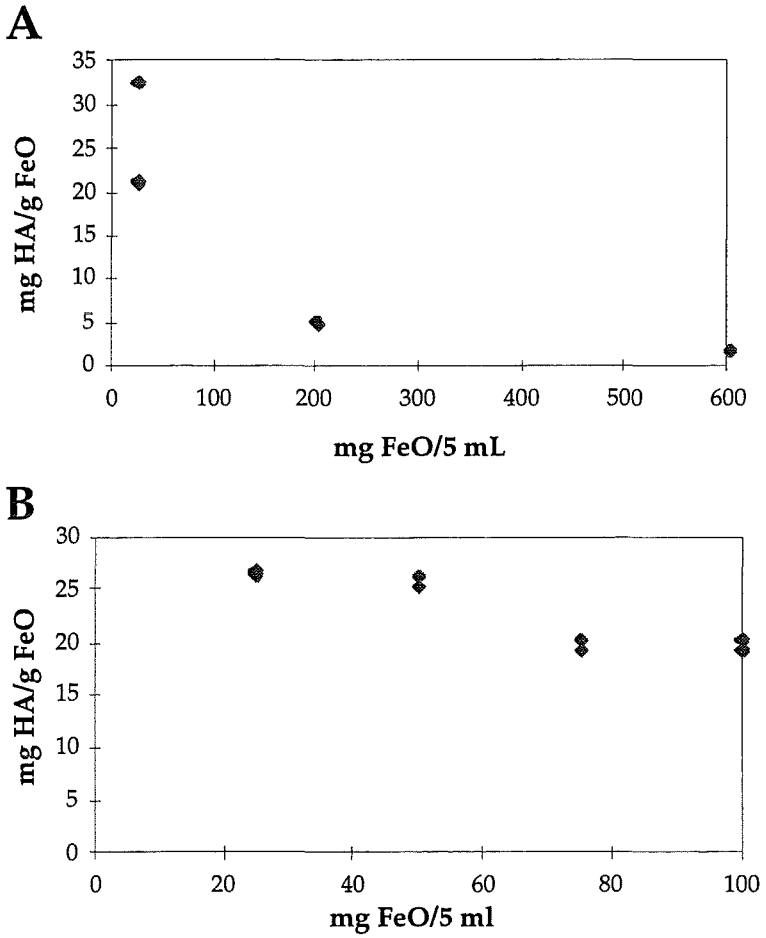

Figure 6. Sorption of humic acids to goethite as function of amount goethite brought into contact with 5 mL of a humic acid solution (A:200 mg/L humic acids, B: 500 mg/L humic acids). The given results are results of experiments carried out in duplicate.

Kaiser and Zech (1997) claim the sorption of higher molecular fractions of dissolved organic matter to be preferred by goethite apparently due to a more favourable sterical arrangement of the functional groups. In agreement with these findings we observed an increase in the E4/E6 ratio when analyzing the humic acid solution resulting from the above experiment summarized in Fig. 6B. In Fig. 7 the variation in the E4/E6 ratio is visualized as function of the amounts of goethite brought into contact with the humic acid solution. In agreement with the rather rapid sorption of humic acids to goethite, we did not observe any change in the E4/E6 ratio as function of time.

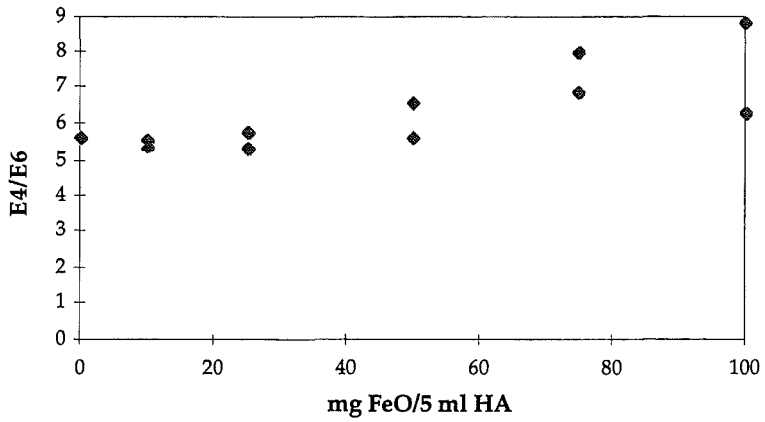

Figure 7. E4/E6 ratios as function of the amount of goethite added to 5 mL of a 500 mg/L humic acid solution.

The above suggested size fractionation of humic acids upon sorption to goethite has not yet been verified by size exclusion chromatography.

Investigations of the possible desorption of humics from the mineral surfaces are pending.

Conclusions

Humic acids are effectively sorbed to kaolinite and goethite surfaces. In both cases the sorption most probably can be described to ligand exchange. However, in the case of kaolinite the sorption takes place at reactive edges exhibiting alumina-like characteristics, whereas in the case of goethite the entire surface apparently is coated with humics. The sorption to kaolinite is best described by a Freundlich type isotherm, whereas the sorption to goethite can be modelled by a Langmuir type isotherm for humic acids concentrations up to approx. 400 mg/L. At higher concentrations a strong increase in sorption was observed probably due to other sorption mechanisms. Goethite sorbs humic acids much more effectively than kaolinite.

In the case of kaolinite no size fractionation of the humic acids was observed as a function of sorption whereas it appears that goethite favours sorption of the larger molecular sizes of the humic acids.

References

Carlsen, L. (1989)The role of organics in the migration of radionuclides in the geosphere, **EUR-12024 EN**, Commision of the European Communities, Nuclear Science and Technology, Luxembourg, 76 pages

Carlsen, L. (1992)*Migration chemistry. Chemical and physico-chemical processes influencing the migration behaviour of pollutants*, NERI Technical Report No. 52, National Environmental Research Institute, Roskilde, 70 pages

Carlsen, L., Lassen, P. and Warwick, P. (1995a)*Sorption of humic acids to alumina: Size effects*, HUMUS - Nordic Humus Newsletter, **2**, 25-32

Carlsen, L., Lassen, P. and Warwick, P. (1995b)*Sorption of humic acids to alumina: Temperature effects*, HUMUS - Nordic Humus Newsletter, **2**, 33-38

Day, G.,McD., Hart, B.T., McKelvie, I.D. and Beckett, R. (1994) *Adsorption of natural organic matter onto goethite*, Colloids and Surfaces A: Phys.Chem. Eng.Aspects 89, 1-13

Haas, C.N. and Horowitz, N.D., (1986) *Adsorption of cadmium to kaolinite in the presence of organic material*, Water, Air, and Soil Pollut. 27, 131-140

Kaiser, K and Zech, W (1997) *Compeditive sorption of dissolved organic matter fraction to soils and related mineral phases*, Soil Sci.Soc.Am.J., 61, 64-69

Keoleian, G.A. and Curl, R.L., (1989) *Effect of humic acid on the adsorption of tetrachlorobiphenyl by kaolinite*, in Adv.Chem. vol. 219, I.H. Suffet and P. McCarthy, Eds, ACS, Washington DC, Ch. 16, 231-250

Kretzschmar, R., Hesterberg, D. and Sticher, H. (1997) *Effects of adsorbed humic acid on surface charge and flocculation of kaolinite*, SoilSci.Soc. Am.J. 61, 101-108

Lassen, P., Carlsen, L. and Warwick, P. (1996)*The interaction between humic acids and γ-Al_2O_3*, Theophrastus' Contributions to Advanced Studies in Geology, **1**, 3-16

Parfitt, R.L., Fraser, A.R. and Farmer, V.C. (1977) . *Fulvic acid and humic acid on goethite, gibbsite and imogolite*, J. Soil Sci., 28, 289-296

Randall, A., Warwick, P., Carlsen, L. and Lassen, P. (1996) *Fundamental studies on the interaction of humic materials*, **EUR-16865 EN**, Commision of the European Communities, Nuclear Science and Technology, Luxembourg, 220 pages

Schwarzenbach, R.P., Gschwend, P.M. and Imboden, D.M. (1993), *Environmental Organic Chemistry*, Wiley, New York, Table 11.5

Takahashi, Y., Minai, Y, Ambe S., Maeda, H., Ambe, F. and Tominaga, T. (1996) *Multitracer study of the influence of humate formation on the adsorption of various ions on kaolinite and silica gel*, RIKEN Review No. 13: Focused on The Multitracer, Its Application to Chemistry, Biochemistry and Biology 11

Varadachari, C. Chattopadhyay, T. and Ghosh, K (1997) *Complexation of humic substances with oxides of iron and aluminium*, Soil Sci. 162, 28-34

Annex 16

Conditioning of Columns and ^{152}Eu Migration Experiments

(Klotz, GSF-IfH)

2st Technical Progress Report

EC Project:

"Effects of Humic Substances on the Migration of Radionuclides:
Complexation and Transport of Actinides"

GSF Contribution to Task 3 (Actinide Transport)

Conditioning of Columns and ^{152}Eu Migration Experiments

D. Klotz

GSF Institut für Hydrologie

Objectives

The objectives are to determine the humate mediated migration behavior of lanthanide and actinide ions in non-tenacious loose sediments of variable grain size. For this purpose, columns experiments are conducted under variation of column length and groundwater flow-velocity. Prior to performing migration experiments, columns need to be conditioned with groundwater over several months. To ensure stable conditions, hydrological and chemical conditions are carefully monitored during conditioning. Initial migration experiments of ^{152}Eu have been conducted with the humic rich Gorleben groundwater Gohy 2227.

Experimental

Five columns with non-tenacious sediments of varying grain size from Lower Saxony (Gorleben) and Bavaria (Dornach and Upper Palatinate) were prepared and installed in an inert gas box. Properties of these columns are shown in Table 1. Preconditioning was done for six weeks with a synthetic groundwater, followed by conditioning for 37 weeks with the Gorleben groundwater Gohy-2227. The flow velocities were about 2×10^{-4} cm/s. Tracer experiments (tritiated water) were used to monitor the hydrological properties during conditioning. Initial migration experiments were conducted with ^{152}Eu at a flow velocity of 2×10^{-4} cm/s.

Development of Hydrological Properties

The five sediment columns were preconditioned by a flow of synthetic "humic matter-free" water for a period of six weeks in order to adjust to a constant grain structure. During conditioning with the humic rich groundwater Gohy-2227, hydrological properties also vary through sorption of humic substances. Development of hydrological properties (effective porosity and longitudinal dispersivity) over the approximately 8.5 months of preconditioning/ conditioning are shown in Table 1.

Table 1: Properties of columns during conditioning. Preconditioning is done for six weeks with synthetic "Gorleben Sweet Water" and conditioning with the Gorleben groundwater Gohy-2227.

Column No.:	1	2	3	4	5
			Sediments		
Origin	Dornach/ Bavaria	Gorleben/ Lower Saxony	Gorleben/ Lower Saxony	Gorleben/ Lower Saxony	Oberpfalz/ Bavaria
Type	Sandy Pebbles/ Gravel	Fine Sand	Fine Sand	Medium Course Sand	Course Sand
Composition	Carbonate	Mixed	Mixed	Mixed	Silicate
Porosity, Total	0.200	0.333	0.343	0.326	0.394
Density (g/cm^3, dry)	2.23	1.76	1.78	1.81	1.69
			Columns		
Preconditioning (six weeks)					
Porosity, Effective	0.12 ± 0.02	0.32 ± 0.01	0.33 ± 0.01	0.31 ± 0.02	0.37 ± 0.01
Dispersivity, Longitudinal (cm)	7.5 ± 1.0	0.17 ± 0.01	0.12 ± 0.05	0.13 ± 0.06	0.15 ± 0.05
Conditioning (Gohy-2227)			Porosity/ Dispersivity:		
Days:					
1	0.086 / 8.7	0.309 / 0.17	0.318 / 0.10	0.287 / 0.17	0.353 / 0.15
7	0.078 / 12.0	0.314 / 0.17	0.312 / 0.13	0.286 / 0.16	0.343 / 0.18
14	0.078 / 14.5	0.285 / 0.19	0.308 / 0.14	0.281 / 0.17	0.341 / 0.18
28	0.099 / 8.5	0.353 / 0.15	0.284 / 0.12	0.318 / 0.13	0.318 / 0.22
42	0.088 / 13.8	0.281 / 0.22	0.313 / 0.23	0.281 / 0.13	0.314 / 0.20
56	0.091 / 15.0	0.267 / 0.19	0.315 / 0.09	0.281 / 0.10	0.320 / 0.23
70	0.080 / 18.4	0.271 / 0.22	0.300 / 0.13	0.265 / 0.18	0.286 / 0.34
84	0.085 / 15.6	0.266 / 0.24	0.299 / 0.13	0.262 / 0.24	0.288 / 0.34
98	0.075 / 20.0	0.265 / 0.27	0.295 / 0.15	0.258 / 0.26	0.285 / 0.35
112	0.082 / 14.2	0.273 / 0.23	0.300 / 0.13	0.261 / 0.25	0.288 / 0.29
140	0.091 / 10.3	0.260 / 0.28	0.292 / 0.17	0.264 / 0.27	0.285 / 0.36
168	0.091 / 20.0	0.260 / 0.23	0.282 / 0.15	0.259 / 0.22	0.272 / 0.33
196	0.087 / 23.2	0.270 / 0.24	0.298 / 0.17	0.272 / 0.26	0.282 / 0.36
224	0.089 / 21.9	0.278 / 0.21	0.296 / 0.13	0.262 / 0.24	0.286 / 0.27
259	0.085 / 14.5	0.288 / 0.15	0.290 / 0.14	0.261 / 0.25	0.283 / 0.31
Development during Conditioning (in % of extrapolated starting value / day)					
Porosity	- 0.03	- 0.05	- 0.03	- 0.05	- 0.09
Dispersivity	0.32	0.07	0.07	0.34	0.04

Linear regression

$$y = A + B \cdot t$$

where y = effective porosity n_{eff} or dispersivity α

t = time [d]

A = intercept of the axes

B = slope of the curve

show the following tendencies during approximately 8.5 months conditioning:

1. Decrease in effective porosity with time.
2. Increase in longitudinal dispersivity with time.

When water containing humic matter flows through the sediments, the humic matter is bound in the grain structure. These thin humic matter films reduce the effective flow volume, whereas the grain size and possibly the non-uniformity are increased. An increase in these two grain characteristics leads to an increase in hydrodynamic dispersion.

^{152}Eu Migration

Initial ^{152}Eu migration experiment were conducted at a filter velocity of about 2.3 x 10^{-4} cm/s. The ^{152}Eu spiked humate solution (0.37 MBq) were conditioned for approximately three months prior to migration experiments. The migration results are presented in Table 2. Eu humate is transported without retardation (retardation factor approx. 1). The negatively charged Eu humate particles are found to be somewhat in front of the water transport in the fine-grained loose sediments having a large surface and a negative surface charge, as determined using tritiated water (retardation factor $R_f \geq 0.94$). The recovery as a measure of the physical migration of the Eu humate particles increases with growing grain size, as expected.

Table 2: Results of ^{152}Eu migration experiments in different columns (cf. Table 1) with the humic rich groundwater Gohy-2227.

Column No.:	1	2	3	4	5
			Sediments		
Origin	Dornach/ Bavaria	Gorleben/ Lower Saxony	Gorleben/ Lower Saxony	Gorleben/ Lower Saxony	Oberpfalz/ Bavaria
Type	Sandy Pebbles/ Gravel	Fine Sand	Fine Sand	Medium Course Sand	Course Sand
^{152}Eu Recovery (%)	82.9	77.8	78.8	82.4	82.8
Retardation Factor	0.94	0.96	0.97	1.00	1.03

Annex 17

Complexation Studies of UO_2^{2+} with Humic Acid at Low Metal Ion Concentrations by Indirect Speciation Methods

(Montavon et al., Uni-Mainz)

COMPLEXATION STUDIES OF UO_2^{2+} WITH HUMIC ACID AT LOW METAL ION CONCENTRATIONS BY INDIRECT SPECIATION METHODS

G. Montavon, A. Mansel, A. Seibert, H. Keller, J.V. Kratz and N. Trautmann

Institut für Kernchemie - Fritz-Strassmann-Weg 2 - D-55128 MAINZ

INTRODUCTION

In the context of the safety assessment of high-level nuclear waste repositories, the quantitative description of the interaction between actinides and humic substances (mainly humic and fulvic acids) is of great importance [CHO85, CH88, CHO92]. These polymeric organic molecules are present in natural waters. They contain carboxylic and phenolic hydroxyl groups which make these compounds hydrophilic and enable them to form stable complexes with actinides [CHO88, CHO92]. Thus, they can retard the migration of the actinides when these molecules are sorbed on mineral surfaces or, conversely, increase their migration by forming dissolved complexes or colloids [CHO85, CHO92, SIL95]. The results of previous investigations have provided a wide range of complexation data [CZE97, RAO94] which have been described with numerous models [HUM97].

However, until now, most of these laboratory studies have yielded humate complexation constants for actinide concentrations above 10^{-7} M. Considering the concentration range in which the actinides may exist in nature (below 10^{-10}M), and considering the heterogeneous and irregular nature of these natural compounds [GRE97], it is of major interest to extend the complexation studies to very low metal ion concentrations to assess the applicability of the complexation models used.

This study deals with the interaction of U(VI) with humic acids (HA). U(VI) may also to some extent serve as a chemical homologue for other actinides at the oxidation state VI. Investigations have been performed at pH 4 and 5 for ionic strengths of 0.1 and $4x10^{-3}$ mol/L using metal ion concentrations ranging from 5.10^{-6}M to 10^{-8}M. The studies are based on indirect speciation methods [MAR96]: for quantification of the complexed and uncomplexed forms of the actinide ions. they are separated by (i) continuous electrophoretic ion focusing (EIF) [FRA97, MAR96,

MAN93], and (ii) anion exchange chromatography (AEC) [CZE94]. The metal ion charge neutralization model is used to deduce complexation constants [KIM96].

EXPERIMENTAL SECTION

Chemicals used were reagent grade. Humic acid was purchased from ALDRICH Company. It was purified and protonated according to [KIM90]. Its proton exchange capacity, PEC, was determined to be 4.6 meq/g [MAR96]. Uranium (>90% ^{235}U) was purified as described elsewhere [CZE94]. For experiments carried out for uranium concentrations above 10^{-7} M, ^{235}U was mixed with ^{238}U ($UO_2(NO_3)_2.6H_2O$ from MERCK). All stock and mixed solutions (HA+U(VI)) were prepared with Millipore water in a glove box under Ar atmosphere to avoid the presence of carbonates. Before the separation step, HA and U(VI) were kept in contact overnight to reach equilibrium [CZE94]. The analysis method is based on the detection of delayed-neutrons after the neutron-induced fission of the isotope ^{235}U [RUD77]. Separations by AEC and EIF were performed under normal atmosphere.

Experimental procedures

AEC and EIF allow the separation between the complexed and uncomplexed forms of U(VI), due to the different charges of the two species. Calculation of the distribution of hydrolysis species of U(VI) in solution [GRE92] shows that no anionic species exist under the experimental conditions of this work. The two separation methods are presented in the following.

<Anion Exchange Chromatography>

This technique involves anionic exchangers and is based on selective retention of the polyanionic humate complex but not the free cation. This method, based on column experiments, has been used for a long time for laboratory experiments [CZE94] as well as for environmental investigations [HIR85]. However, several assays with different kinds of exchangers from Varian (SAX, PSA and NH_2), Bio-Rad (AG 1x8) and Fluka (Sephadex DEAE A-25) have shown that this method is not suitable to the experimental conditions of this work. Especially, the adsorption of the free cation on the exchanger was particularly important for low actinide concentrations. It amounted for instance to 30% at pH=4 for [U(VI)]=10^{-8}M when following the procedure described in the literature with the SAX resin [CZE94]. This method, however, can be applied when using batch instead of column experiments: these are easier to perform and the adsorption of the free cation on the exchanger decreases significantly and can be controlled.

More details concerning adsorption effects are given under "Results and Discussion". Moreover, this method is better adapted to this study since the perturbation of the equilibrium U(VI): HA is minimum: the analyte solution is mixed directly with the exchanger and no further treatment is needed as it is the case for column experiments which require an elution step.

Experimental procedure: Before use, the exchanger was washed with methanol, converted into the perchlorate form with 0.1M $NaClO_4$ and equilibrated to the desired pH and ionic strength. The resin was mixed with 2 mL of the solution in a polyethylene tube. After shaking for 10 sec, the sample was centrifuged and 1 mL of the supernatant was taken for analysis. The variation of pH before and after the separation step did not exceed 0.1 pH unit.

<Electrophoretic Ion Focusing>

By this separation technique, the positively charged metal ion is separated from the negatively charged humate complex in an electric field. More details concerning the principle and the experimental set-up are given in [FRA97,MAR96,MAN93]. A brief scheme of the apparatus is depicted in Scheme 1.

Experimental procedure: In the system chosen, the mixed solution, M, was fed in the central region of the chamber through the inlet capillary 6. Under the effect of the electric field, the species separate and migrate towards the electrodes in an analogue solution, A, (same pH and I as those in M) introduced through capillaries 3,4,5,7,8 and 9. To stop this migration, an electrolyte solution E (same pH as that of M and A) was pumped through the four outer inlet capillaries: this solution has a higher I as compared to that of A leading to the creation of a conductivity jump, diminishing the ion migration. This leads to focusing and concentration of the two respective species at the different boundaries between solutions A and E. At the outlet of the chamber, solution was collected through 90 capillaries in 45 tubes. For simplification, the system is called 2(E):3(A):1(M):3(A):2(E).

One possible artifact is that the complex U(VI)-HA, once separated from U(VI), could dissociate in solution A [RAO94]. To examine this possible phenomenon, experiments have been carried out in the system 3(E):2(A):1(M):2(A):3(E), for which the surface of A in the separation chamber was lower. The distribution between both complexed and uncomplexed species measured after separation were similar irrespective of the system used indicating that the complex dissociation, if it occurs, can be neglected. This can be explained mainly by the rapid migration of the complex to the conductivity jump: all solutions were pumped in such a way that the residence time of the species in the separation chamber did not exceed 5 min.

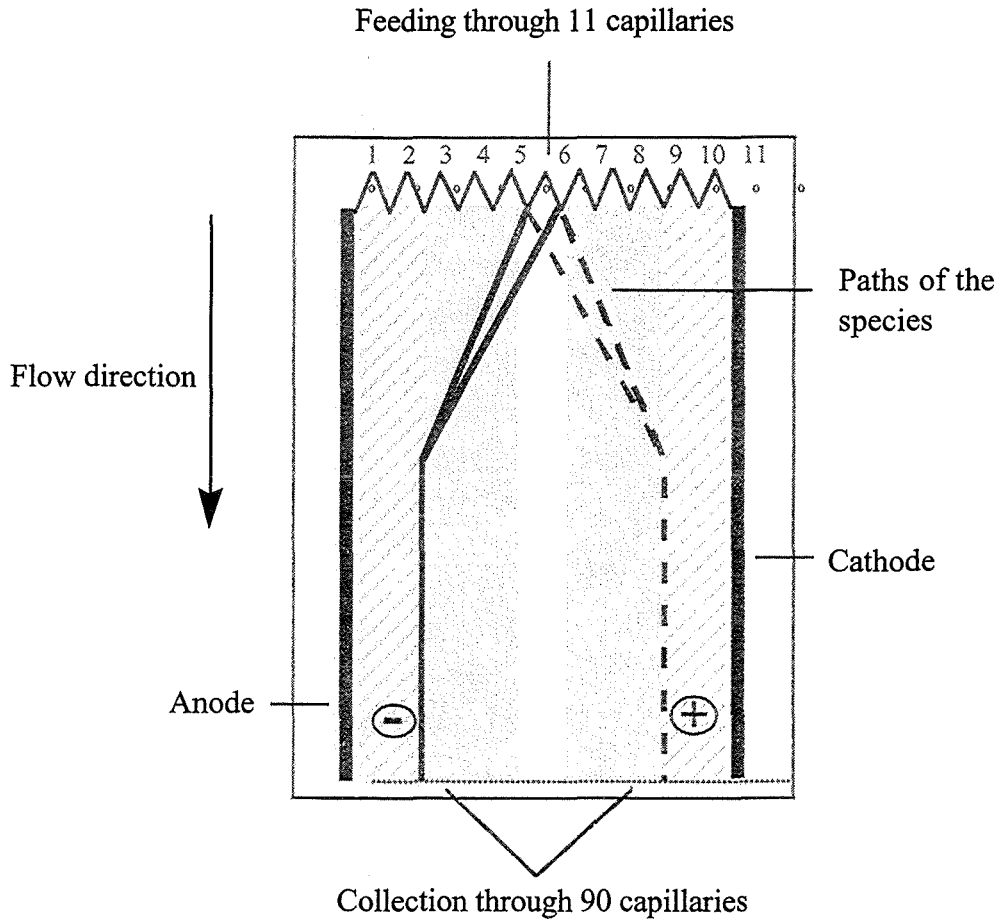

Scheme 1: Upper view of the separation chamber for continuous electrophoretic ion focusing. Mixed (white zone), analogue (gray zone) and electrolyte (dashed zone) solutions are fed via the supply capillaries into the chamber which is made of two horizontal plates kept at a distance of 0.5 mm. The paths of the species under the action of the electric field are symbolized by the full (complexed or free HA) and dashed (free cation) lines.

For illustration, a typical example for an electrophoretic separation is shown in Figure 1. The slight shift of the cationic peak (U(VI)) relative to the theoretical boundary A/E, is due to a plug of some outlet capillaries between fractions 40 and 45.

Before collection, the separation chamber was washed with solutions A, E and M in order to reach an adsorption equilibrium between the plates of the apparatus and the species. In the experimental conditions of this work, 90 min and 180 min of washing were needed for U(VI) concentrations above and below 10^{-6} M, respectively, with (HA)=2.5 mg/L. Furthermore, a buffer (MES) is used to stabilize the pH in the separation chamber.

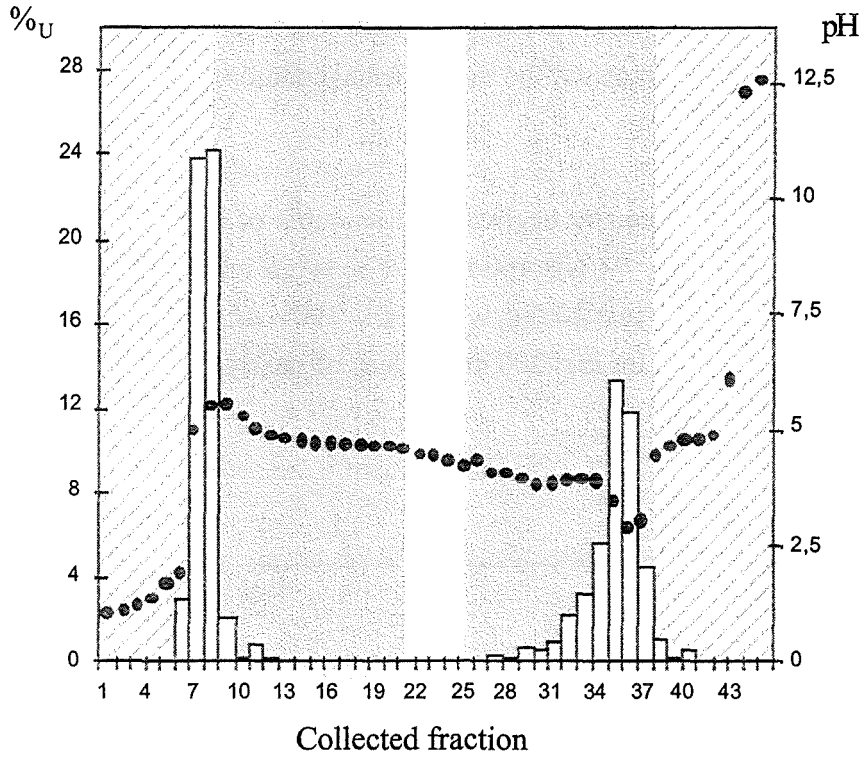

Figure 1: Separation of U(VI)-humate and U(VI) by electrophoretic ion focusing at pH 5: pH and percentage of the total U(VI) amount introduced in the chamber measured in the collected fractions. Voltage applied between the two electrodes: 600V (this resulted in an intensity current of nearly 120 mA passing through the solutions). Feed solutions: M (white zone): $[U(VI)]=1.5.10^{-6}$ M, (HA)=2.5 mg/L, [MES]=0.05 M and $[NaClO_4]=1.10^{-3}$ M; A (gray zone): [MES]=0.05 M and $[NaClO_4]=1.10^{-3}$ M; E (dashed zone): [MES]=0.05 M and $[NaClO_4]\cong 8.10^{-2}$ M.

RESULTS AND DISCUSSION

The first part of this section sums up the K_d values measured by AEC and EIF, which describe quantitatively the distribution between complexed and uncomplexed forms of U(VI). The second part deals with the evaluation of the stability constants by means of the charge neutralization model.

Investigation by AEC

The complexation of U(VI) by HA has been investigated by AEC at pH 4 and 5 with I ranging from 0.004 M to 0.1 M, C_U from 2.10^{-8} M to 5.10^{-6} M and (HA) from 1 to 2.5 mg/L. In a first

step, experiments have been carried out without HA in order to estimate the quantity of free U(VI) adsorbed on the exchanger under the experimental conditions of this work.

<Adsorption of the uranyl ion>

At pH=4, adsorption of U(VI) can be neglected for amounts of exchanger material below 150 mg. On the other hand, at pH 5, the adsorption must be taken into consideration as illustrated in Figure 2: while it is weak for m_R<40 mg, with nearly 100% of U(VI) in solution, it increases with the mass of resin to reach, for m_R=200 mg, values of nearly 30% and 20% for I=0.1 and 0.004 M, respectively.

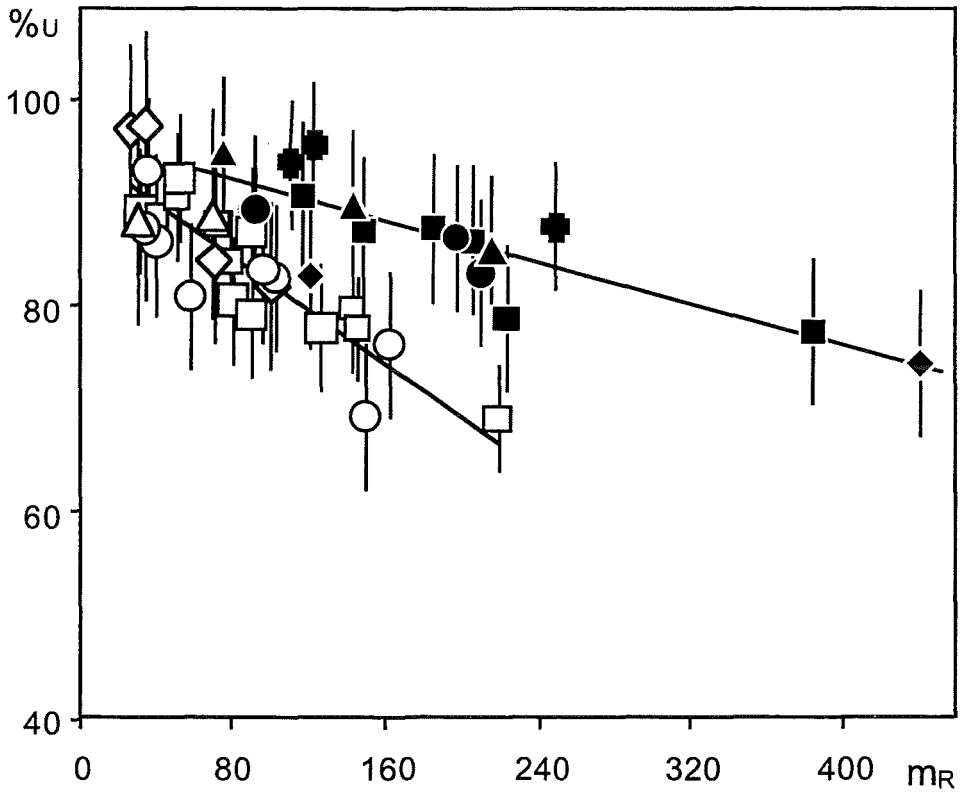

Figure 2: Percentage of U(VI) in solution after mixing with various amounts of resin (in mg) at pH=5 in 0.1 (open symbols) and 4.10^{-3}M (full symbols) $NaClO_4$. C_U=3.2 ( ), 2.8 ( ), 1.5 ( ), 1 ( ), 0.11 ( ), 0.05 ( ), 0.04 (O), 0.03 ( ) and 0.015 µM (Δ). The experimental data are described by linear relationships of the general form $\%_U=am_R+b$, with a=-0.130±0.002 and b=95±3 for I=0.1M and a=-0.051±0.009 and b=96±3 forI=4.10^{-3}M.

According to the literature, this adsorption can be explained by the presence of impurities on the exchanger which behave as cationic exchanger sites [HIR89]. In order to saturate these sites,

the resin has been treated before use with Hf^{4+} ranging from 100 to 1 μM. The results show no significant difference with respect to the data obtained with the non-treated exchanger, indicating that this explanation is not valid in this system. Most probably, this adsorption is related to the presence of hydrolysis species, more important at pH 5 than at pH 4, which are known to sorb on inactive organic material.

The decrease of U(VI) in solution varies linearly with the amount of resin m_R and it is nearly independent of the U(VI) concentration. Based on this, the effect observed can be described in the range of U(VI) concentration and mass of resin investigated by linear relationships (solid lines in Fig 2). These relations have been used for the correction of complexation data for adsorption, as described in the following.

Complexation experiments

The results obtained at pH 4 are presented in Figure 3. The K_d values are not significantly affected by the change of ionic strength, indicating a low I effect on the equilibrium U(VI):HA. At pH=5, the K_d values can be corrected for the adsorption of the free cation on the resin by the following expressions:

$[UHA]=[U(VI)]_R-[U(VI)]_{ads}$, and

$[U(VI)]=[U(VI)]_s+[U(VI)]_{ads}$

with $[U(VI)]_R$, $[U(VI)]_s$ and $[U(V)]_{ads}$ corresponding to the amount of U(VI) fixed on the resin, measured in solution and adsorbed on the resin, respectively.

The two first concentrations are determined experimentally, whereas the last one is calculated through the relation derived from adsorption experiments (see Fig. 2). Note that this correction is valid only if the composition of the free U(VI) in solution (UO_2^{2+} and hydrolysis species) in the presence of HA is not significantly affected as compared to that for a similar uranium solution (same pH and free U(VI) concentration) without complexing agent. Calculations, using the data derived from the charge neutralization model, show that this is true under the experimental conditions of this work (see below).

The K_d values corrected in this way have to be independent of the U(VI) adsorption, and thus of the amount of resin used for the experiment. This is illustrated in Figure 4, for [U(VI)]=0.031 μM, with the exception of the point for m_R=15 mg. For the latter, the lower

calculated value of K_d results from the excess amount of uranium relative to the amount of resin exchange sites.

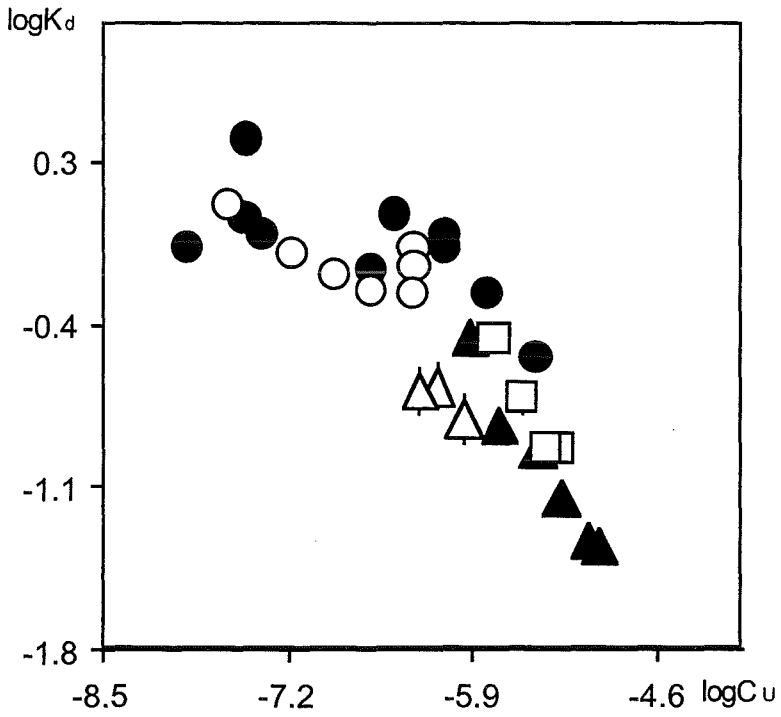

Figure 3: Effect of metal ion concentration on K_d values for humate complexation of U(VI) studied by AEC at pH=4 in 0.1 M (full symbols) and 0.004 M $NaClO_4$ (open symbols) with (HA)=2.5 (●,O), 1.5 (□) and 1 mg/L (▲,Δ).

This experiment has been repeated for other U(VI) concentrations from which mean K_d values were deduced. They are displayed in Figure 5 as a function of the nominal U(VI) concentration, the errors corresponding to the standard deviations.

Experimental data at I=0.004 M are measured in the presence of 0.05 M MES to reproduce the EIF experimental conditions (see experimental section). The good agreement between these values and those obtained at I=0.1 M without MES shows that neither ionic strength nor the buffer significantly affect the equilibrium U(VI):HA. Moreover, the K_d values are close to those measured at pH=4 (circles in dotted line) whereas the complexation ability of HA towards metal ions is known to increase with the deprotonation of HA binding sites and thus with the pH [CHO85,CHO88]. This can be explained by a weak competition between the formation of the hydrolysis species and the humate complex which increases when the pH increases.

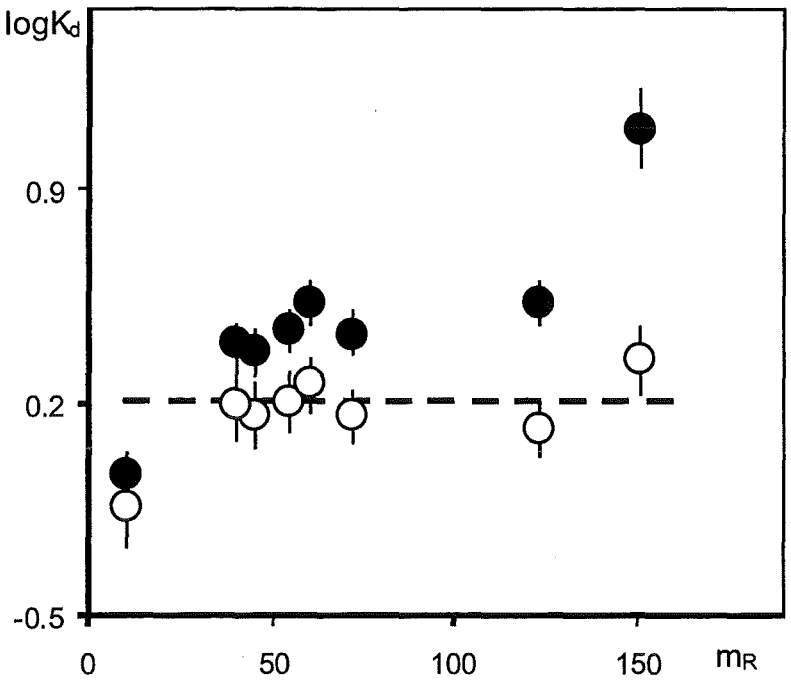

Figure 4: Humate complexation of U(VI) ($3.1.10^{-8}$ M) studied by AEC at pH=5 in 0.1 M $NaClO_4$ with (HA)=2.5 mg/L as a function of the amount of the exchanger. The open symbols correspond to the K_d values corrected from U(VI) adsorption.

Investigation by EIF

Continuous electrophoretic ion focusing is interesting because of the concentration of species occurring at the conductivity jumps; the possibility of handling a high volume of solution; and it allows extension of the complexation studies to much lower metal ion concentrations. In a first approach, however, in order to compare both separation techniques, experiments have been performed at pH 5 in the same range of U(VI) concentrations as that investigated by AEC. The K_d values obtained are shown in Figure 6 (open symbols) together with those measured by AEC (full symbols).

While there is a good agreement between both separation methods for U(VI) concentrations above 10^{-6}M, this is no longer the case when the concentration decreases. Indeed, below 10^{-6} M, the K_d values measured by EIF increase with respect to those measured by AEC to become nearly 40 times higher for the lowest U(VI) concentrations studied.

Experiments carried out without HA showed that all U(VI) was recovered at the cathode. This indicates that a probable interaction U(VI):HA, in addition to the complexation evidenced by

batch experiments, occurs in the separation chamber. In order to confirm this, an experiment was carried out by introducing into the chamber, instead of a mixed solution U(VI):HA, two solutions of free HA and U(VI) through capillaries 7 and 6, respectively. In this system, the complexation is expected to be negligible since (i) the time of contact between both species in the upper part of the chamber is very short (below 2 min) and (ii) the mixing between U(VI) and HA, based on the migration of both species, is poor. In any case, the fraction of U(VI) complexed, according to the known K_d values obtained by AEC, must not exceed approximately 30%.

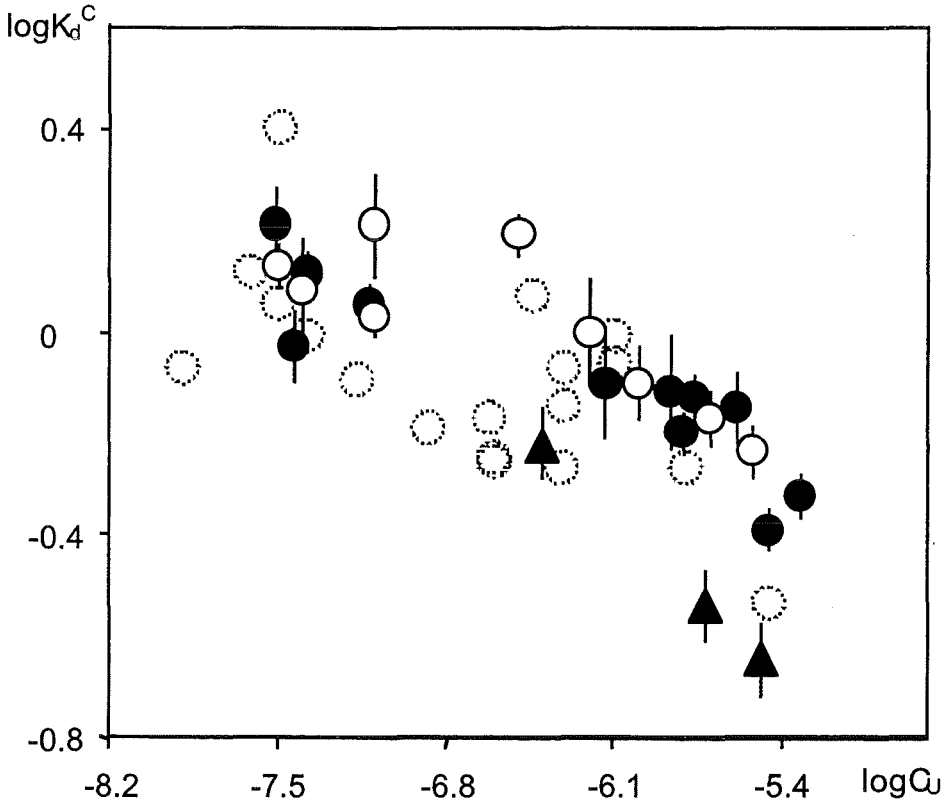

Figure 5: Humate complexation of U(VI) measured by AEC at pH=5 for I=0.1 M (full symbols, $NaClO_4$) and 0.004 M (open symbols, 10^{-3} M $NaClO_4$ + 0.05 M MES) with (HA)=2.5 (circles) and 1.25 mg/L (triangles). Effect of metal concentration on K_d values and comparison with data obtained at pH=4 for (HA)=2.5 mg/L (circles in dotted line).

Results obtained, however, showed that 81% and 67% of U(VI) was complexed for nominal metal ion concentrations of $6x10^{-8}$ and 10^{-6} M, respectively. This confirms the occurrence of an interfering interaction U(VI):HA in the electrophoresis chamber in the course of the species separation. The magnitude of this additional interaction increases with the contact time between

U(VI) and HA in the separation chamber: the analyte solution in the first experiments was introduced through one capillary whereas in the second experiment, two capillaries were used. To confirm this contact time dependence, a third experiment was carried out for $C_U=2.10^{-6}$ M in the system 2(E):2(A):3(M):2(A):2(E), for which 3 capillaries were used to introduce the mixed solution. In agreement with the assumption made above, a K_d value three times higher than that measured in the system 3(E):2(A):1(M):2(A):3(E) was determined.

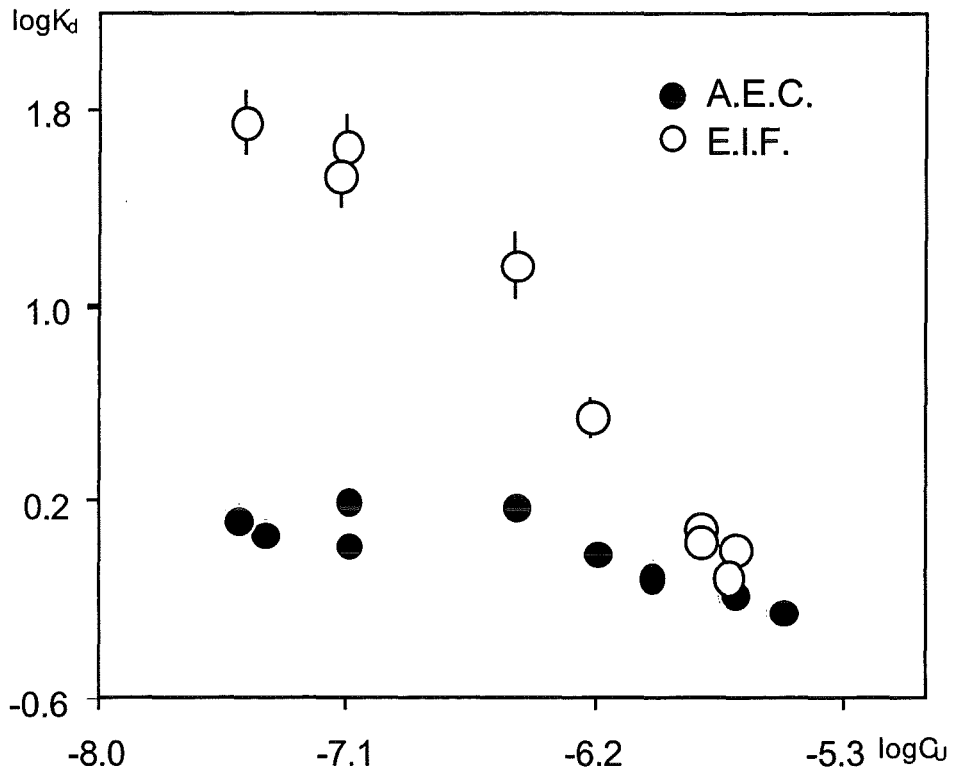

Figure 6: Humate complexation of U(VI) studied by EIF (O) and AEC (●) at pH=5 in 0.001 M $NaClO_4$ and 0.05M MES with (HA)=2.5 mg/L. Effect of metal ion concentration on K_d values.

In conclusion, the evidence for this interference makes the EIF technique not well suited for investigations of the system U(VI):HA. In addition, this effect seems to be particular to the uranyl ion, since such effect was not observed with the system Np(V):HA studied by the same method in similar experimental conditions [MAR96]. The origin of this interference remains however unknown. HA being a polycharged molecule, one could imagine a change of its configuration under the influence of the electric field leading to a change of its complexation properties.

Quantitative treatment of the experimental data obtained by AEC

In this work, the complexation equilibrium is described as a charge neutralization reaction [KIM96], the metal ion neutralizing 2 exchanging groups on the HA:

$$UO_2^{2+} + HA(II) \rightleftarrows UO_2HA(II) \qquad \textbf{(I.1)}$$

The associated stability constant is defined as

$$\beta = \frac{[UO_2HA(II)]}{[UO_2^{2+}]_f[HA(II)]_f} \qquad \textbf{(I.2)}$$

where $[UO_2HA(II)]$, $[UO_2^{2+}]_f$ and $[HA(II)]_f$ are the concentrations of the humate complex, of the free metal ion and the free HA, respectively.

The HA concentration available for complexation, [HA(II)], is calculated with the loading capacity, LC, which represents the portion of HA sites active for metal ion complexation for given pH, I, metal ion and origin of HA [KIM96]. It is related to the amount of HA in solution in g/L, (HA), by the following expression:

$$[HA(II)] = 0.5\,(HA)\,PEC\,LC \qquad \textbf{(I.3)}$$

When $[UO_2^{2+}]_f$ is known, LC is determined graphically by a slope analysis of the experimental data [KIM96]. In this study, hydrolysis species are present and only the total concentration of the free U(VI) is known. Therefore, this method cannot be applied and a new approach for the evaluation of LC values has been examined requiring a series of experimental data i, represented by the K_d^i values, measured at fixed pH and I for various nominal U(VI) concentrations, C_u^i.

In a first step, the stability constant β is fixed arbitrarily and the LC^i values are calculated and plotted as a function of $\log C_U^i$. The curve obtained is fitted by a straight line and its slope a(β) is associated with the couple of values β,LC(β), where LC(β) corresponds to the mean LC value calculated from LC^i. What we assume, is that the LC values are independent of the U(VI) concentration under the experimental conditions of this study, C_U^i being much lower than I. Therefore, in a second step, β is varied and the value of LC(β) retained is that for which a(β) tends to zero.

The method has been firstly applied to complexation data measured with Np(V) at pH 7 and 8, for which no hydrolysis species are expected in solution [MAR98]. The LC values determined correspond within the errors to those obtained by the common graphical method, indicating the validity of the approach. A good agreement between both methods is also observed with data obtained for U(VI) at pH 4, where the hydrolysis species can be neglected [CZE94]. The method has been finally applied to the U(VI) complexation data at pH 5, leading to LC values nearly 1.7 higher than those estimated at pH 4. All the results of the calculation are presented in Table 1.

Table 1: Determination of the loading capacities under the experimental conditions of this work and comparison of LC values estimated with the "new" approach and that currently used with complexation data of the system Np(V):HA [MAR98].

	pH - I	LC (β)	LC
Np(V)	7 - 0.1	0.13±0.02 (3.51-3.53)	0.13±0.01
	8 - 0.1	0.21±0.05 (3.65-6.66)	0.22±0.015
U(VI)	4 - 0.1	0.20±0.05 (6.06-6.10)	0.19±0.01
	4 - 0.004	0.17±0.04 (5.95-5.99)	0.18±0.02
	5 - 0.1	0.34±0.05 (6.04-6.05)	_
	5 - 0.004	0.31±0.04 (6.15-6.17)	_

The LC values obtained at pH 4 and 5 appear nearly independent of the ionic strength. There are indications of a slight decrease of the amount of available sites for U(VI) complexation when I decreases. This variation is not consistent with that currently observed with soluble polyelectrolytes: due to HA configuration change, the surface binding on the polyanion at fixed pH is expected to be more important when I decreases [KRE97,CZE96]. For instance, Czerwinski et al. [CZE96] have shown that measured LC of Am^{3+} with GoHy-573 humic acid at pH 6 varied with I according to the equation $LC = -0.126\sqrt{I} + 0.683$. It remains, however, for U(VI) as well as for Am(III), that the I strength effect remains poor in the range of I studied here and does not affect significantly the values of the stability constants.

Complexation constants calculated for each experimental point i, are displayed in Figure 7. The resulting overall complexation constant $\log\beta=6.08\pm0.15$ is in very good agreement with that determined by other speciation methods [CZE94,POM98] and appears to be invariant of the experimental conditions and in particular of the uranyl concentration. Furthermore, this result shows that the formation of hydrolysis species, as reported by Zeh et al. [ZHE97], is not significant under these experimental conditions.

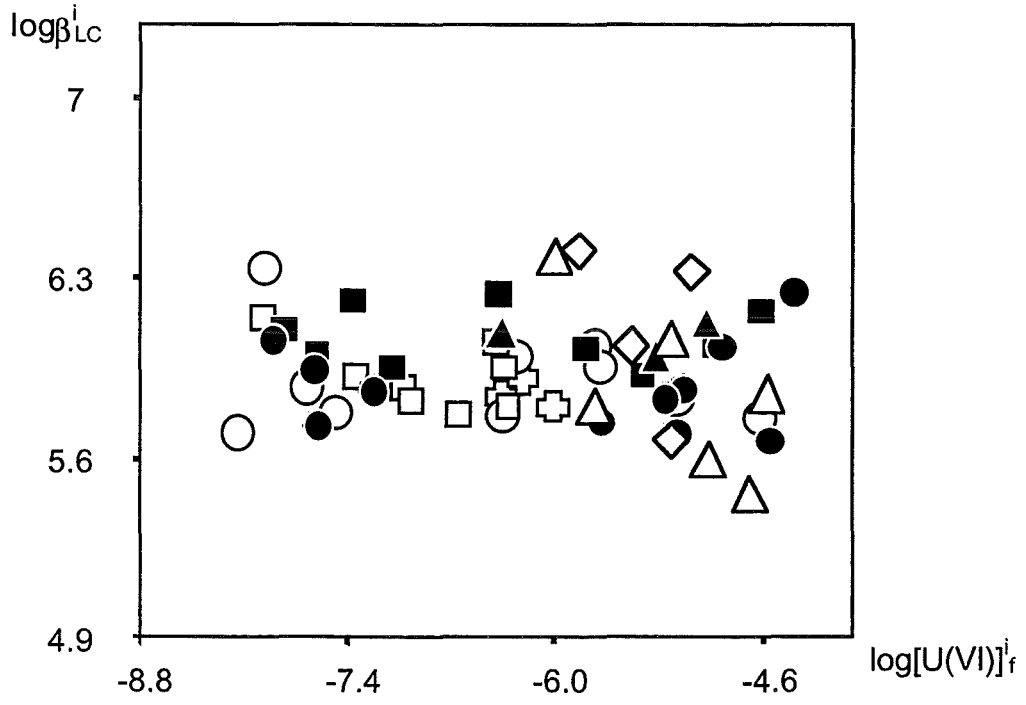

Figure 7: Humate complexation of U(VI) studied by AEC. logβ values calculated and plotted as a function of the logarithm of the free U(VI) concentration in solution. pH=4 (open symbols); I=0.1 M: (HA)=2.5 (O) and 1 mg/L (Δ). I=0.004 M: (HA)=2.5 (□), 1.5 (◇) and 1 mg/L (☆). pH=5 (full symbols); I=0.1 M: (HA)=2.5 (●) and 1.25 mg/L (▲). I=0.004 M: (HA)=2.5 mg/L (■).

CONCLUSIONS

Experimental data on the humate complexation of U(VI) by AEC have been obtained for uranium concentrations down to 10^{-8}M. They can be well described by the charge neutralization model through loading capacity values calculated by a new approach allowing to exempt from the presence of hydrolysis species. Moreover, the investigation of the system U(VI):HA by continuous electrophoretic ion focusing has failed due to the presence of an interfering interaction between U(VI) and HA occurring under the effect of an electric field.

REFERENCES

[CHO85]: Choppin, G.R.: Complexes of Actinides with Naturally Occurring Organic Compounds . In: *Handbook of the Physics and Chemistry of the Actinides*, Vol. 3, eds. A.J. Freeman and C. Keller, Elsevier Sci. Publ. Chap. 11 (1985).

[CHO88]: Choppin, G.R.: Humic and Radionuclide Migration. Radiochim. Acta **44/45**, 23 (1988).

[CHO92]: Choppin, G.R.: The Role of Natural Organics in Radionuclide Migration in Natural Aquifer Systems. Radiochim. Acta **58/59**, 113 (1992).

[CZE94]: Czerwinski, K.R., Buckau, G., Kim, J.I.: Complexation of the Uranyl Ion with Aquatic Humic Acid. Radiochim. Acta **65**, 111 (1994).

[CZE96]: Czerwinski, K.R., Kim, J.I., Rhee, D.S., Buckau, G.: Complexation of Trivalent Actinide Ions (Am^{3+} ; Cm^{3+}) with Humic Acid. The Effect of Ionic Strength. Radiochim. Acta **72**, 179 (1996).

[CZE97]: Czerwinski, K., Kim, J.I.: Complexation of Transuranic Ions by Humic Substances: Application of Laboratory Results to the Natural System. Mater. Res. Soc. Proc., **465** (Scientific Basis for Nuclear Waste Management XX), 743 (1997).

[FRA97]: Franz, C., Herrmann, G., Trautmann, N.: Complexation of Samarium(V) and Americium(III) with Humic Acids at Very Low Metal Concentrations. Radiochim. Acta **77**, 177 (1997).

[GRE92]: Grenthe, I., Fuger, J., Konings, R., Lemire, R., Muller, A., Nguyen-Trung, C., Wanner, H.: Chemical Thermodynamics of Uranium, Elsevier Science Publishers (1992).

[HIR85]: Hiraide, M., Tillekeratne, S.P., Otsuka, K., Mizuike, A.: Separation and Determination of Traces of Heavy Metals Complexed with Humic Substances in Fresh Waters by Sorption on Diethylaminoethyl-Sephadex A-25. Anal. Chim. Acta **172**, 215 (1985).

[HIR89]: Hiraide, M : Separation and Determination of Traces of Heavy Metals Complexed with Humic Substances in River Water. Kontakte (Darmstadt) **3**, 37 (1989).

[HUM97]: Hummel, W.: Binding Models for Humic Substances. In: *Modelling in Aquatic Chemistry*, eds. I. Grenthe and I. Puigdomenech, OECD/NEA, Chap. V (1997).

[KIM90]: Kim, J.I., Buckau, G., Li, G.H., Duschner, H., Psarros, N .: Characterization of Humic anf Fulvic Acids from Gorleben Groundwater: J. Anal. Chem. **338**, 245 (1990).

[KIM96]: Kim, J.I., Czerwinski, K.R.: Complexation of Metal Ions with Humic Acid: Metal Ion Charge Neutralization Model. Radiochim. Acta **73**, 5 (1996).

[KRE97] : Kretzschmar, R., Hesterberg, D., Sticher, H.: Effects of Adsorbed Humic Acid on Surface Charge and Flocculation of Kaolinite. Soil. Sci. Soc. Am. J. **61**, 101 (1997).

[MAN93]: Mang, M. Gehmecker, H., Trautmann, N., Herrmann, G.: Separation of Oxydation States of Neptunium and Plutonium by Continuous Electrophoretic Ion Focusing. Radiochim. Acta **62**, 19 (1993).

[MAR96]: Marquardt, C., Herrmann, G., Trautmann, N.: Complexation of Np(V) with Humic Acids at Very Low Metal Concentrations. Radiochim. Acta **73**, 119 (1996).

[MAR98]: Marquardt, C., Kim, J.I.: Complexation of Np(V) with Humic Acid: Intercomparison of Results from Different Laboratories. In: *First Technical Progress Report, EC Project No.: F14W-CT96-0027*, ed. G. BUCKAU, Forschungszentrum Karlsruhe GmbH, Karlsruhe (1998). Marquardt, C., Kim, J.I.: Complexation of Np(V) with Fulvic Acid. Radiochim. Acta **81**, 143 (1998).

[POM98]: Pompe, S., Brachmann, A., Bubner, M., Geipel, G., Heise, K.H., Bernhard, G., Nitsche, H.: Determination and Comparison of Uranyl Complexation Constants with Natural and Model Humic Acids. Radiochim. Acta **82**, 89 (1998).

[RAO94]: Rao, L., Choppin, G.R., Clark, S.B.: A Study of Metal-Humate Interactions Using Cation Exchange. Radiochim. Acta **66/67**, 141 (1994).

[RIZ94]: Rizkolla, E.N., Rao, L.F., Choppin, G.R., Sullivan, J.C.: Thermodynamics of Uranium(VI) and Plutonium(VI) Hydrolysis. Radiochim. Acta **65**, 23 (1994).

[RUD77]: Rudolph, W., Kratz, K.L., Herrmann, G.: Half-Lives, Fission Yields and Neutron Emission of Neutron-Rich Antimony Isotopes. J. Inor. Nucl. Chem. **39**, 753 (1977).

[SIL95]: Silva, R.J., Nitsche, H.: Actinide Environmental Chemistry. Radiochim. Acta **70/71**, 377 (1995).

[ZHE97]: Zeh, P., Czerwinski, K.R., Kim, J.I.: Speciation of Uranium in Gorleben Groundwaters. Radiochim. Acta **76**, 37 (1997).

ANNEXES

Experimental K_d values measured by AEC for the system U(VI):HA.

pH=4 - I=0.004M

C_U	[HA(II)]	K_D	$\log\beta$
4,93E-07	5,75E-06	0,844	6,08
4,93E-07	5,75E-06	0,710	5,99
4,83E-07	5,75E-06	0,540	5,85
2,50E-07	5,75E-06	0,553	5,82
2,49E-07	5,75E-06	0,562	5,82
1,35E-07	5,75E-06	0,644	5,87
6,80E-08	5,75E-06	0,804	5,96
2,42E-08	5,75E-06	1,304	6,16
1,10E-06	2,30E-06	0,156	5,83
7,00E-07	2,30E-06	0,214	5,93
5,30E-07	2,30E-06	0,205	5,86
5,12E-06	3,45E-06	0,118	6,38
4,15E-06	3,45E-06	0,117	5,91
2,82E-06	3,45E-06	0,190	6,17
1,76E-06	3,45E-06	0,348	6,44

pH=4 - I=0.1M

C_U	[HA(II)]	K_D	$\log\beta$
3,52E-06	5,75E-06	0,291	5,93
1,60E-06	5,75E-06	0,540	5,99
8,10E-07	5,75E-06	0,975	6,14
3,60E-07	5,75E-06	1,177	6,11
9,89E-06	2,30E-06	1,131	6,03
8,28E-06	2,30E-06	0,044	5,75
5,39E-06	2,30E-06	0,047	5,85
3,69E-06	2,30E-06	0,071	6,18
1,90E-06	2,30E-06	0,115	5,84
1,23E-06	2,30E-06	0,144	6,41
3,20E-08	5,75E-06	0,348	6,02
8,10E-07	5,75E-06	0,861	6,07
2,41E-07	5,75E-06	0,678	5,94
4,20E-08	5,75E-06	0,978	5,95
3,26E-08	5,75E-06	2,511	6,36
1,27E-08	5,75E-06	0,848	5,89

pH=5 - I=0.004M

C_U	[HA(II)]	K_d	log β
4,20E-08	5,75E-06	1,190	6,11
3,20E-08	5,75E-06	1,360	6,17
8,60E-08	5,75E-06	1,060	6,07
7,20E-08	5,75E-06	1,610	6,25
6,20E-07	5,75E-06	1,010	6,12
3,20E-07	5,75E-06	1,540	6,27
1,00E-06	5,75E-06	0,794	6,05
2,00E-06	5,75E-06	0,676	6,13
3,00E-06	5,75E-06	0,583	6,22

pH=5 - I=0.1M

C_U	[HA(II)]	K_d	log β
4,70E-06	5,75	0,476	6,27
2,50E-06	5,75	0,705	6,12
1,70E-06	5,75	0,747	6,01
7,30E-07	5,75	0,795	5,92
3,10E-08	5,75	1,624	6,14
4,20E-08	5,75	1,308	6,06
7,40E-08	5,75	1,129	6,00
1,40E-06	5,75	0,761	5,98
3,50E-06	5,75	0,407	5,87
3,70E-08	5,75	0,936	5,91
1,50E-06	5,75	0,633	5,89
4,00E-06	2,880	0,225	6,16
2,50E-06	2,88	0,287	6,07
6,30E-07	2,88	0,602	6,14